

Transverse Momenta in Hard Scattering Processes

postdoctoral thesis ^{1,2}

presented by

Rainer Jakob

to the Department of Physics of the

University of Wuppertal



10th November, 2002

¹ Habilitationsschrift im Sinne von §3 Abs. 2 der Habilitationsordnung des Fachbereiches Physik der Bergischen Universität Gesamthochschule Wuppertal.

²for an electronic version see my homepage at <http://www.theorie.physik.uni-wuppertal.de/~rainer/>

Diese Arbeit wurde ermöglicht durch ein Habilitandenstipendium der Deutschen Forschungsgemeinschaft, für deren Unterstützung ich mich hiermit ausdrücklich bedanken möchte.

Contents

Foreword	1
1 Introduction	5
2 Light-Cone quantisation	17
3 Transverse momenta in (semi-)inclusive reactions	25
3.1 the concept of PDFs and PFFs in (semi-)inclusive reactions	25
3.2 transverse momentum dependent PDFs and PFFs	31
3.2.1 PDFs of a spin-1/2 hadron	31
3.2.2 transverse momentum dependent PDFs	37
3.2.3 PFFs of a spin-1/2 hadron	42
3.2.4 the naming scheme	48
3.2.5 towards a global analysis of transversity	50
3.2.5.1 Collins effect in SIDIS	53
3.2.5.2 Collins effect in e^+e^- annihilation	57
3.2.5.3 SSA in $\pi\pi$ production	60
3.2.5.4 DSA in inclusive ρ production	66
3.3 model calculations of PDFs and PFFs	66
3.3.1 PDF and PFF in a spectator model	67
3.3.2 results and discussion	71
3.3.2.1 PDFs of the nucleon	71
3.4 transverse momentum dependence and evolution	79
3.5 summary	83
4 Transverse momenta in exclusive reactions	85
4.1 advantages of being exclusive	85
4.2 exclusive reactions at large momentum transfer	87
4.2.1 reaction mechanisms	87

4.2.2	form factors at large $ t $	97
4.2.2.1	form factor of the pion $F_\pi(Q^2)$	97
4.2.2.2	elastic form factor of the nucleon	99
4.2.2.3	pion- γ transition form factor	102
4.2.3	wide angle Compton scattering	104
4.2.3.1	WACS off protons in the hard scattering approach	104
4.2.3.2	WACS of protons in the soft-overlap approach	106
4.2.3.3	wide angle meson production	110
4.3	deeply virtual exclusive reactions	110
4.4	generalised parton distributions	115
4.4.1	LCWF overlap representation of GPDs	120
4.4.1.1	the region $\xi < \bar{x} < 1$	122
4.4.1.2	the region $-1 < \bar{x} < -\xi$	123
4.4.1.3	the region $-\xi < \bar{x} < \xi$	123
4.4.1.4	interpretation of overlap formulas	124
4.4.2	orbital angular momentum	124
4.4.3	transverse localisation of partons	126
4.5	summary	131
5	Conclusions and outlook	133
A	Dirac matrices in chiral (Weyl) representation	137
B	Sudakov factor	141
C	Reference frames for elastic FFs and CS	143
C.1	elastic FF, different reference frames	144
C.1.1	“Breit-brick wall”	144
C.1.2	“Breit-symmetric”	145
C.1.3	“hadron-in” frame	146
C.1.4	“hadron-out” frame	146
C.1.5	arguments of Ψ^{out} in terms of “hadron-in” quantities	146
C.1.6	scheme of different reference frames	147
C.2	RCS, different reference frames	148
C.2.1	“CMS-symmetric”	148
C.2.2	scheme of different reference frames	149
C.2.3	“hadron-in frame”	150

C.2.4	“hadron-out” frame	150
C.2.5	arguments of Ψ^{out} in terms of “hadron-in” quantities	151
C.2.6	“CMS-in”	152
C.2.7	“CMS-out”	152
C.3	DVCS, different reference frames	153
C.3.1	“average” frame	153
C.3.2	“hadron-in” frame	157
C.3.3	“hadron-out” frame	158
C.3.4	arguments of LCWFs in terms of auxiliary variables	159
C.3.5	arguments of Ψ^{out} in terms of “hadron-in” quantities	160
C.3.6	“ γ^* -nucleon c.m.”-frame	161
C.3.7	relation to X and ζ variables	162
D	Acronyms	163
	Bibliography	165

Foreword

One of the most successful concepts in hadron physics is the basic idea of the *naive parton model*, where fast moving hadrons are considered as a jet of quasi-free partons moving almost collinear. Over more than three decades this simple and beautiful picture has proven to be an extremely valuable guideline for the description of a large variety of hard scattering processes. The main physics effects were indeed correctly - qualitatively and quantitatively - explained by proper applications of the parton model ideas to hard processes involving hadrons in the initial state and/or detected hadrons in the final state.

the parton
model...

The topic of the present thesis is the discussion of one of the possible directions to go beyond the naive parton model, i.e., the effect of transverse motion of partons. The picture of ‘... a jet of partons moving *almost* collinear...’ in fact implies that individually partons may have small momentum components transverse to the momentum of their parent hadrons. Clearly, the effects of transverse parton momenta play the rôle of corrections to the dominant ones, but they can be of quite some importance for the detailed understanding of hadronic substructure:

...and beyond

- the corrections can be of substantial numerical magnitude, as is the case for many *exclusive quantities* at presently accessible momentum transfers,
- or the corrections can lead to the existence of new tensor structures not possible without transverse momenta and resulting in unambiguous angular dependencies which allow to single out the transverse momentum effects, as is known from many *(semi-)inclusive scattering processes*.

Clearly, the investigation on transverse momentum effects results in a more detailed - in a sense, more refined - knowledge on the structure of hadronic matter and the inner workings of QCD. Often the dependence on transverse momenta can be combined with the transverse spin structure of hadrons to investigate the angular momentum aspects of the hadron substructure.

Detailed measurements of semi-inclusive and exclusive processes have become feasible in running experiments (HERMES, H1 and ZEUS at DESY, experiments at CEBAF/JLAB, at the SLC/SLAC, at LEP/CERN), and will become even more precise with the experiments presently starting (COMPASS/CERN), or discussed and planned for the mid-term future (ELFE@TESLA, TESLA-N, an upgraded version of CEBAF, or EIC into which the former EPIC and eRHIC proposals have merged). A new generation of accelerators and detectors make possible experiments with unprecedented precision and kinematic range. The

experiment
and theory

considerable progress in the experimental precision asks for clear theoretical concepts beyond the well-understood and tested parton model ideas, like for instance the transverse momentum effects. In turn, the outcome of experiments stimulates, and will further stimulate, the theoretical understanding of our fundamental picture of hadronic substructure.

semi-inclusive
and exclusive
hard processes

In this thesis I will try to give a detailed discussion of transverse momentum effects in exclusive and (semi-)inclusive hard processes with a comparison of similarities and differences between the two distinct classes of reactions. It is based on the experience gained in the field in the last 10-15 years which showed considerable new developments for both, exclusive and semi-inclusive hard processes leading to deeper insights. A partial synthesis of the concepts used in the description of the two distinct classes of reactions was triggered by the discussion of *deeply virtual exclusive processes* and the notion of the *skewed* or *generalised parton distributions*³ which were first considered in the mid of the '80, and recently received an enormous revived interest which jump started vibrant activities in the last 6 years.

a coherent picture

During the last decade I was happy to participate and contribute to fundamental research activities in hadronic physics, being involved in the theoretical investigation of various exclusive and (semi-)inclusive scattering processes. With retrospective, I was lucky having worked on both classes of reactions, distinct but with vast similarities, in a period when new ideas and concepts were developed merging existing ones in a much more coherent picture. In the present thesis I will try to review these aspects of coherence in notions and concepts. Therefore, often I will refer for technical details to the original publications and instead point to and emphasise the underlying physical picture.

Much of the insights I could gain in the physics topics covered in the present report I owe to friends and colleagues. Many fruitful discussions and enjoyable collaborations during the last 10-12 years are gratefully acknowledged. In particular, I would like to thank

Alessandro Bacchetta, Michael Bergmann, Nicola Bianchi,
Andrea Bianconi, Daniel Boer, Sigfrido Boffi, Jan Bolz, Sabrina Casanova,
Matthias Dahm, Markus Diehl, Thorsten Feldmann, Marco Radici,
Martin Raulfs, Joao Rodrigues, Manfred Schürmann, Wolfgang Schweiger,
and Carsten Vogt,

who will find parts of their results obtained in collaboration with me in the present report. Special thanks go to

Peter Kroll, Piet Mulders and Nico Stefanis

who guided my – still ongoing – learning in physics and supported me in different stages of my scientific work.

³The name *skewed parton distributions* was invented to amalgamate the different terms (non-forward, off-forward, non-diagonal, off-diagonal) which can be found in the literature for closely related quantities. Throughout this thesis I will instead use the notion of *generalised parton distributions* which emphasises the aspect of generalisation and replaces the - somewhat unfortunate - older naming convention in the more recent literature.

Further I would like to mention all colleagues which made working in the field so much enjoyable by participating in lively discussions, scientific exchange on the numerous meetings, workshops and conferences where we have met. Being part of the community – only vaguely characterised by the label of *hadronic physics* – for me was a mostly very pleasant experience far beyond sensing the shared interest in the fundamental questions about the substructure of hadronic matter. Dedication to physics in general is the basis for our relationship, beyond it many colleagues became good friends.

Last but certainly not least, special thanks go to Petra Engels and her daughter Olivia, who had to suffer so much from all the negative consequences it brings to live with a physicist, i.e. somebody who is always absent when needed most, who moves every second year to a different place, with whom you never can make plans beyond the next step, and who comes home late in the evenings and is always busy, ... to name but a few of the consequences. Since more than 16 years I keep on promising that the situation will change and I will spend more time with you. I am very much indebted to you for your continuous support during my diploma, Ph.D., the post-doc period and habilitation. We have to find out together what future will bring.

Wuppertal, 12th November, 2002

1

Introduction

Quantum Chromodynamics (QCD) is well established as the theory which describes all known phenomena of strong interactions in the realm of short distance/short time effects where the powerful technical tool of perturbation theory applies. The successes of perturbative QCD (pQCD) are based on the fundamental property of *asymptotic freedom*, i.e., the strength of the QCD coupling decreases when going to the regime of short distance scales. Here effectively the dynamics of hard subprocesses between quasi-free *partons* (*quarks* and *gluons*) dominates the physical phenomena. A number of so-called infrared safe observables in high energy physics, like ratios of cross sections or event shape variables, can be very successfully calculated entirely within pQCD.

QCD as the theory
of strong
interactions

Moreover, QCD is presumed to describe also the long distance/long time effects of strong interactions like the binding of hadrons. Actually, it was the symmetry patterns observed in the properties of bound hadrons which lead to the development of the theory: baryon spectroscopy revealed the colour degrees of freedom, and flavour symmetry was first seen clearly in hadron spectroscopy. Unfortunately, the standard tool, perturbation theory, is not applicable in the long distance regime. There are promising attempts of developing non-perturbative techniques, or effective theories which incorporate the main features of QCD in the low energy domain. Lattice gauge theory, has developed into a powerful and essential tool in QCD, and in principal, will be able to determine the observables connected to long distance phenomena in hadron physics from first principles. But still enormous conceptual and technical difficulties have to be overcome.

Thus, it seems fair to state that currently there is no rigorous analytical explanation for the way partons are bound by strong interactions to form hadrons, the only objects involved in hard processes which reach our macroscopic physical world by hitting a detector and producing a signal which finally is transformed into something suitable for human perception. The missing link for a full description of all phenomena of strong interactions within QCD is the transition from the elementary objects of the Quantum Field Theory, *quark* and *gluon fields*, to the real physical objects, the *hadrons*.

quarks & gluons
↓
hadrons

A way out of the dilemma is provided by the concepts of the *parton model* which turned out to be extremely successful in the phenomenology of inclusive processes, and are also generally accepted for the description of exclusive reactions

the parton model

at very high momentum transfers.

The basic ideas of the parton model applied to inclusive processes are

- (a) to treat a rapidly moving hadron as a jet of quasi-free partons moving almost collinear, and
- (b) to calculate the cross section of the hadronic process as a convolution of a partonic cross section and parton distribution functions (PDFs) summed incoherently over all partons.

In the application of the *parton model* ideas to exclusive processes the second step is done on the level of the scattering amplitudes, i.e., (b) is replaced by

- (b') hadronic scattering amplitudes are calculated from partonic hard scattering amplitudes convoluted with distribution amplitudes (DAs).

The prescriptions (b) and (b') go under the name of *factorisation*, which is of fundamental importance for all considerations in hadron physics and, therefore, this concept deserves a closer look:

Loosely speaking, *factorisation* is the - well-defined - splitting of an unsolvable problem into a tractable part, and a part which we do not know how to handle within the theory. The intractable part of the problem gets a name and its solution accordingly can be simply postponed. From a practical minded point of view we just “parameterise our lack of knowledge in terms of unknown functions”.

A certainly better view at *factorisation* is that there is a well founded underlying physical picture: The description of hard processes involving hadrons in the initial or final states is divided in the partonic subprocess taking place at short distances/times and in the long distance binding effects embodied in hadronic matrix elements of parton field operators. Thus, partonic subprocesses and binding effects to a good approximation decouple and do not influence each other. The former are calculable within pQCD, in principal to arbitrary accuracy, although sometimes quite tedious in practice. The latter are parametrised in form of *a priori* unknown phenomenological functions like PDFs, or DAs. In Fig. 1.1 a schematic view of the general concept of *factorisation* is displayed.

Whereas firstly factorisation in the parton model was introduced as a concept motivated by physical intuition, it was realised shortly after that the parton model description is the lowest order of a systematic expansion within the appropriate Quantum Field Theory, namely QCD. Consequently, the property of factorisation can be proven to hold to all orders of a perturbative QCD expansion, and at least to leading or even next-to-leading order in an expansion in inverse powers of the relevant hard scale. For many hard processes formal field theoretical proofs of the factorisation property, so-called *factorisation theorems* have been worked out [1]. Still for other hard processes factorisation theorems are lacking due to technical difficulties, but nevertheless factorisation is generally assumed to be plausible at least at leading order in an $1/Q$ expansion, where Q is the hard scale of the process.

the concept of
factorisation

parton model is
limiting case of
QFT

common feature in description of hard processes: factorisation	
hard physics short distance/time effects	soft physics long distance/time effects
calculable in perturbative QCD	parameterised as <i>a priori</i> unknown fcts.
perturbative (Wilson) coefficients	hadronic matrix elements of (bilocal/multilocal) quark/gluon field operators ↓↓ • parton distribution fcts. (PDF) • parton fragmentation fcts. (PFF) • distribution amplitudes (DA) • ...
process dependence	universality PDFs, PFFs and DAs are process independent

Figure 1.1: Schematic view of the concepts of *factorisation* and *universality*.

In the line of arguments within the parton model, or in the context of factorisation theorems, respectively, the connection between *quark* and *gluon fields* on one side, and *hadrons* on the other side is given by hadronic matrix elements of operators constructed from the elementary field operators [2, 3, 4, 5, 6]. These hadronic matrix elements are in turn parametrised in form of phenomenological functions which are process independent. Depending on the type of process under consideration the matrix elements involved can be, for instance,

- transition matrix elements between a hadronic state and the vacuum defining a *distribution amplitude* (DA),
- a forward matrix element (expectation value) between the same initial and final hadronic state defining a *parton distribution function* (PDF)
- a non-forward matrix element between hadronic states characterised by different momenta (and eventually different hadronic content) defining a *generalised parton distribution* (GPD).

hadronic matrix
elements define
phenomenological
functions

DA

PDF

GPD

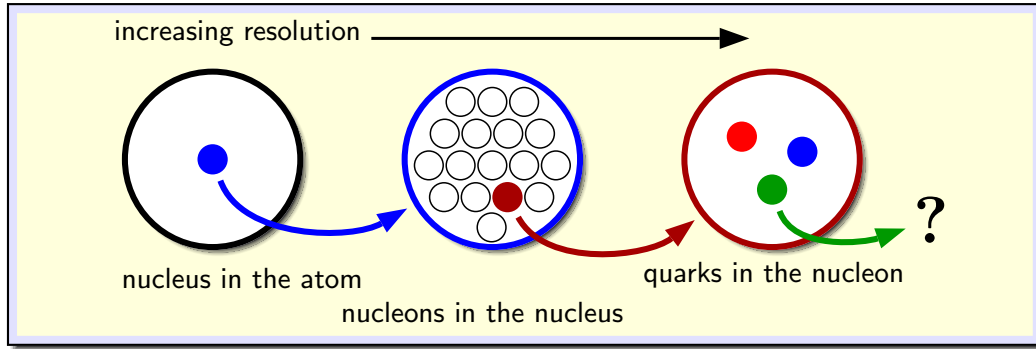


Figure 1.2: Different fundamental layers of matter as subsequently probed with increasing resolution, i.e., increasing momentum transfer.

the property of
universality

Once measured in a hard process, the DAs, PDFs, or GPDs can be inserted into the calculation of other hard processes involving the same type of functions unchanged, or at most subjected to a perturbatively controlled rescaling which results in a logarithmic dependence on the hard scale. This property of process independence is called *universality*; and this is the indispensable foundation stone of the predictive power of the formalism.

The hadronic matrix elements, and the phenomenological functions defined from them, are the main objects of interest in this thesis. The ultimate goal for the far future will be to calculate those objects and their properties from first principles within QCD. Presently, in lack of the necessary technical tools for the big deal, one follows a standard practice: From hard scattering experiments as much information as possible on the hadron substructure in partonic degrees of freedom should be extracted. In particular, hard scattering processes with electroweak probes are well suited for this investigation. The information gained from experiments may be compared with model calculations. Models can be simple-minded or sophisticated; as far as feasible, they should incorporate at least some basic symmetry principles and features of QCD. Finally, the experiences from model considerations shall prepare the path to a consistent QCD treatment of the bound hadrons.

The very principle of exploring the internal substructure of a target by hard scattering with a known probe is not new at all. It stands in the long tradition of the pioneering Rutherford experiment [7], in which by scattering of α -particles on a foil of gold the existence of the nucleus inside the atom was discovered. The process of deep inelastic scattering (DIS) of leptons on a nucleon target

$$\text{lepton} + \text{nucleon} \rightarrow \text{lepton} + \text{anything}$$

is probably the closest analogue to the Rutherford experiment on much smaller scales (compare Fig. 1.2), and of course in a more refined way using the advanced technology of today.

In DIS the known probe is represented by the electroweak interaction mediated by the exchange of gauge bosons (photons, Z -, and W -bosons) and the resolution is high enough to scatter directly on the partons inside the nucleon, i.e., quarks and gluons. The information on hadron substructure is extracted in form of PDFs (cf. Fig. 1.3).

processes involving
PDFs

exploring the
substructure of
hadronic matter in
experiments

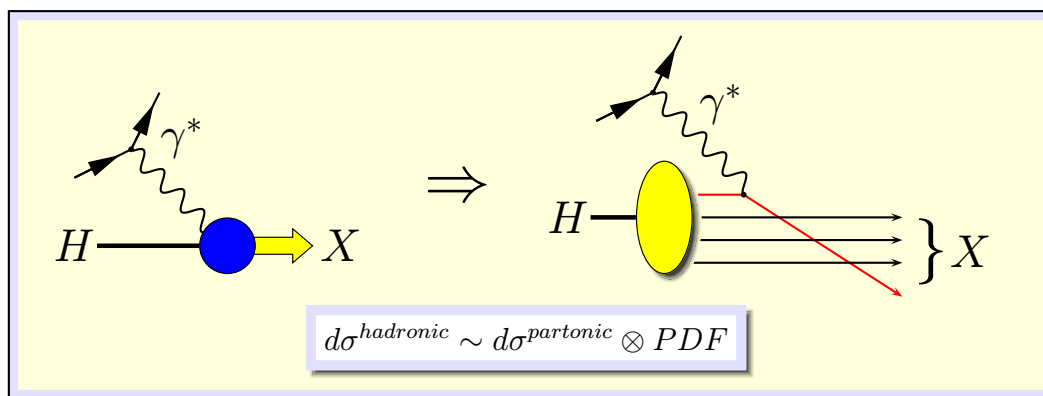


Figure 1.3: Lepton-nucleon deep inelastic scattering (DIS) interpreted in the parton model.

Any other (semi-)inclusive hard scattering process with hadrons in the initial state employs the very same PDFs in its parton model description. A prominent example is the high mass dimuon production or Drell-Yan process [8, 9] (see Fig. 1.4)

$$\text{hadron} + \text{hadron} \rightarrow \text{lepton} + \text{anti-lepton} + \text{anything}$$

which played a major rôle in confirming parton model ideas developed in the context of the DIS process.

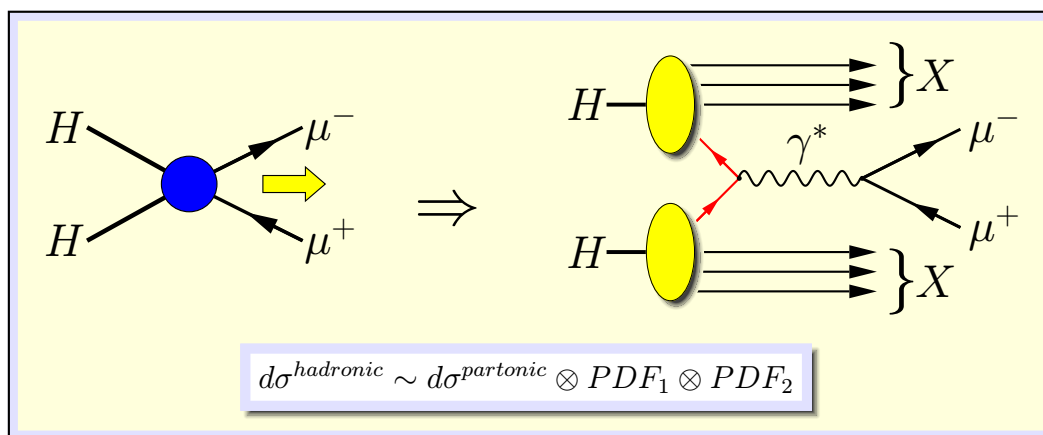


Figure 1.4: Parton model description of the Drell-Yan process $H_1 H_2 \rightarrow \mu^+ \mu^- X$.

Hard scattering processes involving the measurement of hadrons in the final state provide access to the investigation of the hadronisation dynamics. This kind of information is stored up in form of parton fragmentation functions (PFFs) defined again from hadronic matrix elements of quark and gluon field operators. A prominent, perhaps the most simple, example for a hard semi-inclusive process involving PFFs is the one-hadron inclusive electron-positron annihilation (see Fig. 1.5)

$$e^+ + e^- \rightarrow \text{hadron} + \text{anything}$$

from which most of our experimental knowledge on hadronisation originates.

Whereas PDFs give the probabilities of finding a specific parton in a hadron with a certain momentum relative to the one of the parent hadron, the PFFs

processes involving
PFFs

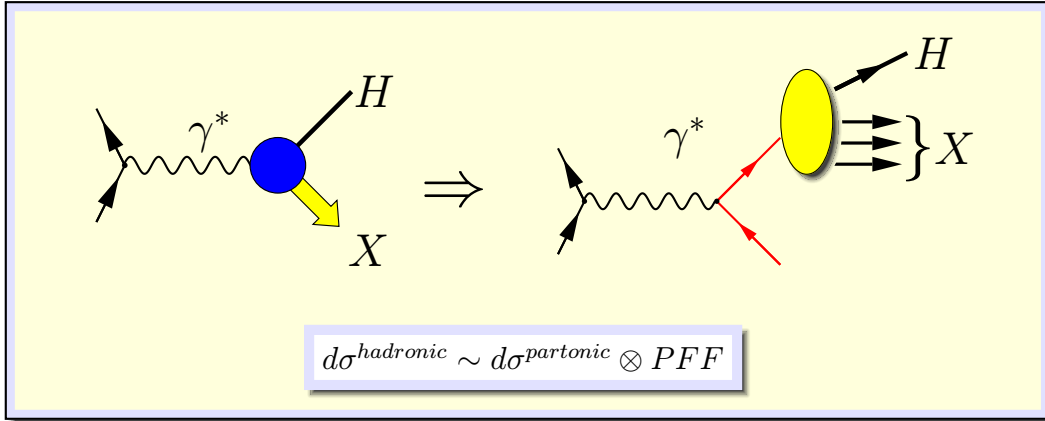


Figure 1.5: One-hadron inclusive electron-positron annihilation $e^+e^- \rightarrow hX$ in the parton model interpretation.

comprise information on the probability that a parton fragments into a certain hadron. In a sense the PFF are the time-like counterparts of PDFs, and encode probabilistic information on the formation process of confined hadrons. One could say that PDFs are related to the *results of confinement*, and PFFs show the *formation of confinement*.

More complicated semi-inclusive processes can involve both, PDFs and PFFs at the same time. Examples for these types of processes are, for instance, the semi-inclusive deep inelastic lepton-nucleon scattering (SIDIS)

$$\text{lepton} + \text{nucleon} \rightarrow \text{lepton} + \text{hadrons} + \text{anything}$$

or jet production in hadron-hadron scattering

$$\text{hadron} + \text{hadron} \rightarrow \text{hadrons} + \text{anything}.$$

Based on the *universality* property, the experimental information from all hard processes can be combined to extract PDFs and PFFs from global fits.

probabilities
vs. amplitudes

It is typically for the class of (semi-)inclusive reactions that information on the hadron substructure is obtained in form of distributions, i.e., probabilities of finding, for instance, a parton in an initial state hadron depending on the partons momentum relative to the hadrons momentum, or probabilities of finding a final state hadron in the fragments of a parton. There is no information on the phase of amplitudes.

processes involving
DAs

Information on hadron substructure on the level of amplitudes can be obtained from the measurement of *exclusive* reactions in which the final state is completely determined, i.e., all outgoing particles are registered. In this sense exclusive reactions are complementary to the inclusive ones. Well known examples are the elastic form factors, like the one of the nucleon

$$\text{nucleon} + \text{lepton} \rightarrow \text{nucleon} + \text{lepton}$$

from which for instance the distribution of electric charge and of the magnetic moment in the nucleon can be learned.

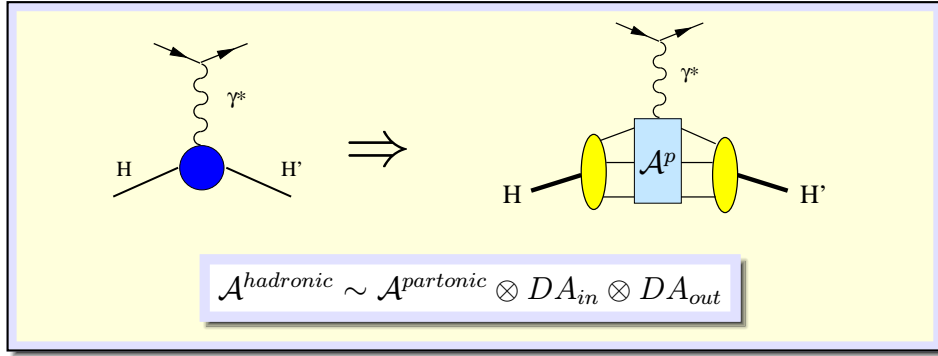


Figure 1.6: Elastic form factor of the nucleon in the parton model interpretation.

The parton model view of the elastic form factor is schematically given in Fig. 1.6. A few words are in order here about two remarkable consequences induced by the extra constraints stemming from the specified final state:

remarkable
features specific to
hard excl. reactions

1. Hard exclusive reactions at high momentum transfer receive their dominant contributions from configurations with the least number of partons, i.e., from the valence Fock state of the hadron. Loosely speaking, the smaller the number of involved partons, the easier it is for them to recombine appropriately into the required final state hadrons.
2. There is a systematic expansion of the partonic amplitude in inverse powers of the hard scale $1/Q$ and in powers of the strong coupling α_s . The constraint of the recombination of partons into final state hadrons results in another remarkable feature; the asymptotically dominant term is of lowest order in the $1/Q$ expansion, but not of lowest order in α_s .

valence Fock state

asymptotically
leading term is of
higher order in α_s

Thus, for kinematic regions of intermediate large Q , where the numerical size of $1/Q$ is not too different from $1/\ln(Q^2)$, one has to investigate carefully the size of the pre-factors of terms which come with a higher power of $1/Q$ but lower power of α_s compared to the powers of asymptotically leading term.

The second point above was the reason why the partonic amplitude was not further specified in Fig. 1.6. In Fig. 1.7 two diagrams are displayed which generically stand for competing mechanisms contributing to the elastic FF of the nucleon.

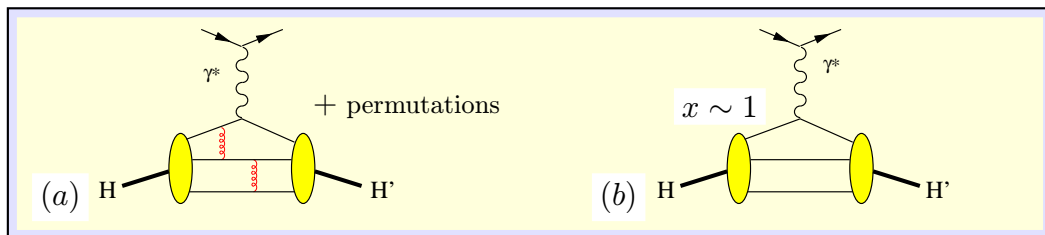


Figure 1.7: Competing mechanisms for the elastic form factor of the nucleon at intermediate large momentum transfer.

In diagram (a) the partonic scattering amplitude contains the minimum number of hard gluon lines necessary to connect all valence Fock state parton lines. The overall momentum transfer is completely redistributed in the hard subprocess. This diagram and those obtained from it by permutations are the dominant ones in the asymptotic limit of very high momentum transfers. Note that all parton lines actively take part in the hard scattering; there are no pure ‘spectator lines’. This is the criterion which results in the lowest possible power of $1/Q$ selecting the asymptotically dominant contributions.

In diagram (b), on the other hand, there are two spectator lines, but also two hard gluons less resulting in a higher power of $1/Q$, but lower order in α_s . Notice that the exact power in the $1/Q$ expansion depends on details of light-cone wave functions describing the initial and final nucleon. Although, in the asymptotic limit subleading, the contributions from diagram (b) can take the lead at intermediate large momentum transfers. There is also another class of diagrams ‘between’ type (a) and (b) with one spectator and one hard gluon.

It is instructive to take a closer look at the parton model picture of another hard exclusive process, the Compton scattering [10]

$$\textit{photon} + \textit{charged target} \rightarrow \textit{charged target} + \textit{photon}$$

which historically provided early evidence that the electromagnetic wave is quantised, and hence has the nature of particles.

Let us consider Compton scattering off the nucleon in kinematic regimes where the nucleon can be replaced by a jet of quasi-free partons. It is important to realize that there are two dimensional scales which potentially can be large and thus justify the application of parton model ideas: the virtuality of the initial photon Q^2 , and the square of the momentum transfer $|t|$. Therefore, in Fig. 1.8 the distinction is made between the regime of ‘deep virtual Compton scattering’ (DVCS), characterised by large Q^2 and small $|t|$, and the regime of ‘wide angle Compton scattering’ (WACS) characterised by large $|t|$ and small Q^2 .

In the DVCS regime the amplitude for the partonic subprocess is given by the Compton scattering off a single parton, the long distance/time part of the process is described with the help of recently introduced, rather new quantities. The close similarity to the DIS process – the total cross section of DIS is related to the imaginary part of the forward Compton scattering amplitude via the optical theorem – has lead to the introduction of a generalisation of PDFs, the *generalised parton distributions* (GPDs). All Fock states contribute to the DVCS process, since the partonic scattering dominantly takes place on one quark line only and an increasing number of spectator partons does not lead to a significant suppression.

In the WACS regime the situation parallels the one discussed above for the example of elastic form factors. Since the momentum transfer is high, it is the lowest Fock state configurations of initial and final nucleon that dominate the process. For asymptotically large momentum transfer $|t|$ the dominant contributions come from partonic subdiagrams which contain the minimum number of hard gluons necessary to connect all parton lines, i.e., two hard gluons in the process under consideration (for instance, the diagram shown in Fig. 1.9(a)). All parton lines are involved in the hard subprocess, and diagrams obtained by

Compton
scattering
a two-scale process

DVCS regime

WACS regime

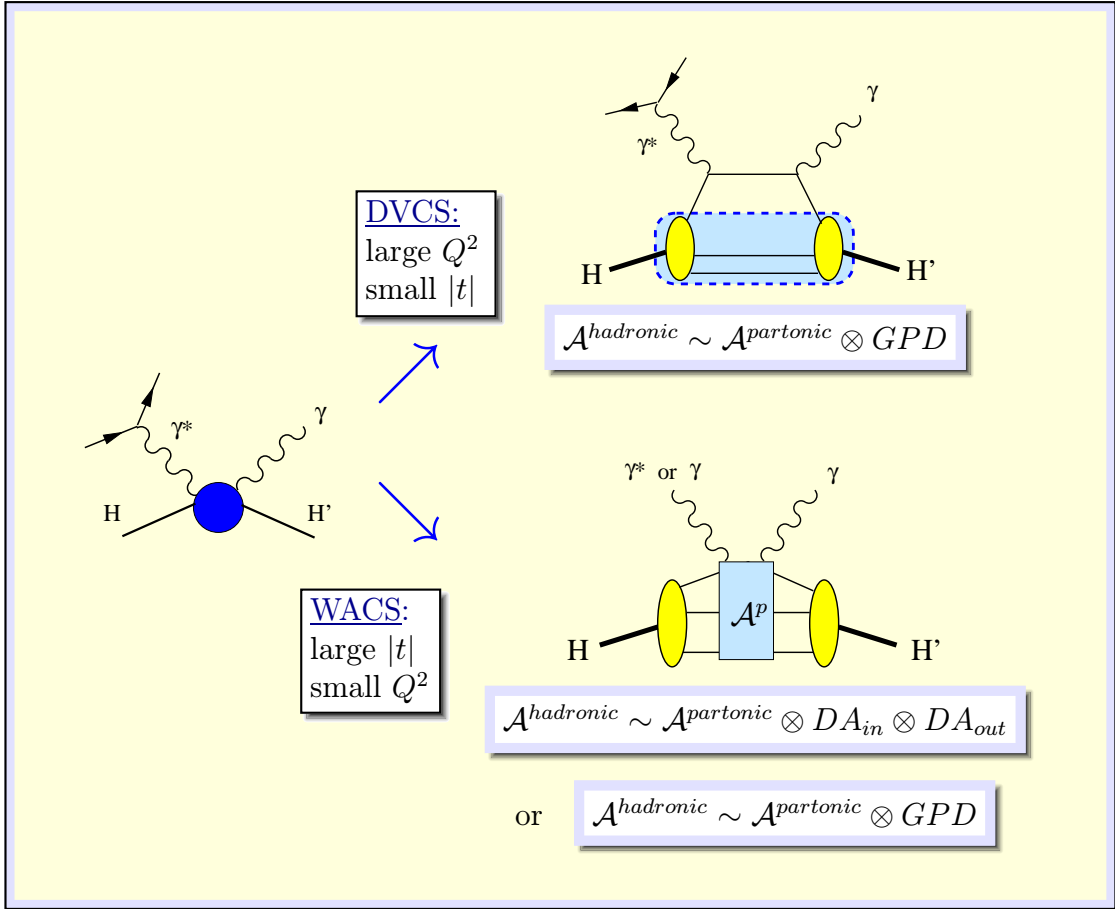


Figure 1.8: Compton scattering off the nucleon in the parton model interpretation, which has a somewhat different representation in the DVCS and WACS kinematic domains. The overlaid dashed box for the DVCS regime indicates a generalised parton distribution.

all possible permutations of parton lines and photon-parton couplings *a priori* contribute at the same order. At intermediate momentum transfer, however, the cross section may be dominated by the partonic diagram without any hard gluons – but two more ‘spectator’ lines – where the photons couple to the same quark line (for instance, the diagram shown in Fig. 1.9(b)). For this *handbag* diagram the soft physics part is comprised in a GPD, actually at a certain kinematical point, as we shall see later.

The introduction of the concept of GPDs in fact was a big step forward in our understanding of the transition between hadronic and partonic degrees of freedom, since formally they link PDFs and form factors, and thus unify conceptual ideas developed for *inclusive* and *exclusive* processes.

GPDs unify conceptual ideas of inclusive and exclusive processes

In particular, GPDs allow a simultaneous study of longitudinal and transverse degrees of freedom of the partonic motion. Combining the all information contained in GPDs, at least in principle, for the first time an *absolute localisation* of partons inside hadrons seems feasible.

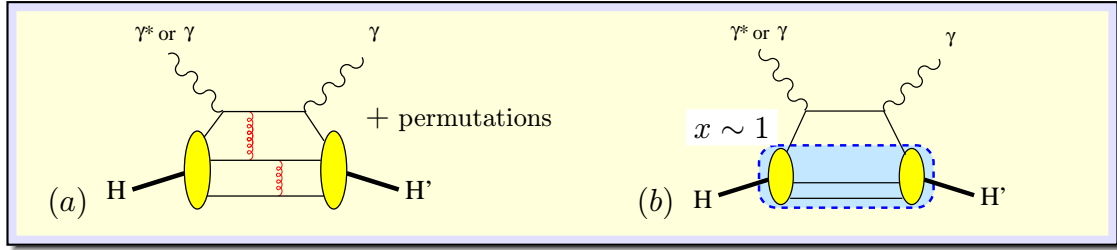


Figure 1.9: Diagrams contributing to WACS. Diagram (a) is an example for the class of diagrams dominant at asymptotically large momentum transfer. Diagram (b) can be leading at intermediate momentum transfer.

...beyond the parton model

Several aspects of the partonic substructure of hadrons *beyond the basic ideas of the parton model* have been investigated in a systematic way:

$(\alpha_s)^n$ corrections

- Higher orders in perturbation theory manifest themselves as *QCD loop corrections*. The absorption of collinear singularities via a redefinition of soft physics objects (PDFs, PFFs, DAs, and GPDs) leads to a scale dependence of these objects. Finite terms give $(\alpha_s)^n$ suppressed corrections to the physical observables like structure functions. The systematic inclusion of perturbative corrections into the *naive parton model* is known as the *QCD improved parton model*.

$(1/Q)^n$ corrections

- The inclusion of hadron mass effects leads to *corrections suppressed by powers of $1/Q$* – the so-called kinematical power corrections. There are also dynamical power corrections from non-leading projections of hadronic matrix elements, and from multi-parton correlations or higher Fock state components. The incorporation of these classes of corrections is extremely difficult. Numerical estimates can sometimes be obtained from model considerations or lattice gauge theory.

To the extent that *factorisation* is expected to hold often the next-to-leading order power corrections can be systematically classified.

intrinsic transverse momenta

- *Intrinsic transverse momenta* of partons relative to their parent hadrons, sometimes combined with (transverse) spin degrees of freedom.

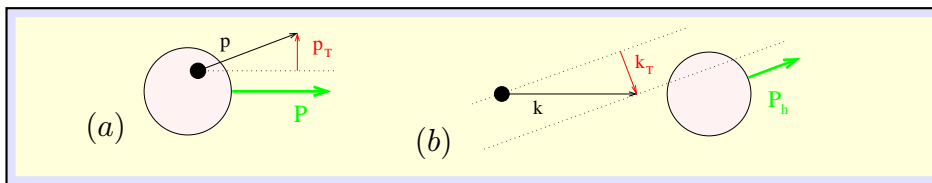


Figure 1.10: Illustration of partonic transverse momenta. In diagram (a) the component of a parton momentum transverse relative to the momentum of the parent hadron is indicated as p_T . In (b) the transverse parton momentum k_T relative to the momentum of a produced hadron in a fragmentation process is displayed.

This thesis is devoted to the comparative study of the latter point, i.e., the effect of *intrinsic transverse momenta* in the phenomenology of hard (semi-)inclusive and exclusive reactions.

The notion of *transverse momenta* needs some clarification. Clearly, referring to components of a four-vector separately, results in frame dependent statements. In fact, a particularly convenient set of frames are those, where the momentum vector of a hadron has no transverse components. These systems will be called “hadron frames”, and the transverse parton momenta $\mathbf{p}_{\perp i}$ in an appropriate hadron frame will be referred to as *intrinsic transverse momenta*. Partonic transverse momenta in frames related to a hadron frame by a *transverse boost* take the form $\mathbf{p}_{\perp i} + x_i \mathbf{P}_{\perp}$ when \mathbf{P}_{\perp} is the transverse part of the hadron momentum in the new frame. In other frames of reference transverse momentum effects may manifest themselves as effects from higher Fock states, with additional gluons or quark-antiquark pairs, and the simple relations may be obscured. Similarly, as much as possible, the parton model picture will be used, which implies the use of an axial gauge, in particular a light cone gauge. Of course, any physical quantity may be calculated using an arbitrary frame of reference and an arbitrary gauge, but interpretations as partonic probabilities (or at least partonic probability amplitudes) are not always applicable.

In that sense, the present thesis will focus on effects related to *transverse momenta* in appropriate *hadron frames* in the framework of a *parton picture*.

intrinsic transverse
momenta

2

Light-Cone Quantisation

Light-Cone
quantisation

In this section I review some basic features of Light-Cone (LC) quantisation [11, 12, 13, 14, 15]. The discussion of hard processes is particularly simple in the context of LC quantisation. Concepts and notions introduced appeal to imagination and follow closely the basic ideas of the *parton model*, to which in fact they provide the formal theoretical background.

The presentation I give in this section is by no means exhaustive, but rather limited and merely serves as reference for some points used in the discussions of the later sections. The larger question whether LC quantisation has principal advantages over the canonical equal-time quantisation will not be pursued here. Also the known severe problems of LC quantisation connected with *zero modes* are beyond the scope of this section.

To set the stage some notation has to be introduced. Here and in the following I will use the component notation

$$a^\mu = [a^+, a^-, \mathbf{a}_\perp] \quad (2.1)$$

for any four-vector a^μ with the LC components $a^\pm = (a^0 \pm a^3)/\sqrt{2}$ and the 2-dimensional transverse part $\mathbf{a}_\perp = (a^1, a^2)$. Square brackets are reserved for LC component notation. With the non-diagonal metric tensor ($\mu, \nu = +, -, 1, 2$)

$$g^{\mu\nu} = \begin{bmatrix} 0 & 1 & 0 & 0 \\ 1 & 0 & 0 & 0 \\ 0 & 0 & -1 & 0 \\ 0 & 0 & 0 & -1 \end{bmatrix} \quad (2.2)$$

the scalar product of two four-vectors is given as

$$a \cdot b = a^\mu b_\mu = g^{\mu\nu} a_\mu b_\nu = a^+ b^- + a^- b^+ - \mathbf{a}_\perp \cdot \mathbf{b}_\perp. \quad (2.3)$$

Notice that the non-zero off-diagonal entries in the metric tensor make the conversion of contravariant and covariant vectors somewhat confusing, resulting for instance in $a^\pm = a_\mp$, and $\partial^\pm \equiv \partial/\partial z_\pm = \partial/\partial z^\mp$. Hence I will work with upper (contravariant) indices as much as possible. Frequently, I will use two light-like unit vectors n_\pm

$$n_+ \equiv [1, 0, \mathbf{0}_\perp] , \quad n_- \equiv [0, 1, \mathbf{0}_\perp] \quad (2.4)$$

satisfying $n_+^2 = n_-^2 = 0$ and $n_+ \cdot n_- = 1$. With the help of n_\pm LC components can be projected out by

$$a^+ = n_- \cdot a , \quad a^- = n_+ \cdot a . \quad (2.5)$$

longitudinal boost A Lorentz transformation which boosts coordinates from the rest frame of a particle to a frame where the particle moves with velocity v along the z -axis changes the ordinary components according to

$$\tilde{x}^0 = \frac{x^0 - vx^3}{\sqrt{1-v^2}} , \quad \tilde{x}^3 = \frac{x^3 - vx^0}{\sqrt{1-v^2}} , \quad \tilde{x}^1 = x^1 , \quad \tilde{x}^2 = x^2 . \quad (2.6)$$

The same relations written in LC components take the form

$$\tilde{x}^+ = x^+ e^\psi , \quad \tilde{x}^- = x^- e^{-\psi} , \quad \tilde{\mathbf{x}}_\perp = \mathbf{x}_\perp , \quad (2.7)$$

where the hyperbolic angle ψ is $\ln((1-v)/(1+v))/2$, so that $v = -\tanh \psi$ [16]. The momentum of a particle with mass m obtained by a boost with ψ from the rest frame is

$$\tilde{p}^\mu = \left[p^+ , \frac{m^2}{2p^+} , \mathbf{0}_\perp \right] = \left[\frac{m}{\sqrt{2}} e^\psi , \frac{m}{\sqrt{2}} e^{-\psi} , \mathbf{0}_\perp \right] . \quad (2.8)$$

transverse boost A particularly useful Lorentz transformation is a *transverse boost* (cf. e.g. [12, 14]) which leaves the *plus* component of *any* momentum vector a unchanged, and which involves a parameter b^+ and a transverse vector \mathbf{b}_\perp :

$$\begin{aligned} a^\mu &= [a^+ , a^- , \mathbf{a}_\perp] \\ \longrightarrow \quad \tilde{a}^\mu &= \left[a^+ , a^- - \frac{\mathbf{a}_\perp \cdot \mathbf{b}_\perp}{b^+} + \frac{a^+ \mathbf{b}_\perp^2}{2(b^+)^2} , \mathbf{a}_\perp - \frac{a^+}{b^+} \mathbf{b}_\perp \right] \end{aligned} \quad (2.9)$$

with

$$\begin{aligned} \tilde{a}^2 &= 2a^+a^- - 2a^+ \frac{\mathbf{a}_\perp \cdot \mathbf{b}_\perp}{b^+} + 2a^+ \frac{a^+ \mathbf{b}_\perp^2}{2(b^+)^2} - \mathbf{a}_\perp^2 + 2 \frac{a^+}{b^+} \mathbf{a}_\perp \cdot \mathbf{b}_\perp - \left(\frac{a^+}{b^+} \right)^2 \mathbf{b}_\perp^2 \\ &= 2a^+a^- - \mathbf{a}_\perp^2 = a^2 . \end{aligned} \quad (2.10)$$

Note the distinction of a transverse boost from a rotation. There is always a rotation in coordinate space which has the same effect on the transverse momentum components. But a rotation leaves the energy component unchanged and thus changes the *plus* LC component. Rotations and transverse boosts in general do not commute.

It turns out useful to define projectors

$$\mathcal{P}_\pm = \frac{1}{2} \gamma^\mp \gamma^\pm \quad (2.11)$$

with

$$\mathcal{P}_+ + \mathcal{P}_- = 1, \quad \mathcal{P}_+ \mathcal{P}_- = \mathcal{P}_- \mathcal{P}_+ = 0, \quad \mathcal{P}_\pm^2 = \mathcal{P}_\pm, \quad (2.12)$$

which satisfy

$$\mathcal{P}_\pm \gamma^\mp = \gamma^\mp \mathcal{P}_\mp, \quad \mathcal{P}_\pm \gamma^\pm = 0, \quad \mathcal{P}_\pm \gamma_\perp = \gamma_\perp \mathcal{P}_\pm. \quad (2.13)$$

The canonical way of quantising field theories proceeds via imposing commutation relations between the dynamically independent fields at equal-time, for instance $z^0 = 0$. As a direct consequence of Lorentz invariance any other space-like hyper-plane in Minkowski space is equally well suited. A light-front hyper-plane, as for instance defined by $z^+ = 0$, can be viewed as the limiting case of a sequence of space-like hyper-planes.

At given light-cone time, say $z^+ = 0$, the independent dynamical fields of QCD are the so-called “good” LC components of the fields, namely $\phi_q^c \equiv \mathcal{P}_+ \psi_q^c$ for quarks of flavour q and colour c and the transverse components of the gluon potential A_i^c (where $i \in \{1, 2\}$ is a transverse index and c again denotes colour). The dependent fields, or “bad” components are $\chi_q^c \equiv \mathcal{P}_- \psi_q^c$ for the quarks and the *minus* component of the gluon potential A^{-c} (see, for instance, [15]).

In order to illustrate the different rôle of “good” and “bad” components of the quark fields, one can use \mathcal{P}_\pm to project the Dirac equation down to two separate equations (colour indices suppressed)

$$i \gamma^+ D^- \phi = i \vec{\gamma}_\perp \cdot \mathbf{D}_\perp \chi + m \chi \quad (2.14)$$

$$i \gamma^- D^+ \chi = i \vec{\gamma}_\perp \cdot \mathbf{D}_\perp \phi + m \phi, \quad (2.15)$$

where $D^\pm = \partial/\partial z^\mp + i g A^\pm$. Only Eq. (2.14) describes the propagation of physical degrees of freedom. In Eq. (2.15) the “light-cone time” z^+ does not occur at all, and thus it is rather a constraint valid at any LC time. In LC gauge $A^+ = 0$ it takes the form

$$i \gamma^- \frac{\partial}{\partial z^-} \chi = \vec{\gamma}_\perp \cdot \mathbf{D}_\perp \phi + m \phi \quad (2.16)$$

and constrains χ in terms of ϕ and \mathbf{A}_\perp , which therefore should be regarded as composite $\chi = F[\phi, \mathbf{A}_\perp]$. Similar considerations on the gluon equations of motion reveal that A^- is a constrained variable, too.

The independent dynamical fields have Fourier expansions in momentum space (see e.g. [14], Appendix II)

$$\begin{aligned} \phi_q^c(z^-, \mathbf{z}_\perp) &= \int \frac{dp^+ d^2 \mathbf{p}_\perp}{p^+ 16\pi^3} \Theta(p^+) \sum_\mu \\ &\left\{ \begin{aligned} &b_q(w) u_+(w) \exp\left(-i p^+ z^- + i \mathbf{p}_\perp \cdot \mathbf{z}_\perp\right) \\ &+ d_q^\dagger(w) v_+(w) \exp\left(+i p^+ z^- - i \mathbf{p}_\perp \cdot \mathbf{z}_\perp\right) \end{aligned} \right\} \quad (2.17) \end{aligned}$$

\mathcal{P}_\pm projectors

“good” & “bad”
field components

equations of
motion

expansion in
momentum space

for the free quark field, and $(\alpha \in \{1, 2\})$

$$A_\alpha^c(z^-, \mathbf{z}_\perp) = \int \frac{dp^+ d^2\mathbf{p}_\perp}{p^+ 16\pi^3} \Theta(p^+) \sum_\mu \left\{ \begin{aligned} & a(w) \epsilon_\alpha(w) \exp(-ip^+ z^- + i\mathbf{p}_\perp \cdot \mathbf{z}_\perp) \\ & + a^\dagger(w) \epsilon_\alpha^*(w) \exp(+ip^+ z^- - i\mathbf{p}_\perp \cdot \mathbf{z}_\perp) \end{aligned} \right\}. \quad (2.18)$$

for the free gluon field, where $\Theta(p^+)$ denotes the usual step function. A collective notation is used for the dependence on the *plus* and transverse parton momentum components, the helicity, and the colour in the form

$$w = (p^+, \mathbf{p}_\perp, \mu, c). \quad (2.19)$$

The operators b and d^\dagger are the annihilator of the ‘‘good’’ component of the quark fields and the creator of the ‘‘good’’ component of the antifields, respectively, and $u_+(w) \equiv \mathcal{P}_+ u(w)$ and $v_+(w) \equiv \mathcal{P}_+ v(w)$ are the projections of the usual quark and antiquark spinors. a and a^\dagger are the annihilation and creation operators for transverse gluons, and $\epsilon_\alpha(w)$ is a transverse component of the gluon polarisation vector. The operators fulfil the anticommutation relations

$$\begin{aligned} \{b_{q'}(w'), b_q^\dagger(w)\} &= \{d_{q'}(w'), d_q^\dagger(w)\} \\ &= 16\pi^3 p^+ \delta(p'^+ - p^+) \delta^{(2)}(\mathbf{p}'_\perp - \mathbf{p}_\perp) \delta_{q'q} \delta_{\mu'\mu} \delta_{c'c}, \end{aligned} \quad (2.20)$$

and the gluon operators a and a^\dagger satisfy the commutation relation

$$[a(w'), a^\dagger(w)] = 16\pi^3 p^+ \delta(p'^+ - p^+) \delta^{(2)}(\mathbf{p}'_\perp - \mathbf{p}_\perp) \delta_{\mu'\mu} \delta_{c'c}. \quad (2.21)$$

Fock state decomposition

A key ingredient for a probabilistic interpretation of phenomenological functions involved in the description of hard processes is the Fock state decomposition [14], i.e., the replacement of a hadron state by a superposition of partonic Fock states containing free quanta of the ‘‘good’’ LC components of (anti)quark and gluon fields. Single-parton, quark, antiquark or gluon, momentum eigenstates are created by b^\dagger , d^\dagger and a^\dagger acting on the perturbative vacuum,¹

$$\begin{aligned} |q; w\rangle &= b_q^\dagger(w) |0\rangle, \\ |\bar{q}; w\rangle &= d_q^\dagger(w) |0\rangle, \\ |g; w\rangle &= a^\dagger(w) |0\rangle, \end{aligned} \quad (2.22)$$

and the (anti)commutation relations (2.20) and (2.21) translate into the normalisation of these states,

$$\langle s'; w' | s; w \rangle = 16\pi^3 p^+ \delta(p'^+ - p^+) \delta^{(2)}(\mathbf{p}'_\perp - \mathbf{p}_\perp) \delta_{s's} \delta_{\mu'\mu} \delta_{c'c} \quad (2.23)$$

¹A ‘trivial’ perturbative vacuum is assumed, i.e., $b|0\rangle = d|0\rangle = a|0\rangle = 0$, and possible problems arising from zero modes are ignored, which are beyond the scope of this investigation.

for partons s, s' of any kind. A hadronic state characterised by the momentum P and helicity λ is written as

$$|H; P, \lambda\rangle = \sum_{N, \beta} \int [dx]_N [d^2 \mathbf{p}_\perp]_N \Psi_{N, \beta}^\lambda(r) |N, \beta; p_1, \dots, p_N\rangle, \quad (2.24)$$

where $\Psi_{N, \beta}^\lambda(r)$ is the momentum LCWF of the N -parton Fock state denoted by $|N, \beta; p_1, \dots, p_N\rangle$. The index β labels its parton composition, and the helicity and colour of each parton.

Apart from their discrete quantum numbers (flavour, helicity, colour) the partons are characterised by their momenta $k_i = [p_i^+, p_i^-, \mathbf{p}_{\perp i}]$. The LCWFs, on the other hand, do not depend on the momentum of the hadron, but only on the momentum coordinates of the partons *relative* to the hadron momentum. In other words, the centre of mass motion can be separated from the relative motion of the partons [11]. The arguments of the LCWF, namely $x_i \equiv p_i^+/P^+$ and the transverse momenta $\mathbf{p}_{\perp i}$, can most easily be identified in reference frames where the hadron has zero transverse momentum. Such frames are called “hadron-frames” and again a collective notation is used

$$r_i = (x_i, \mathbf{p}_{\perp i}) \quad (2.25)$$

and $\Psi_{N, \beta}^\lambda(r) = \Psi_{N, \beta}^\lambda(r_1, \dots, r_N)$ for the arguments of the LCWFs.² An N -parton state is defined as

$$|N, \beta; p_1, \dots, p_N\rangle = \frac{1}{\sqrt{f_{N, \beta}}} \prod_i \frac{b_{q_i}^\dagger(w_i)}{\sqrt{x_i}} \prod_j \frac{d_{q_j}^\dagger(w_j)}{\sqrt{x_j}} \prod_l \frac{a^\dagger(w_l)}{\sqrt{x_l}} |0\rangle. \quad (2.26)$$

The hadron states are normalised as

$$\langle H; P', \lambda' | H; P, \lambda \rangle = 16\pi^3 P^+ \delta(P'^+ - P^+) \delta^{(2)}(\mathbf{P}'_\perp - \mathbf{P}_\perp) \delta_{\lambda'\lambda}, \quad (2.27)$$

with

$$\sum_{N, \beta} \int [dx]_N [d^2 \mathbf{p}_\perp]_N |\Psi_{N, \beta}^\lambda(r)|^2 = 1. \quad (2.28)$$

The integration measures in Eqs. (2.24) and (2.28) are defined by

$$[dx]_N \equiv \prod_{i=1}^N dx_i \delta\left(1 - \sum_{i=1}^N x_i\right), \quad (2.29)$$

$$[d^2 \mathbf{p}_\perp]_N \equiv \frac{1}{(16\pi^3)^{N-1}} \prod_{i=1}^N d^2 \mathbf{p}_{\perp i} \delta^{(2)}\left(\sum_{i=1}^N \mathbf{p}_{\perp i} - \mathbf{P}_\perp\right). \quad (2.30)$$

Note that the parton states (2.26) do not refer to a specific hadron, rather they are characterised by a set β of flavour, helicity and colour quantum numbers. Their coupling to a colour singlet hadron with definite quantum numbers such as isospin is incorporated in the LCWFs $\Psi_{N, \beta}^\lambda(r)$. Many of them are zero, and several of the non-zero ones are related to each other. The three-quark (valence) Fock state of the nucleon, for instance, has only one independent LCWF for all configurations where the quark helicities add up to the helicity of the nucleon [13]. For higher Fock states there are in general several independent LCWFs.

²This notation resembles the definition of the w in (2.19), but refers now to the *relative* momentum coordinates.

parton density
operator $\bar{\psi} \gamma^+ \psi$

With the above outlined concepts and notions at hand it is instructive to take a closer look at the bilocal quark field operator $\bar{\psi}(z_1) \gamma^+ \psi(z_2)$ which occurs in the definitions of the unpolarised leading-order quark PDFs and GPDs, and – in its localised version with $z_1 = z_2$ – in electromagnetic form factors.

From the identities

$$\begin{aligned}\gamma^0 \gamma^+ &= \frac{1}{\sqrt{2}} (\gamma^0 \gamma^0 + \gamma^0 \gamma^3) = \frac{1}{\sqrt{2}} (1 + \gamma^0 \gamma^3) \\ \gamma^3 \gamma^+ &= \frac{1}{\sqrt{2}} (\gamma^3 \gamma^0 + \gamma^3 \gamma^3) = \frac{1}{\sqrt{2}} (\gamma^3 \gamma^0 - 1)\end{aligned}\quad (2.31)$$

one readily obtains by summing

$$\begin{aligned}\gamma^- \gamma^+ &= \frac{1}{\sqrt{2}} (\gamma^0 \gamma^+ - \gamma^3 \gamma^+) = \frac{1}{\sqrt{2}} (2 + \gamma^0 \gamma^3 - \gamma^3 \gamma^0) \\ &= 1 + \gamma^0 \gamma^3 = \gamma^0 \gamma^0 + \gamma^0 \gamma^3 = \sqrt{2} \gamma^0 \gamma^+\end{aligned}\quad (2.32)$$

or

$$\gamma^0 \gamma^+ = \sqrt{2} \mathcal{P}_+ = \sqrt{2} \mathcal{P}_+ \mathcal{P}_+ \quad (2.33)$$

and the bilocal quark field operator under consideration becomes

$$\bar{\psi}(z_1) \gamma^+ \psi(z_2) = \psi^\dagger(z_1) \gamma^0 \gamma^+ \psi(z_2) = \sqrt{2} (\mathcal{P}_+ \psi)^\dagger(z_1) (\mathcal{P}_+ \psi)(z_2) \quad (2.34)$$

since $(\mathcal{P}_+)^\dagger = \mathcal{P}_+$. With the help of the Fourier expansion in momentum space for the good components of the quark fields $\mathcal{P}_+ \psi = \phi$ in Eq. (2.17) the density operator can be cast in the form

$$\begin{aligned}\frac{1}{\sqrt{2}} \bar{\psi}(z_1) \gamma^+ \psi(z_2) &= \phi^\dagger(z_1) \phi(z_2) \\ &= 2 \int \frac{dp'^+ d^2 \mathbf{p}'_\perp}{p'^+ 16\pi^3} \Theta(p'^+) \int \frac{dp^+ d^2 \mathbf{p}_\perp}{p^+ 16\pi^3} \Theta(p^+) \sum_{\mu, \mu'} \\ &\quad \times \left\{ \exp\left(+i p'^+ z_1^- - i \mathbf{p}'_\perp \cdot \mathbf{z}_{1\perp} - i p'^+ z_2^- + i \mathbf{p}'_\perp \cdot \mathbf{z}_{2\perp}\right) \right. \\ &\quad \times b^\dagger(w') b(w) u_+^\dagger(w') u_+(w) \\ &\quad + \exp\left(-i p^+ z_1^- + i \mathbf{p}_\perp \cdot \mathbf{z}_{1\perp} + i p^+ z_2^- - i \mathbf{p}_\perp \cdot \mathbf{z}_{2\perp}\right) \\ &\quad \times d(w') d^\dagger(w) v_+^\dagger(w') v_+(w) \\ &\quad + \exp\left(-i p^+ z_1^- + i \mathbf{p}_\perp \cdot \mathbf{z}_{1\perp} - i p^+ z_2^- + i \mathbf{p}_\perp \cdot \mathbf{z}_{2\perp}\right) \\ &\quad \times d(w') b(w) v_+^\dagger(w') u_+(w) \\ &\quad \left. + \exp\left(+i p^+ z_1^- - i \mathbf{p}_\perp \cdot \mathbf{z}_{1\perp} + i p^+ z_2^- - i \mathbf{p}_\perp \cdot \mathbf{z}_{2\perp}\right) \right. \\ &\quad \left. \times b^\dagger(w') d^\dagger(w) u_+^\dagger(w') v_+(w) \right\},\end{aligned}\quad (2.35)$$

from which the probabilistic interpretation – in terms of only “good” LC components – becomes manifest: The operators $b^\dagger(w') b(w)$ and $d^\dagger(w') d(w)$ count the number of quarks and antiquarks, respectively, whereas $d(w') b(w)$ and $b^\dagger(w') d^\dagger(w)$ annihilate/create a quark-/antiquark pair.

The chiral structure of the operator can easily be included in our considerations by defining chiral projectors

$$\mathcal{P}_{R/L} = \frac{1}{2} (\mathbb{1} + \gamma_5) \quad (2.36)$$

which commute with the projectors on “good” and “bad” components such that

$$\bar{\psi}(z_1) \gamma^+ \psi(z_2) = \sqrt{2} \left(\phi_R^\dagger(z_1) \phi_R(z_2) + \phi_L^\dagger(z_1) \phi_L(z_2) \right) . \quad (2.37)$$

where I have used the notation

$$\phi_{R/L} \equiv \mathcal{P}_{R/L} \phi = \mathcal{P}_{R/L} \mathcal{P}_+ \psi . \quad (2.38)$$

The density operator thus counts the sum of right- and lefthanded “good” quark field quanta.

The above example can be generalised for a bilocal quark field operator with an arbitrary 4×4 matrix A , such as $\bar{\psi}(z_1) A \psi(z_2)$. In the chiral representation (Weyl representation) defined by

general bilocal
quark field
operator

$$\gamma^0 = \begin{pmatrix} 0 & \mathbb{1} \\ \mathbb{1} & 0 \end{pmatrix}; \quad \vec{\gamma} = \begin{pmatrix} 0 & -\vec{\sigma} \\ \vec{\sigma} & 0 \end{pmatrix}; \quad \gamma_5 = \begin{pmatrix} \mathbb{1} & 0 \\ 0 & -\mathbb{1} \end{pmatrix} \quad (2.39)$$

where σ are the usual Pauli matrices, the projectors to “good” and “bad” LC components take the explicit form

$$\mathcal{P}_+ = \begin{pmatrix} 1 & 0 & 0 & 0 \\ 0 & 0 & 0 & 0 \\ 0 & 0 & 0 & 0 \\ 0 & 0 & 0 & 1 \end{pmatrix}, \quad \mathcal{P}_- = \begin{pmatrix} 0 & 0 & 0 & 0 \\ 0 & 1 & 0 & 0 \\ 0 & 0 & 1 & 0 \\ 0 & 0 & 0 & 0 \end{pmatrix}, \quad (2.40)$$

such that

$$\mathcal{P}_+ \begin{pmatrix} a \\ b \\ c \\ d \end{pmatrix} = \begin{pmatrix} a \\ 0 \\ 0 \\ d \end{pmatrix}, \quad \mathcal{P}_- \begin{pmatrix} a \\ b \\ c \\ d \end{pmatrix} = \begin{pmatrix} 0 \\ b \\ c \\ 0 \end{pmatrix}, \quad (2.41)$$

i.e., the 1st and 4th component of a four-spinor in Weyl representation represent the “good” components of the fields, whereas the 2nd and 3rd represent the “bad” ones. The chiral projectors in Weyl representation have the simple form

$$\mathcal{P}_R = \begin{pmatrix} 1 & 0 & 0 & 0 \\ 0 & 1 & 0 & 0 \\ 0 & 0 & 0 & 0 \\ 0 & 0 & 0 & 0 \end{pmatrix}, \quad \mathcal{P}_L = \begin{pmatrix} 0 & 0 & 0 & 0 \\ 0 & 0 & 0 & 0 \\ 0 & 0 & 1 & 0 \\ 0 & 0 & 0 & 1 \end{pmatrix}, \quad (2.42)$$

such that

$$\mathcal{P}_R \begin{pmatrix} a \\ b \\ c \\ d \end{pmatrix} = (a, b, 0, 0), \quad \mathcal{P}_L \begin{pmatrix} a \\ b \\ c \\ d \end{pmatrix} = (0, 0, c, d) . \quad (2.43)$$

In other words the upper two components of a four-spinor represent the right-handed part of the field, whereas the lower components represent the left-handed one. Combining Eqs. (2.41) and (2.43) a four-spinor in Weyl representation can be written generically

$$\psi = \begin{pmatrix} \phi_R \\ \chi_R \\ \chi_L \\ \phi_L \end{pmatrix}, \quad (2.44)$$

and a matrix has the general structure

$$\begin{pmatrix} \phi_R^\dagger \phi_R & \chi_R^\dagger \phi_R & \chi_L^\dagger \phi_R & \phi_L^\dagger \phi_R \\ \phi_R^\dagger \chi_R & \chi_R^\dagger \chi_R & \chi_L^\dagger \chi_R & \phi_L^\dagger \chi_R \\ \phi_R^\dagger \chi_L & \chi_R^\dagger \chi_L & \chi_L^\dagger \chi_L & \phi_L^\dagger \chi_L \\ \phi_R^\dagger \phi_L & \chi_R^\dagger \phi_L & \chi_L^\dagger \phi_L & \phi_L^\dagger \phi_L \end{pmatrix} \quad (2.45)$$

where the generic notation indicates that a matrix element labelled for instance by $\phi_L^\dagger \chi_R$ relates a left-handed “good” component of a quark field with a right-handed “bad” one, and so on.

Equipped with these tools one can read off the properties of the operator combination $\bar{\psi}(z_1) A \psi(z_1) = \psi^\dagger(z_1) (\gamma^0 A) \psi(z_2)$ from its explicit form in Weyl representation. For instance, with $A = \gamma^+$ a comparison of

$$\gamma^0 \gamma^+ = \sqrt{2} \begin{pmatrix} 1 & 0 & 0 & 0 \\ 0 & 0 & 0 & 0 \\ 0 & 0 & 0 & 0 \\ 0 & 0 & 0 & 1 \end{pmatrix} \quad (2.46)$$

with (2.45) results in rediscovering the observation that $\bar{\psi}(z_1) \gamma^+ \psi(z_2)$ counts the sum of right- and left-handed “good” quarks components, i.e. Eq.(2.37). And with $A = \gamma^+ \gamma_5$ a comparison of

$$\gamma^0 \gamma^+ \gamma_5 = \sqrt{2} \begin{pmatrix} 1 & 0 & 0 & 0 \\ 0 & 0 & 0 & 0 \\ 0 & 0 & 0 & 0 \\ 0 & 0 & 0 & -1 \end{pmatrix} \quad (2.47)$$

with (2.45) reveals that $\bar{\psi}(z_1) \gamma^+ \gamma_5 \psi(z_2)$ counts the difference of “good”, right-handed and “good”, left-handed quarks

$$\bar{\psi}(z_1) \gamma^+ \gamma_5 \psi(z_2) = \sqrt{2} \left(\phi_R^\dagger(z_1) \phi_R(z_2) - \phi_L^\dagger(z_1) \phi_L(z_2) \right). \quad (2.48)$$

In Appendix A I list an appropriate basis of 4×4 matrices M_i ($i=1, \dots, 16$) in Weyl representation which by simple comparison with the generic pattern given in (2.45) reveals its chiral structure in terms of “good” and “bad” quark field components.

3

Transverse momenta in (semi-)inclusive reactions

3.1 the concept of PDF and PFF in (semi-)inclusive reactions

The deep inelastic scattering of leptons on nucleons (DIS) has led to the discovery of partons, and is certainly the archetype of all hard reactions involving the concept of parton distribution functions.

PDFs in DIS

When a high-energetic lepton beam is scattered on a nucleon target, or alternatively a lepton and a nucleon beam are brought to collision, the electroweak interaction is mediated by the exchange of a highly virtual gauge boson: a photon, Z - or W -boson. Gravitation is too weak to be of any importance in this context, and leptons are not subject to strong interactions.

The kinematics of the reaction is characterised by the Lorentz invariants which

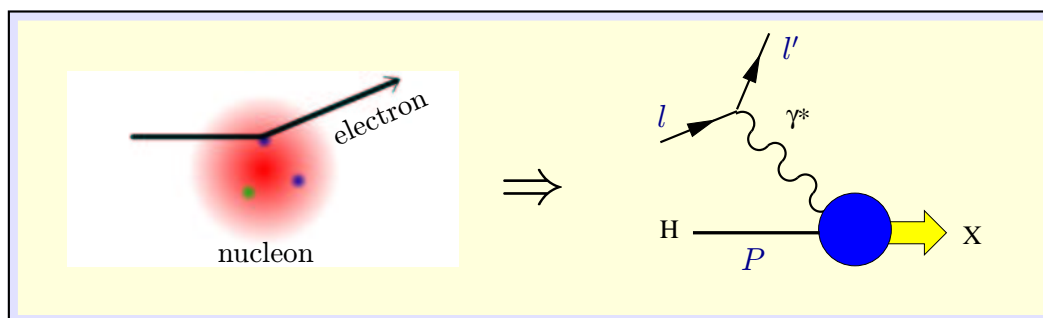


Figure 3.1: Representation of (deep inelastic) lepton-nucleon scattering in a diagrammatic language.

can be built from the momenta of the lepton before and after the scattering, l and l' , and from the momentum of the nucleon P . Conventionally one chooses as independent invariants the square of the centre of mass energy

$$s = (P + l)^2, \quad (3.1)$$

the virtuality of the gauge boson

$$q^2 = (l' - l)^2 \equiv -Q^2 \quad (3.2)$$

and

$$\nu = \frac{P \cdot q}{M}, \quad (3.3)$$

where M is the nucleon mass. In the rest frame of the nucleon ν has the interpretation of the transferred energy. The remaining possible invariants to be built from l , l' and P are fixed by the on-shell conditions $P^2 = M^2$, and $l^2 = l'^2 = m_\ell^2$, with m_ℓ the lepton mass.

Two crucial steps have led to the discovery of partons and the formulation of the parton model:

Bjorken scaling

elastic scattering
on point-like
particles

1. The observation of a phenomenon called *Bjorken scaling* and its interpretation: At very large Q^2 there is a relation between the energy and the momentum transfer innate to *elastic scattering processes* which leads to a characteristic behaviour of structure functions defined from the differential cross section as

$$\frac{d\sigma}{d\Omega dE'} = \frac{4\alpha_{em}E'^2}{Q^4} \left\{ 2 \sin^2 \left(\frac{\Theta}{2} \right) W_1(\nu, Q^2) + \cos^2 \left(\frac{\Theta}{2} \right) W_2(\nu, Q^2) \right\}, \quad (3.4)$$

where E' is the energy and Ω the solid angle of the outgoing lepton, and Θ the scattering angle in the nucleon rest frame.

In the limit $Q^2 \rightarrow \infty$ for a fixed ratio of $Q^2/P \cdot q$, the so-called Bjorken limit, the structure functions F_1 and F_2 , defined from W_1 and W_2 , depend to a good approximation only on a certain combination of Q^2 and ν

$$x_{Bj} = \frac{Q^2}{2P \cdot q} = \frac{Q^2}{2M\nu}. \quad (3.5)$$

and not on both invariants independently

$$\begin{aligned} 2MW_1(\nu, Q^2) &= F_1(\nu, Q^2) \rightarrow F_1(x_{Bj}) \\ \nu W_2(\nu, Q^2) &= F_2(\nu, Q^2) \rightarrow F_2(x_{Bj}). \end{aligned} \quad (3.6)$$

The fact that the dimensionless structure functions F_1 and F_2 depend on the dimensionless combination of invariants indicates that the elastic scattering takes place on *point-like particles* – otherwise dimensionful form factors would show up.

2. A natural interpretation of the phenomenon arises in *Feynmans parton model* the basic idea of which can be summarised by two simple rules:

Feynmans parton model

- (a) a rapidly moving hadron is treated as a *jet of quasi-free partons* moving almost collinear, and
- (b) the cross section of the hadronic process is calculated as a *convolution of a partonic cross section and parton distribution functions (PDFs)* summed incoherently over all partons.

jet of quasi-free partons

The parton model interpretation of the dominant contribution to deep inelastic lepton nucleon scattering is depicted in Fig. 1.3; its contribution to the cross section of DIS is given by the famous ‘handbag’ diagram shown in Fig. 3.2, where also the factorisation in *soft* and *hard* parts is indicated.

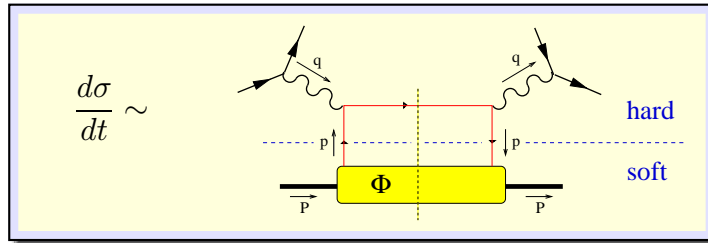


Figure 3.2: The ‘handbag’ diagram leading to the dominant contribution to the cross section of DIS.

This intuitive simple picture of the ‘naive’ *parton model* turned out to be very successful, and in fact, to have a more rigorous basis in the underlying quantum field theory, QCD. In systematic expansions of observables in powers of the strong coupling (α_s) and in powers of $1/Q$ in the context of QCD, the parton model is known to reproduce exactly the leading order terms. This holds true in both approaches, the operator product expansion, as well as in the diagrammatic approaches.

The non-perturbative information is encoded as quark-quark correlation function which in a light-cone gauge takes the form [2, 3, 4, 5, 6]

quark-quark correlation function

$$\Phi_{ij}(p, P, S) = \int \frac{d^4z}{(2\pi)^4} e^{ip \cdot z} \langle P, S | \bar{\psi}_j(0) \psi_i(z) | P, S \rangle \quad (3.7)$$

depending on the quark momentum p , the target nucleon momentum P , and possibly on the spin of the nucleon, i.e. the spin vector S . The link operator normally needed to render the definition gauge-invariant does not appear because we choose the gauge $A^+ = 0$, which together with an integration path along the minus direction reduces the link operator to unity. At higher orders in the expansions in powers of $1/Q$ more complicated non-perturbative objects are involved, like for instance hadronic matrix elements of gluon fields, or matrix elements of one gluon and two quark fields, etc.

In the totally inclusive DIS process the quark-quark correlation function (3.7) occurs traced with certain Dirac matrices, and integrated over three of the four

quark momentum components

$$\Phi^{[\Gamma]}(x) = \frac{1}{2} \int dp^- d^2 \mathbf{p}_T \text{Tr}(\Phi \Gamma) \Big|_{p^+ = xP^+}, \quad (3.8)$$

where Γ is a 4×4 Dirac matrix. For instance it can be an element of the basis (A.5), which is particularly convenient, since its use leads to an automatic ordering in powers of $1/Q$ as will be argued in the next subsections. The integrations on the RHS of Eq.(3.8) restricts the non-locality of the quantity $\Phi^{[\Gamma]}(x)$ to a light like separation, hence it depends only on the light-cone momentum fraction $x = p^+/P^+$.

The spin-independent quark distribution function occurring at leading order for instance is defined by

$$\Phi^{[\gamma^+]}(x) = f_1(x), \quad (3.9)$$

and the two rules of the parton model cited above together with the definition (3.4) establish a direct relation between the observable structure functions and theoretical constructed PDF

$$2F_1(x_{Bj}) = \frac{F_2(x_{Bj})}{x_{Bj}} = \sum_a e_a^2 f_1^a(x_{Bj}), \quad (3.10)$$

where the index a runs over all types of quarks. The PDF $f_1(x)$ – often denoted $q(x)$ where q may take any flavour value u, d, s, \dots – has a simple probabilistic interpretation within the parton model.

- The function $f^a(x)$, or $q(x)$, gives the probability to find a quark of flavour a in the parent hadron carrying the light cone momentum fraction x .

Ultimately, this interpretation is justified in the context of Quantumchromodynamics in its light cone quantised form, i.e. the notion of *quarks* is to be replaced by *quanta of the good components of the quark field*.

PDFs in
electron/positron
annihilation

Whenever hadrons in the final state are observed in a hard (semi-)inclusive process, another bit of non-perturbative information is needed to describe the reaction: the hadronisation process of a parton. The most simple process involving hadronisation is the annihilation of an electron/positron pair into hadrons, one of which is observed, $e^+e^- \rightarrow h X$ (see Fig. 1.5).

The dominant contribution to the differential cross section of this process involves the annihilation of electron and positron into a highly virtual photon (or Z boson), and the creation of a quark/antiquark pair (see Fig. 3.3). The hadronisation of one member of the pair, say the final state hadron is observed in the quark jet, is of non-perturbative nature and described by another quark-quark correlation function defined as Fourier transform of a hadronic matrix element of a bilocal quark field operator

quark-quark
correlation
function

$$\Delta_{ij}(k, P_h, S_h) = \sum_{X'} \frac{1}{(2\pi)^4} \int d^4 z e^{ik \cdot z} \times \langle 0 | \psi_i(z) | P_h, S_h; X' \rangle \langle P_h, S_h; X' | \bar{\psi}_j(0) | 0 \rangle \quad (3.11)$$

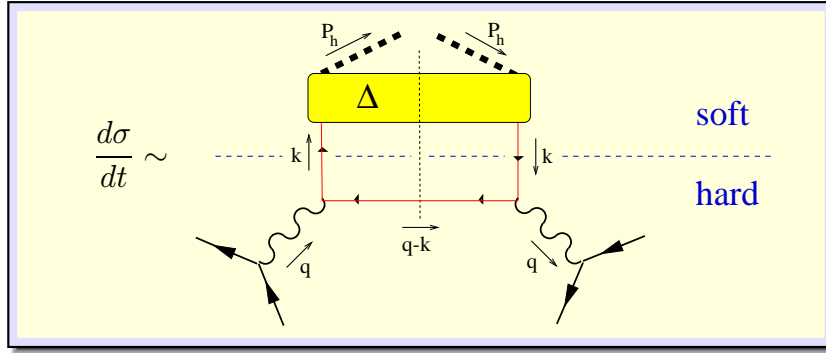


Figure 3.3: The dominant contribution to the differential cross section of electron/positron annihilation with one observed hadron in the final state $e^+e^- \rightarrow hX$.

depending on the momentum of the fragmenting quark k , the momentum of the observed hadron P_h , and possibly its spin, e.g. the spin vector S_h for a spin 1/2 hadron as assumed in the definition above. Here, in this definition X' denotes the rest of the quark initiated jet modulo the one observed hadron. Again the link operator normally needed to render the definition gauge-invariant is not shown adopting a light cone gauge and a suitable choice of the integration path.

For convenience, parton fragmentation functions are defined from Δ by tracing the quark-quark correlation function with certain Dirac matrices, and integrating over three of the four momentum components of the fragmenting quark

$$\Delta^{[\Gamma]}(z) \equiv \frac{1}{4z} \int dk^+ d^2\mathbf{k}_T \text{Tr} [\Delta\Gamma] \Big|_{k^- = P_h^-/z}, \quad (3.12)$$

since these are the quantities encountered in the description of the process $e^+e^- \rightarrow hX$.¹ The non-locality in the expression for $\Delta^{[\Gamma]}(z)$ is again restricted to a light-like separation. The spin-independent PDF for instance is given as

$$\Delta^{[\gamma^-]}(z) = D_1(z) \quad (3.13)$$

which gives the probability to find a hadron which carries the light cone momentum fraction $z = P_h^-/k^-$.

PDFs and PFFs occur together in the description of semi-inclusive hard processes which involve hadrons in the initial and final state, like for instance the one-hadron inclusive lepton nucleon scattering, $\ell H \rightarrow \ell' hX$ (see Fig. 3.4). Here the differential cross section is calculated as a convolution of:

PDFs and PFFs
together in
semi-inclusive
processes

¹ Note that throughout this work whenever possible I assume initial state hadrons to move from left to right with a large plus momentum component, and hadrons in the final state moving from right to left with a large minus momentum component. This assumption is behind the interchange of plus and minus components in the definitions of PDFs and PFFs, and corresponds to a convenient choice of frame for the description of one-hadron semi-inclusive DIS, but has no fundamental meaning beyond this arbitrary choice of reference.

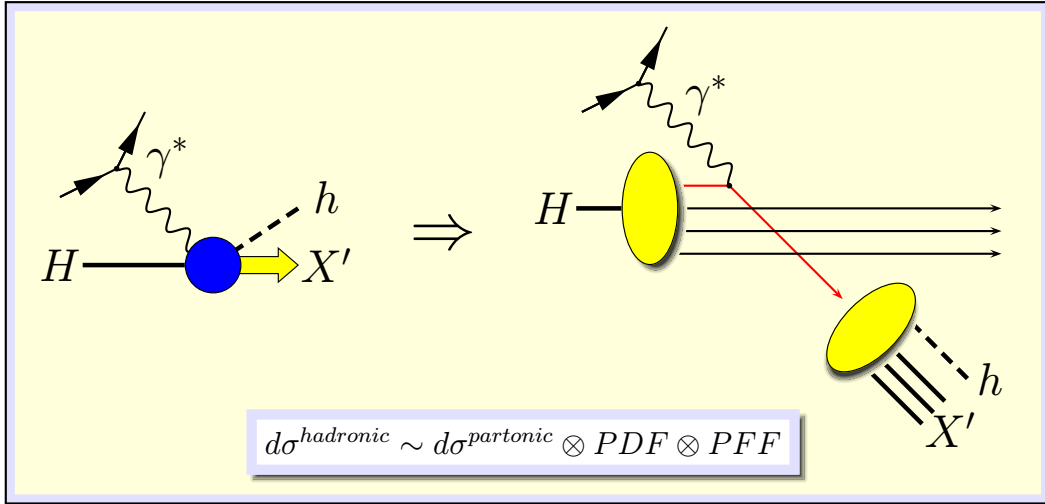


Figure 3.4: Semi-inclusive lepton-nucleon scattering interpreted in the parton model.

- a PDF for the probability to find a quark in the target nucleon,
- a partonic cross section describing the scattering of the photon on the struck quark,
- and the PFF for the hadronisation of the quark forming the observed hadron and all the unobserved rest of the current jet.

The diagram for the leading contribution to the differential cross section is an extension of the ‘handbag’ diagram as shown in Fig. 3.5.

sensitivity to quark
transverse
momenta

For the example of this process we can discuss a peculiarity of all processes which involve a larger number of external momenta. For the description of totally inclusive DIS one can always choose a frame of reference where the target momentum P and the photon momentum q are collinear. If one hadron in the final state is measured, in general there is no frame where all three relevant four-vectors P , q , and P_h are collinear; one of them will unavoidably have transverse momentum components. Observables which are unintegrated in this external

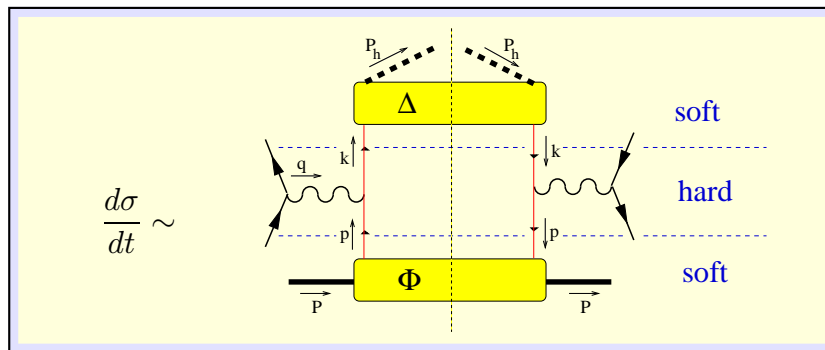


Figure 3.5: The diagram leading to the dominant contribution to the cross section of SIDIS.

transverse momentum component will have a sensitivity to the transverse momentum components which quarks can have relative to their parents momenta. Let us exemplify the situation by assuming a frame, where the momenta P and P_h are collinear, but the photon momentum q has a transverse component. The formula for the differential cross section $d\sigma/d\dots d^2\mathbf{q}_T$ will involve a delta-function $\delta^2(\mathbf{p}_T + \mathbf{q}_T - \mathbf{k}_T)$ induced by momentum conservation at the photon-quark vertex as illustrated in Fig. 3.6.

This way one can access transverse momentum dependent PDFs and PFFs related to the integrated ones for instance like

$$\int d^2\mathbf{p}_T f_1(x, \mathbf{p}_T^2) = f_1(x), \quad \int d^2\mathbf{k}'_T D_1(z, \mathbf{k}'_T{}^2) = D_1(z)$$

with $\mathbf{k}'_T = z\mathbf{k}_T$ (see Fig.3.7).

More examples for observables which are indirectly sensitive to intrinsic transverse parton momenta are differential cross sections of two hadron inclusive electron-positron annihilation, the Drell-Yan process, or (semi-)inclusive hadron-hadron scattering. Generally, for any hard process involving two or more soft hadronic matrix elements, there are observables which reveal sensitivity to partonic transverse momentum effects. Those observables at leading order in α_s contain the non-integrated PDFs and PFFs.

There is a classification scheme based on *LC quantisation* and the notions of *effective twist* and *chirality* which allows to give a systematic and rather simple overview for all (spin-dependent) PDFs and PFFs occurring at leading and next to leading order in semi-inclusive processes. The next subsections will be devoted to this classification scheme.

3.2 transverse momentum dependent PDFs and PFFs

3.2.1 PDFs of a spin-1/2 hadron

The discussion of quark distribution functions of a spin-1/2 hadron, say a nucleon target in DIS, may serve to exemplify a general method for the classification of independent functions derived from the correlation functions. This method lends itself to an easy generalisation to other situations, thus it provides classification schemes also for gluon distribution functions, for distribution functions of a spin-0 or spin-1 hadron, for one- or multiple-hadron fragmentation functions, etc.

In a first step formal properties of the quark-quark correlation function Eq.(3.7) can be considered which lead to three constraints arising from the hermiticity properties of the fields, and invariance under parity and time-reversal operations

$$\Phi^\dagger(k, P, S) = \gamma_0 \Phi(k, P, S) \gamma_0 \quad [\text{Hermiticity}] \quad (3.14)$$

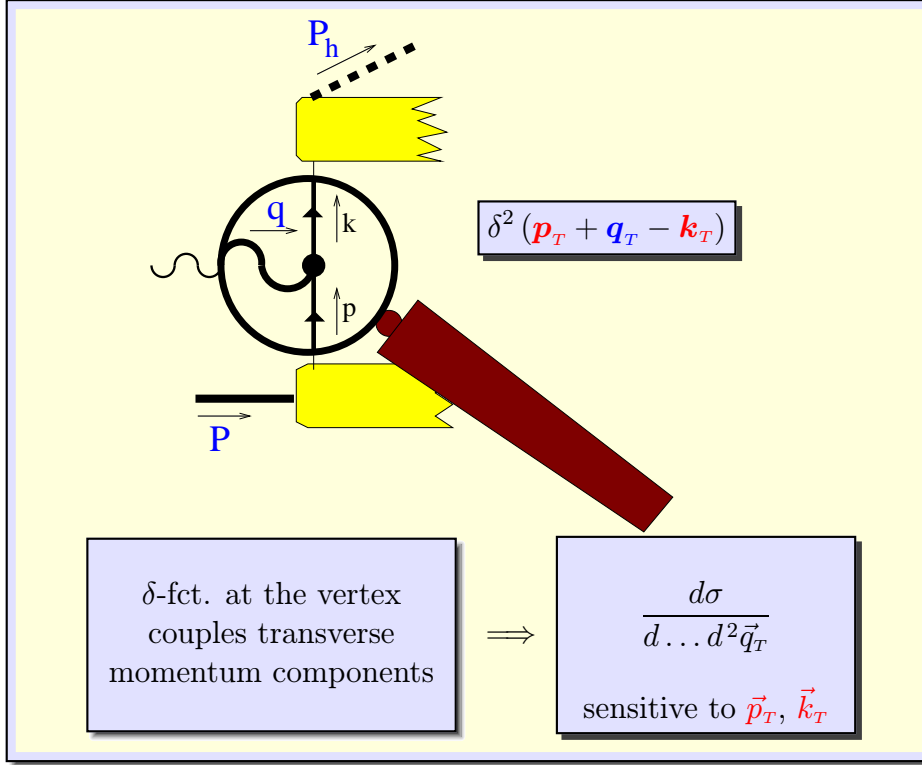


Figure 3.6: Illustration how momentum conservation induces quark transverse momentum sensitivity in observables unintegrated in external transverse momentum components.

$$\Phi(k, P, S) = \gamma_0 \Phi(\bar{k}, \bar{P}, -\bar{S}) \gamma_0 \quad [\text{Parity}] \quad (3.15)$$

$$\Phi^*(k, P, S) = (-i\gamma_5 C) \Phi(\bar{k}, \bar{P}, \bar{S}) (-i\gamma_5 C) \quad [\text{Time reversal}] \quad (3.16)$$

with the shorthand notation $\bar{P} \equiv (P^0, -P^i)$, etc. for four-vectors with reversed sign in their spatial components. From the definition (3.7) it is obvious that Φ_{ij} is a 4×4 matrix in Dirac space, and depends on the four-vectors p , P , and S only. The most general expression for Φ consistent with the constraints from

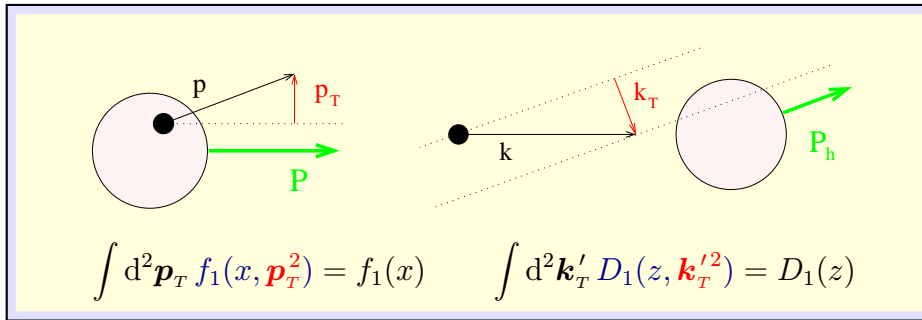


Figure 3.7: Illustration of transverse momentum components quarks can have relative to their parent hadrons momenta, and transverse momentum dependent PDFs and PFFs.

hermiticity and parity is [17, 18]:

$$\begin{aligned}
 \Phi(p, P, S) = & \\
 & M A_1 + A_2 \not{P} + A_3 \not{p} + (A_4/M) \sigma^{\mu\nu} P_\mu p_\nu \\
 & + i A_5 (p \cdot S) \gamma_5 + M A_6 \not{S} \gamma_5 + (A_7/M) (p \cdot S) \not{P} \gamma_5 + (A_8/M) (p \cdot S) \not{p} \gamma_5 \\
 & + i A_9 \sigma^{\mu\nu} \gamma_5 S_\mu P_\nu + i A_{10} \sigma^{\mu\nu} \gamma_5 S_\mu p_\nu + i (A_{11}/M^2) (p \cdot S) \sigma^{\mu\nu} \gamma_5 p_\mu P_\nu \\
 & + (A_{12}/M) \epsilon_{\mu\nu\rho\sigma} \gamma^\mu P^\nu p^\rho S^\sigma, \tag{3.17}
 \end{aligned}$$

where the amplitudes $A_i = A_i(\sigma, \tau)$ depend on the invariants $\sigma \equiv 2p \cdot P$ and $\tau \equiv p^2$. Hermiticity requires all amplitudes $A_i(\sigma, \tau)$ to be real. Note that the dependence on the spin-vector S is at most linear [15], and it has been made explicit. The corresponding expression for spin-0 hadrons (or the for description of hadrons with averaged polarisation) is obtained by keeping the terms with amplitudes $A_1, A_2, A_3,$ and $A_4,$ and discarding the spin-dependent ones.

The constraint from time-reversal invariance would require the amplitudes $A_4, A_5,$ and A_{12} to be purely imaginary and hence to vanish, since this is in contradiction with the requirements from hermiticity. But there are several situations conceivable where this constraint is not applicable. So for the moment we keep the terms in the ansatz and will comment in detail on the issue in the next subsections. Those terms are conventionally, albeit quite misleading, called (*naive*) *time-reversal odd*.

For a further discussion it is convenient to chose specific frames, where the hadron momentum P has no transverse components, i.e. $P = [P^+, P^-, \mathbf{0}_T]$. I will call those systems “hadron frames” and refer to transverse parton momenta in appropriate hadron frames as “intrinsic” transverse momenta. The on-shell condition for a physical hadron implies a further relation between the LC components $P^- = M^2/(2P^+)$, where M is the mass of the hadron. One component, say P^+ , can be freely chosen to fix the system within the class of hadron frames. This freedom correspond to longitudinal boosts along the z -axis.

Up to now, all considerations on the quark-quark correlation functions were completely process independent. But actually we are interested in those objects only in the context of hard processes. The hard momentum scale of such a process will impose a dominant light-like direction along which the correlation function is probed. By trivial boosts one can change the frames for the description of any hard process such that the correlation function under consideration are probed along the same light-like direction, and results from different processes can be related to each other. For instance we can chose to have Φ being probed always along the minus direction and Δ along the plus direction (compare also footnote 1). In a process involving two correlation functions for initial hadrons we chose a frame that one Φ is probed along the plus direction, the other along the minus direction. The relation between the two expressions is straightforward, and the PDFs involved are identical, only their accompanying tensors differ by trivial exchanges of LC components. The situation is analogous for processes involving for instance two hadrons in the final state. In this sense, the aforementioned universality of PDFs and PFFs is to be understood.

parametrisation of
momenta

All this will become clear from an explicit example. For instance, in deep-inelastic lepton-nucleon scattering, a standard choice is to define two light-like unit vectors n_{\pm} (satisfying $n_+^2 = n_-^2 = 0$ and $n_+ \cdot n_- = 1$) from the photon momentum q and the hadron momentum P and parameterise

$$P = P^+ n_+ + \frac{M^2}{2P^+} n_- = \frac{Q}{x_{Bj}\sqrt{2}} n_+ + \frac{M^2 x_{Bj}}{Q\sqrt{2}} n_- \quad (3.18)$$

and

$$q = \frac{Q}{\sqrt{2}} n_+ - \frac{Q}{\sqrt{2}} n_- \quad (3.19)$$

in agreement with the definition (3.5) of x_{Bj} . With this choice the component P^+ scales in the Bjorken limit like Q and P^- like $1/Q$. The correlation function Φ will be probed along a light-like distance z in *minus* direction. The spin vector S and the quark momentum p are also expanded in the lightlike vectors and transverse components in a Sudakov decomposition:

$$p = \frac{xQ}{x_{Bj}\sqrt{2}} n_+ + \frac{x_{Bj}(p^2 + \mathbf{p}_T^2)}{xQ\sqrt{2}} n_- + p_T, \quad (3.20)$$

$$S = \frac{\lambda Q}{Mx_{Bj}\sqrt{2}} n_+ - \frac{\lambda Mx_{Bj}}{Q\sqrt{2}} n_- + S_T, \quad (3.21)$$

where $p_T^\mu = [0, 0, \mathbf{p}_T]$ (and similar S_T) is a four-vector with transverse components only. Thus x represents the fraction of the momentum in the plus direction carried by the quark inside the hadron. The spin vector satisfies $P \cdot S = 0$ and for a pure state $-S^2 = \lambda^2 + \mathbf{S}_T^2 = 1$. For later use the following projectors can be defined in the transverse space

$$g_T^{\mu\nu} = g^{\mu\nu} - n_+^{\{\mu} n_-^{\nu\}}, \quad (3.22)$$

$$\epsilon_T^{\mu\nu} = \epsilon^{-+\mu\nu}. \quad (3.23)$$

Considering transverse momentum integrated observables in a hard scattering process up to order $1/Q$, the components of p along n_- and in transverse direction are irrelevant, and one encounters the quantities

$$\Phi^{[\Gamma]}(x) = \frac{1}{2} \int dp^- d^2 \mathbf{p}_T \text{Tr}(\Phi \Gamma) \Big|_{p^+ = xP^+} = \int [d\sigma d\tau \theta(\cdot)] \frac{\text{Tr}(\Phi \Gamma)}{4P^+}, \quad (3.24)$$

where the shorthand notation

$$[d\sigma d\tau \theta(\cdot)] = \pi d\sigma d\tau \theta(x\sigma - x^2 M^2 - \tau) \quad (3.25)$$

was used. The projections of Φ on different Dirac structures define PDFs. They are related to integrals over linear combinations of the amplitudes.

In the context of LC quantisation – as sketched in chapter 2 – the Dirac projections determine the spin structure on the quark side. The occurrence of the light cone helicity λ , or a transverse component of the spin vector S_T^i signals the polarisation state of the hadron. A complete list of independent 4×4 Dirac matrices together with their explicit form in the chiral (Weyl) representation is




	$\begin{aligned} \bar{\psi} \gamma^+ \psi &= \sqrt{2} \psi_+^\dagger (P_R P_R + P_L P_L) \psi_+ \\ &= \bar{R}R + \bar{L}L \end{aligned}$
	$\begin{aligned} \bar{\psi} \gamma^+ \gamma_5 \psi &= \sqrt{2} \psi_+^\dagger (P_R P_R - P_L P_L) \psi_+ \\ &= \bar{R}R - \bar{L}L \end{aligned}$
	$\begin{aligned} \bar{\psi} i\sigma^{i+} \gamma_5 \psi &= \sqrt{2} \psi_+^\dagger (P_L \gamma^i P_R - P_R \gamma^i P_L) \psi_+ \\ &= \bar{L}R - \bar{R}L \end{aligned}$

Figure 3.8: Dirac projections determine the quark spin information encoded in PDFs. The table summarises findings from chapter 2, where also the projectors P_R and P_L are defined.

given in appendix A. The chiral quark structure of the leading PDFs obtained by projections with γ^+ , $\gamma^+\gamma_5$, and $i\sigma^{i+}\gamma_5$ is summarised in Fig. 3.8. Note that the chiral structure induced by the projections with γ^+ and $\gamma^+\gamma_5$ is $(\bar{R}R + \bar{L}L)$ and $(\bar{R}R - \bar{L}L)$, respectively. The resulting PDFs are called *chiral even*. The chiral structure induced by the projection with $i\sigma^{i+}\gamma_5$ is $(\bar{L}R - \bar{R}L)$, i.e. it evokes a change of chirality and the associated PDFs are called *chiral odd*. The diagram for the $i\sigma^{i+}\gamma_5$ projection in Fig. 3.8 instead indicates a transverse quark spin, which amounts to a change of representations of the γ -matrices from a chiral one to a transverse spin representation. We will comment on this point in some detail in a following subsection.

The projections

leading PDFs(x)

$$\begin{aligned} \Phi^{[\gamma^+]}(x) &\equiv f_1(x) \\ &= \int [d\sigma d\tau \theta(\cdot)] [A_2 + xA_3] , \end{aligned} \quad (3.26)$$

$$\begin{aligned} \Phi^{[\gamma^+\gamma_5]}(x) &\equiv \lambda g_1(x) \\ &= \lambda \int [d\sigma d\tau \theta(\cdot)] \left[-A_6 - \left(\frac{\sigma - 2xM^2}{2M^2} \right) (A_7 + xA_8) \right] , \end{aligned} \quad (3.27)$$

$$\begin{aligned} \Phi^{[i\sigma^{i+}\gamma_5]}(x) &\equiv S_T^i h_1(x) \\ &= S_T^i \int [d\sigma d\tau \theta(\cdot)] \left[-(A_9 + xA_{10}) + \frac{x\sigma - x^2M^2 + \tau}{2M^2} A_{11} \right] \end{aligned} \quad (3.28)$$

are leading in $1/Q$. For the distribution functions, this is indicated by the sub-

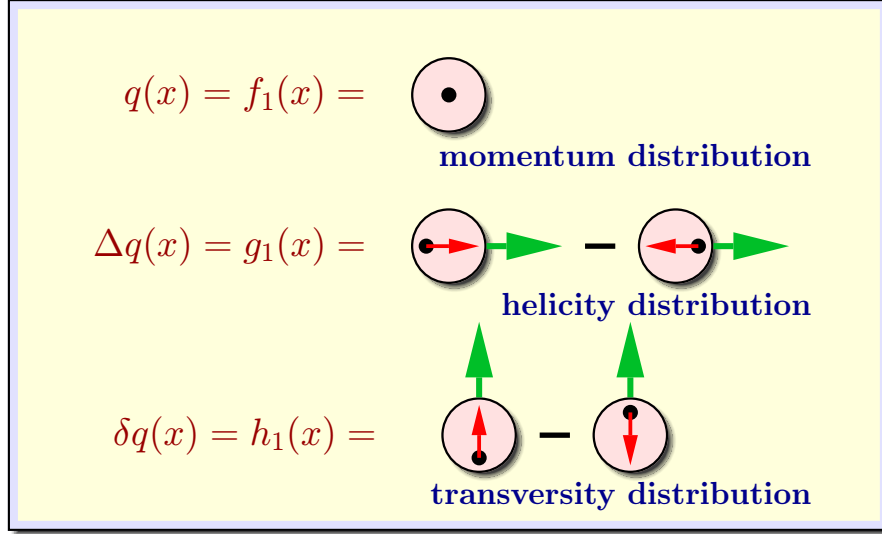


Figure 3.9: Probability interpretation of leading order integrated PDFs. The identification with the more popular names $q(x)$, $\Delta q(x)$, and $\delta q(x)$ is shown. The hadron is assumed to move from left to right, which defines the longitudinal direction. Green external arrows symbolise the hadron spin, red internal arrows the spin state of the quark.

script 1 in the names of the functions. The naming scheme adopted here [18], and extended where necessary, has the advantage of being flexible enough to encase higher order and transverse momentum dependent PDFs and PFFs. The more popular names $q(x)$, $\Delta q(x)$, and $\delta q(x) = \Delta_T q(x)$ lack this flexibility. The probability interpretation of the leading order PDFs is shown in Fig. 3.9.

subleading
PDFs(x)

The following projections occur with a pre-factor M/P^+ , which signals the subleading (or higher twist) nature of the corresponding distribution functions

$$\begin{aligned}\Phi^{[1]}(x) &\equiv \frac{M}{P^+} e(x) \\ &= \frac{M}{P^+} \int [d\sigma d\tau \theta(\cdot)] [A_1],\end{aligned}\quad (3.29)$$

$$\begin{aligned}\Phi^{[i\gamma_5]}(x) &\equiv \frac{M}{P^+} \lambda e_L(x) \\ &= \frac{M}{P^+} \lambda \int [d\sigma d\tau \theta(\cdot)] \left[- \left(\frac{\sigma - 2x M^2}{2M^2} \right) A_5 \right],\end{aligned}\quad (3.30)$$

$$\begin{aligned}\Phi^{[\gamma^i]}(x) &\equiv \frac{M}{P^+} \epsilon_T^{ij} S_{Tj} f_T(x) \\ &= \frac{M}{P^+} \epsilon_T^{ij} S_{Tj} \int [d\sigma d\tau \theta(\cdot)] \left[- \left(\frac{\sigma - 2x M^2}{2M^2} \right) A_{12} \right],\end{aligned}\quad (3.31)$$

$$\Phi^{[\gamma^i \gamma_5]}(x) \equiv \frac{M}{P^+} S_T^i g_T(x)$$

$$= \frac{M}{P^+} S_T^i \int [d\sigma d\tau \delta(\cdot)] \left[-A_6 + \frac{x\sigma - x^2 M^2 + \tau}{2M^2} A_8 \right], \quad (3.32)$$

$$\begin{aligned} \Phi^{[i\sigma^{ij}\gamma_5]}(x) &\equiv \frac{M}{P^+} \epsilon_T^{ij} h(x) \\ &= \frac{M}{P^+} \epsilon_T^{ij} \int [d\sigma d\tau \theta(\cdot)] \left[\left(\frac{\sigma - 2x M^2}{2M^2} \right) A_4 \right], \end{aligned} \quad (3.33)$$

$$\begin{aligned} \Phi^{[i\sigma^{+-}]}(x) &\equiv \frac{M}{P^+} \lambda h_L(x) \\ &= \frac{M}{P^+} \lambda \int [d\sigma d\tau \theta(\cdot)] \left[-(A_9 + x A_{10}) \right. \\ &\quad \left. - \left(\frac{\sigma - 2x M^2}{2M^2} \right) A_{10} + \left(\frac{\sigma - 2x M^2}{2M^2} \right)^2 A_{11} \right]. \end{aligned} \quad (3.34)$$

The functions $e_L(x)$, $f_T(x)$ and $h(x)$ are (naive) time reversal-odd as can be easily seen from the fact that they involve the amplitudes A_4 , A_5 and A_{12} .

3.2.2 transverse momentum dependent PDFs of a spin-1/2 hadron

As anticipated in the previous subsection there are observables for which the integration over quark transverse momenta can not be carried out. For instance, the cross section for one-hadron inclusive DIS kept differential in \mathbf{q}_T is of the general structure

PDFs(x, \mathbf{p}_T^2)

$$\begin{aligned} \frac{d\sigma}{dx dz d\cdots d^2\mathbf{q}_T} &\propto \int d^2\mathbf{p}_T d^2\mathbf{k}_T \delta^2(\mathbf{k}_T - \mathbf{p}_T + \mathbf{q}_T) \\ &\quad \times w(\mathbf{p}_T, \mathbf{k}_T) f(x, \mathbf{p}_T^2) D(z, \mathbf{k}_T^2) \end{aligned} \quad (3.35)$$

where $f(x, \mathbf{p}_T^2)$ (or $D(z, \mathbf{k}_T^2)$) generically stands for a PDF (or PFF), and $w(\mathbf{p}_T, \mathbf{k}_T)$ is a specific weight function which may depend on \mathbf{p}_T , \mathbf{k}_T and additional angular dependencies (not indicated here). On integration of the observable over $d^2\mathbf{q}_T$ the expression is deconvoluted in the transverse space and one obtains a formula involving the the usual integrated PDFs and PFFs.

The quark-quark correlation function Φ integrated over the p^- component and projected on different Dirac structures

$$\Phi^{[\Gamma]}(x, \mathbf{p}_T) = \frac{1}{2} \int dp^- \text{Tr}(\Phi \Gamma) \Big|_{p^+ = xP^+, p_T} = \int [d\sigma d\tau \delta(\cdot)] \frac{\text{Tr}(\Phi \Gamma)}{4P^+}, \quad (3.36)$$

with the shorthand notation (note the occurrence of a δ -function instead of the θ -function)

$$[d\sigma d\tau \delta(\cdot)] = d\sigma d\tau \delta\left(\tau - x\sigma + x^2 M^2 + \mathbf{p}_T^2\right), \quad (3.37)$$

defines \mathbf{p}_T dependent PDFs.

leading
PDFs(x, \mathbf{p}_T)

The projections leading in $1/Q$ are

$$\begin{aligned}\Phi^{[\gamma^+]}(x, \mathbf{p}_T) &\equiv f_1(x, \mathbf{p}_T^2) + \frac{\epsilon_T^{ij} p_{Ti} S_{Tj}}{M} f_{1T}^\perp(x, \mathbf{p}_T^2) \\ &= \int [d\sigma d\tau \delta(\cdot)] \left\{ [A_2 + x A_3] + \frac{\epsilon_T^{ij} p_{Ti} S_{Tj}}{M} [-A_{12}] \right\},\end{aligned}\quad (3.38)$$

$$\begin{aligned}\Phi^{[\gamma^+\gamma_5]}(x, \mathbf{p}_T) &\equiv \lambda g_{1L}(x, \mathbf{p}_T^2) + \frac{\mathbf{p}_T \cdot \mathbf{S}_T}{M} g_{1T}(x, \mathbf{p}_T^2) \\ &= \int [d\sigma d\tau \delta(\cdot)] \left\{ \lambda \left[-A_6 - \left(\frac{\sigma - 2x M^2}{2M^2} \right) (A_7 + x A_8) \right] \right. \\ &\quad \left. + \frac{\mathbf{p}_T \cdot \mathbf{S}_T}{M} (A_7 + x A_8) \right\},\end{aligned}\quad (3.39)$$

$$\begin{aligned}\Phi^{[i\sigma^{i+}\gamma_5]}(x, \mathbf{p}_T) &\equiv S_T^i h_{1T}(x, \mathbf{p}_T^2) + \frac{p_T^i}{M} \left(\lambda h_{1L}^\perp(x, \mathbf{p}_T^2) + \frac{\mathbf{p}_T \cdot \mathbf{S}_T}{M} h_{1T}^\perp(x, \mathbf{p}_T^2) \right) \\ &\quad + \frac{\epsilon_T^{ij} p_T^j}{M} h_1^\perp(x, \mathbf{p}_T^2) \\ &= \int [d\sigma d\tau \delta(\cdot)] \left\{ -S_T^i (A_9 + x A_{10}) + \frac{\epsilon_T^{ij} p_T^j}{M} [-A_4] \right. \\ &\quad \left. + \frac{\lambda p_T^i}{M} \left[A_{10} - \left(\frac{\sigma - 2x M^2}{2M^2} \right) A_{11} \right] + \frac{p_T^i}{M} \frac{\mathbf{p}_T \cdot \mathbf{S}_T}{M} A_{11} \right\}.\end{aligned}\quad (3.40)$$

The probabilistic interpretation of the leading transverse momentum dependent PDFs is schematically shown in Fig. 3.10. There are two groups of additional PDFs possible because of the presence of a non-vanishing transverse quark momentum. The functions $g_{1T}(x, \mathbf{p}_T^2)$, $h_{1L}^\perp(x, \mathbf{p}_T^2)$, and $h_{1T}^\perp(x, \mathbf{p}_T^2)$ are non-vanishing, if there is a correlation between longitudinal quark polarisation (helicity) and transverse hadron polarisation, or vice versa. This possibilities, surprising at first glance, do exist because of the extra distinction of a direction by the transverse quark momentum components; otherwise they would be forbidden simply by rotational invariance. Note that the existence of two transverse directions x and y is reflected in the number of independent chiral-odd functions. The second group of additional functions consists of the (naive) time-reversal odd PDFs $f_{1T}^\perp(x, \mathbf{p}_T^2)$ (the so-called Sivers function [19]) and $h_1^\perp(x, \mathbf{p}_T^2)$ correlating transverse quark momentum to transverse hadron spin, or transverse quark momentum to transverse quark spin, respectively.²

A symmetric integration over \mathbf{p}_T relates the transverse momentum dependent PDFs with their integrated counterparts

$$f(x) = \int d^2 \mathbf{p}_T f(x, \mathbf{p}_T^2) \quad (3.41)$$

for a generic PDF $f(x, \mathbf{p}_T^2)$. Note that a symmetric integration of $\Phi^{[i\sigma^{i+}\gamma_5]}(x, \mathbf{p}_T)$ over \mathbf{p}_T receives two non-vanishing contributions resulting in the identification

$$h_1(x) = \int d^2 \mathbf{p}_T \left(h_{1T}(x, \mathbf{p}_T^2) + \frac{\mathbf{p}_T^2}{2M^2} h_{1T}^\perp(x, \mathbf{p}_T^2) \right). \quad (3.42)$$

²A discussion on the possible existence of non-vanishing time-reversal odd PDFs is given in comparison with time-reversal odd PFFs in the next subsection 3.2.3.

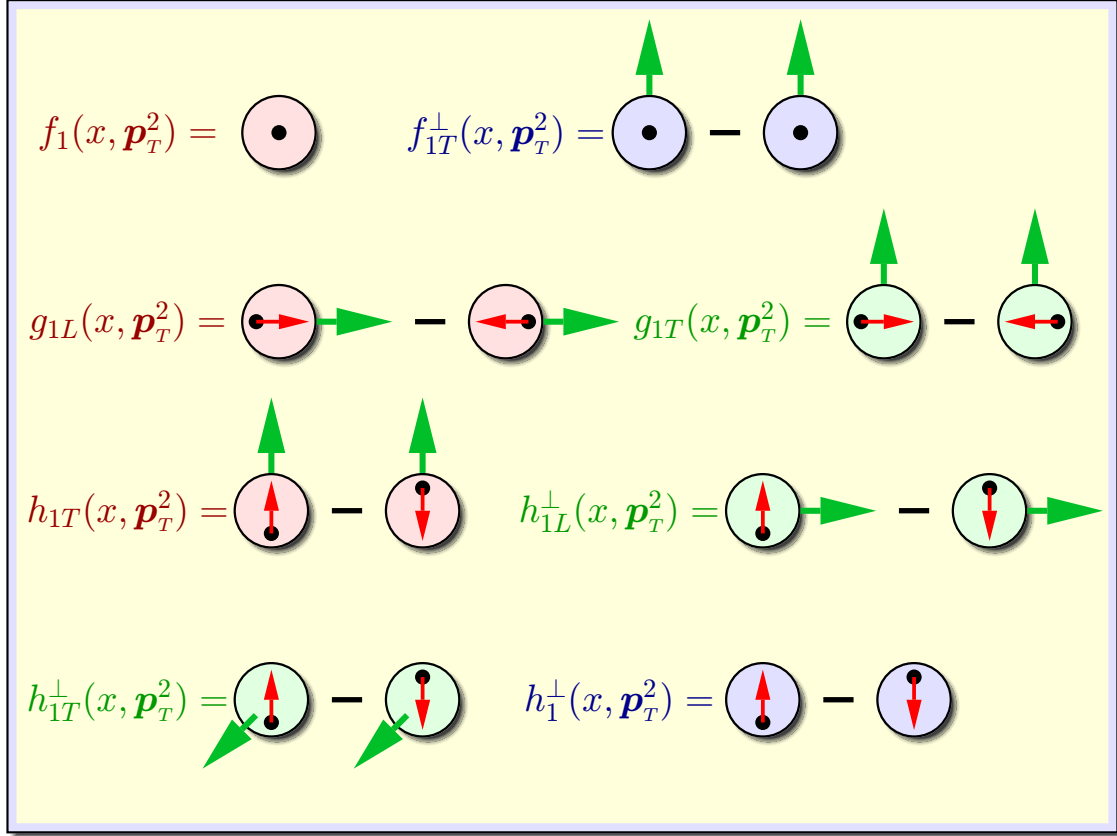


Figure 3.10: Probability interpretation of leading order transverse momentum dependent PDFs. Compared to the integrated leading order PDFs there are two additional time-reversal odd functions f_{1T}^\perp and h_1^\perp (indicated with blue shaded hadrons), and three additional functions g_{1T} , h_{1L} , h_{1T}^\perp (indicated with green shaded hadrons) which correlate quark and hadron spin orientation in different directions.

The following projections occur with a pre-factor M/P^+ , which signals the subleading (or higher twist) nature of the corresponding distribution functions

subleading
PDFs(x, \mathbf{p}_T)

$$\begin{aligned} \Phi^{[1]}(x, \mathbf{p}_T) &\equiv \frac{M}{P^+} e(x, \mathbf{p}_T^2) \\ &= \frac{M}{P^+} \int [d\sigma d\tau \delta(\cdot)] A_1, \end{aligned} \quad (3.43)$$

$$\begin{aligned} \Phi^{[i\gamma_5]}(x, \mathbf{p}_T) &\equiv \frac{M}{P^+} \left\{ \lambda e_L(x, \mathbf{p}_T^2) + \frac{\mathbf{p}_T \cdot \mathbf{S}_T}{M} e_T(x, \mathbf{p}_T^2) \right\} \\ &= \frac{M}{P^+} \int [d\sigma d\tau \delta(\cdot)] \\ &\quad \left\{ \lambda \left[- \left(\frac{\sigma - 2x M^2}{2M^2} \right) A_5 \right] + \frac{\mathbf{p}_T \cdot \mathbf{S}_T}{M} A_5 \right\}, \end{aligned} \quad (3.44)$$

$$\begin{aligned} \Phi^{[\gamma^i]}(x, \mathbf{p}_T) &\equiv \frac{M}{P^+} \left\{ \frac{p_T^i}{M} f^\perp(x, \mathbf{p}_T^2) + \lambda \frac{\epsilon_T^{ij} \mathbf{p}_{Tj}}{M} f_L^\perp(x, \mathbf{p}_T^2) + \epsilon_T^{ij} S_{Tj} f_T(x, \mathbf{p}_T^2) \right\} \\ &= \frac{M}{P^+} \int [d\sigma d\tau \delta(\cdot)] \left\{ \frac{p_T^i}{M} A_3 + \lambda \frac{\epsilon_T^{ij} \mathbf{p}_{Tj}}{M} A_{12} \right\} \end{aligned}$$

$$+ \epsilon_T^{ij} S_{Tj} \left[\left(\frac{\sigma - 2x M^2}{2M^2} \right) A_{12} \right] \Big\}, \quad (3.45)$$

$$\begin{aligned} \Phi^{[\gamma^i \gamma_5]}(x, \mathbf{p}_T) &\equiv \frac{M}{P^+} \left\{ S_T^i g_T'(x, \mathbf{p}_T^2) \right. \\ &\quad \left. + \frac{p_T^i}{M} \left(\lambda g_L^\perp(x, \mathbf{p}_T^2) + \frac{\mathbf{p}_T \cdot \mathbf{S}_T}{M} g_T^\perp(x, \mathbf{p}_T^2) \right) \right\} \\ &= \frac{M}{P^+} \int [d\sigma d\tau \delta(\cdot)] \left\{ S_T^i [-A_6] \right. \\ &\quad \left. - \frac{\lambda p_T^i}{M} \left(\frac{\sigma - 2x M^2}{2M^2} \right) A_8 + \frac{p_T^i}{M} \frac{\mathbf{p}_T \cdot \mathbf{S}_T}{M} A_8 \right\}, \quad (3.46) \end{aligned}$$

$$\begin{aligned} \Phi^{[i\sigma^{ij} \gamma_5]}(x, \mathbf{p}_T) &\equiv \frac{M}{P^+} \left\{ \frac{S_T^i p_T^j - S_T^j p_T^i}{M} h_T^\perp(x, \mathbf{p}_T^2) + \epsilon_T^{ij} h(x, \mathbf{p}_T^2) \right\} \\ &= \frac{M}{P^+} \int [d\sigma d\tau \delta(\cdot)] \left\{ \frac{S_T^i p_T^j - S_T^j p_T^i}{M} [-A_{10}] \right. \\ &\quad \left. + \epsilon_T^{ij} \left[\left(\frac{\sigma - 2x M^2}{2M^2} \right) A_4 \right] \right\}, \quad (3.47) \end{aligned}$$

$$\begin{aligned} \Phi^{[i\sigma^{+-}]}(x, \mathbf{p}_T) &\equiv \frac{M}{P^+} \left\{ \lambda h_L(x, \mathbf{p}_T^2) + \frac{\mathbf{p}_T \cdot \mathbf{S}_T}{M} h_T(x, \mathbf{p}_T^2) \right\} \\ &= \frac{M}{P^+} \int [d\sigma d\tau \delta(\cdot)] \left\{ \lambda \left[-A_9 - \frac{\sigma}{2M^2} A_{10} + \left(\frac{\sigma - 2x M^2}{2M^2} \right)^2 A_{11} \right] \right. \\ &\quad \left. - \frac{\mathbf{p}_T \cdot \mathbf{S}_T}{M} \left(\frac{\sigma - 2x M^2}{2M^2} \right) A_{11} \right\}. \quad (3.48) \end{aligned}$$

A symmetric integration of $\Phi^{[\gamma^i \gamma_5]}(x, \mathbf{p}_T)$ over \mathbf{p}_T receives two non-vanishing contributions resulting in the identification

$$g_T(x) = \int d^2 \mathbf{p}_T \left(g_T'(x, \mathbf{p}_T^2) + \frac{\mathbf{p}_T^2}{2M^2} g_T^\perp(x, \mathbf{p}_T^2) \right). \quad (3.49)$$

The constraint of the δ -function in the integration over σ and τ is indicated in Fig. 3.11. Furthermore, the integration is restricted to the region $M_R^2 \equiv (P - p)^2 \geq 0$. This leads to the vanishing of the distribution functions at $x = 1$.

The relation of transverse momentum dependent PDFs and their integrated counterparts finds its simple reflection in the expressions in terms of the amplitudes $A_i(\sigma, \tau)$ by a change of the integration measure. If a generic distribution function is written as

$$f(x, \mathbf{p}_T^2) = \int [d\sigma d\tau \delta(\cdot)] G(A_i(\sigma, \tau), \sigma, x) \quad (3.50)$$

with the shorthand notation (3.25) for $[d\sigma d\tau \delta(\cdot)]$, symmetric integration over \mathbf{p}_T gives

$$f(x) = \int [d\sigma d\tau \theta(\cdot)] G(A_i(\sigma, \tau), \sigma, x), \quad (3.51)$$

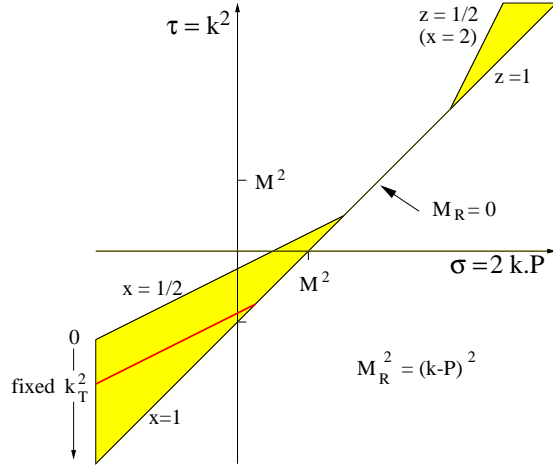


Figure 3.11: The δ -function constraint in the σ - τ plane (using quark momentum k and hadron momentum P) coming from fixing x and \mathbf{k}_T^2 in the expression for the distribution functions $F(x, \mathbf{k}_T^2)$ (and similarly for the fragmentation functions $D(z, z^2 \mathbf{k}_T^2)$) and the full integration regions for the \mathbf{k}_T integrated functions $F(x)$ (and similarly for $D(z)$). The latter region is determined by $\mathbf{k}_T^2 \geq 0$ and $M_R^2 \geq 0$.

with $[d\sigma d\tau \theta(\)]$ defined by (3.37). The region covered by the θ -function (for $x = 1/2$) is the lower shaded region in Fig. 3.11 corresponding to $\mathbf{p}_T^2 \geq 0$. Only the terms involving the distribution functions $f_1, g_1 = g_{1L}, h_1 = h_{1T} + (\mathbf{p}_T^2/2M^2) h_{1T}^\perp, e, e_L, f_T, g_T = g'_T + (\mathbf{p}_T^2/2M^2) g_{1T}^\perp, h$ and h_L are non-vanishing upon integration over \mathbf{p}_T . The integrated functions $f_1(x), g_1(x)$ and $h_1(x)$ have the well known probabilistic interpretations. The twist three functions have no intuitive partonic interpretation. Nevertheless, they are well defined as hadronic matrix elements via Eqs. (3.7) and (3.11), and their projections.

We note the appearance of higher \mathbf{p}_T^2 -moments,

$$\begin{aligned} f^{(n)}(x) &\equiv \int d^2 \mathbf{p}_T \left(\frac{\mathbf{p}_T^2}{2M^2} \right)^n f(x, \mathbf{p}_T^2) \\ &= \pi \int [d\sigma d\tau \theta(\)] \left(\frac{x\sigma - x^2 M^2 - \tau}{2M^2} \right)^n G(A_i(\sigma, \tau), \sigma, x), \end{aligned} \quad (3.52)$$

such as $h_{1T}^{\perp(1)}$ and $g_T^{\perp(1)}$. The equality in Eq. (3.52) is obtained using the azimuthal symmetry of the distribution functions, which depend only on x and \mathbf{p}_T^2 . In the weighted integration, $\int d^2 \mathbf{p}_T p_T^i \dots$ one will encounter the functions $g_{1T}^{(1)}$ and $h_{1L}^{\perp(1)}$.

The distribution functions cannot be all independent because their number is larger than the number of amplitudes A_i . This is reflected in relations such as

$$f_T(x) = -\frac{d}{dx} f_{1T}^{\perp(1)}(x), \quad (3.53)$$

$$e_L(x) = -\frac{d}{dx} e_T^{(1)}(x), \quad (3.54)$$

$$g_T(x) = g_1(x) + \frac{d}{dx} g_{1T}^{(1)}(x), \quad (3.55)$$

$$h_L(x) = h_1(x) - \frac{d}{dx} h_{1L}^{\perp(1)}(x), \quad (3.56)$$

$$h(x) = -\frac{d}{dx} h_1^{\perp(1)}(x), \quad (3.57)$$

$$h_T^{(1)}(x) = -\frac{1}{2} \frac{d}{dx} h_{1T}^{\perp(2)}(x), \quad (3.58)$$

which can be obtained using their explicit expressions in terms of the amplitudes [20, 21].

The functions $g_2 = g_T - g_1$ and $h_2 = 2(h_L - h_1)$ thus satisfy the sum rules

$$\int_0^1 dx g_2(x) = -g_{1T}^{(1)}(0), \quad (3.59)$$

$$\int_0^1 dx h_2(x) = 2 h_{1L}^{\perp(1)}(0), \quad (3.60)$$

which are a direct consequence of (3.55) and (3.56). If the functions $g_{1T}^{(1)}$ and $h_{1L}^{\perp(1)}$ vanish at the origin, we rediscover the Burkhardt-Cottingham sum rule [22] and the Burkardt sum rule [23]. These sum rules (Eqs. (3.59) and (3.60) with vanishing right-hand sides) can also be derived using Lorentz covariance for the expectation values of local operators [24]. In our approach this would imply constraints on the amplitudes A_i .

3.2.3 PFFs of a spin-1/2 hadron

PFFs (z)

The correlation function Δ defined in Eq. (3.11) is also constrained by the hermiticity properties of the fields and invariance under parity operation, leading to an expansion identical to that in Eq. (3.17) with the replacements $\{p, P, S, M\} \rightarrow \{k, P_h, S_h, M_h\}$ [18] and with real amplitudes, say B_i , now depending on $\tau_h \equiv k^2$ and $\sigma_h \equiv 2k \cdot P_h$. Time reversal invariance does not imply any constraints on the amplitudes, thus B_4 , B_5 and B_{12} , referred to as ‘time-reversal odd’, are, in general, non-vanishing.

In hard processes one encounters the quantities

$$\Delta^{[\Gamma]}(z) = \frac{1}{4z} \int dk^+ d^2\mathbf{k}_T \text{Tr}(\Delta\Gamma) \Big|_{k^- = P_h^-/z} = \int [d\sigma_h d\tau_h \theta(\cdot)] \frac{\text{Tr}(\Delta\Gamma)}{8z P_h^-}, \quad (3.61)$$

with the shorthand notation

$$[d\sigma_h d\tau_h \theta(\cdot)] = d\sigma_h d\tau_h \theta\left(\frac{\sigma_h}{z} - \frac{M_h^2}{z^2} - \tau_h\right). \quad (3.62)$$

A convenient parametrisation of the momentum of the produced hadron (with mass M_h) in a hadron frame is

$$P_h = \frac{M_h^2}{2P_h^-} n_+ + P_h^- n_- = \frac{M_h^2}{z_h Q \sqrt{2}} n_+ + \frac{z_h Q}{\sqrt{2}} n_-, \quad (3.63)$$

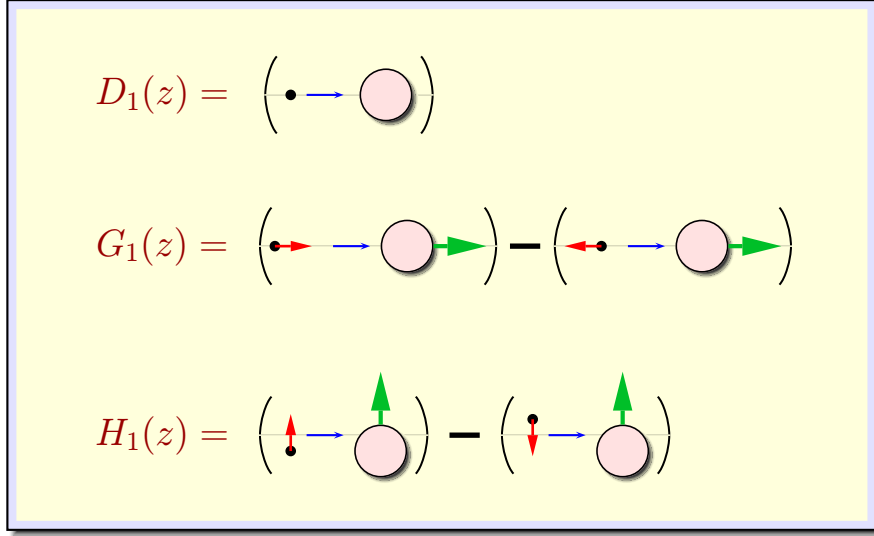


Figure 3.12: Probability interpretation of leading order integrated PFFs. The quark is assumed to move from left to right, which defines the longitudinal direction. Green arrows symbolise the hadron spin, red arrows the spin state of the quark.

where the Lorentz invariant quantity $z_h = 2P_h \cdot q/q^2$ is used in analogy to the Bjorken variable. A Sudakov decomposition of the quark momentum and the spin vector can be written

$$k = \frac{z(k^2 + \mathbf{k}_T^2)}{z_h Q \sqrt{2}} n_+ + \frac{z_h Q}{z \sqrt{2}} n_- + k_T, \quad (3.64)$$

$$S_h = -\frac{\lambda_h M_h}{z_h Q \sqrt{2}} n_+ + \frac{\lambda_h z_h Q}{M_h \sqrt{2}} n_- + S_{hT}. \quad (3.65)$$

Thus z is the fraction of the momentum in the minus direction carried by the hadron h originating from the fragmentation of the quark. The spin vector satisfies $P_h \cdot S_h = 0$ and for a pure state $-S_h^2 = \lambda_h^2 + \mathbf{S}_{hT}^2 = 1$.

The projections

leading PFFs(z)

$$\Delta^{[\gamma^-]}(z) = D_1(z), \quad (3.66)$$

$$\Delta^{[\gamma^- \gamma_5]}(z) = \lambda_h G_1(z), \quad (3.67)$$

$$\Delta^{[i\sigma^{i-} \gamma_5]}(z) = S_{hT}^i H_1(z) \quad (3.68)$$

are leading in $1/Q$. We use for the names of the fragmentation functions capital letters corresponding to the names of the PDFs (with the only exception for the counterparts of f_{\cdot} functions which are called D_{\cdot}). Probabilistic interpretation of the leading order integrated PFFs is shown in Fig. 3.12.

subleading
PFFs(z)

The following projections occur with a pre-factor M_h/P_h^- , which signals the subleading (or higher twist) nature of the corresponding fragmentation functions

$$\Delta^{[1]}(z) = \frac{M_h}{P_h^-} E(z), \quad (3.69)$$

$$\Delta^{[i\gamma_5]}(z) = \frac{M_h}{P_h^-} \lambda_h E_L(z), \quad (3.70)$$

$$\Delta^{[\gamma^i]}(z) = \frac{M_h}{P_h^-} \epsilon_T^{ij} S_{hTj} D_T(z), \quad (3.71)$$

$$\Delta^{[\gamma^i \gamma_5]}(z) = \frac{M_h}{P_h^-} S_{hT}^i G_T(z), \quad (3.72)$$

$$\Delta^{[i\sigma^{ij} \gamma_5]}(z) = \frac{M_h}{P_h^-} \epsilon_T^{ij} H(z), \quad (3.73)$$

$$\Delta^{[i\sigma^{-+} \gamma_5]}(z) = \frac{M_h}{P_h^-} \lambda_h H_L(z). \quad (3.74)$$

PFFs(z, \mathbf{k}'_T)

In observables differential in transverse momenta there occur also the associated unintegrated quantities

$$\Delta^{[\Gamma]}(z, \mathbf{k}_T) = \frac{1}{4z} \int dk^+ \text{Tr}(\Delta\Gamma) \Big|_{k^- = P_h^- / z, k_T} = \int [d\sigma_h d\tau_h \delta(\cdot)] \frac{\text{Tr}(\Delta\Gamma)}{8z P_h^-}, \quad (3.75)$$

with the shorthand notation

$$[d\sigma_h d\tau_h \delta(\cdot)] = d\sigma_h d\tau_h \delta\left(\tau_h - \frac{\sigma_h}{z} + \frac{M_h^2}{z^2} + \mathbf{k}'_T\right), \quad (3.76)$$

which lead to the definition of transverse momentum dependent PFFs.

leading
PFFs(z, \mathbf{k}_T)

The projections

$$\Delta^{[\gamma^-]}(z, -z\mathbf{k}_T) = D_1(z, \mathbf{k}'_T) + \frac{\epsilon_T^{ij} k_{Ti} S_{hTj}}{M_h} D_{1T}^\perp(z, \mathbf{k}'_T), \quad (3.77)$$

$$\Delta^{[\gamma^- \gamma_5]}(z, -z\mathbf{k}_T) = \lambda_h G_{1L}(z, \mathbf{k}'_T) + \frac{\mathbf{k}_T \cdot \mathbf{S}_{hT}}{M_h} G_{1T}(z, \mathbf{k}'_T), \quad (3.78)$$

$$\Delta^{[i\sigma^{i-} \gamma_5]}(z, -z\mathbf{k}_T) = S_{hT}^i H_{1T}(z, \mathbf{k}'_T) + \frac{\epsilon_T^{ij} k_{Tj}}{M_h} H_1^\perp(z, \mathbf{k}'_T) \quad (3.79)$$

$$+ \frac{k_T^i}{M_h} \left(\lambda_h H_{1L}^\perp(z, \mathbf{k}'_T) + \frac{\mathbf{k}_T \cdot \mathbf{S}_{hT}}{M_h} H_{1T}^\perp(z, \mathbf{k}'_T) \right) \quad (3.80)$$

are leading in $1/Q$. Their partonic interpretation is depicted in Fig. 3.13.

The functions D_{1T}^\perp and H_1^\perp are examples of what are generally called ‘time-reversal odd’ functions. This somewhat misleading terminology refers to the behaviour of the functions under the so-called *naive* time-reversal operation T_N [25], which acts as follows on the correlation functions:

$$\Delta(P_h, S_h; k) \xrightarrow{T_N} (\gamma_5 C \Delta(\bar{P}_h, \bar{S}_h; \bar{k}) C^\dagger \gamma_5)^* \quad (3.81)$$

where $\bar{k} = (k^0, -\mathbf{k})$, etc. If T_N invariance would apply, the functions D_{1T}^\perp , H_1^\perp , D_L^\perp , D_T , E_L , E_T and H would be purely imaginary. On the other hand, hermiticity requires the functions to be real, so these functions should then vanish.

The operation T_N differs from the actual time-reversal operation T in that the former does not transform *in* into *out*-states, and *vice versa*. Due to final state interactions, the *out*-state $|P_h, S_h; X\rangle$ in $\Delta(P_h, S_h; k)$ is not a plane wave state and thus, is not simply related to an *in*-state. Therefore, one has $T_N \neq T$ and since T itself does not pose any constraints on the functions, they need not vanish.

In the analogous case of distribution functions, which are derived from matrix elements with plane wave states, $T = T_N$ and therefore it was generally believed there are no ‘time-reversal odd’ distribution functions [26].

The effects of so-called gluonic poles in twist-three quark-gluon-quark hadronic matrix elements, as first considered by Qiu and Sterman in the Drell-Yan process [27] and direct photon production [28], were shown to be indistinguishable from those of time-reversal odd PDFs. In particular, both gluonic poles and time-reversal odd distribution functions can lead to the same single spin asymmetries [29]. This is one of the reasons why the time-reversal odd structures have been listed in subsections 3.2.1 and 3.2.2. With the working hypothesis of non-vanishing time-reversal odd PDFs some phenomenology has been done on observable effects [30, 31, 29, 32, 33].

Recently, the discussion about the possibility for non-vanishing time-reversal odd PDFs was reopened by a model calculation of a single-spin asymmetry including the effects of final state interactions by Brodsky, Hwang and Schmidt [34]. This calculation provided a counterexample and thus invalidated the earlier argument against time-reversal odd PDFs, since the effects amount to the existence a non-vanishing Sivers function f_{1T}^\perp as soon after was shown by Collins [35]. It was demonstrated that the effects of final state interactions can be taken into account by a proper careful treatment of a gauge link operator at infinity [36, 37] and related questions on the density interpretation of PDFs have been raised [38]. The topic is still not settled and under debate.

The following projections occur with a pre-factor M_h/P_h^- , which signals the subleading (or higher twist) nature of the corresponding fragmentation functions

$$\begin{aligned} \Delta^{[1]}(z, -z\mathbf{k}_T) &= \frac{M_h}{P_h^-} E(z, \mathbf{k}_T^{\prime 2}), \\ \Delta^{[\gamma^i]}(z, -z\mathbf{k}_T) &= \frac{k_T^i}{P_h^-} D^\perp(z, \mathbf{k}_T^{\prime 2}) + \lambda_h \frac{\epsilon_T^{ij} k_{Tj}}{P_h^-} D_L^\perp(z, \mathbf{k}_T^{\prime 2}) \end{aligned}$$

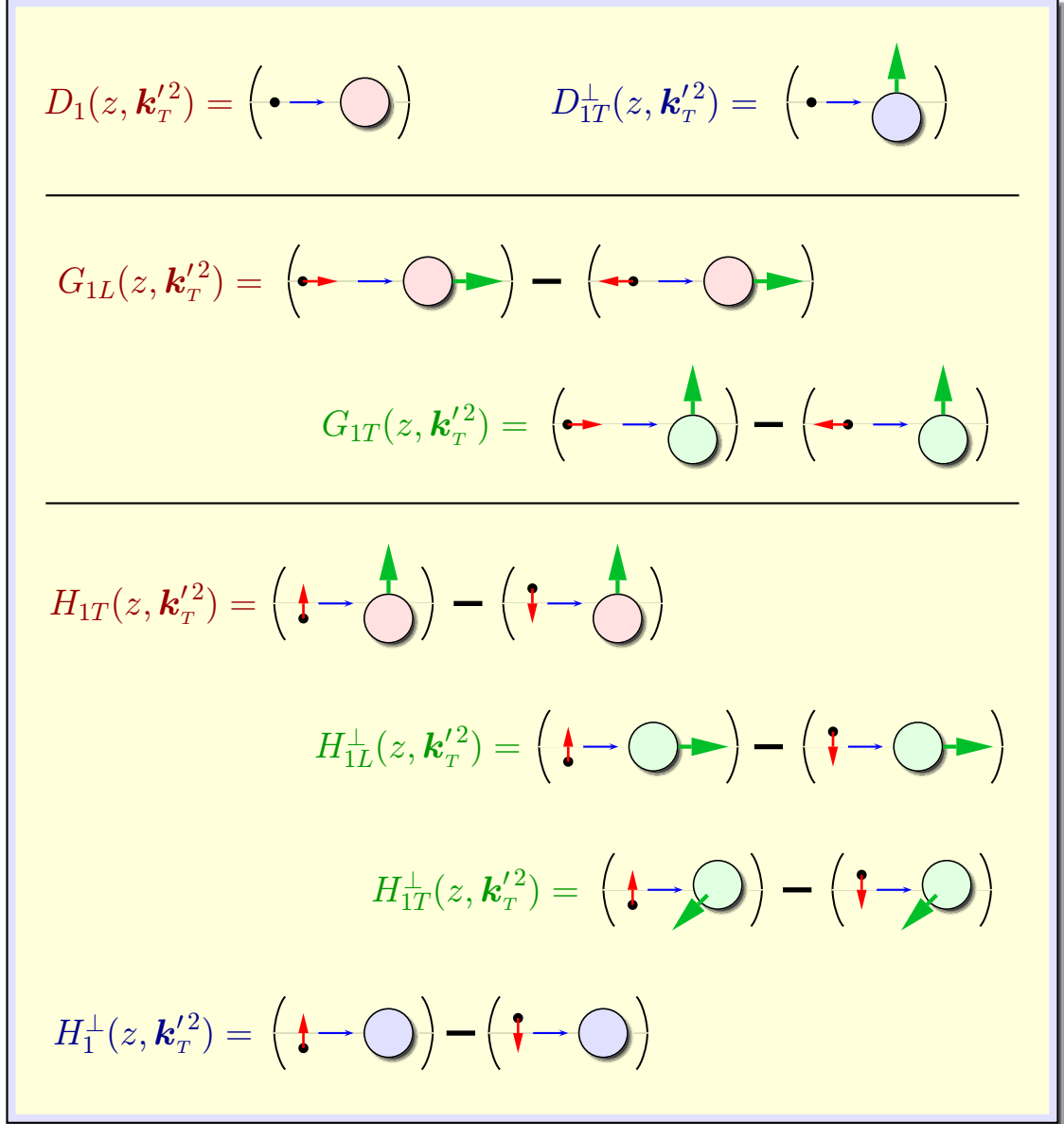


Figure 3.13: Probability interpretation of leading order transverse momentum dependent PFFs. Compared to the integrated leading order PFFs there are two additional time-reversal odd functions D_{1T}^\perp and H_1^\perp (indicated with blue shaded hadrons), and three additional functions G_{1T} , H_{1L}^\perp , H_{1T}^\perp (indicated with green shaded hadrons) which correlate quark and hadron spin orientation in different directions.

$$\begin{aligned}
 & + \frac{M_h}{P_h} \epsilon_T^{ij} S_{hTj} D_T(z, \mathbf{k}'_T{}^2), \\
 \Delta^{[i\gamma_5]}(z, -z\mathbf{k}_T) & = \frac{M_h}{P_h} \left(\lambda_h E_L(z, \mathbf{k}'_T{}^2) + \frac{\mathbf{k}_T \cdot \mathbf{S}_{hT}}{M_h} E_T(z, \mathbf{k}'_T{}^2) \right), \\
 \Delta^{[\gamma^i\gamma_5]}(z, -z\mathbf{k}_T) & = \frac{M_h}{P_h} S_{hT}^i G'_T(z, \mathbf{k}'_T{}^2) \\
 & + \frac{k_T^i}{M_h} \left(\lambda_h G_L^\perp(z, \mathbf{k}'_T{}^2) + \frac{\mathbf{k}_T \cdot \mathbf{S}_{hT}}{M_h} G_T^\perp(z, \mathbf{k}'_T{}^2) \right),
 \end{aligned}$$

$$\begin{aligned}\Delta^{[i\sigma^{ij}\gamma_5]}(z, -z\mathbf{k}_T) &= \frac{M_h S_{hT}^i k_T^j - S_{hT}^j k_T^i}{P_h^- M_h} H_T^\perp + \frac{M_h}{P_h^-} \epsilon_T^{ij} H, \\ \Delta^{[i\sigma^{-+}\gamma_5]}(z, -z\mathbf{k}_T) &= \frac{M_h}{P_h^-} \left(\lambda_h H_L(z, \mathbf{k}'_T) + \frac{\mathbf{k}_T \cdot \mathbf{S}_{hT}}{M_h} H_T(z, \mathbf{k}'_T) \right)\end{aligned}$$

Comparing the above equations with the case of the distribution functions, one sees that the relations between the Dirac projections $2z \Delta^{[\Gamma]}(z, \mathbf{k}_T)$ and the amplitudes are identical to those for $\Phi^{[\Gamma]}(x, \mathbf{p}_T)$ after the replacements

$$\begin{aligned}\{x, \sigma, \tau, \mathbf{p}_T, P, S_T, \lambda, M, A_i, \text{plus/minus-components}\} \\ \implies \{1/z, \sigma_h, \tau_h, \mathbf{k}_T, P_h, S_{hT}, \lambda_h, M_h, B_i, \text{minus/plus-components}\} .\end{aligned}\quad (3.82)$$

Furthermore, the definition of fragmentation functions follow the general procedure used to define distribution functions. For example,

$$\begin{aligned}\Delta^{[\gamma^-]}(z, \mathbf{k}_T) &\equiv D_1(z, \mathbf{k}'_T) + \frac{\epsilon_T^{ij} k_{Ti} S_{hTj}}{M_h} D_{1T}^\perp(z, \mathbf{k}'_T) \\ &= \frac{1}{2z} \int [d\sigma_h d\tau_h \delta(\)] \left\{ \left[B_2 + \frac{1}{z} B_3 \right] + \frac{\epsilon_T^{ij} k_{Ti} S_{hTj}}{M_h} B_{12} \right\},\end{aligned}\quad (3.83)$$

where $\mathbf{k}'_T = -z\mathbf{k}_T$. The choice of arguments z and \mathbf{k}'_T in the fragmentation functions is worth a comment. In the expansion of k in Eq. (3.64) the quantities $1/z$ and \mathbf{k}_T appear in a natural way. However, in the interpretation of Δ as a decay function of quarks, the variable z as the ratio of P_h^-/k^- is more adequate. Applying a Lorentz transformation that leaves the minus component (and hence the definition of z) unchanged, one finds that $\mathbf{k}'_T = -z\mathbf{k}_T$ is the transverse component of hadron h with respect to the quark momentum.

The constraint imposed by the δ -function in the σ_h - τ_h plane is also indicated in Fig. 3.11. The integration is restricted to the region $M_R^2 = (P_h - k)^2 \geq 0$, which implies that the fragmentation functions vanish at $z = 1$. We note the reciprocity of x and z , i.e., the constraint for $z = 1/2$ is the same as one would have for $x = 2$. Note, however, that the integration involves different regions. For the distributions one has (roughly) spacelike quark momenta, for the fragmentation timelike quark momenta. If a generic quark fragmentation function is given by

$$D(z, \mathbf{k}'_T) = \frac{1}{2z} \int [d\sigma_h d\tau_h \delta(\)] G(B_i(\sigma_h, \tau_h), \sigma_h, z),\quad (3.84)$$

the integrated functions are given by

$$\begin{aligned}D^{(n)}(z) &\equiv z^2 \int d^2\mathbf{k}_T \left(\frac{\mathbf{k}_T^2}{2M_h^2} \right)^n D(z, \mathbf{k}'_T) \\ &= \frac{\pi z}{2} \int [d\sigma_h d\tau_h \theta(\)] \left(\frac{\sigma_h - 2M_h^2/z}{2M_h^2} \right)^n G(B_i(\sigma_h, \tau_h), \sigma_h, z),\end{aligned}\quad (3.85)$$

relations between
leading and
subleading PFFs

where

$$[d\sigma_h d\tau_h \theta(\cdot)] = d\sigma_h d\tau_h \theta \left(\frac{\sigma_h}{z} - \frac{M_h^2}{z^2} - \tau_h \right). \quad (3.86)$$

Non-vanishing upon integration over \mathbf{k}_T are the fragmentation functions D_1 , $G_1 = G_{1L}$, $H_1 = H_{1T} + (\mathbf{k}_T^2/2M_h^2) H_{1T}^\perp$, E , $G_T = G'_T + (\mathbf{k}_T^2/2M_h^2) G_T^\perp$, H_L and D_T .

As for the distributions, the integrated fragmentation functions are not all independent. Using Eq. (3.85) one obtains relations such as

$$E_L(z) = z^3 \frac{d}{dz} \left[\frac{E_T^{(1)}(z)}{z} \right], \quad (3.87)$$

$$D_T(z) = z^3 \frac{d}{dz} \left[\frac{D_{1T}^{\perp(1)}(z)}{z} \right], \quad (3.88)$$

$$G_T(z) = G_1(z) - z^3 \frac{d}{dz} \left[\frac{G_{1T}^{(1)}(z)}{z} \right], \quad (3.89)$$

$$H_L(z) = H_1(z) + z^3 \frac{d}{dz} \left[\frac{H_{1L}^{\perp(1)}(z)}{z} \right], \quad (3.90)$$

$$H(z) = z^3 \frac{d}{dz} \left[\frac{H_1^{\perp(1)}(z)}{z} \right], \quad (3.91)$$

leading to

$$\int_0^1 dz \frac{E_L(z)}{z^3} = \lim_{z \rightarrow 0} \frac{E_T^{(1)}(z)}{z}, \quad (3.92)$$

and similar ones for D_T , $G_2 = G_T - G_1$, $H_2 = 2(H_L - H_1)$ and H . Provided that the functions labelled with superscript (1) vanish at the origin faster than one power of z , the right hand side vanishes. Finally, let us remark that this formalism can be easily extended to include antiquarks [18, 21].

3.2.4 the naming scheme

a consistent
naming scheme

At first glance, the names of PDFs and PFFs look unnecessary complicated with all their sub- and superscripts. But in fact, they follow a simple systematics reflecting the unambiguous way of the determination of all independent functions from quark-quark correlation functions spelled out in the previous subsections. Last but not least, the names publicly announce the physical situation to be considered, in which these quantities can be accessed. The scheme is based on works by Jaffe and Ji, was largely extended by Mulders, Levelt and Tangerman [39, 18], and recently ported to the cases of gluon PDFs and PFFS by Rodrigues and Mulders [40], to spin-one functions by Bacchetta and Mulders [41], and to 2-hadron PFFs by Bianconi, Boffi, Jakob and Radici [42].

The naming scheme can be summarised with the following set of five rules: exemplified for the $\mathbf{k}_T^2/(2M_h^2)$ moment of the fragmentation function D_{1T}^\perp in Fig. 3.14.

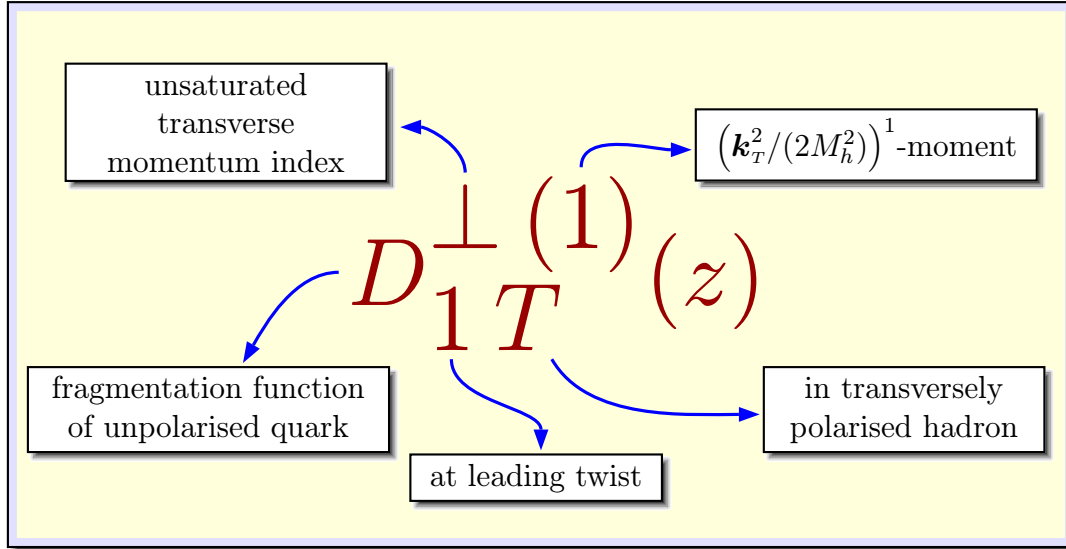


Figure 3.14: Application of the name scheme exemplified for the $D_{1T}^{\perp(1)}(z)$ fragmentation function. The name reveals that the fragmentation of an unpolarised quark into a transversely polarised hadron at leading order is described. There is a non-contracted transverse momentum index in the accompanying tensor structure, and the $(\mathbf{k}_T^2/(2M_h^2))^1$ -moment of the unintegrated PFF is to be taken.

1. the Dirac projection of the correlation function, i.e., the matrix Γ , determines the letter of the resulting PDF or PFF:

Dirac projection with Γ		PDF	PFF
vector	$\gamma^+, \gamma^i, \gamma^-$	f	D
axial vector	$\gamma^+ \gamma_5, \gamma^i \gamma_5, \gamma^- \gamma_5$	g	G
tensor	$\sigma^{+i} \gamma_5, \sigma^{ij} \gamma_5, \sigma^{+-} \gamma_5, \sigma^{-i} \gamma_5,$	h	H
(pseudo) scalar	$1, \gamma_5$	e	E

Note that corresponding PDFs and PFFs are denoted with the same small and capital letter; with the only exception that the counterparts of the f -PDFs are denoted with a capital D for consistence with widespread used names for spin-independent PFFs.

2. the first subscript indicates the ‘effective twist’ of the function:

effective twist	subscript
“2”	1
“3”	none (or 2)
“4”	3

3. the second subscript indicates the polarisation of the hadron:

hadron polarisation	subscript
unpolarised	none
longitudinal	L
transverse	T

4. non-contracted transverse index of a quark momentum \rightarrow superscript \perp

5. higher \mathbf{p}_T^2 -moments (or \mathbf{k}_T^2 -moments) \rightarrow superscript (n)

$$f^{(n)}(x) \equiv \int d^2\mathbf{p}_T \left(\frac{\mathbf{p}_T^2}{2M^2} \right)^n f(x, \mathbf{p}_T^2)$$

The application of the name scheme is exemplified for the $\mathbf{k}_T^2/(2M_h^2)$ moment of the D_{1T}^\perp fragmentation function in Fig. 3.14.

3.2.5 towards a global analysis of transversity

spin of the nucleon

The spin of the nucleon is certainly a key issue in the investigation of its structure. It is nowadays well confirmed that only 20-30% of the longitudinal spin of the nucleon is carried by its quark and antiquark constituents. The rest is provided by the polarisation of gluons and by orbital angular momenta of quarks and gluons. First indications on the sign and size of the gluon polarisation have been seen (HERMES@DESY), and precision measurements are on the way (COMPASS@CERN, RHIC-spin@BNL, E-161@SLAC).

transversity distribution

For the full picture still another fundamental piece of the puzzle is missing: to complete the knowledge of the nucleon spin in the parton model sector one has to consider the third leading twist PDF, the *transversity distribution* $h_1(x)$ (frequently also called $\delta q(x)$, or $\Delta_T q(x)$), which is associated to a situation where the nucleon spin is oriented transverse to the direction of its motion. As an example for the rôle of intrinsic transverse momentum in semi-inclusive reactions and its interplay with spin degrees of freedom in this subsection we will elaborate on the issue of possible measurements of $h_1(x)$, one of the hot topics of present-days hadron physics.

The problem with $h_1(x)$ is related to its unusual spin property, it is one of the *chiral-odd* PDFs, which requires for compensation the occurrence of a second *chiral-odd* object with similar unusual spin property. Therefore, as a matter of principle it can not be accessed in the inclusive lepton-nucleon scattering measurements mostly performed so far. Hence $h_1(x)$ escaped notice until 1979, when it was discussed by Ralston and Soper in a paper on Drell-Yan spin asymmetries [17].

The chirality properties of $h_1(x)$ deserve a closer look, which is best done in the context of light-cone quantisation as sketched in chapter 2, and using the Weyl (or

chiral) representation of appendix A. In Eq. (3.26) the transversity distribution $h_1(x)$ (multiplied by a transverse component of the spin vector S_T^i) is defined as the projection $\Phi^{[i\sigma^{i+}\gamma_5]}(x)$. From the discussion of different operator structures in appendix A, in particular Eqs. (A.9) and (A.10), the operator under consideration is readily identified as density of good light-cone components $\phi \equiv \mathcal{P}_+\psi$ of the quark fields

$$\bar{\psi} i\sigma^{i+}\gamma_5 \psi = \sqrt{2} \phi^\dagger \left(P_L \gamma^i P_R - P_R \gamma^i P_L \right) \phi \quad (3.93)$$

with the chirality structure $\overline{LR} - \overline{RL}$ expressed by the chiral projectors $\mathcal{P}_{R/L} = (1 + \gamma_5)/2$ (cf. Eq.(2.36)). Thus a situation is considered where a right-handed quark is taken out from the hadron and a left-handed quark is reinserted, or *vice versa*: $h_1(x)$ involves a flip of quark chirality. The notion of a ‘chiral-odd’ function is used precisely in this sense. Since for the good component of the (massless) quark fields helicity and chirality are identical, $h_1(x)$ is also often referred to as ‘helicity-flip’ distribution. Strong interactions are helicity (or chirality) conserving up to negligible quark mass terms. As a consequence the helicity-flip of $h_1(x)$ cannot be compensated for by the hard part of a diagram, in order to form a physical observable. The occurrence of a *chiral-odd* projection of a second soft hadronic matrix element is mandatory for $h_1(x)$ to be observable in a hard process. This is the reason why $h_1(x)$ is not seen in inclusive lepton-nucleon scattering – a process whose dominant contribution is described by the hand-bag diagram involving only one soft matrix element. More complex processes, like Drell-Yan scattering or semi-inclusive DIS instead allow for the extraction of $h_1(x)$, if the observables are chosen carefully. The situation is schematically exemplified in Fig. 3.15

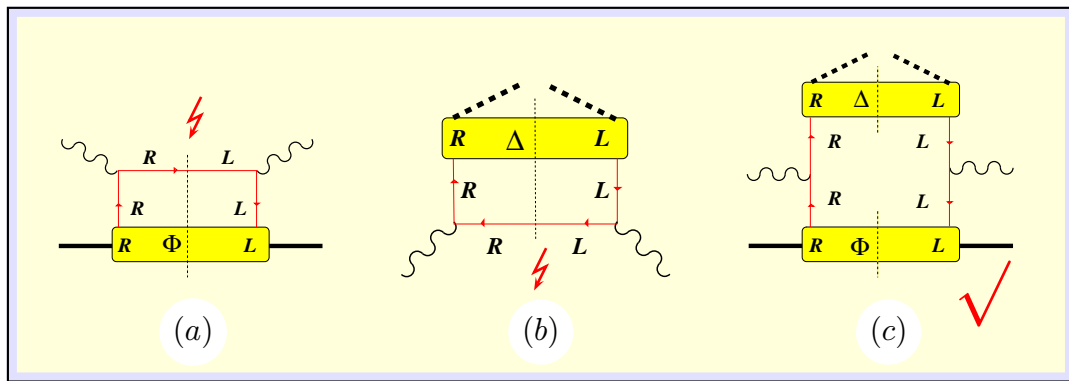


Figure 3.15: Chiral odd functions can hardly be probed in the simple processes (a) DIS and (b) $e^+e^- \rightarrow hX$, where they contribute only via (suppressed) quark mass effects. But they are accessible when combined with another chiral odd quantity like e.g. in (c) ($\ell H \rightarrow \ell' hX$).

With the above discussion $h_1(x)$ appears to have a very special rôle within the three leading twist nucleon PDFs. Actually, though this is certainly true for its experimental accessibility, from a theoretical point of view and the information comprised on the spin decomposition of the nucleon, the transversity distribution is on the same footing as the helicity distribution $g_1(x)$. In a helicity or chirality basis (compare the Weyl representation in appendix A), where γ_5 and $\Sigma^3 = \frac{i}{2} [\gamma^1, \gamma^2]$ are diagonal, the $h_1(x)$ function appears to be non-diagonal and

thus behaves different from $f_1(x)$ and $g_1(x)$. A different choice of basis, for instance the so-called transversity basis, where γ^1 (or equivalently γ^2) is diagonal reveals that there is nothing special about $h_1(x)$. In fact, in the transversity basis $f_1(x)$ and $h_1(x)$ are diagonal, and $g_1(x)$ is non-diagonal. It is in this basis, that $h_1(x)$ acquires a simple interpretation in terms of transverse spin orientations as indicated for instance in Fig. 3.9. These considerations show that the spin information obtained in $h_1(x)$ and $g_1(x)$ are on the same level; it is just the conventional choice of the helicity basis which makes $h_1(x)$ seemingly so unusual [15, 43, 44].

ideal strategy to
extract transversity

An ideal strategy to extract the transversity distribution from data would roughly have the following steps:

1. Identify and measure an observable in a process which involves $h_1(x)$ together with a second chiral odd function, say a fragmentation function generically called $H(z)$.
2. If possible, measure the second chiral odd function $H(z)$ in a different process and combine the information to eliminate the $H(z)$ dependence in order to isolate $h_1(x)$.
3. Repeat steps 1 and 2 with two more processes for a second independent determination of $h_1(x)$ to check *universality*.

complications

Evidently, the analysis requires the combination of a number of rather complicated measurements on different processes. A reliable determination of $h_1(x)$ furthermore is complicated by the following items:

- To relate the chiral odd PDFs and PFFs from different experiments, and thus naturally obtained at different scales, one has to control the scale dependence of the functions. Evolution presently is known at least for the leading twist integrated PDFs and PFFs, but for instance only in the theoretical limit of large- N_C for the transverse momentum dependent functions [45].
- Next to leading order α_s corrections to the asymmetries involving $h_1(x)$ are largely unknown though expected to be significant. Of particular importance is the dilution of asymmetries by Sudakov factors in process which do not have a strict collinear factorisation [26]; fortunately, theoretical considerations and numerical estimates do exist for this problem [46].
- In many of the relevant observables the transversity distribution $h_1(x)$ occurs together with the second chiral-odd function as a convolution integral in transverse momentum space.

global fit of $h_1(x)$

Given the complexity of the task it is more likely that a combined fit of a model ansatz to the available data is more promising to learn about $h_1(x)$, than following the above outlined procedure step by step. Of course, to the best knowledge as much as possible of the listed ingredients should be included in such a global fitting.

In the following we will list and discuss several processes involving $h_1(x)$: [43]

- In the Drell-Yan process with two transversely polarised protons $h_1^{q/p}(x)$ occurs together with its counterpart for an antiquark $h_1^{\bar{q}/p}(x)$. This process is understood to next to leading order, but the function $h_1^{\bar{q}/p}(x)$ for an antiquark in a proton presumably is very small, and Drell-Yan rates are generically low compared to purely hadronic processes at colliders. Moreover, an upper limit for this double spin asymmetry derived in a next-to-leading order analysis by using the Soffer bounds on transversity was found to be discouragingly low [47].
- In pion production in DIS at twist three level $h_1^{q/p}(x)$ occurs together with the chiral-odd fragmentation function $E(z)$. But the process is power suppressed and there is a competing chiral-even mechanism $g_T(x) \otimes D_1(z)$ which must be subtracted.
- The transversity distribution $h_1^{q/p}(x)$ occurs at leading twist together with the chiral-odd PFF $H_1(z)$ in Λ production in electron scattering $ep^\uparrow \rightarrow \Lambda^\uparrow X$ on a transversely polarised target, or proton scattering $pp^\uparrow \rightarrow \Lambda^\uparrow X$ on a transversely polarised target [48]. By the kinematics of the observed decay of the Λ its polarisation can be determined. But semi-inclusive data with Λ in the final state are scarce. The relevant quantity here in both cases is a double spin asymmetry.

There are more observables involving $h_1(x)$ in different hard semi-inclusive processes (for discussions of various options see [49, 50]). Some of them deserve special consideration in the context of this report and will be discussed in more detail in the following, since they exemplify the rôle of quark transverse momenta.

3.2.5.1 Collins effect in SIDIS ($\ell H \rightarrow \ell' h X$):

Following Collins and collaborators a very promising option to access transversity is given by a single spin asymmetry (SSA) in semi-inclusive DIS, if the transverse momentum of the produced hadron, say a pion, is determined relative to the current fragmentation jet. The kinematical situation is sketched in Fig. 3.16.

SSA in SIDIS

The relevant terms in the differential cross section at leading order for DIS with an unpolarised beam and a transversely polarised target are [26, 18, 33, 51]

$$\begin{aligned} \frac{d\sigma_{OT}}{dx_{Bj} dy dz_h d\phi^\ell d^2P_{h\perp}} &= \frac{2\alpha^2 x_{Bj} S}{Q^4} |\mathbf{S}_\perp| \sum_{\mathbf{a}, \bar{\mathbf{a}}} \mathbf{e}_\mathbf{a}^2 \\ &\times \left\{ (1-y) \sin(\phi_h^\ell + \phi_S^\ell) \mathcal{F} \left[\frac{\hat{\mathbf{h}} \cdot \mathbf{k}_T}{M_h} h_1^{\mathbf{a}} H_1^{\perp \mathbf{a}} \right] \right. \\ &\quad \left. + (1-y) \sin(3\phi_h^\ell - \phi_S^\ell) \right. \\ &\quad \left. \times \mathcal{F} \left[\frac{4(\hat{\mathbf{h}} \cdot \mathbf{p}_T)^2 (\hat{\mathbf{h}} \cdot \mathbf{k}_T) - 2(\hat{\mathbf{h}} \cdot \mathbf{p}_T)(\mathbf{p}_T \cdot \mathbf{k}_T) - \mathbf{p}_T^2 (\hat{\mathbf{h}} \cdot \mathbf{k}_T)}{M^2 M_h^2} h_{1T}^{\perp \mathbf{a}} H_1^{\perp \mathbf{a}} \right] \right\} \end{aligned}$$

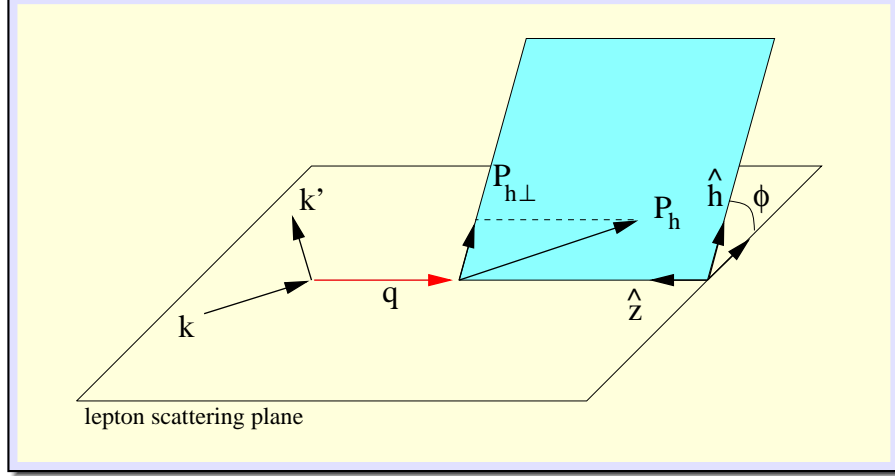


Figure 3.16: Kinematics for one-hadron inclusive DIS. The final hadron is observed in a direction out of the lepton scattering plane. The photon momentum defines the longitudinal direction. A decomposition of the P_h momentum in longitudinal and perpendicular components, defines the azimuthal angle ϕ_h^ℓ relative to the lepton scattering plane. It is convenient to introduce a normalised vector by $\hat{\mathbf{h}} = \mathbf{P}_{h\perp} / |\mathbf{P}_{h\perp}|$.

$$\begin{aligned}
 & + \left(1 - y + \frac{y^2}{2} \right) \sin(\phi_h^\ell - \phi_S^\ell) \mathcal{F} \left[\frac{\hat{\mathbf{h}} \cdot \mathbf{p}_T}{M} f_{1T}^{\perp a} D_1^a \right] \\
 & + \mathcal{O} \left(\frac{1}{Q} \right) + \mathcal{O}(\alpha_s) + \dots \} \quad (3.94)
 \end{aligned}$$

with the azimuthal angles ϕ_h^ℓ of the momentum of the produced hadron P_h , and the azimuthal angle ϕ_S^ℓ of the target spin vector, each taken with respect to the lepton scattering plane, and the convolution

$$\begin{aligned}
 \mathcal{F} [w(\mathbf{p}_T, \mathbf{k}_T) fD] & \equiv \\
 & \int d^2 \mathbf{p}_T d^2 \mathbf{k}_T \delta^2(\mathbf{p}_T + \mathbf{q}_T - \mathbf{k}_T) w(\mathbf{p}_T, \mathbf{k}_T) f(x, \mathbf{p}_T) D(z, \mathbf{k}_T). \quad (3.95)
 \end{aligned}$$

The occurrence of this convolution reveals the link between the observable momentum components $\mathbf{P}_{h\perp}$ in which the cross section is kept differential and the quark transverse momenta \mathbf{p}_T and \mathbf{k}_T . The connection is induced by momentum conservation on partonic vertices as schematically illustrated in Fig. 3.7. Note that an integration over $d^2 P_{h\perp}$ can be easily carried out by using the δ -function in Eq. (3.95) and the kinematical relation $\mathbf{P}_{h\perp}^\mu = -\mathbf{z} \mathbf{q}_T^\mu$. Both contributions in (3.94) vanish under symmetric integration over $d^2 P_{h\perp}$.

The part (3.94) can be isolated from the rest of the cross section by reversing the target polarisation and subtracting the results. The first term involving $H_1(x)$ is known as the ‘Collins effect’ [26, 52], the second term was found in [18], the third term involves the time-reversal odd PDF $f_{1T}^\perp(x)$ [33, 51]. The three terms have distinct angular dependences which can be used to discriminate between the contributions. The big advantages of accessing transversity via the Collins effect are that it occurs at leading order, and there is no determination of a spin state of a final hadron necessary. In a sense, a necessary second spin vector was traded for a dependence on transverse momentum relative to the jet.

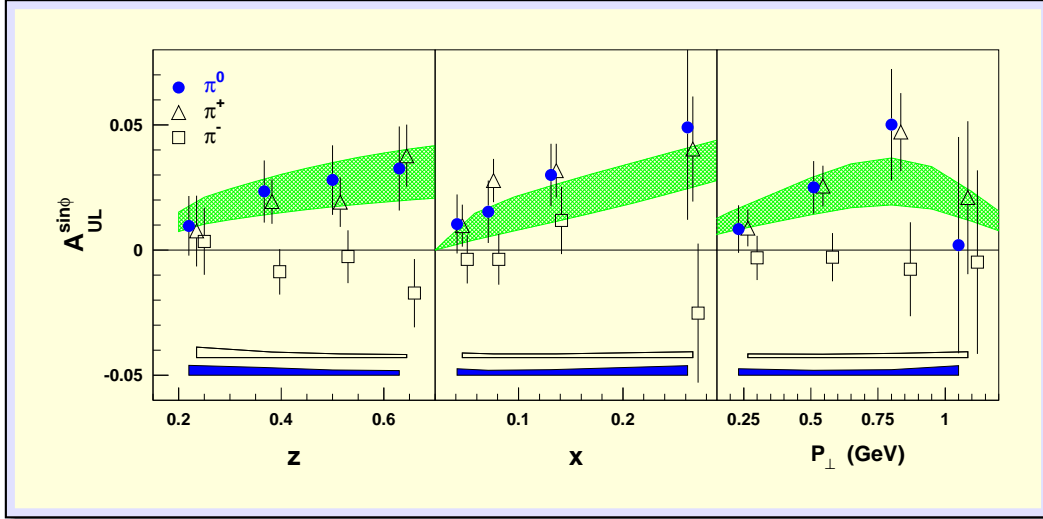


Figure 3.17: Single spin azimuthal asymmetry in electroproduction of pions in deep inelastic scattering (Collins effect) measured at HERMES. Shown is the $\sin(\phi)$ moment $A_{UL}^{\sin\phi}$ for unpolarised beam and longitudinally polarised target vs. z, x , and p_T .

Though the possibility was mentioned in the original proposal by Collins [26] the importance of a dilution of the effect by Sudakov factors was quantitatively estimated only recently [46]. The origin for this additional complication lies in the fact that collinear factorisation does not apply, since it is a multiple scale process depending on Q^2 , $|P_{h\perp}|$ (with $|P_{h\perp}| \ll Q^2$). However, one can avoid this problem by considering an asymmetry expression that is weighted with a power of the observed transverse momentum [33]

$$\frac{\langle \sin(\phi_h^\ell + \phi_S^\ell) Q_T/M_h \rangle}{4\pi \alpha^2 s/Q^4} = |\mathbf{S}_\perp| (1-y) \sum_{a,\bar{a}} e_a^2 x h_1^a(x) H_1^{\perp(1)a}(z) \quad (3.96)$$

with $Q_T \equiv |P_{h\perp}|/z$, the moment

$$H_1^{\perp(1)a}(z) \equiv z^2 \int d^2\mathbf{k}_T \left(\frac{\mathbf{k}_T^2}{2M_h^2} \right) H_1^{\perp a}(z, \mathbf{k}_T^2), \quad (3.97)$$

and where the weighting of a cross section is defined by

$$\langle W(Q_T, \phi_h^\ell, \phi_S^\ell) \rangle \equiv \int d\phi^\ell d^2q_T W(Q_T, \phi_h^\ell, \phi_S^\ell) \frac{d\sigma}{dx_{Bj} dy dz_h d\phi^\ell d^2q_T} \quad (3.98)$$

The observation of a $\sin(\phi_h^\ell)$ asymmetry in semi-inclusive DIS has been reported by HERMES [53] and SMC [54]. In Fig. 3.17 the HERMES data are shown as $\sin(\phi)$ weighted asymmetry.

Though the asymmetry was measured with a longitudinal polarised target, it involves the weighted cross section of Eq. (3.96), since the direction of polarisation experimentally refers to the lepton beam, which results in large spin

components longitudinal to the photon, but also – on the average small – components transverse to the photon. Therefore, the asymmetry receives two different contributions, from Eq. (3.96) and from the weighted cross section [18, 55]

$$\begin{aligned} \left\langle \frac{Q_T}{M} \sin(\phi_h^\ell) \right\rangle_{OL} &= \frac{4\pi\alpha^2 s}{Q^4} \lambda(2-y) \sqrt{1-y} \frac{2M_h}{Q} \\ &\times \sum_{a,\bar{a}} e_a^2 \left\{ x_{B_j} h_{1L}^{\perp(1)a}(x_{B_j}) \frac{\tilde{H}^a(z)}{z} \right. \\ &\left. - x_{B_j} \left[x_{B_j} h_L^a(x_{B_j}) - \frac{m}{M} g_{1L}^a(x_{B_j}) \right] H_1^{\perp(1)a}(z) \right\}, \end{aligned} \quad (3.99)$$

where $\tilde{H}(z)$ is an interaction dependent twist three PFF defined by the relation

$$H(z, \mathbf{k}'_T{}^2) = -\frac{\mathbf{k}'_T{}^2}{M_h^2} z H_1^\perp(z, \mathbf{k}'_T{}^2) + \tilde{H}(z, \mathbf{k}'_T{}^2). \quad (3.100)$$

There is some confusion in the literature about the relative sign between the two contributions caused by a typo in Ref. [18], which was corrected in [55] (see also the Erratum to Ref. [56]³).

Since the target polarisation is in the lepton plane, the azimuthal angle of the spin vector components transverse to the photon ϕ_S^ℓ can take only the values $\phi_S^\ell = \{\pi, 0\}$ leading to $\sin(\phi_h^\ell + \phi_S^\ell) \rightarrow \{\sin(\phi_h^\ell), -\sin(\phi_h^\ell)\}$. Consequently, both contributions Eqs. (3.96) and (3.99) feed into the same $\sin(\phi_h^\ell)$ asymmetry. Although the contributions from (3.99) are power suppressed compared to (3.96), they cannot be neglected for the asymmetry shown in Fig. 3.17, since they are enhanced by the large longitudinal polarisation components compared to the small transverse polarisation components accompanying (3.96). Thus, for a direct extraction of $h_1(x)$ — even if one would know the function $H_1^{\perp(1)}(z)$ — these data are not sufficient; the sensitivity of the SSA in an experiment with longitudinally polarised target to $h_1(x)$ is very small. On the other hand, utilising theoretical estimates and approximation, like the neglect all interaction dependent functions known as Wandzura-Wilczek approximation [58], combined with model calculations for all involved functions a good agreement with data can be achieved [57]. The positive conclusions from the experimental observation of this single spin asymmetry is that a significant large moment of the Collins fragmentation function $H_1^{\perp(1)}(z)$ is very likely.

A similar positive conclusion on $H_1^{\perp(1)}(z)$ can be drawn from the observed large asymmetry in pionproduction in pp scattering, $p^\uparrow p \rightarrow \pi X$, at the Tevatron (Fermilab) [59]. However, an extraction of the function here is even more difficult, because the description of this process involves three soft matrix elements. A phenomenological analysis relating the asymmetry to the Collins effect has been done [60].

In the near future measurements will be done at HERMES and COMPASS with targets polarised transverse to the lepton beam. Here the polarisation components transverse to the photon direction will be dominant on the average,

³Contrary to a statement in the Erratum to Ref. [56] the sign was taken correctly in References [57] (private communication by K. Oganessian).

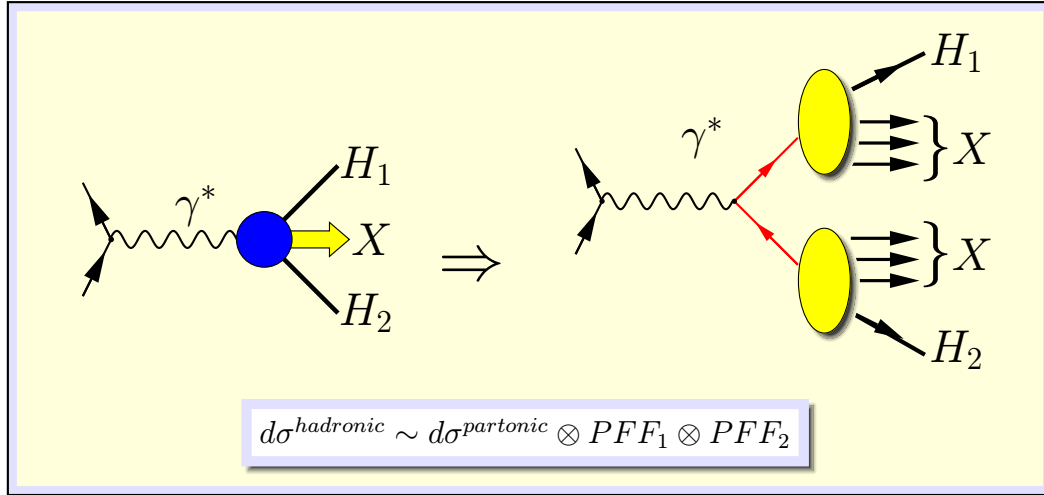


Figure 3.18: Two-hadron (in separate jets) inclusive electron-positron annihilation in the parton model interpretation.

which allows a much more direct access to the cross section of Eq. (3.94), and the asymmetry of Eq. (3.96).

3.2.5.2 Collins effect in e^+e^- annihilation ($e^+e^- \rightarrow h_1h_2X$):

Information on the time-reversal odd and chiral-odd fragmentation function, $H_1^\perp(z)$, can be obtained from the electron-positron annihilation with two hadrons observed, each in a separate jet, $e^+e^- \rightarrow h_1h_2X$ (see Fig. 3.18).

H_1^\perp from e^+e^- annihilation

The complete differential cross section to next-to-leading twist accuracy (albeit at tree-level in the strong coupling) was discussed in [61], and the leading twist asymmetries at the Z -pole where the bulk of the data is available in [62]. The leading contribution to the process is described by a handbag-type diagram involving two soft matrix elements for the quark(antiquark) hadronisation (see Fig. 3.19), up to order $1/Q$ gluonic corrections connecting soft and hard scattering parts have to be included (see Fig. 3.20).

The physical picture of the process at tree-level is the following. Electron and positron annihilate forming a photon or Z -boson which creates a quark-antiquark pair. The spin of the quark and antiquark will be anticorrelated for each single event. If the quark spin has a transverse component, it can be correlated to the transverse momentum a produced hadron has relative to the jet via the Collins effect described by the function $H_1^\perp(z)$. The same holds true for the antiquark; its transverse spin component can be correlated to the transverse momentum of a hadron relative to the antiquark jet by a function $\overline{H}_1^\perp(z)$. As the net effect of the double occurrence of the Collins effect in each of the two jets, the azimuthal distributions of two hadrons relative to their respective jet directions can be correlated in a measurable way.

The kinematics of the process in a lepton centre of mass frame is shown in Fig. 3.21. The hadron momenta are denoted P_1 and P_2 , one of the hadron momenta, say P_2 , serves to define the longitudinal direction, the other hadron

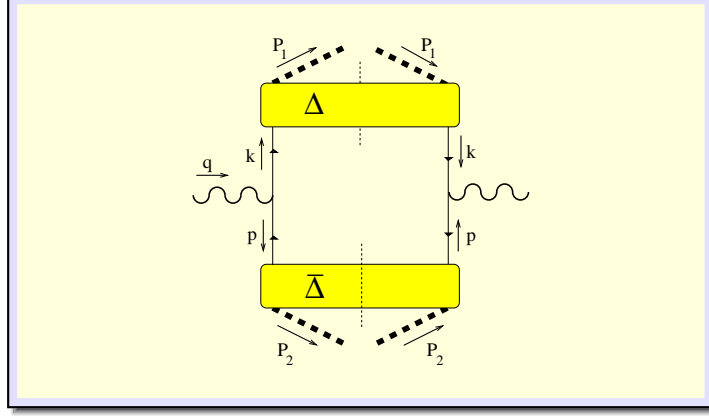


Figure 3.19: Quark diagram contributing to e^+e^- annihilation in leading order. There is a similar diagram with reversed fermion flow.

momenta in general is out of the lepton plane and its perpendicular direction defines the azimuthal angle ϕ_1 . For convenience normalised vectors $\hat{\mathbf{h}} = \mathbf{P}_{1\perp}/|\mathbf{P}_{1\perp}|$ (in the hadron plane) and $\hat{\mathbf{l}}_{\perp}$ (in the lepton plane) are defined.

Considering the asymmetry at the Z -pole where most of the electron/positron data are available (and where contributions from photons and $\gamma - Z$ interference can safely be neglected) the the vector and axial couplings of the Z boson to quark lines occur, which are given by:

$$g_V^j = T_3^j - 2Q^j \sin^2 \theta_W, \quad (3.101)$$

$$g_A^j = T_3^j, \quad (3.102)$$

where Q^j denotes the charge and T_3^j the weak isospin of particle j (i.e., $T_3^j = +1/2$ for $j = u$ and $T_3^j = -1/2$ for $j = e^-, d, s$). Combinations of the couplings occurring frequently in the formulas are

$$\begin{aligned} c_1^j &= (g_V^{j2} + g_A^{j2}), \\ c_2^j &= (g_V^{j2} - g_A^{j2}), \quad j = \ell \text{ or } u, d, s \\ c_3^j &= 2g_V^j g_A^j. \end{aligned} \quad (3.103)$$

In leading order in $1/Q$ and α_s the following expression for the cross section are obtained in case of unpolarised (or spinless) final state hadrons:

$$\begin{aligned} \frac{d\sigma(e^+e^- \rightarrow h_1 h_2 X)}{d\Omega dz_1 dz_2 d^2\mathbf{q}_T} &= \sum_{a,\bar{a}} \frac{3\alpha_w^2 Q^2}{(Q^2 - M_Z^2)^2 + \Gamma_Z^2 M_Z^2} z_1^2 z_2^2 \\ &\times \left\{ \left(c_1^\ell c_1^a \left(\frac{1}{2} - y + y^2 \right) - \frac{1}{2} c_3^\ell c_3^a (1 - 2y) \right) \mathcal{F} [D_1^a \bar{D}_1^a] \right. \\ &\left. + \cos(2\phi_1) c_1^\ell c_2^a y(1 - y) \mathcal{F} \left[\left(2\hat{\mathbf{h}} \cdot \mathbf{k}_T \hat{\mathbf{h}} \cdot \mathbf{p}_T - \mathbf{k}_T \cdot \mathbf{p}_T \right) \frac{H_1^{\perp a} \bar{H}_1^{\perp a}}{M_1 M_2} \right] \right\}, \end{aligned} \quad (3.104)$$

where $d\Omega = 2dy d\phi^l$ and ϕ^l gives the orientation of \hat{l}_1^μ . The convolution notation

$$\mathcal{F} [D^a \bar{D}^a] \equiv \int d^2\mathbf{k}_T d^2\mathbf{p}_T \delta^2(\mathbf{p}_T + \mathbf{k}_T - \mathbf{q}_T) D^a(z_1, z_1^2 \mathbf{k}_T^2) \bar{D}^a(z_2, z_2^2 \mathbf{p}_T^2) \quad (3.105)$$

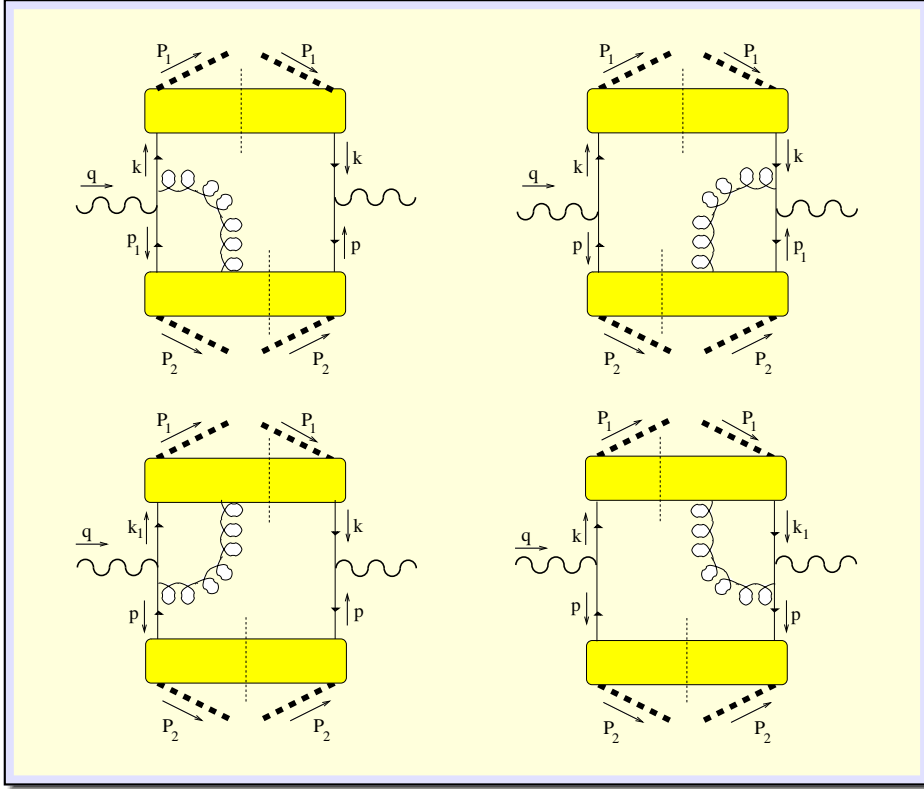


Figure 3.20: Diagrams contributing to e^+e^- annihilation at order $1/Q$.

was used. The angle ϕ_1 is the azimuthal angle of \hat{h} (see Fig. 3.21). In order to deconvolute these expressions one can define weighted cross sections

$$\langle W \rangle = \int \frac{d\phi^\ell}{2\pi} d^2\mathbf{q}_T W \frac{d\sigma(e^+e^- \rightarrow h_1 h_2 X)}{d\Omega dz_1 dz_2 d^2\mathbf{q}_T}, \quad (3.106)$$

where $W = W(Q_T, \phi_1, \phi_2, \phi_{S_1}, \phi_{S_2})$. To access the relevant information one utilises the weighted cross sections

$$\begin{aligned} \langle 1 \rangle_O &= \frac{3\alpha_w^2 Q^2}{(Q^2 - M_Z^2)^2 + \Gamma_Z^2 M_Z^2} \sum_{a,\bar{a}} \\ &\times \left(c_1^\ell c_1^a \left(\frac{1}{2} - y + y^2 \right) - \frac{1}{2} c_3^\ell c_3^a (1 - 2y) \right) D_1^a(z_1) \bar{D}_1^a(z_2), \end{aligned} \quad (3.107)$$

and

$$\begin{aligned} \left\langle \frac{Q_T^2}{4M_1 M_2} \cos(2\phi_1) \right\rangle &= \frac{3\alpha_w^2 Q^2}{(Q^2 - M_Z^2)^2 + \Gamma_Z^2 M_Z^2} \sum_{a,\bar{a}} \\ &\times c_1^\ell c_2^a y(1 - y) H_1^{\perp(1)a}(z_1) \bar{H}_1^{\perp(1)a}(z_2), \end{aligned} \quad (3.108)$$

where the \mathbf{k}_T^2 -moments for a generic fragmentation function F are defined by

$$F^{(n)}(z_i) = z_i^2 \int d^2\mathbf{k}_T \left(\frac{\mathbf{k}_T^2}{2M_i^2} \right)^n F(z_i, z_i^2 \mathbf{k}_T^2). \quad (3.109)$$

Note that the same moment of $H_1^\perp(z, \mathbf{k}_T^2)$ enters Eq. (3.108) as in the weighted cross section of SIDIS (3.96).

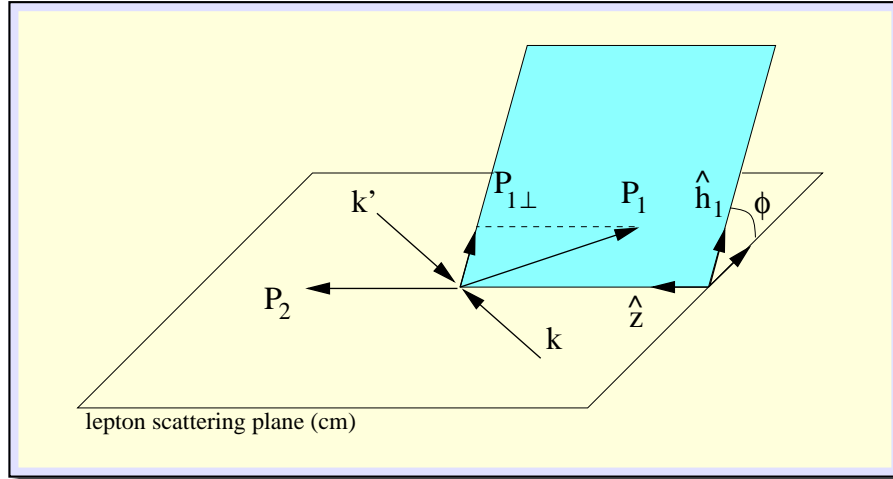


Figure 3.21: Kinematics of the annihilation process in the lepton centre of mass frame for a back-to-back jet situation. P_1 (P_2) is the momentum of a fast hadron in jet one (two).

A first indication of a nonzero correlation comes from a preliminary analysis [63] of the 91-95 LEP data (DELPHI). Several phenomenological analyses used this information together with additional assumptions, for instance on isospin relations, or model input to look for possible agreement with data.

The $\cos(2\phi)$ asymmetry of $e^+e^- \rightarrow h_1 h_2 X$ is a very clear example for the interplay of spin degrees of freedom and the intrinsic transverse momenta of partons with respect to their parent hadrons. Even without determining polarisation of a final state hadron a subtle test of our understanding of spin transfer mechanisms in perturbative QCD can be done here. The information on the production of a transversely polarised quark-antiquark pair, which subsequently fragment into unpolarised (or spinless) hadrons with probabilities depending on the orientation of the (anti)quarks spin vector relative to its transverse momentum, is contained in an azimuthal asymmetry. This is in fact *spin physics with spin-0 hadrons*.

3.2.5.3 SSA in $\pi\pi$ production – interference fragmentation functions:

There is another very promising option to access the transversity distribution in processes where two hadrons in the same jet are detected [52, 64, 65, 43, 44]. As in the previous subsection, again there is no determination of spin of final state hadrons necessary, which facilitates the experimental requirements. The measured hadrons for instance can be a pair of pions (or Kaons) which are abundant in energetic jets and provide large counting rates.

Before proceeding with the discussion on the strategies for a possible extraction of $h_1(x)$ making use of the two-hadron interference fragmentation functions we have to set up some definitions, thereby generalising the methods and the classification scheme of subsection 3.2.3 for the case of a single detected spin-1/2 hadron to the present case. The notation will largely follow Reference [42].

In analogy with the quark-quark correlation function involving one detected hadron in the final state, the simplest matrix element for the hadronisation into

two hadrons is the quark-quark correlation function describing the decay of a quark with momentum k into two hadrons with momenta P_1, P_2 (see Fig. 3.22), namely

$$\Delta_{ij}(k; P_1, P_2) = \not{\int}_X \int \frac{d^4\zeta}{(2\pi)^4} e^{ik\cdot\zeta} \times \langle 0 | \psi_i(\zeta) a_2^\dagger(P_2) a_1^\dagger(P_1) | X \rangle \langle X | a_1(P_1) a_2(P_2) \bar{\psi}_j(0) | 0 \rangle, \quad (3.110)$$

where $a^\dagger(P)$ ($a(P)$) are hadronic creation (annihilation) operators, and the sum runs over all the possible intermediate states involving the two final hadrons P_1, P_2 . For the Fourier transform only the two space-time points 0 and ζ matter, i.e. the positions of quark creation and annihilation, respectively. Their relative distance ζ is the conjugate variable to the quark momentum k .

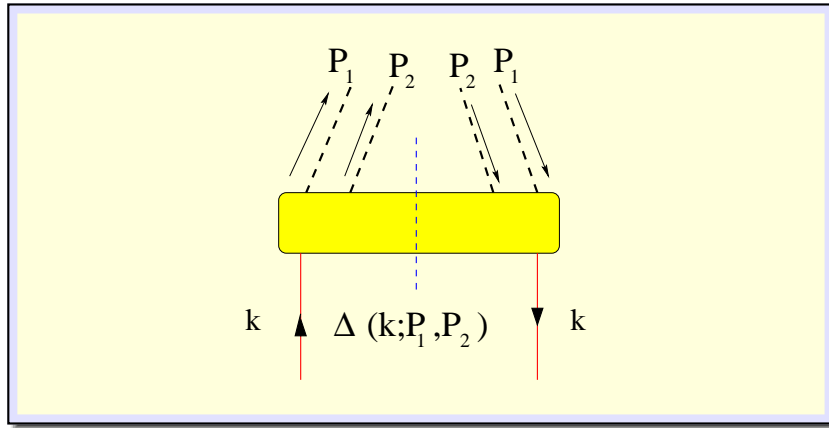


Figure 3.22: Quark-quark correlation function for the fragmentation of a quark into a pair of hadrons.

By generalising the Collins-Soper light-cone formalism [66, 5] for fragmentation into multiple hadrons [64, 44], the cross sections for semi-inclusive processes with two-hadron detected in the same jet can be expressed in terms of specific Dirac projections of $\Delta(k; P_1, P_2)$ after integrating over the (hard-scale suppressed) light-cone component k^+ and, consequently, taking ζ as light-like [18], i.e.

$$\begin{aligned} \Delta^{[\Gamma]} &= \frac{1}{4z_h} \int dk^+ \text{Tr}[\Delta\Gamma] \Big|_{\zeta^-=0} \\ &= \frac{1}{4z_h} \int dk^+ \int dk^- \delta\left(k^- - \frac{P_h^-}{z_h}\right) \text{Tr}[\Delta\Gamma]. \end{aligned} \quad (3.111)$$

Let us discuss the kinematical variables the projection $\Delta^{[\Gamma]}$ depends on. The integrand of (3.111) in principal depends on all the invariants which can be built from the momenta k, P_1, P_2 and the light-like vector $n_+ = [1, 0, \mathbf{0}_T]$ induced by the δ -function. We choose for convenience a frame where the total pair momentum $P_h = P_1 + P_2$ has no transverse component. The constraint to reproduce on-shell hadrons with fixed mass ($P_1^2 = M_1^2, P_2^2 = M_2^2$) and the condition $n_+^2 = 0$ reduces to seven the number of independent degrees of freedom. They can conveniently be reexpressed in terms of the light-cone component of the hadron

pair momentum, $P_h^- = P_h \cdot n_+$, of the light-cone fraction of the quark momentum carried by the hadron pair, $z_h = P_h^-/k^- = z_1 + z_2$, of the fraction of hadron pair momentum carried by each individual hadron, $\xi = z_1/z_h = 1 - z_2/z_h$, and of the four independent invariants that can be formed by means of the momenta k, P_1, P_2 at fixed masses M_1, M_2 , i.e.

$$\begin{aligned}\tau_h &= k^2, \\ \sigma_h &= 2k \cdot (P_1 + P_2) \equiv 2k \cdot P_h, \\ \sigma_d &= 2k \cdot (P_1 - P_2) \equiv 4k \cdot R, \\ M_h^2 &= (P_1 + P_2)^2 \equiv P_h^2,\end{aligned}\tag{3.112}$$

with $R \equiv (P_1 - P_2)/2$ being (half of) the relative momentum between the hadron pair. An explicit parametrisation for the three momenta external to Δ is

$$\begin{aligned}k &= \left[\frac{P_h^-}{z_h}, z_h \frac{k^2 + \vec{k}_T^2}{2P_h^-}, \vec{k}_T \right] \\ P_1 &= \left[P_h^- \frac{z_1}{z_h}, \frac{z_h(M_1^2 + \vec{R}_T^2)}{2z_1 P_h^-}, \vec{R}_T \right] \\ P_2 &= \left[P_h^- \frac{z_2}{z_h}, \frac{z_h(M_2^2 + \vec{R}_T^2)}{2z_2 P_h^-}, -\vec{R}_T \right].\end{aligned}\tag{3.113}$$

After the two integrations the projection $\Delta^{[\Gamma]}$ now depends on five variables, apart from the Lorentz structure of the Dirac matrix Γ . In order to make this more explicit and to reexpress the set of variables in a more convenient way, let us rewrite the integrations in Eq. (3.111) in a covariant way using

$$2P_h^- = \frac{d\sigma_h}{dk^+}, \quad 2k^+ = \frac{d\tau_h}{dk^-},\tag{3.114}$$

and the relation

$$\begin{aligned}\frac{1}{2k^+} \delta\left(k^- - \frac{P_h^-}{z_h}\right) &= \delta\left(2k^+ k^- - \frac{2k^+ P_h^-}{z_h}\right) \\ &= \delta\left(\tau_h + \vec{k}_T^2 - \frac{\sigma_h}{z_h} + \frac{M_h^2}{z_h^2}\right)\end{aligned}\tag{3.115}$$

which leads to the result

$$\begin{aligned}\Delta^{[\Gamma]}(z_h, \xi, \vec{k}_T^2, M_h^2, \sigma_d) &= \int d\sigma_h d\tau_h \delta\left(\tau_h + \vec{k}_T^2 - \frac{\sigma_h}{z_h} + \frac{M_h^2}{z_h^2}\right) \\ &\quad \times \frac{\text{Tr}[\Delta(z_h, \xi, P_h^-, \tau_h, \sigma_h, M_h^2, \sigma_d) \Gamma]}{8z_h P_h^-},\end{aligned}\tag{3.116}$$

where the dependence on the transverse quark momentum \vec{k}_T^2 through σ_h is made explicit by means of

$$\sigma_h = 2k \cdot P_h = \left\{ \frac{M_1^2 + \vec{R}_T^2}{z_h \xi} + \frac{M_2^2 + \vec{R}_T^2}{z_h (1 - \xi)} \right\} + z_h (\tau_h + \vec{k}_T^2)\tag{3.117}$$

and

$$\vec{R}_T^2 = \xi(1 - \xi) M_h^2 - (1 - \xi) M_1^2 - \xi M_2^2 . \quad (3.118)$$

with $\xi = z_1/z_h$.

Using further the relations

$$\begin{aligned} \tau_h &= k^2 \\ \sigma_d &= 2k \cdot (P_1 - P_2) \\ &= \left\{ \frac{M_1^2 + \vec{R}_T^2}{z_h \xi} - \frac{M_2^2 + \vec{R}_T^2}{z_h (1 - \xi)} \right\} + z_h(2\xi - 1)(\tau_h + \vec{k}_T^2) - 4\vec{k}_T \cdot \vec{R}_T \\ M_h^2 &= P_h^2 \\ &= 2P_h^+ P_h^- = \left\{ \frac{M_1^2 + \vec{R}_T^2}{\xi} + \frac{M_2^2 + \vec{R}_T^2}{1 - \xi} \right\} \end{aligned} \quad (3.119)$$

makes it possible to reexpress $\Delta^{[\Gamma]}$ as a function of z_h , ξ , \vec{k}_T^2 and \vec{R}_T^2 , $\vec{k}_T \cdot \vec{R}_T$, where \vec{R}_T is (half of) the transverse momentum between the two hadrons in the considered frame. In this manner $\Delta^{[\Gamma]}$ depends on how much of the fragmenting quark momentum is carried by the hadron pair (z_h), on the way this momentum is shared inside the pair (ξ), and on the “geometry” of the pair, namely on the relative momentum of the two hadrons (\vec{R}_T^2) and on the relative orientation between the pair plane and the quark jet axis (\vec{k}_T^2 , $\vec{k}_T \cdot \vec{R}_T$, see also Fig. 3.23). The kinematical dependencies derived by general considerations have been rewritten to quantities in a specific frame, which have an obvious geometric meaning.

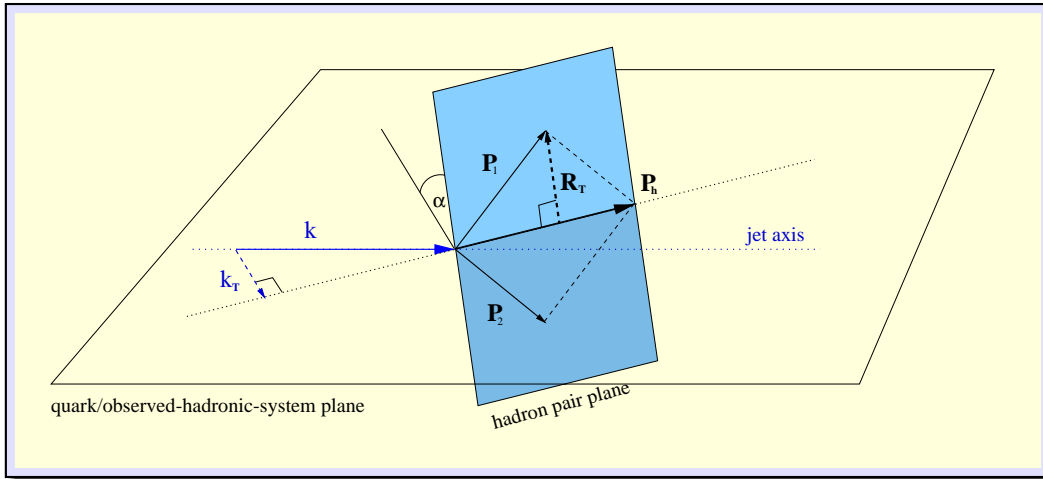


Figure 3.23: Kinematics for a fragmenting quark jet containing a pair of leading hadrons.

If the polarisations of the two final hadrons are not observed, the quark-quark correlation $\Delta(k; P_1, P_2)$ of Eq. (3.110) can be generally expanded, according to hermiticity and parity invariance, as a linear combination of the independent Dirac structures of the process

$$\Delta(k; P_1, P_2) = B_1 (M_1 + M_2) + B_2 \not{P}_1 + B_3 \not{P}_2 + B_4 \not{k}$$

$$\begin{aligned}
& + \frac{B_5}{M_1} \sigma^{\mu\nu} P_{1\mu} k_\nu + \frac{B_6}{M_2} \sigma^{\mu\nu} P_{2\mu} k_\nu + \frac{B_7}{M_1 + M_2} \sigma^{\mu\nu} P_{1\mu} P_{2\nu} \\
& + \frac{B_8}{M_1 M_2} \gamma_5 \epsilon^{\mu\nu\rho\sigma} \gamma_\mu P_{1\nu} P_{2\rho} k_\sigma .
\end{aligned} \tag{3.120}$$

Symmetry constraints are obtained in the form

$$\gamma_0 \Delta^\dagger(k; P_1, P_2) \gamma_0 = \Delta(k; P_1, P_2) \quad [\text{Hermiticity}] , \tag{3.121}$$

$$\gamma_0 \Delta(\bar{k}; \bar{P}_1, \bar{P}_2) \gamma_0 = \Delta(k; P_1, P_2) \quad [\text{Parity}] , \tag{3.122}$$

$$\left(\gamma_5 C \Delta(\bar{k}; \bar{P}_1, \bar{P}_2) C^\dagger \gamma_5 \right)^* = \Delta(k; P_1, P_2) \quad [\text{Time reversal}] , \tag{3.123}$$

where $\bar{a} = (a^0, -\vec{a})$ and $C = i \gamma^2 \gamma^0$. From the hermiticity of the fields it follows that

$$B_i^* = B_i \quad \text{for } i = 1, \dots, 12 \tag{3.124}$$

and, if constraints from time-reversal invariance can be applied, that

$$B_i^* = B_i \quad \text{for } i = 1, \dots, 4 \quad B_i^* = -B_i \quad \text{for } i = 5, \dots, 8 , \tag{3.125}$$

which means in that case $B_5 = B_6 = B_7 = B_8 = 0$, i.e. terms involving B_5, \dots, B_8 are naive ‘‘T-odd’’.

Inserting the ansatz (3.120) in Eq. (3.116) and reparametrising the momenta k, P_1, P_2 with the indicated new set of variables, one gets the following Dirac projections

$$\begin{aligned}
\Delta^{[\gamma^-]}(z_h, \xi, \vec{k}_T^2, \vec{R}_T^2, \vec{k}_T \cdot \vec{R}_T) & \equiv D_1(z_h, \xi, \vec{k}_T^2, \vec{R}_T^2, \vec{k}_T \cdot \vec{R}_T) \\
& = \frac{1}{2z_h} \int [d\sigma_h d\tau_h] \left[B_2 \xi + B_3 (1 - \xi) + B_4 \frac{1}{z_h} \right]
\end{aligned} \tag{3.126}$$

$$\begin{aligned}
\Delta^{[\gamma^- \gamma_5]}(z_h, \xi, \vec{k}_T^2, \vec{R}_T^2, \vec{k}_T \cdot \vec{R}_T) & \equiv \frac{\epsilon_T^{ij} R_{Ti} k_{Tj}}{M_1 M_2} G_1^\perp(z_h, \xi, \vec{k}_T^2, \vec{R}_T^2, \vec{k}_T \cdot \vec{R}_T) \\
& = \frac{\epsilon_T^{ij} R_{Ti} k_{Tj}}{M_1 M_2} \frac{1}{2z_h} \int [d\sigma_h d\tau_h] [-B_8]
\end{aligned} \tag{3.127}$$

$$\begin{aligned}
\Delta^{[i\sigma^{i-} \gamma_5]}(z_h, \xi, \vec{k}_T^2, \vec{R}_T^2, \vec{k}_T \cdot \vec{R}_T) & \equiv \frac{\epsilon_T^{ij} R_{Tj}}{M_1 + M_2} H_1^\perp(z_h, \xi, \vec{k}_T^2, \vec{R}_T^2, \vec{k}_T \cdot \vec{R}_T) \\
& + \frac{\epsilon_T^{ij} k_{Tj}}{M_1 + M_2} H_1^\perp(z_h, \xi, \vec{k}_T^2, \vec{R}_T^2, \vec{k}_T \cdot \vec{R}_T) \\
& = \frac{\epsilon_T^{ij} R_{Tj}}{M_1 + M_2} \frac{1}{2z_h} \int [d\sigma_h d\tau_h] \left[-B_5 \left(\frac{M_1 + M_2}{z_h M_1} \right) + B_6 \left(\frac{M_1 + M_2}{z_h M_2} \right) - B_7 \right] \\
& + \frac{\epsilon_T^{ij} k_{Tj}}{M_1 + M_2} \frac{1}{2z_h} \int [d\sigma_h d\tau_h] \left[B_5 \xi \left(\frac{M_1 + M_2}{M_1} \right) + B_6 (1 - \xi) \left(\frac{M_1 + M_2}{M_2} \right) \right] ,
\end{aligned} \tag{3.128}$$

where $\epsilon_T^{\mu\nu} \equiv \epsilon^{-+\mu\nu}$ (such that i, j are transverse indices) and

$$\int [d\sigma_h d\tau_h] \equiv \int d\sigma_h d\tau_h \delta \left(\tau_h + \vec{k}_T^2 - \frac{\sigma_h}{z_h} + \frac{M_h^2}{z_h^2} \right) . \tag{3.129}$$

Transverse 4-vectors are defined as $a_T^\mu = g_T^{\mu\nu} a_\nu = [0, 0, \vec{a}_T]$ (with $g_T^{\mu\nu} = g^{\mu\nu} - n_+^\mu n_-^\nu - n_-^\mu n_+^\nu$).

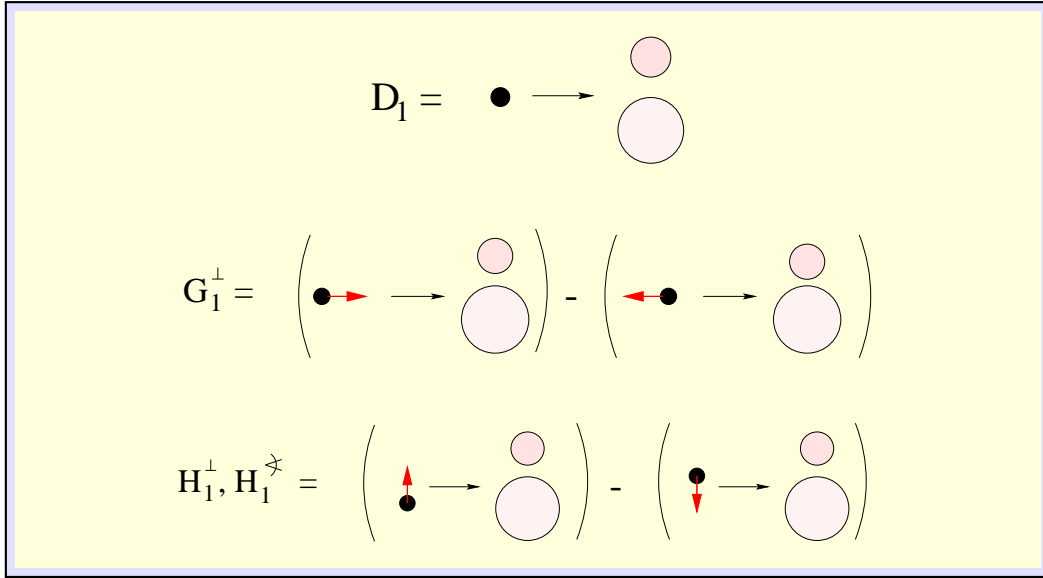


Figure 3.24: Probabilistic interpretation for the leading order FF arising in the decay of a current quark into a pair of unpolarised hadrons.

The functions D_1 , G_1^\perp , $H_1^{\star\perp}$, H_1^\perp are the FF that arise to leading order in $1/Q$ for the fragmentation of a current quark into two unpolarised hadrons inside the same jet. The different Dirac structures used in the projections are related to different spin states of the fragmenting quark and lead to a nice probabilistic interpretation [42]. As illustrated in Fig. 3.24, D_1 is the probability for an unpolarised quark to produce a pair of unpolarised hadrons; G_1^\perp is the difference of probabilities for a quark with opposite chiralities to produce a pair of unpolarised hadrons; $H_1^{\star\perp}$ and H_1^\perp both are differences of probabilities for a transversely polarised quark with opposite spins to produce a pair of unpolarised hadrons.

The interference functions G_1^\perp , $H_1^{\star\perp}$ and H_1^\perp are (naive) “T-odd”. In fact, the probability for an anyway polarised quark with observed transverse momentum to fragment into unpolarised hadrons is non-vanishing only if there are residual interactions in the final state. In this case, the constraint (3.123) still holds, but does not imply the condition (3.125) and indeed the projections (3.128), (3.129) are non-vanishing. A measure of these functions would directly give the size and importance of such FSI inside the jet.

G_1^\perp is chiral even; it has a counterpart in the FF for one-hadron semi-inclusive production. In that case, from the $\Delta^{[\gamma^-]}$ projection a “T-odd” FF arises, named D_{1T}^\perp , which describes the probability for an unpolarised quark with observed transverse momentum to fragment in a transversely polarised hadron [18]. It is known also in a different context [67] that the similarity is recovered by substituting an axial vector (the hadron transverse spin) with a vector (the momentum of a second detected hadron) and by balancing this change in parity with the introduction of the quark polarisation.

The functions $H_1^{\star\perp}$ and H_1^\perp are chiral odd and can, therefore, be identified as the chiral partners needed to access the transversity h_1 . Given their probabilistic interpretation, they can be considered as a sort of “double” Collins effect [26].

They differ just by geometrical weighting factors that are selectively sensitive either to the relative momentum of the final hadrons (\vec{R}_T) or to the relative orientation of the total pair momentum with respect to the jet axis (\vec{k}_T , see also Fig. 3.23).

3.2.5.4 DSA in inclusive ρ production:

The consideration of spin-one hadrons in the final state, for instance in semi-inclusive ρ production by deep inelastic scattering on a transversely polarised nucleon target provides additional options to access the transversity distribution. Since the ρ will be identified by its decay into two pions, it is obvious that the involved spin-one PFFs have a close relationship to the two-hadron PFFs. A complete analysis of the relations has been performed recently [68]. Here only the most interesting asymmetry in the cross section is quoted from [41]

$$\frac{2\pi d\sigma_{UT}(l + \vec{H} \rightarrow l' + \vec{h} + X)}{d\phi^l dx_{Bj} dz_h dy} = \frac{-4\pi\alpha^2 s}{Q^4} x_{Bj}(1-y) |\mathbf{S}_T| |\mathbf{S}_{hLT}| \sin(\phi_{hLT}^l + \phi_S^l) h_1(x_{Bj}) H_{1LT}(z_h) \quad (3.130)$$

involving the spin-one fragmentation function H_{1LT} corresponding to the p -wave part the H_1^{\triangleleft} two-hadron PFF [68].

3.3 model calculations of PDFs and PFFs

The transverse momentum dependence of PDFs and PFFs is often modelled in form of Gaussian distributions (as for instance in [39, 18, 69, 57]). A typical ansatz for a PDF would be

$$f(x, \mathbf{p}_T^2) = f(x, 0) \exp(-R_H^2 \mathbf{p}_T^2) = f(x) \frac{R_H^2}{\pi} \exp(-R_H^2 \mathbf{p}_T^2) \quad (3.131)$$

or similarly

$$D(z, \mathbf{k}_T^{\prime 2}) = D(z, 0) \exp(-R_h^2 \mathbf{k}_T^2) = D(z) \frac{R_h^2}{z^2 \pi} \exp(-R_h^2 \mathbf{k}_T^2) \quad (3.132)$$

for a PFF, with radii R_H and R_h governing the fall-off of the functions in a way specific for the hadron under consideration. In principle, these radii again may depend on the LC fractional momentum and on the specific function, i.e. $R_H = R_H^f(x)$ and $R_h = R_h^D(z)$.

Instead of directly guessing an ansatz for transverse momentum dependence, alternatively suitable model calculations can be used. Of course, the behaviour of PDFs and PFFs resulting from such a calculation depends on the model assumptions put in the first place. The advantage is merely that transverse momentum dependence such is linked to model properties which influence other phenomena. For instance, models typically relate the longitudinal and transverse momentum

dependence of the functions in a specific way. Ultimately all those ideas and assumptions will have to be checked against experiments.

More generally, in order to investigate the structure of the quark-quark correlation functions it is instructive to employ models which illustrate the consequences of the various constraints. Model calculations of PDFs and PFFs serve several purposes:

- Realistic model predictions for unknown PDFs and PFFs are needed to estimate the size of observables for future experiments. In particular, in planning the measurements of small quantities like azimuthal asymmetries it is crucial to have an idea in advance of what can be expected.
- From a comparison of results from model calculations with the actually measured functions relevant mechanisms and properties can be identified which are responsible for characteristic features of the functions.

Many models for PDFs and PFFs are on the market, like bag models [70, 71, 72, 73], quark models [74, 75, 76], soliton models [77, 78], or spectator models [79, 80, 20, 21, 81, 82, 83], to name but a few.

In the following we will focus on a spectator model where the spectrum of intermediate states, which can be inserted in the definition of the correlation function Φ in Eq. (3.7), or which are explicitly displayed in the definition of the correlation function Δ in Eq. (3.11), is replaced by one state with a definite mass.

Though simple in its physical input, it has the advantage of being covariant and producing the right support. It incorporates the properties of quark-quark correlation functions discussed in the subsections 3.2.1, 3.2.2 and 3.2.3. Its structural simplicity results in analytical expressions for these functions, which can be projected in order to obtain transverse momentum dependent and integrated PDFs and PFFs.

3.3.1 PDF and PFF in a spectator model

Estimates not only for the usual spin-independent PDFs and PFFs, but also for spin-dependent ones and for subleading (higher twist) functions for the nucleon have been obtained in the spectator model [20]. Also PDFs and PFFs up to subleading order are discussed in the same publication.

The treatment of intermediate states, to be inserted in the definition of Φ in Eq. (3.7) and explicitly present in Eq. (3.11) for Δ , as a spectator state with a definite mass amounts to making a specific ansatz for the spectral decomposition of these correlation functions. This may be best illustrated using the support plot in $\sigma \equiv 2p \cdot P$ and $\tau \equiv p^2$. In this plot the mass M_R of the remainder, called the spectator, is constant along the lines $(P - k)^2 = \tau - \sigma + M^2 = M_R^2$, as indicated in Fig. 3.25. The quantum numbers of the intermediate state are those determined by the action of the quark field on the state $|P, S\rangle$, hence the name *diquark spectator*. In the most naive picture of the quark structure of the nucleon, such that in its rest frame all quarks are in $1/2^+$ orbitals, the spin of

basic assumption
of the
spectator model

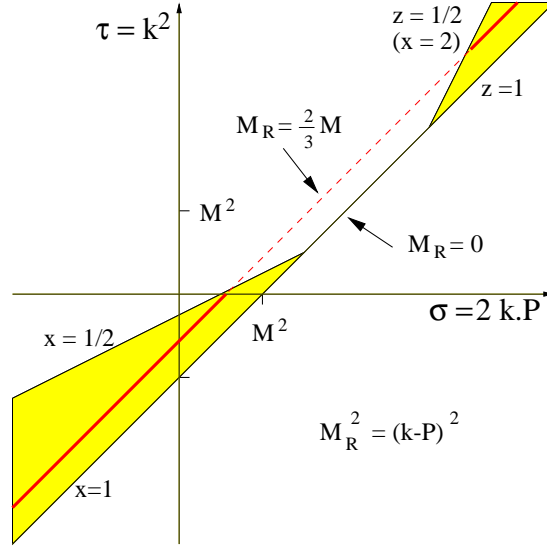


Figure 3.25: The constraint in the $\sigma - \tau$ plane coming from fixing the spectator mass M_R (compare with Fig. 3.11).

the diquark system can be either 0 (scalar diquark s) or 1 (axial vector diquark a). For a pion state we have an *antiquark spectator*. The inclusion of antiquark and gluon distributions would require a more complex spectral decomposition of intermediate states; for an exploratory study the restriction to the simplest case seems reasonable [20]. The correlation function Φ (the correlation function Δ will be treated later) is then given in the spectator model by

calculation of Φ in
the spectator
model

$$\begin{aligned} \Phi_{ij}^R(p, P, S) &= \frac{1}{(2\pi)^3} \langle P, S | \bar{\psi}_j(0) | X^{(\lambda)} \rangle \theta(P_R^+) \\ &\times \delta \left[(p - P)^2 - M_R^2 \right] \langle X^{(\lambda)} | \psi_i(0) | P, S \rangle, \end{aligned} \quad (3.133)$$

where $P_R = P - p$ and $X^{(\lambda)}$ represents the spectator and its possible spin states (indicated with λ). One projects onto different spins in the intermediate state and allows for different spectator masses.

To start with the correlation function Φ for a nucleon, the matrix element appearing in the RHS of (3.133) is given by

$$\langle X_s | \psi_i(0) | P, S \rangle = \left(\frac{i}{\not{p} - m} \right)_{ik} \Upsilon_{kl}^s U_l(P, S), \quad (3.134)$$

in the case of a scalar diquark, or by

$$\langle X_a^{(\lambda)} | \psi_i(0) | P, S \rangle = \epsilon_\mu^{*(\lambda)} \left(\frac{i}{\not{p} - m} \right)_{ik} \Upsilon_{kl}^{a\mu} U_l(P, S), \quad (3.135)$$

for a vector diquark. The matrix elements consist of a nucleon-quark-diquark vertex $\Upsilon(N)$ yet to be specified, the Dirac spinor for the nucleon $U_l(P, S)$, a quark propagator for the untruncated quark line (m is the constituent mass of the quark) and a polarisation vector $\epsilon_\mu^{*(\lambda)}$ in the case of an axial vector diquark.

The next step is to fix the Dirac structure of the nucleon-quark-diquark vertex Υ . A possible assumption are the following structures:

$$\Upsilon^s(N) = \mathbf{1} g_s(p^2), \quad (3.136)$$

$$\begin{aligned} \Upsilon^{a\mu}(N) &= \frac{g_a(p^2)}{\sqrt{3}} \gamma_\nu \gamma_5 \frac{\not{P} + M}{2M} \left(-g^{\mu\nu} + \frac{P^\mu P^\nu}{M^2} \right) \\ &= \frac{g_a(p^2)}{\sqrt{3}} \gamma_5 \left(\gamma^\mu + \frac{P^\mu}{M} \right). \end{aligned} \quad (3.137)$$

The functions $g_R(p^2)$ (where R is s or a) are form factors that take into account the composite structure of the nucleon and the diquark spectator. In the choice of vertices, the factors and projection operators are chosen to assure that in the target rest frame, where the nucleon spinors have only upper components, the diquark spin 1 states are purely spatial and in which case the axial vector diquark vertex reduces to $\chi_N^\dagger \sigma \cdot \epsilon \chi_q$. The most general structure of the vertices can be found in [84]. With the choices of Eqs.(3.136), one finds

$$\begin{aligned} \Phi^R(p, P, S) &= \frac{|g_R(p^2)|^2}{2(2\pi)^3} \frac{\delta(\tau - \sigma + M^2 - M_R^2)}{(p^2 - m^2)^2} \\ &\times (\not{p} + m) (\not{P} + M) (1 + a_R \gamma_5 \not{S}) (\not{p} + m), \end{aligned} \quad (3.138)$$

where a_R is a spin factor, which takes the values $a_s = 1$ and $a_a = -1/3$. In obtaining this result the polarisation sum for the axial vector diquark was used in the form $\sum_\lambda \epsilon_\mu^{*(\lambda)} \epsilon_\nu^{(\lambda)} = -g_{\mu\nu} + P_\mu P_\nu / M^2$, which is consistent with the choice that the axial vector diquark spin states are purely spatial in the nucleon rest frame. The same form factors for scalar and axial vector diquark is used:

$$g(\tau) = N \frac{\tau - m^2}{|\tau - \Lambda^2|^\alpha}. \quad (3.139)$$

The quantity Λ is another parameter of the model which ensures that the vertex is cut off if the virtuality of the quark leg is much larger than Λ^2 . N is a normalisation constant. This choice of form factor has the advantage of killing the pole of the quark propagator as suggested in [84].

In passing one may note that in the same way a simple spectator model for the pion can be obtained. The matrix element can be written as

$$\langle X^{(\alpha)} | \psi_i(0) | P_\pi \rangle = \left(\frac{i}{\not{p} - m} \right)_{ik} \Upsilon_{kl} v_l^{(\alpha)}. \quad (3.140)$$

The spinor $v_l^{(\alpha)}$ describes the spin state of the antiquark spectator. The simplest vertex is given by

$$\Upsilon(\pi) = \frac{g(p^2)}{\sqrt{2}} \frac{\not{P}_\pi + M_\pi}{2M_\pi} \gamma_5. \quad (3.141)$$

Taking for the spectator antiquark spin sum $\sum_\alpha v_l^{(\alpha)} \bar{v}_l^{(\alpha)} = \not{P}_\pi - M_\pi$ one arrives at precisely the same expression as for the nucleon (Eq. (3.138)) with $a_R = 0$. This option will not be pursued further here, but the focus will be on the example of nucleon PDFs to exemplify transverse momentum dependence in the model.

From the correlation function Φ one easily obtains the distribution functions. Taking out the explicit δ -function,

$$\Phi^R(p, P, S) = \tilde{\Phi}(p, P, S) \delta(\tau - \sigma + M^2 - M_R^2), \quad (3.142)$$

one finds immediately from Eq. (3.36) the result

$$\Phi^{[\Gamma]}(x, \mathbf{p}_T) = \frac{\text{Tr}(\tilde{\Phi}\Gamma)}{4(1-x)P^+} \Big|_{\tau = p^2(x, \mathbf{p}_T^2)}, \quad (3.143)$$

with

$$-p^2(x, \mathbf{p}_T^2) = \frac{\mathbf{p}_T^2}{1-x} + \frac{x}{1-x} M_R^2 - x M^2. \quad (3.144)$$

For completeness the calculation of fragmentation functions is sketched in the following, which is very similar to the case of the distribution functions, involving the same type of matrix elements. Further assuming that the hadron h has no interactions with the spectator allows to use a free spinor to describe this outgoing hadron. Then it is seen that the correlation function Δ is the same as the one needed for the distributions, after obvious replacements in the arguments, namely

$$\begin{aligned} \Delta^R(k, P_h, S_h) &= \frac{|g_R(k^2)|^2}{2(2\pi)^3} \frac{\delta(\tau_h - \sigma_h + M_h^2 - M_R^2)}{(k^2 - m^2)^2} \\ &\times (\not{k} + m) (\not{P}_h + M_h) (1 + a_R \gamma_5 \not{S}_h) (\not{k} + m). \end{aligned} \quad (3.145)$$

A direct consequence is

$$\Delta^{[\Gamma]}(z, \mathbf{k}_T) = \frac{1}{2z} \Phi^{[\Gamma']}\left(\frac{1}{z}, \mathbf{k}_T\right) = \frac{1}{2z} \Phi^{[\Gamma]}\left(\frac{1}{z}, -\frac{\mathbf{k}'_T}{z}\right), \quad (3.146)$$

where Γ' and Γ involve an interchange of $+$ and $-$ components. Defining $\tilde{\Delta}$ by $\Delta(k, P_h, S_h) = \tilde{\Delta}(k, P_h, S_h) \delta((k - P_h)^2 - M_R^2)$, Eq. (3.75) leads to

$$\Delta^{[\Gamma]}(z, \mathbf{k}_T) = \frac{\text{Tr}x(\tilde{\Delta}\Gamma)}{8(1-z)P_h^-} \Big|_{\tau_h = k^2(z, \mathbf{k}_T^2)}, \quad (3.147)$$

with

$$k^2(z, \mathbf{k}_T^2) = \frac{z}{1-z} \mathbf{k}_T^2 + \frac{M_R^2}{1-z} + \frac{M_h^2}{z}. \quad (3.148)$$

The consequence of using free spinors to describe the outgoing hadron in this variant of the spectator model is that all T-odd fragmentation functions vanish and there is a one-to-one correspondence between distribution and fragmentation functions. As can be seen in Fig. 3.25 the actual behaviour of the distribution and fragmentation functions comes from different regions in τ , roughly spacelike and timelike, respectively. Therefore, the above reciprocity (Eq. (3.146)) is of use for the analytic expressions, less for the actual values.

3.3.2 results and discussion

Complete results and discussions can be found in the original publication [20]. The results of the spectator model calculation for PDFs and PFFs have been used to discuss properties of the structure functions of one-hadron inclusive DIS [85]. Here the focus will be on the transverse momentum dependence of nucleon PDFs only. Since the dependence for PFFs of the nucleon, and PDFs and PFFs of pions is very similar, this serves as a typical example.

3.3.2.1 PDFs of the nucleon:

Using the expression in Eq. (3.138) one can compute the amplitudes A_i of the ansatz in Eq. (3.17). Taking out some common factors by defining

$$A_i = \frac{N^2}{2(2\pi)^3} \frac{\delta(\tau - \sigma + M^2 - M_R^2)}{|\tau - \Lambda^2|^{2\alpha}} \tilde{A}_i, \quad (3.149)$$

one obtains, as expected from the absence of final state interaction in the present form of the model, the T-odd amplitudes $\tilde{A}_4 = \tilde{A}_5 = \tilde{A}_{12} = 0$, and

$$\tilde{A}_1 = \frac{m}{M} \left((M + m)^2 - M_R^2 \right) + (\tau - m^2) \left(1 + \frac{m}{M} \right), \quad (3.150)$$

$$\tilde{A}_2 = -(\tau - m^2), \quad (3.151)$$

$$\tilde{A}_3 = (M + m)^2 - M_R^2 + (\tau - m^2), \quad (3.152)$$

$$\tilde{A}_6 = -a_R \left[\frac{m}{M} \left((M + m)^2 - M_R^2 \right) + (\tau - m^2) \left(1 + \frac{m}{M} \right) \right], \quad (3.153)$$

$$\tilde{A}_7 = 2 a_R m M, \quad (3.154)$$

$$\tilde{A}_8 = 2 a_R M^2, \quad (3.155)$$

$$\tilde{A}_9 = a_R (\tau - m^2), \quad (3.156)$$

$$\tilde{A}_{10} = -a_R \left[(M + m)^2 - M_R^2 + (\tau - m^2) \right], \quad (3.157)$$

$$\tilde{A}_{11} = -2 a_R M^2. \quad (3.158)$$

Introducing the function $\lambda_R^2(x)$ such that

$$\Lambda^2 - p^2 = \frac{\mathbf{p}_T^2 + \lambda_R^2(x)}{1 - x}, \quad (3.159)$$

which implies

$$\lambda_R^2(x) = \Lambda^2(1 - x) + xM_R^2 - x(1 - x)M^2, \quad (3.160)$$

one gets the following results for the \mathbf{p}_T^2 -dependent distribution functions,

$$f_1(x, \mathbf{p}_T^2) = \frac{N^2 (1 - x)^{2\alpha-1}}{16\pi^3} \frac{(xM + m)^2 + \mathbf{p}_T^2}{(\mathbf{p}_T^2 + \lambda_R^2)^{2\alpha}}, \quad (3.161)$$

$$g_{1L}(x, \mathbf{p}_T^2) = a_R \frac{N^2 (1 - x)^{2\alpha-1}}{16\pi^3} \frac{(xM + m)^2 - \mathbf{p}_T^2}{(\mathbf{p}_T^2 + \lambda_R^2)^{2\alpha}}, \quad (3.162)$$

$$g_{1T}(x, \mathbf{p}_T^2) = a_R \frac{N^2 (1-x)^{2\alpha-1}}{8\pi^3} \frac{M(xM+m)}{(\mathbf{p}_T^2 + \lambda_R^2)^{2\alpha}}, \quad (3.163)$$

$$h_{1T}(x, \mathbf{p}_T^2) = a_R f_1(x, \mathbf{p}_T^2), \quad (3.164)$$

$$h_{1L}^\perp(x, \mathbf{p}_T^2) = -g_{1T}(x, \mathbf{p}_T^2), \quad (3.165)$$

$$h_{1T}^\perp(x, \mathbf{p}_T^2) = -a_R \frac{N^2 (1-x)^{2\alpha-1}}{8\pi^3} \frac{M^2}{(\mathbf{p}_T^2 + \lambda_R^2)^{2\alpha}}, \quad (3.166)$$

$$e(x, \mathbf{p}_T^2) = \frac{N^2 (1-x)^{2\alpha-2}}{16\pi^3} \times \frac{(1-x)(xM+m)(M+m) - M_R^2 \left(x + \frac{m}{M}\right) - \left(1 + \frac{m}{M}\right) \mathbf{p}_T^2}{(\mathbf{p}_T^2 + \lambda_R^2)^{2\alpha}}, \quad (3.167)$$

$$f^\perp(x, \mathbf{p}_T^2) = \frac{N^2 (1-x)^{2\alpha-2}}{16\pi^3} \times \frac{(1-x^2)M^2 + 2mM(1-x) - M_R^2 - \mathbf{p}_T^2}{(\mathbf{p}_T^2 + \lambda_R^2)^{2\alpha}}, \quad (3.168)$$

$$g'_T(x, \mathbf{p}_T^2) = a_R e(x, \mathbf{p}_T^2), \quad (3.169)$$

$$g_L^\perp(x, \mathbf{p}_T^2) = -a_R \frac{N^2 (1-x)^{2\alpha-2}}{16\pi^3} \frac{(1-x)^2 M^2 - M_R^2 - \mathbf{p}_T^2}{(\mathbf{p}_T^2 + \lambda_R^2)^{2\alpha}}, \quad (3.170)$$

$$g_T^\perp(x, \mathbf{p}_T^2) = a_R \frac{N^2 (1-x)^{2\alpha-1}}{8\pi^3} \frac{M^2}{(\mathbf{p}_T^2 + \lambda_R^2)^{2\alpha}}, \quad (3.171)$$

$$h_T^\perp(x, \mathbf{p}_T^2) = a_R f^\perp(x, \mathbf{p}_T^2), \quad (3.172)$$

$$h_L(x, \mathbf{p}_T^2) = a_R \frac{N^2 (1-x)^{2\alpha-2}}{16\pi^3} \times \frac{(1-x)(xM+m)(M+m) - \left(x + \frac{m}{M}\right) M_R^2 + \left(1 - 2x - \frac{m}{M}\right) \mathbf{p}_T^2}{(\mathbf{p}_T^2 + \lambda_R^2)^{2\alpha}}, \quad (3.173)$$

$$h_T(x, \mathbf{p}_T^2) = -g_L^\perp(x, \mathbf{p}_T^2). \quad (3.174)$$

Although there is a certain freedom in the choice of the parameters, one immediately sees that the occurrence of singularities in the integration region (see Fig. 3.25) will cause problems which are avoided if there is no zero in the denominator. The requirement that $\lambda_R^2(x)$ is positive implies for the distribution functions ($0 \leq x \leq 1$)

$$M_R > M - \Lambda, \quad (3.175)$$

while for the fragmentation functions (using reciprocity, we have to look at $x \geq 1$) it leads to

$$M_R > \Lambda - M_h. \quad (3.176)$$

Provided condition (3.175) is fulfilled, one obtains the integrated distribution functions,

$$f_1(x) = \frac{N^2 (1-x)^{2\alpha-1}}{32\pi^2 (\alpha-1)(2\alpha-1)} \frac{2(\alpha-1)(xM+m)^2 + \lambda_R^2(x)}{(\lambda_R^2(x))^{2\alpha-1}}, \quad (3.177)$$

$$g_1(x) = \frac{N^2 a_R (1-x)^{2\alpha-1}}{32\pi^2 (\alpha-1)(2\alpha-1)} \frac{2(\alpha-1)(xM+m)^2 - \lambda_R^2(x)}{(\lambda_R^2(x))^{2\alpha-1}}, \quad (3.178)$$

$$h_1(x) = \frac{N^2 a_R (1-x)^{2\alpha-1}}{16\pi^2 (2\alpha-1)} \frac{(xM+m)^2}{(\lambda_R^2(x))^{2\alpha-1}}, \quad (3.179)$$

$$e(x) = \frac{N^2 (1-x)^{2\alpha-2}}{32\pi^2 (\alpha-1)(2\alpha-1)} \times \frac{2(\alpha-1) \left(x + \frac{m}{M}\right) [(1-x)(M+m)M - M_R^2] - \left(1 + \frac{m}{M}\right) \lambda_R^2(x)}{(\lambda_R^2(x))^{2\alpha-1}}, \quad (3.180)$$

$$g_T(x) = \frac{N^2 a_R (1-x)^{2\alpha-2}}{32\pi^2 (\alpha-1)(2\alpha-1)} \times \frac{2(\alpha-1) \left(x + \frac{m}{M}\right) [(1-x)(M+m)M - M_R^2] - \left(x + \frac{m}{M}\right) \lambda_R^2(x)}{(\lambda_R^2(x))^{2\alpha-1}}, \quad (3.181)$$

$$h_L(x) = \frac{N^2 a_R (1-x)^{2\alpha-2}}{32\pi^2 (\alpha-1)(2\alpha-1)} \times \frac{2(\alpha-1) \left(x + \frac{m}{M}\right) [(1-x)(M+m)M - M_R^2] + \left(1 - 2x - \frac{m}{M}\right) \lambda_R^2(x)}{(\lambda_R^2(x))^{2\alpha-1}}. \quad (3.182)$$

Examples of the $\mathbf{p}_T^2/2M^2$ -weighted distributions are

$$g_{1T}^{(1)}(x) = -h_{1L}^{\perp(1)}(x) = \frac{N^2 a_R (1-x)^{2\alpha-1}}{32\pi^2 (\alpha-1)(2\alpha-1)} \frac{x + \frac{m}{M}}{(\lambda_R^2(x))^{2\alpha-2}}. \quad (3.183)$$

These latter functions do not vanish at $x = 0$, implying non-vanishing sum rules for g_2 and h_2 , in accordance with Eqs. (3.59) and (3.60), except if the quarks are massless.

The functions g_2 and h_2 are given by

$$g_2(x) = \frac{h_2(x)}{2} = \frac{N^2 a_R (1-x)^{2\alpha-2}}{32\pi^2 (\alpha-1)(2\alpha-1)} \times \frac{2(\alpha-1) \left(x + \frac{m}{M}\right) [M^2(1-x)^2 - M_R^2] + \left(1 - 2x - \frac{m}{M}\right) \lambda_R^2(x)}{(\lambda_R^2(x))^{2\alpha-1}}. \quad (3.184)$$

A direct check reveals that Eqs. (3.55) and (3.56) are satisfied.

Up to now, flavour in the distributions is not specified. For the nucleon only two types of distributions, f_1^s and f_1^a , etc. are distinguished. Since spin 0 diquarks are in a flavour singlet state and spin 1 diquarks are in a flavour triplet state, in order to combine to a symmetric spin-flavour wave function as demanded by the Pauli principle, the proton wave function has the well-known $SU(4)$ structure,

$$\begin{aligned} |p \uparrow\rangle &= \frac{1}{\sqrt{2}} |u \uparrow S_0^0\rangle + \frac{1}{\sqrt{18}} |u \uparrow A_0^0\rangle \\ &\quad - \frac{1}{3} |u \downarrow A_0^1\rangle - \frac{1}{3} |d \uparrow A_1^0\rangle + \sqrt{\frac{2}{9}} |d \downarrow A_1^1\rangle, \end{aligned} \quad (3.185)$$

where S (A) represents a scalar (axial vector) diquark and the upper (lower) indices represent the projections of the spin (isospin) along a definite direction. Since the coupling of the spin has already been included in the vertices, the flavour coupling is needed

$$|p\rangle = \frac{1}{\sqrt{2}} |u S_0\rangle + \frac{1}{\sqrt{6}} |u A_0\rangle - \frac{1}{\sqrt{3}} |d A_1\rangle, \quad (3.186)$$

to find that for the nucleon the flavour distributions are

$$f_1^u = \frac{3}{2} f_1^s + \frac{1}{2} f_1^a, \quad (3.187)$$

$$f_1^d = f_1^a, \quad (3.188)$$

and similarly for the other functions. The proportionality of the numbers is obtained from Eq. (3.186), while the overall factor is chosen to reproduce the sum rules for the number of up and down quarks if f_1^s and f_1^a are normalised to unity upon integration over \mathbf{p}_T and x . This will fix the normalisation N in the form factor in Eq. (3.139). Notice that the factors $a_s = 1$ and $a_a = -1/3$ in the distribution functions will produce different u and d weighting for unpolarised and polarised distributions. Further differences between u and d distributions can also be induced by different choices of M_R , Λ or α . For the nucleon $\alpha = 2$ reproduces the right large x behaviour of f_1^u , i.e. $(1-x)^3$, as predicted by the Drell-Yan-West relation and reasonably well confirmed by data. Though tuning the large x behaviour of f_1^d to match the $(1-x)^4$ form indicated by data could be easily obtained by choosing a different form factor for the vector diquarks, since f_1^d is only affected by the latter, such a fine-tuning would probably take things too far with the simple model under consideration. Similarly, only one common value for Λ is used. However, different masses for scalar and vector diquark spectators are considered. The colour magnetic hyperfine interaction, held responsible for the nucleon-delta mass difference of 300 MeV, will also produce a mass difference between singlet and triplet diquark states. Neglecting dynamical effects, group-theoretical factors lead to a difference $M_a - M_s = 200$ MeV [86].

The remaining parameters of the model are fixed as follows. In Ref. [20] it is argued that a satisfactory qualitative agreement with the valence distributions of Glück, Reya and Vogt (GRV) calculated at the low scale $\mu_{LO}^2 = 0.23$ GeV² [87] can be obtained with the choices $m = 0.36$ GeV, $M_s = 0.6$ GeV and $M_a = 0.8$ GeV, given the fact that the neglect of sea-quark and gluon spectator components is

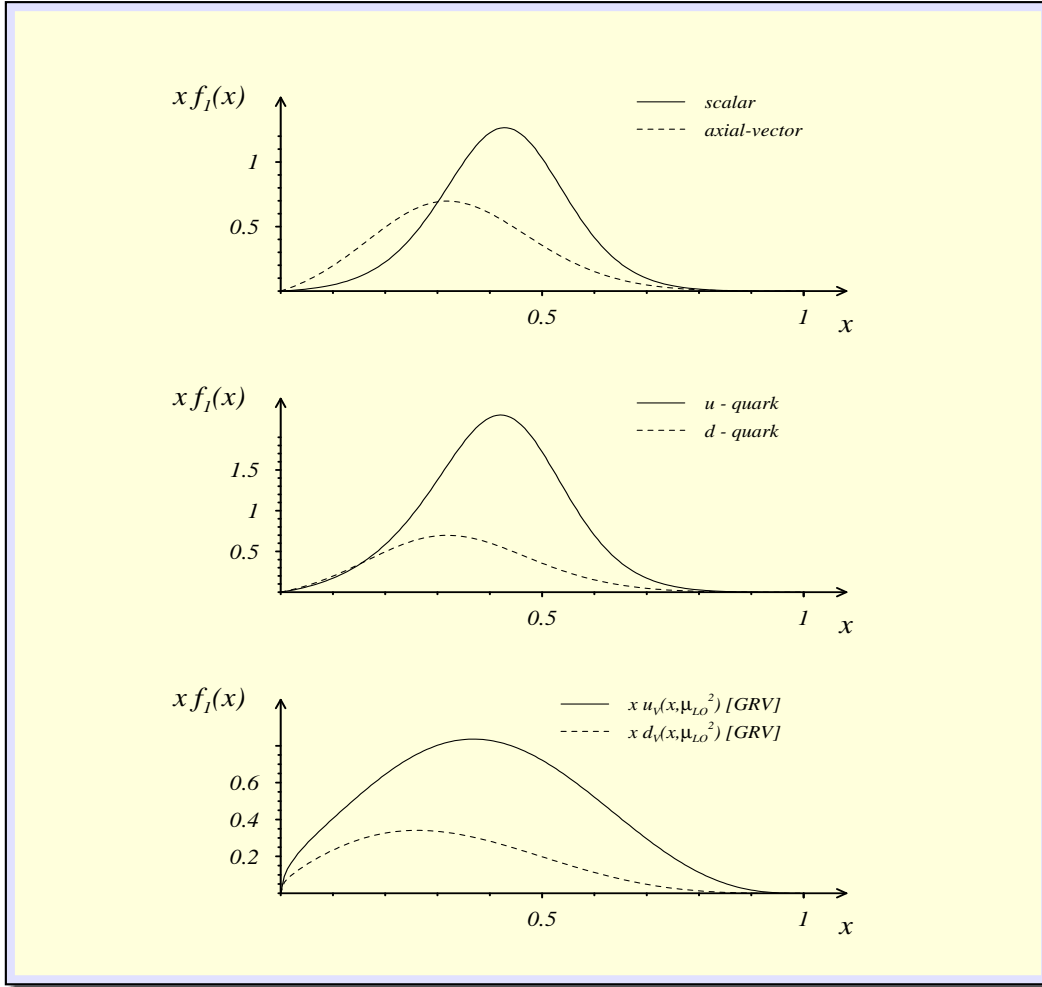


Figure 3.26: Twist two distributions for the nucleon. The plot at the top shows $x f_1^s(x)$ (full line) and $x f_1^a(x)$ (dashed line) for $M_s = 0.6$ GeV, $M_a = 0.8$ GeV and $\Lambda = 0.5$ GeV. The plot on the middle shows $x f_1^u(x)$ (full line) and $x f_1^d(x)$ (dashed line) for the same values of the parameters. The third plot shows the low scale ($\mu^2 = 0.23$ GeV²) valence distributions of Glück, Reya and Vogt [87].

known to lead to more narrow distributions than the ones observed in experiment. It turns out the distributions are rather insensitive to the quark mass value.

Another important constraint comes from the axial charge of the nucleon, given by

$$g_A = \int_0^1 dx [g_1^u(x) - g_1^d(x)] = \int_0^1 dx \left[\frac{3}{2} g_1^s(x) - \frac{1}{2} g_1^a(x) \right]. \quad (3.189)$$

This constraint is used to fix Λ . The value $\Lambda = 0.5$ GeV gives $g_A = 1.28$, close to the experimental value.

Fig. 3.26 shows the distribution $f_1(x)$ multiplied by x in comparison with the valence distributions of Glück, Reya and Vogt (GRV) [87]. For u and d quarks, the first moment of $f_1(x)$ is clearly larger in the spectator model, which would imply that these results describe the nucleon at an even lower scale than GRV. Fig. 3.27 shows the distributions $g_1^u(x)$ and $g_1^d(x)$ multiplied by x . Again,

a qualitative agreement with the polarised valence distributions of Glück *et al.* [88] is found.

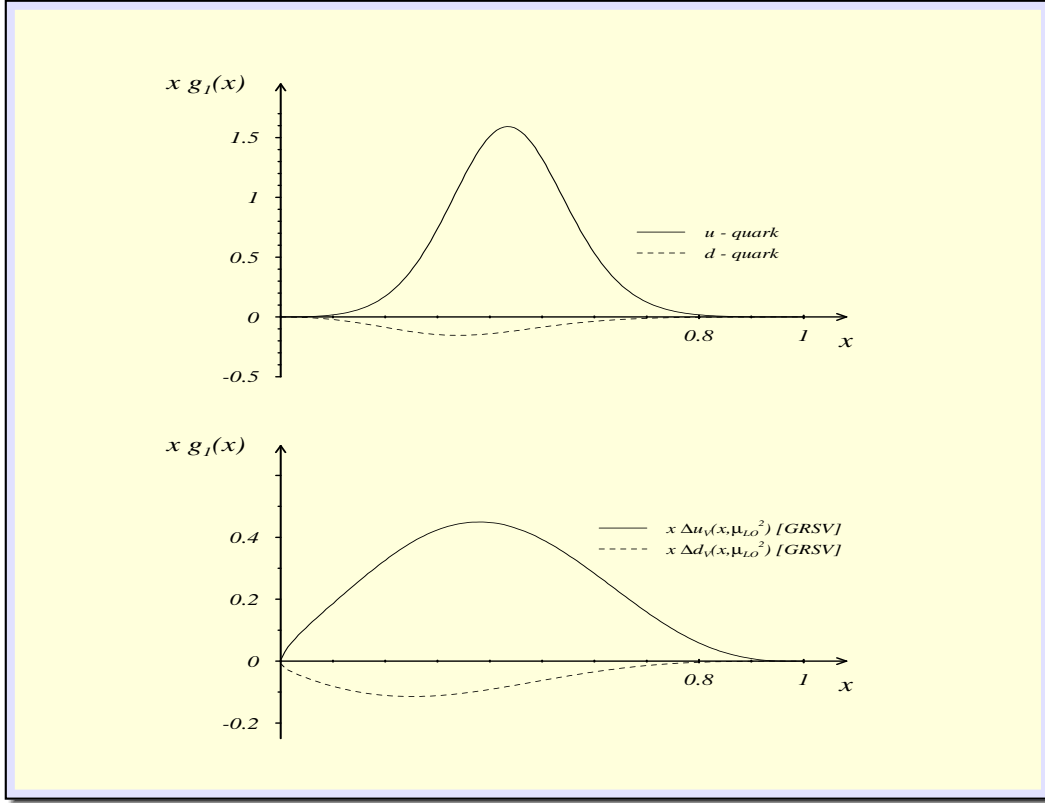


Figure 3.27: Polarised proton distributions $g_1^u(x)$ and $g_1^d(x)$. The first plot shows the model estimates for $xg_1^u(x)$ (full line) and $xg_1^d(x)$ (dashed line). The second plot shows the low scale $\mu_{LO}^2 = 0.23 \text{ GeV}^2$ parametrisation of Glück, *et al.* [88] for the same functions.

After having fixed all parameters by the requirement of a rough qualitative agreement of the integrated distribution functions, $f_1(x)$ and $g_1(x)$, with phenomenological parametrisations, the transverse momentum dependence as predicted by the model can be considered. In Fig. 3.28 the spin-independent PDFs $xf_1^u(x, \mathbf{p}_T^2)$ and $xf_1^d(x, \mathbf{p}_T^2)$ are displayed. In comparison the spin-dependent PDFs, $xg_{1L}^u(x, \mathbf{p}_T)$ and $xg_1^d(x, \mathbf{p}_T)$, are shown in Fig. 3.29. Finally, in Fig. 3.30 the combination

$$x h_1(x, \mathbf{p}_T) = x h_{1T}(x, \mathbf{p}_T) + x \frac{\mathbf{p}_T^2}{2M^2} h_{1T}^\perp(x, \mathbf{p}_T) \quad (3.190)$$

is displayed for u - and d -quarks.

Though the three distributions, say for u -quarks, look very similar at first glance in the 3-dimensional plots, a closer inspection reveals that the transverse momentum dependence indeed is different in each case. This is due to the different \mathbf{p}_T^2 dependence in the numerators of the Eqs. (3.161), (3.162), (3.164) and (3.166). From the same equations one reads off that in the scalar diquark sector the Soffer inequality [89]

$$|h_1| \leq \frac{1}{2} |f_1 + g_1| \quad (3.191)$$

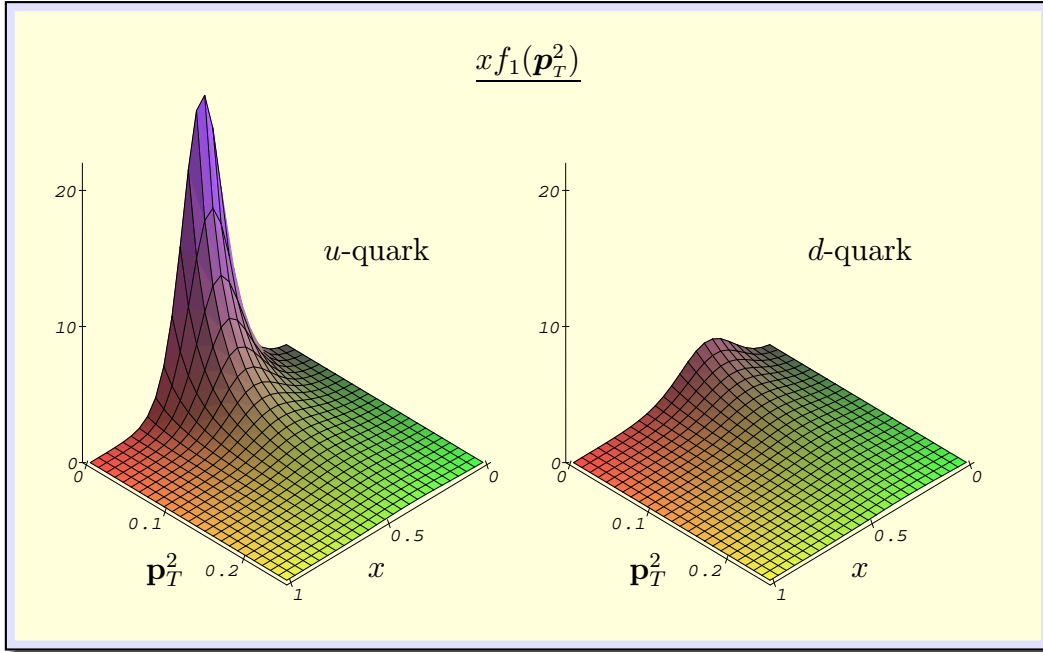


Figure 3.28: The transverse momentum dependent distribution $x f_1(x, \mathbf{p}_T^2)$ plotted against $0 \leq x \leq 1$ and $0 \leq \mathbf{p}_T^2 \leq 0.25 \text{ GeV}^2$ for the u -quark (left panel) and the d -quark (right panel).

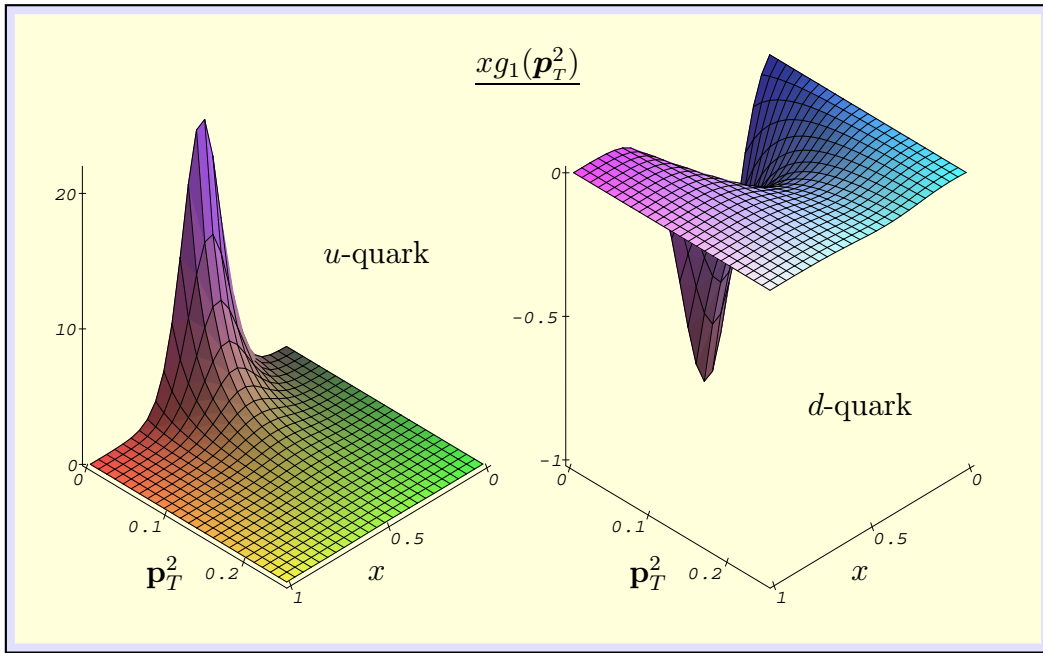


Figure 3.29: The transverse momentum dependent distribution $x g_1(x, \mathbf{p}_T^2)$ plotted against $0 \leq x \leq 1$ and $0 \leq \mathbf{p}_T^2 \leq 0.25 \text{ GeV}^2$ for the u -quark (left panel) and the d -quark (right panel).

is saturated, i.e. $|h_1(x, \mathbf{k}_T^2)|$ takes the allowed maximum for each value of \mathbf{k}_T^2 . In the vector diquark sector the inequality is not saturated because a_R differs from unity.

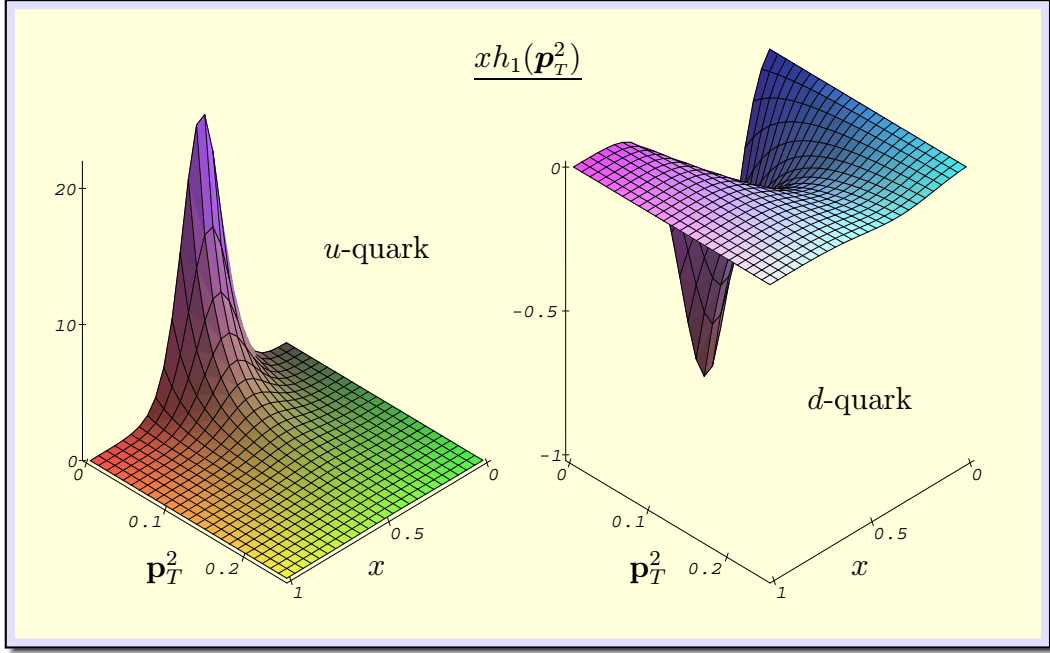


Figure 3.30: The transverse momentum dependent distribution $xh_1(x, \mathbf{p}_T^2) = xh_{1T}(x, \mathbf{p}_T^2) + (x\mathbf{p}_T^2/2M^2)h_{1T}^\perp(x, \mathbf{p}_T^2)$ plotted against $0 \leq x \leq 1$ and $0 \leq \mathbf{p}_T^2 \leq 0.25 \text{ GeV}^2$ for the u -quark (left panel) and the d -quark (right panel).

Not surprisingly the transverse momentum dependence at asymptotical large \mathbf{p}_T^2 follows a power law; this behaviour merely reflects the choice of the form factors of the scalar and vector diquark in Eq. (3.139), and thus is a consequence of the model assumption with rather limited predicting power. However, more interesting to note is that covariant kinematics, and flavour structure (with different spin couplings in the scalar and vector diquark sector) enforce a different transverse momentum dependence on the specific PDF projections. Thus, this simple model shows that generally not only relations between longitudinal and transverse momentum dependence are to be expected, but also interrelations with the spin-dependence of the functions. This feature is very likely to hold more generally beyond the model, since it rather follows from general properties than from assumptions specific to the model. Thus, phenomenologically motivated ansätze which ascribe uniformly the same \mathbf{p}_T^2 -dependence to all PDFs likely miss the full complexity of nucleon structure, though possibly can very well be good approximations depending on the context they are used for.

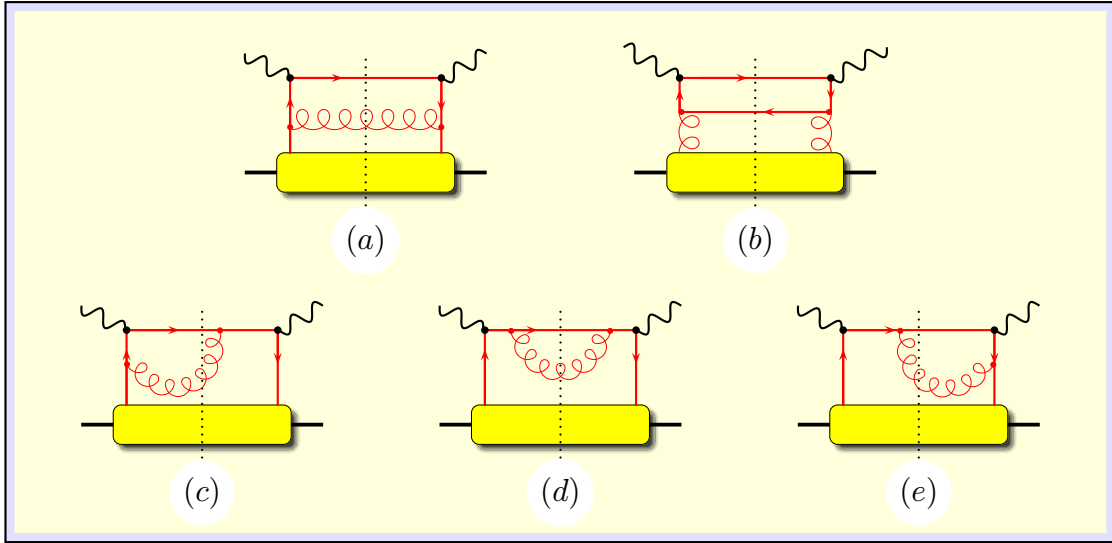


Figure 3.31: Real one-loop corrections to the DIS handbag diagram.

3.4 transverse momentum dependence and evolution

Up to here the question about the origin of the partonic transverse momentum was left untouched. Implicitly it was assumed that there is some non-perturbative mechanism – the same which is responsible for the confinement effect in general – which allows partons to have transverse momentum components relative to their parent hadrons of the order of a typical hadronic mass scale, say 1 GeV. This transverse momentum inherent to all partons is usually called *intrinsic*.

intrinsic transverse momenta

On top of it there is another source for partons to develop transverse momenta relative to parent hadrons: the perturbative radiation of fellow partons leading to the famous logarithmic scale dependence of PDFs and PFFs known as *evolution*.

radiative transverse momenta

The partonic interpretation of evolution is sketched in the following for the example of totally inclusive DIS. One-loop corrections to the leading order handbag diagram for DIS can be sorted into two separately gauge-invariant subgroups: real corrections where a perturbative gluon crosses the final state cut (shown in Fig. 3.31 together with the quark box diagram (b), which completes the set of one-loop diagrams), and virtual loop corrections (shown in Fig. 3.32).

In the calculation of these loop diagrams one encounters two different types of singularities:

1. *Soft divergencies* where all components of an internal momentum become infinitely small, such that a pole in the denominator of a propagator emerges. The soft divergencies mutually cancel when all real and virtual corrections are summed up.
2. *Collinear divergences* where an internal momentum k becomes collinear to an external momentum P such that $P \cdot k \rightarrow 0$ which also leads to a propagator pole in the case of massless particles.

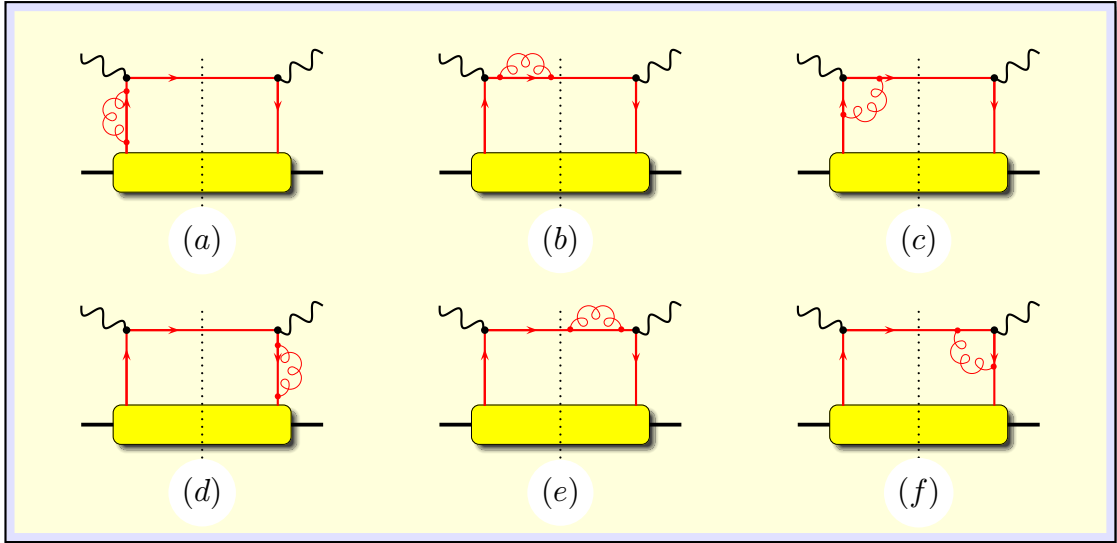


Figure 3.32: Virtual one-loop corrections to the DIS handbag diagram.

Both types of divergencies are conventionally named *infrared divergencies*⁴. In an axial gauge the collinear divergencies occur only in the ladder-type diagrams Fig. 3.31 (a) and (b), but not in the diagrams Fig. 3.31 (c), (d), (e), neither in the diagrams Fig. 3.31 (a) – (f). The principle observation actually holds true also at higher orders: in an axial gauge the *leading logs* (i.e. those terms with the highest powers of logarithms in a given order of α_s) result from ladder diagrams (cf. Fig. 3.33, here the naming *ladder* becomes more apparent, since the ladder has more than just one rung). Collinear divergencies can be absorbed by a redefinition of the integrated PDFs, thus relating *bare* PDFs with the *physical* ones, very much in the spirit of the renormalisation program, which absorbs UV divergencies in the redefinition of charge, mass, wave function etc. The redefinition of PDFs is unique up to finite terms; the precise prescription defines a factorisation scheme like the popular DIS scheme, or \overline{MS} scheme, or any other scheme one might think of. Depending on the scheme the finite corrections to the partonic cross sections differ exactly corresponding to the choice which parts of the finite terms were absorbed in the PDFs. Thus, the arbitrariness in choosing a certain scheme vanishes (to the order in α_s of a given calculation) when putting together soft parts, PDFs and PFFs, and the partonic cross section in order to derive a physical quantity.

DGLAP equations

As a consequence of the redefinition physical (integrated) PDFs acquire a logarithmic scale dependence described by the famous DGLAP evolution [90]

$$\frac{dq(x, Q^2)}{d \ln Q^2} = \frac{\alpha_s(Q^2)}{2\pi} \int_x^1 \frac{dy}{y} \left\{ q(y, Q^2) P_{qq} \left(\frac{x}{y} \right) + G(y, Q^2) P_{qG} \left(\frac{x}{y} \right) \right\}, \quad (3.192)$$

for a generic quark distribution $q(x, Q^2)$ and similarly for the gluon distribution functions

$$\frac{dG(x, Q^2)}{d \ln Q^2} = \frac{\alpha_s(Q^2)}{2\pi} \int_x^1 \frac{dy}{y} \left\{ q(y, Q^2) P_{Gq} \left(\frac{x}{y} \right) + G(y, Q^2) P_{GG} \left(\frac{x}{y} \right) \right\}, \quad (3.193)$$

⁴In the literature the usage of the notions of *soft* and *infrared divergencies* is not uniform.

where P_{qq} , P_{qG} , P_{Gq} , P_{GG} are the *splitting functions*, formally given as inverse Mellin transforms of the anomalous dimensions of the operators defining the distribution functions. *Splitting functions* also have a partonic interpretation. For instance, $P_{qq}(x/y)$ is the probability for a quark with LC momentum fraction y to split into a quark-gluon pair where the quark carries the reduced fraction x . Similar interpretation hold for the other splitting functions.

Thus, DGLAP evolution at $\mathcal{O}(\alpha_s)$ takes into account that the quark with momentum fraction x which is struck by the highly virtual photon, may have started off as quark with the larger momentum fraction y before radiating off a gluon (with probability P_{qq}). It even may have started off as gluon with momentum fraction y which turned into a $q\bar{q}$ -pair (with probability P_{qG}) taken into account by the 2nd term in Eq. (3.192). Evolution at higher order in $\mathcal{O}(\alpha_s)$ is interpreted as iteration of the basic radiation processes.

Here a detailed discussion of evolution of PDFs and PFFs shall no be pursued (in extenso treatments can be found in the vast literature, see for instance [91] as a good starting point for further reading), but the aspect of perturbative origin of partonic transverse momenta is commented on. To this end one may look at the example of a 3-rung quark ladder diagram as shown in Fig. 3.33. For the sake of simplicity of the argument regularisation of singularities by momentum cut-off is assumed, thereby neglecting for the moment the known problems with gauge-invariance and translational invariance introduced by this regularisation method.

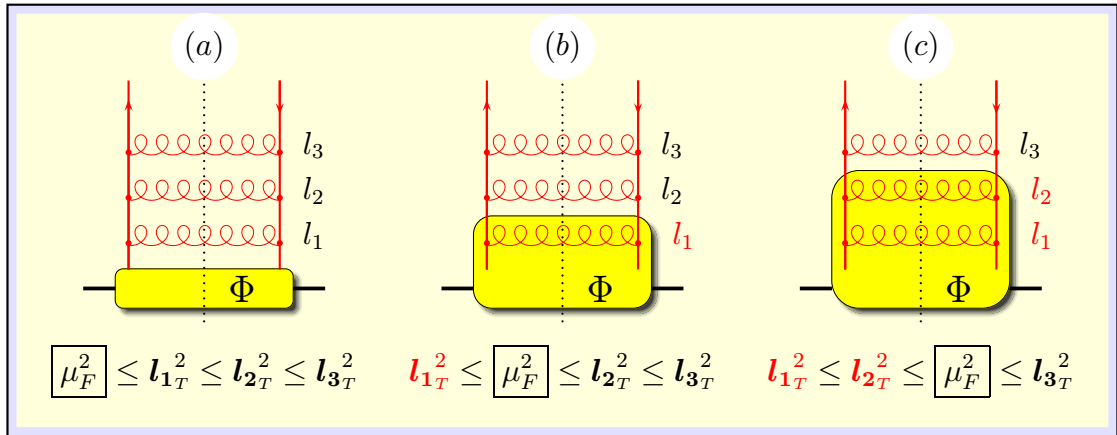


Figure 3.33: Schematic interpretation of the scale dependence of PDFs. An analogous picture can be drawn for PFFs.

An explicit calculation reveals that only those regions of phase space are responsible for *leading logs* where the gluon momenta along the ladder reveal a *strong ordering* [92, 93]

$$\mathbf{l}_{1T}^2 \ll \mathbf{l}_{2T}^2 \ll \dots \ll \mathbf{l}_{nT}^2 \quad \beta_1 \gg \beta_2 \dots \gg \beta_n \quad (3.194)$$

β_i being the LC fraction of the quarks momentum lead away by the i -th gluon. The interpretation is that the quark-quark correlation dependent on a cut-off factorisation scale, $\Phi = \Phi(\mu_F^2)$, contains information an all soft gluons with $\mathbf{l}_{Ti}^2 \leq \mu_F^2$, whereas all harder gluons with $\mu_F^2 \leq \mathbf{l}_{Ti}^2$ have to be taken into account explicitly

by perturbative calculations. By shifting up the factorisation scale μ_F^2 more and more gluons are absorbed into Φ as indicated by the sequence of diagrams in Fig. 3.33 (a) – (c). The effect of shifting the factorisation scale is described by the logarithmic scale dependence of the DGLAP evolution equations for PDFs (and similarly for PFFs) as long as μ_F^2 stays in the perturbative regime⁵. Shifting μ_F^2 below the perturbative regime would require non-perturbative modifications to the evolution equations not known at present days.

From the above intuitive picture it becomes clear that partonic transverse momenta play a double rôle. Undoubtedly, there is some non-perturbative confinement mechanism responsible for the *intrinsic* transverse momenta inherent to partons. Hard radiation off further partons results in an increase of transverse momentum on the perturbative level. The perturbative transverse momenta, when integrated over for the ladder diagrams, produce the leading logarithmic scale dependence of integrated PDFs and PFFs. There is no clear-cut distinction between non-perturbative and perturbative partonic transverse momenta, but a smooth transition. Factorisation scheme and scale independence of observables guarantees that the net effect of both is taken correctly into account.

Because of this inextricable intertwining of the double rôle the theoretical understanding of evolution of transverse momentum dependent PDFs and PFFS is yet in its infancy, only few exploratory studies [94] and large N_C -limit considerations [45] exist.

⁵It is generally believed that the perturbative regime in this context can be safely extended down to values as small as 1 GeV²; perhaps to even smaller values with some additional courage.

3.5 summary

In this section different aspects of transverse momentum effects in (semi-)inclusive reactions have been discussed. Starting from the definitions of non-integrated, i.e. transverse momentum dependent PDFs and PFFS the decisive rôle of observables like azimuthal asymmetries in a global analysis of the transversity distribution function has been emphasised. These observables typically show sensitivity to transverse momentum components, either of parton momenta, or of the relative momentum in a produced hadron pair. Angular distributions thus can be used to unravel the spin content of nucleons.

The transverse momentum dependence of PDFs and PFFs resulting in a simple spectator model calculation has been revealed. The actual outcome of the model is a consequence of the assumptions build in on a more elemental level. In the model under consideration the transverse momentum dependence of correlation functions is entirely governed by the assumed fall-off of elementary form factors for composite objects. Furthermore, it was observed that transverse momentum behaviour is not only entangled with the longitudinal momentum dependence, but also with the spin projections used to reduce correlation functions to PDFs and PFFs. This is very likely to be a general property: different PDFs in general have different transverse momentum dependence. For instance, a model using a Gaussian shape with the same constant radius in the exponent for all PDFs can be a reasonable approximation for phenomenology, but does not describe the full complexity of nucleon spin structure.

Finally, the double rôle of partonic transverse momenta from *intrinsic* non-perturbative origin, and resulting from perturbative hard radiation has been commented on. The relation to the DGLAP evolution behaviour of integrated PDFs and PFFs has been indicated.

4

Transverse momenta in exclusive reactions

4.1 advantages of being exclusive

By definition, *exclusive hard reactions* are subject to stricter constraints than inclusive reactions. The requirement of a specific final state has the unavoidable consequence of low counting rates in an experiment, since most events with possible final states of an comparable inclusive measurement are simply discarded for the exclusive measurement. The situation is even worse, there is not only the suppression by the fact that only one out of many possible channels is retained in the measurement, but moreover, typically one is interested in a channel with final states that are quite unlikely to occur. For practical reasons one considers reactions with final states having a rather low number of hadrons in order to allow full experimental determination. The occurrence of a hard scale, on one hand necessary in order to probe hadron substructure on the level of quarks and gluons, on the other hand conflicts with the requirement of low multiplicities in the final state. Loosely speaking: it is difficult to hit a composite complex object very hard and avoid the break-up into many fragments. Expressed in technical terms this means that cross sections of exclusive hard reactions typically fall off with increasing hard scale according to a power-law behaviour. Dimensional arguments known as *dimensional power counting* relate the number of partons in the valence Fock states of the involved hadrons to the powers of the asymptotical fall-off. Practically, these general considerations result in the conclusion that hard exclusive reactions are very difficult to measure, though not impossible as experience has taught us. What is the motivation to take such an effort ?

exclusive hard
reactions are
difficult to measure

Exclusive hard reactions allow for a complementary view and in fact reveal a richer information on hadron substructure compared to inclusive hard reactions. Since factorisation into soft and hard physics takes places on the level of amplitudes, phase information on soft hadronic matrix elements is accessible in exclusive processes by utilising interference phenomena. The price to pay is an indirect and tedious extraction of the soft hadronic matrix elements from observ-

complementary
view on hadron
substructure

ables: typically only moments of hadronic matrix elements enter cross sections.

As will be argued in the following (partonic) transverse momenta play a crucial rôle in exclusive hard reactions in many different aspects. A distinction between processes at large momentum transfer and those with small momentum transfer but a highly virtual external photon is useful.

large momentum
transfer

- In most processes with large momentum transfer – think of form factors or wide angle exclusive scatterings – an internal redistribution of the momentum is necessary to prevent break-up of the struck hadron, and allow for the formation of the requested final state. The redistribution of momentum is easier with fewer partons involved, thus *the lowest Fock states dominate the process*. This effect becomes more pronounced with increasing momentum transfer, and thus the behaviour of exclusive reactions in this respect is in contrast to the one of inclusive reactions, where conversely, higher Fock states with additional gluons and sea-quarks become more and more important with increasing external scale.

The relevant scale for the distinction of soft and hard regimes is the one of the internal redistribution instead of the overall momentum transfer. As all internal variables are integrated over, the internal scale is not always large, but contributes over the full kinematical range. Compared to the internal scale partonic transverse momentum components can be significant or even dominant in some regions of phase space, even so they may be always small compared to the external hard scale. *A strong enhancement of the importance of partonic transverse momentum effects is thus observed in many exclusive reactions at large momentum transfer.*

high photon
virtuality

- Also at small momentum transfer exclusive reactions allow access to partonic degrees of freedom of the hadron structure, if a second scale is hard instead. An incoming photon can have a high virtuality as for instance in deeply virtual Compton scattering (DVCS) or deeply virtual exclusive meson production. If the momentum transfer is small, no internal redistribution of momentum transfer is necessary and consequently there is no *a priori* preference for configurations with low number of partons. In fact, all Fock states generally contribute to an observable quantity, though with different importance in the course of integrations over internal variables. The relevant scale for distinction of soft and hard physics is the virtuality of the photon. A very close similarity to DIS is noticeable. In fact, the treatment of DVCS and deeply virtual meson production is a generalisation of the one of DIS; GPDs are generalisations of PDFs.

Also in the deeply virtual kinematical regime transverse momenta effects play a crucial rôle, since they offer opportunities to study a uniquely new aspect of hadronic substructure, *the localisation of partons in the plane transverse to the motion of the hadron.*

A complete, exhaustive discussion of exclusive reactions is beyond the scope of this paper; in the following the focus will be on the specific effects induced by transverse momentum dependence exemplified for different exclusive quantities in hard reactions.

4.2 exclusive reactions at large momentum transfer

4.2.1 reaction mechanisms

It is instructive to discuss the principles of different possible reaction mechanisms for elastic electromagnetic form factors at large momentum transfer, before considering the specific consequences of transverse momentum effects in those quantities. In the present subsection it will be done – in an admittedly schematic and strongly simplified manner. The basic principles of the presented simplified view though hold true and are confirmed in more explicit and elaborate calculations.

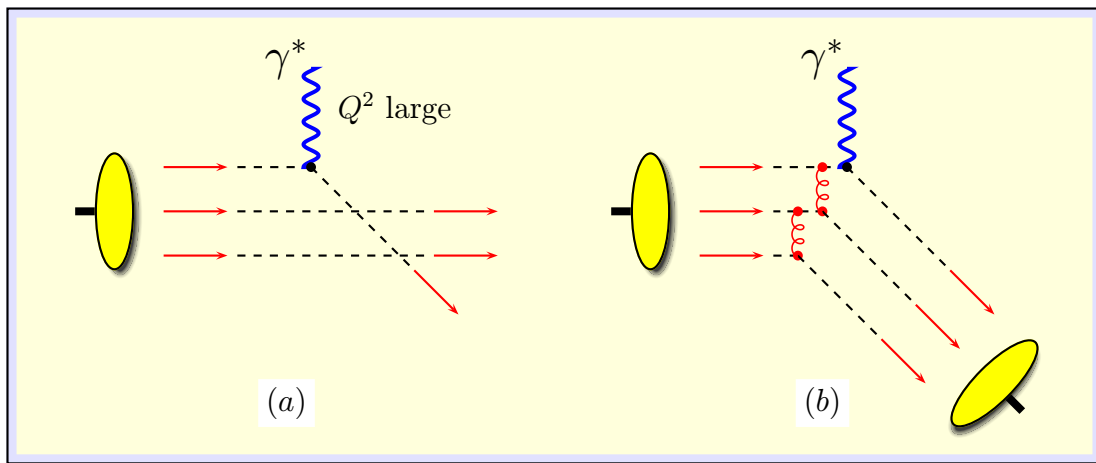


Figure 4.1: Schematical view of the internal momentum redistribution in the hard scattering mechanism for elastic form factor of the nucleon. (a) One parton taking all of the momentum transfer leads to a configuration very unlikely to form a nucleon in the final state. (b) Internal redistribution of the momentum by hard gluons allows formation of the final state nucleon.

In Fig. 4.1 the need for internal momentum redistribution by hard gluons is schematically indicated for the example of the elastic nucleon form factor. An incoming nucleon is replaced by three valence quarks, i.e. the lowest possible Fock state with correct quantum numbers, carrying roughly equal longitudinal momentum fractions. One quark is hit by a highly virtual photon and deflected in its direction as indicated in (a) (in the drawing arbitrarily the momentum transfer is assumed to have a large transverse component, an assumption which is inessential for the argument). In order to allow a reformation of the three quarks to the final nucleon with a reasonable non-vanishing probability, as requested by the definition of an *elastic form factor*, the overall momentum transfer has to be redistributed internally by exchange of additional hard gluons as shown in (b).

The internal redistribution of momentum transfer is the characterising principle of the so-called *hard scattering mechanism*. The corresponding Feynman diagrams to lowest order in α_s are shown in Fig. 4.2 for the elastic pion form factor and in Fig. 4.3 for the Dirac form factor of the nucleon. Each additional hard gluon needed for the redistribution of momentum transfer introduces a suppression of the amplitude by the large momentum flow and a power of α_s . Therefore,

hard scattering
mechanism

dominance of
lowest Fock states

the *lowest Fock states* with a minimal number of parton lines, and corresponding diagrams with a minimal number of hard gluons necessary to connect all parton lines, contribute dominantly to the hard scattering mechanism. Dimensional arguments, in fact, allow to relate the minimum number of partons in initial (final) state hadrons n_i (n_f) to the asymptotic power-law fall-off predicted by the hard scattering mechanism for differential cross-sections of hard exclusive processes

$$\frac{d\sigma}{dt}(s, t) = f(s/t) s^{2-n_i-n_f} \quad (\text{modulo logs}), \quad (4.1)$$

for a fixed ratio of Mandelstam variables $s/t = \text{const.}$ equivalent to a fixed scattering angle. These relations are known as *dimensional counting rules*. For instance, for the Dirac form factor of the nucleon with $n_i = n_f = 3$ the dimensional counting rules imply

$$F_1(Q^2 \rightarrow \infty) \sim Q^{-4} \quad (\text{modulo logs}) \quad (4.2)$$

and for the elastic form factor of the pion with $n_f = n_i = 2$

$$F_\pi(Q^2 \rightarrow \infty) \sim Q^{-2} \quad (\text{modulo logs}). \quad (4.3)$$

The formalism describing the hard scattering mechanism was developed in the late 70's [95, 96, 97, 98, 99, 100]. The leading order contribution to an elastic form factor takes the form

$$F^h(Q^2) = (N_N^h)^2 \int_0^1 [dx]_N \int_0^1 [dx']_N \phi_N^*(x'_j, \mu_F) T_H(x_i, x'_j, Q^2, \mu_F) \phi_N(x_i, \mu_F) \quad (4.4)$$

where N_N^h is a normalisation specific to the N -particle Fock State of the hadron h . The distribution amplitudes are obtained from LCWFs by integration over transverse momenta up to a factorisation scale μ_F^2

$$\phi_N(x_i, \mu_F) = \frac{1}{N_N^h} \int^{\mu_F^2} [d^2\mathbf{p}_\perp]_N \Psi_N(x_i, \mathbf{p}_\perp i) \quad (4.5)$$

with the integration measures

$$[dx]_N = \delta\left(1 - \sum_{i=1}^N x_i\right) \prod_{i=1}^N dx_i, \quad (4.6)$$

$$[d^2\mathbf{p}_\perp]_N = 16\pi^3 \delta^{(2)}\left(\sum_{i=1}^N \mathbf{p}_\perp i\right) \prod_{i=1}^N \frac{d^2\mathbf{p}_\perp i}{16\pi^3}. \quad (4.7)$$

The normalisation N_N^h is determined such that

$$\int_0^1 [dx]_N \phi_N(x_i) = 1, \quad (4.8)$$

which implies for instance

$$N_2^\pi = \frac{f_\pi}{2\sqrt{6}}, \quad N_3^N = \frac{f_N}{8\sqrt{6}}, \quad (4.9)$$

dimensional
counting rules

where $f_\pi (= 133 \text{ MeV})$ is the usual pion decay constant and f_N plays the rôle of the nucleon wave function at the origin of coordinate space. The hard scattering amplitude T_H describes the scattering of collinear partons calculated perturbatively from connected Feynman diagrams. The diagrams contributing at lowest order in α_s in a calculation of the hard scattering amplitude for the pion form factor F_π are shown in Fig. 4.2.

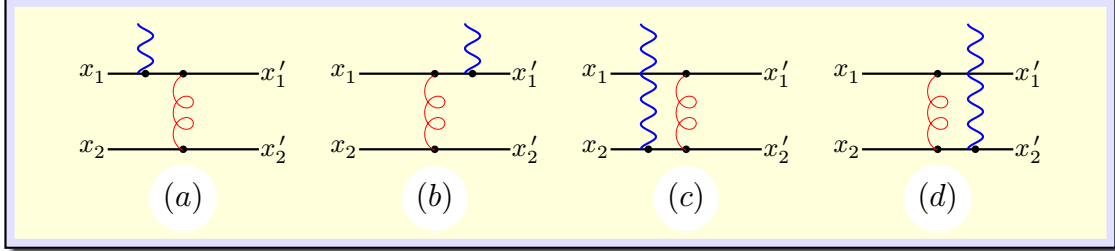


Figure 4.2: Lowest order diagrams to the hard scattering amplitude T_H of the pion form factor F_π .

Neglecting pion masses, it is convenient to choose for the evaluation of the diagrams a special Breit frame, a brick wall frame (cf. appendix C.1.1), where the incoming pion moves fast in positive z -direction and photon and outgoing pion move in the negative z -direction. With the notations of Chapter 2, i.e. $a^\mu = (a_0, a_1, a_2, a_3) = [a^+, a^-, \mathbf{a}_\perp]$ the parametrisation reads

$$\begin{aligned} P^\mu &= (1, 0, 0, 0) Q/2 = [1, 0, \mathbf{0}_\perp] Q/\sqrt{2} && \text{incoming pion} \\ q^\mu &= (0, 0, 0, -1) Q = [-1, 1, \mathbf{0}_\perp] Q/\sqrt{2} && \text{virtual photon} \\ P'^\mu &= (1, 0, 0, 0) Q/2 = [0, 1, \mathbf{0}_\perp] Q/\sqrt{2} && \text{outgoing pion} \end{aligned} \quad (4.10)$$

such that $q^2 = -Q^2$ and $P + q = P'$, and momenta of collinear partons (partons which have no transverse momentum components relative to their parent nucleons) are given as

$$\begin{aligned} p_i^\mu &= [x_i, 0, \mathbf{0}_\perp] Q/\sqrt{2} && \text{incoming parton} \\ p_i'^\mu &= [0, x'_i, \mathbf{0}_\perp] Q/\sqrt{2} && \text{outgoing parton.} \end{aligned} \quad (4.11)$$

Using symmetry of the pion wave function under the replacement $x_1 \leftrightarrow x_2$ (from C invariance) with collinear partons one arrives at

$$T_H(x_1, x'_1, Q^2, \mu_F) = \frac{16\pi \alpha_s(\mu) C_F}{x_1 x'_1 Q^2} \quad (4.12)$$

where $C_F = 4/3$ is the colour factor given as the value of the Casimir operator in $SU(3)_C$. The denominator of the gluon propagator involves the scale $x_1 x'_1 Q^2$, which is the virtuality of the exchanged hard gluon in the collinear approximation. In fact, the observation that the scales of internal momentum flow are related to the external momentum transfer by multiplication with momentum fractions holds true generally for hard scattering amplitudes calculated in the approximation of partons moving collinear to their parent hadrons.

the relevant hard scale

$x_1 x'_1 Q^2$

For a further example of this rule one may look at a little more complex object, the hard scattering amplitude T_H for the Dirac form factor of the nucleon F_1^N . It has to be calculated from 14 diagrams (10 with non-zero contributions) [96, 98, 101, 99] as shown in Fig. 4.3. For the present purpose it is sufficient to have a look at typical scales occurring in the denominators of quark and gluon propagators. As an example Fig. 4.3 (1a) shall be considered (the same diagram as discussed in [102]).

In the Breit-brick wall frame (cf. appendix C.1.1) with the approximation of collinear moving partons (4.11) the scales in the denominators of quark and gluon propagators are readily calculated as

$$\begin{aligned} f_1 &\approx p_1 + q = [x_1 - 1, 1, \mathbf{0}_\perp] Q/\sqrt{2} \\ &\rightarrow f_1^2 \approx -(1 - x_1) Q^2 \end{aligned} \quad (4.13)$$

$$\begin{aligned} g_1 &\approx f_1 - p'_1 = p_1 + q - p'_1 = [x_1 - 1, 1 - x'_1, \mathbf{0}_\perp] Q/\sqrt{2} \\ &\rightarrow g_1^2 \approx -(1 - x_1)(1 - x'_1) Q^2 \end{aligned} \quad (4.14)$$

$$\begin{aligned} f_2 &\approx p_2 + g_1 = p_2 + p_1 + q - p'_1 = [-x_3, 1 - x'_1, \mathbf{0}_\perp] Q/\sqrt{2} \\ &\rightarrow f_2^2 \approx -x_3(1 - x'_1) Q^2 \end{aligned} \quad (4.15)$$

$$\begin{aligned} g_2 &\approx p'_3 - p_3 = [-x_3, x'_3, \mathbf{0}_\perp] Q/\sqrt{2} \\ &\rightarrow g_2^2 \approx -x_3 x'_3 Q^2, \end{aligned} \quad (4.16)$$

where use of the identities

$$\sum_{i=1}^3 x_i = \sum_{i=1}^3 x'_i = 1 \quad (4.17)$$

was made.

Going through the full calculation with all contributing diagrams one finds that scales in the denominators of gluon propagators are given by Q^2 multiplied with two momentum fractions, i.e. of the generic form $x_i x'_j Q^2$, and the corresponding scales in fermion propagators come in two classes, Q^2 either multiplied with one momentum fraction, $x_i Q^2$ or $x'_j Q^2$, or multiplied with two momentum fractions $x_i x'_j Q^2$.

Since the calculation of the elastic form factors involves integrals over the full range $0 \leq \{x_i, x'_j\} \leq 1$ of all momentum fractions in Eq.(4.4), it is obvious that contributions from the end-point regions, $\{x_i, x'_j\} \approx 0$ or $\{x_i, x'_j\} \approx 1$, are unavoidable. In the kinematical end-point regions the gluons become very soft, and the basic assumption of the rescattering by hard perturbative gluons is invalid. The severeness of this inconsistency, i.e. how much end-point regions contribute to the full result, depends on the value for Q^2 , but also on the weighting by the *a priori* unknown distribution amplitudes $\phi(x_i)$.

In fact, the assumption of dominance of the hard scattering mechanism has been criticised [103, 104] on account of large end-point contributions to form factors in the kinematical regions where data are presently available, i.e. up to about

$x_i x'_j Q^2$ or
 $x_i Q^2, x'_j Q^2$

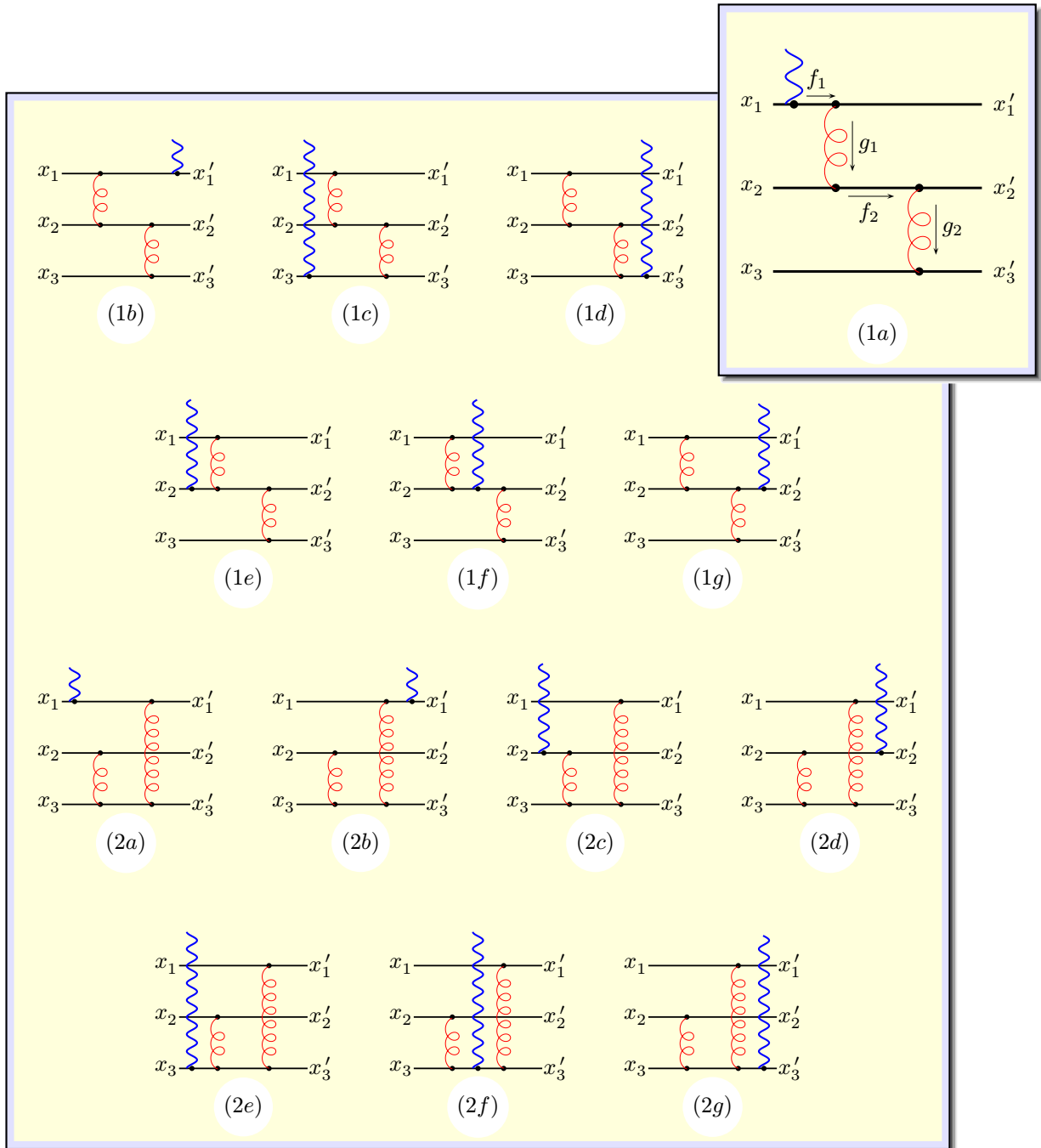


Figure 4.3: The 14 lowest order diagrams to be calculated for the hard scattering amplitude T_H to the Dirac form factor of the nucleon F_1^N . The momentum flow through quark and gluon propagators for the example of diagram (1a) is indicated (see text).

$Q^2 = 10 \text{ GeV}^2$ for $F_\pi(Q^2)$ and up to about $Q^2 = 30 \text{ GeV}^2$ for F_1^p . In particular, in calculations with end-point concentrated DAs, like the Chernyak-Zhitnitsky DA type for the pion [105], and of the Chernyak-Ogloblin-Zhitnitsky [106], Gari-Stefanis [107], King-Sachrajda [108], or the heterotic (HET) [109] type DAs for the nucleon, the contradictory situation emerges that the main part of the results originates from kinematic regions where the basic assumptions of the formalism, as for instance the one-gluon-exchange approximation, are unreliable. With DAs closer to the asymptotic form, $\phi_{asy,\pi}(x_i) \sim x_1 x_2$ and $\phi_{asy,N}(x_i) \sim x_1 x_2 x_3$, the end-point regions contribute less, but the full results are way below the data.

Another aspect – of special relevance in the present context – is the quality of the collinear approximation for the lowest order hard scattering amplitude. Intrinsic transverse momenta of the partons, typically permitted by LCWFs to be up to about a few hundred MeV, have to be compared with the size of the longitudinal scales $\sqrt{x_i x'_j} Q$ or $\sqrt{x_i} Q$. In the end-point regions of the integrations over momentum fractions the neglect of transverse momenta is clearly not justified at all.

These considerations have led to the development of the modified hard scattering approach (mHSA). [110, 111, 112, 113, 114, 115, 116, 117, 118]. The main ingredients of the mHSA are (without going into details here; for a recent review see [102]):

- *Transverse momenta of partons in the hard scattering amplitude* are taken into account in the form that T_H is calculated with (off-shell) partonic momenta

$$\begin{aligned} p_i^\mu &= [x_i Q/\sqrt{2}, 0, \mathbf{p}_{\perp i}] \\ p_i'^\mu &= [0, x'_i Q/\sqrt{2}, \mathbf{p}'_{\perp i}]. \end{aligned} \quad (4.18)$$

For instance, the hard scattering amplitude for the elastic form factor of the pion now takes the form (compare to Eq.(4.12))

$$T_H(x_1, x'_1, Q^2, \mu_F) = \frac{16\pi \alpha_s(\mu_F) C_F}{x_1 x'_1 Q^2 + (\mathbf{p}_{\perp 1} + \mathbf{p}'_{\perp 1})^2} \frac{x_1 Q^2}{x_1 Q^2 + \mathbf{p}_{\perp 1}^2} \quad (4.19)$$

Similar modifications apply to the hard scattering amplitude of the Dirac form factor of the nucleon (see [112, 114] for the detailed formulae).

As a consequence transverse momenta can not be integrated out on the level of the soft hadronic matrix elements, such that elastic form factors are calculated from

$$\begin{aligned} F^h(Q^2) &= (N_N^h)^2 \int_0^1 [dx]_N \int [d^2 \mathbf{p}_\perp]_N \int_0^1 [dx']_N \int [d^2 \mathbf{p}'_\perp]_N \\ &\times \Psi_{0,N}^*(x'_i, \mathbf{p}'_{\perp i}, \mu_F) T_H(x_i, x'_i, \mathbf{p}_{\perp i}, \mathbf{p}'_{\perp i}, Q^2, \mu_F) \Psi_{0,N}(x_i, \mathbf{p}_{\perp i}, \mu_F) \end{aligned} \quad (4.20)$$

with a convolution involving LCWFs $\Psi_{0,N}(x_i, \mathbf{p}_{\perp i}, \mu_F)$ for N -particle Fock states instead of DAs $\Phi_N(x_i, \mu_F)$. The LCWFs $\Psi_{0,N}$ carry an additional

importance of
transverse
momentum effects
in (m)HSA

the modified hard
scattering
approach

index “0” to remind that those are merely the soft parts of the wave functions, i.e. the full wave functions with the perturbative tail removed, since it is taken care of explicitly in the hard scattering amplitude T_H .

- Double logarithmic, radiative gluon corrections – resummed to all orders of α_s by exponentiation – generate *Sudakov type form factors*. These form factors have been derived [66] and adapted to hard exclusive reactions [110] in a mixed representation, where the LC *plus* and *minus* momentum components are kept, but the two transverse momentum components are Fourier transformed to impact parameter space. The leading order diagrams contributing dominantly in an axial gauge are shown in Fig. 4.4; diagrams with radiative gluons connecting parton lines from different LCWFs are subdominant in this gauge. Thus, the Sudakov factors can be taken into account by multiplying the LCWFs (in the mixed representation) by exponentials. The (partly) Fourier transformed expression for an elastic form factor thus takes the form

$$\begin{aligned}
 F^h(Q^2) &= (N_N^h)^2 \int_0^1 [dx]_N \int [d^2\mathbf{b}_\perp]_N \int_0^1 [dx']_N \int [d^2\mathbf{b}'_\perp]_N \\
 &\times \hat{\Psi}_{0,N}^*(x'_j, \mathbf{b}'_{\perp j}, \mu_F) \hat{T}_H^k(x_i, x'_j, \mathbf{b}_{\perp i}, \mathbf{b}'_{\perp j}, Q^2, t) \hat{\Psi}_{0,N}(x_i, \mathbf{b}_{\perp i}, \mu_F) \\
 &\times \exp \left[-S_k(x_i, x'_j, \mathbf{b}_{\perp i}, \mathbf{b}'_{\perp j}, Q, t_k) \right]
 \end{aligned} \tag{4.21}$$

where the index “ k ” indicates a summation over Feynman diagrams. The impact parameter integration measure is

$$[d^2\mathbf{b}_\perp]_N = 4\pi \delta^{(2)} \left(\sum_{i=1}^N \mathbf{b}_{\perp i} \right) \prod_{i=1}^N \frac{d^2\mathbf{b}_{\perp i}}{4\pi}, \tag{4.22}$$

and the convention

$$\hat{f}(\mathbf{b}_\perp) = \frac{1}{(2\pi)^2} \int d^2\mathbf{p}_\perp \exp(-i\mathbf{b}_\perp \cdot \mathbf{p}_\perp) f(\mathbf{p}_\perp) \tag{4.23}$$

for a Fourier transformed function $\hat{f}(\mathbf{b}_\perp)$ is used. As argument of the strong coupling the largest mass scale appearing in the hard scattering amplitude (in diagram “ k ”) is taken. For instance for the pion form factor the argument of $\alpha_s(t_k)$ is

$$t_k = \max \left(\sqrt{x_1 x'_1} Q, \sqrt{x_1} Q, 1/\mathbf{b}_{\perp i}, 1/\mathbf{b}'_{\perp j} \right). \tag{4.24}$$

The Sudakov form factor is defined as

$$\begin{aligned}
 S_k(x_i, x'_j, \mathbf{b}_{\perp i}, \mathbf{b}'_{\perp j}, Q, t_k) &= \\
 &\exp \left[- \sum_{i=1}^N \left(s(x_i, \mathbf{b}_{\perp i}, Q) + \int_{1/b_{\perp i}}^{t_k} \frac{d\bar{\mu}}{\bar{\mu}} \gamma_q(g(\bar{\mu}^2)) \right) \right] \\
 &+ \exp \left[- \sum_{j=1}^N \left(s(x'_j, \mathbf{b}'_{\perp j}, Q) + \int_{1/b'_{\perp j}}^{t_k} \frac{d\bar{\mu}}{\bar{\mu}} \gamma_q(g(\bar{\mu}^2)) \right) \right],
 \end{aligned} \tag{4.25}$$

where " k " is a generic index for the contributing diagrams; the scale t_k is chosen corresponding to the scales in the hard scattering diagram [114, 102]. The function $s(x_i, \mathbf{b}_{\perp i}, Q)$ for a single parton line is listed in appendix B.

- *Intrinsic transverse momentum dependence of the soft wave functions* has to be taken into account in form of a phenomenological model (constrained by electromagnetic charge radii and the probability limit $P_N \leq 1$ valid for any N particle Fock state). For practical purposes in almost all applications a Gaussian form of the transverse momentum is assumed, which is based on a harmonic oscillator model in LC coordinates [119]. A typical ansatz for the LCWF has the form [113, 114, 118, 120]

$$\Psi_N(x_i, \mathbf{p}_{\perp i}) = N_N^h \phi_N(x_i) \Omega_N(x_i, \mathbf{p}_{\perp i}) \quad (4.26)$$

with the normalisation conditions Eq. (4.8) and

$$\int [d^2 \mathbf{p}_{\perp}]_N \Omega_N(x_i, \mathbf{p}_{\perp i}) = 1 \quad (4.27)$$

and a Gaussian for the \mathbf{p}_{\perp} -dependence

$$\Omega_N(x_i, \mathbf{p}_{\perp i}) = \frac{(16\pi^2 a_N^2)^{N-1}}{x_1 x_2 \dots x_N} \exp \left[-a_N^2 \sum_{i=1}^N \frac{\mathbf{p}_{\perp i}^2}{x_i} \right]. \quad (4.28)$$

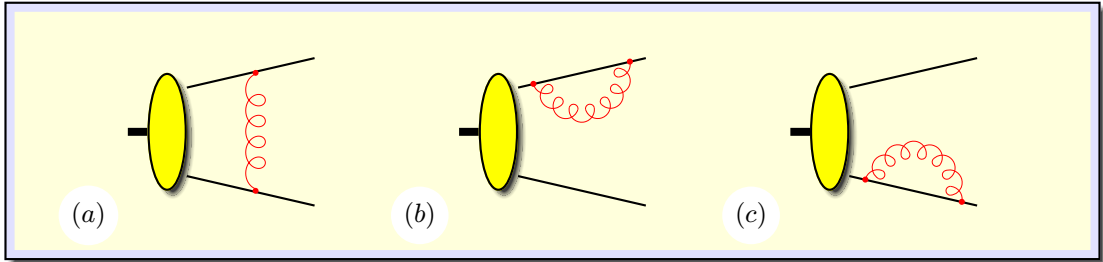


Figure 4.4: Diagrams contributing at leading order in an axial gauge to the Sudakov corrections to the pion LCWF.

In the mHSA perturbative calculations are rendered self-consistent in the sense that most of the contributions picked up in integrations are truly from hard regions, and the singularities from (the one-loop pQCD form of) the running coupling are regularised, since contributions from soft end-point regions are sufficiently suppressed by transverse momentum effects and Sudakov factors.

The price to pay is that results for exclusive quantities calculated in the mHSA typically are significantly smaller than results obtained in HSA. The phenomenological implications will be discussed for some examples in following subsections.

Feynman
mechanism

A competing reaction mechanism, originally proposed by Feynman [121], also known under the names *soft-overlap mechanism* or *handbag mechanism*, is shown in Fig. 4.5 for the elastic nucleon FF. Here an asymmetric, and thus rare, configuration for the longitudinal momentum fractions in the incoming nucleon is

assumed as indicated by the different length of momentum vectors. If the quark struck by the highly virtual photon carries most of the momentum of the nucleon, it can recombine with the two ‘wee’ spectator partons without the need for a redistribution of the momentum transfer. The spectators carry practically no information about a direction; as a perfect null-vector is not oriented in (Euclidean) space at all. The corresponding Feynman diagram is the one shown in Fig. 1.7(b).

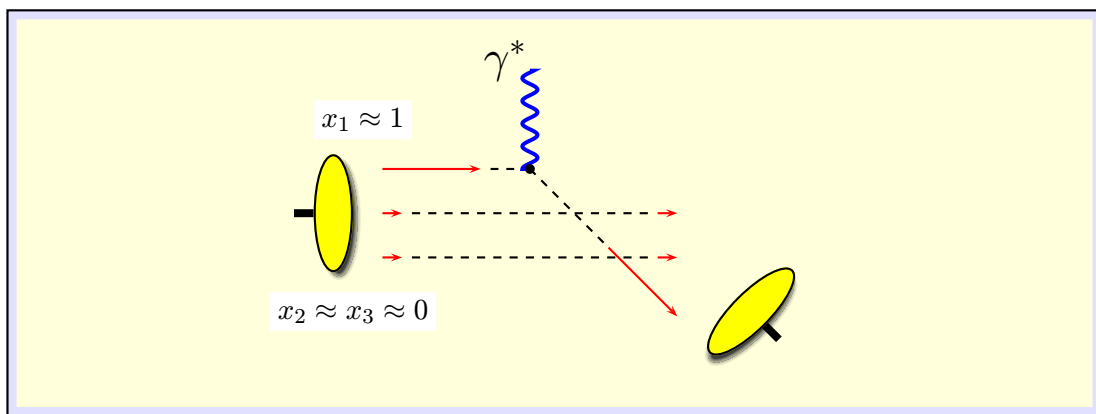


Figure 4.5: Schematical indication of the Feynman mechanism. For an asymmetric initial state configuration ($x_1 \approx 1$ and $x_2 \approx x_3 \approx 0$) no internal redistribution of the momentum transfer is necessary.

The Feynman mechanism receives no suppression by large momentum flow and powers of α_s from the hard gluons; instead the price has to be paid on the level of the wave functions as probability amplitudes to find a certain parton configuration in the nucleon. A configuration where one parton carries (almost) all of the nucleon momentum is extremely rare which is reflected by a strong suppression by the wave function. From the nature of the suppression it is clear that in the asymptotical limit, $Q^2 \rightarrow \infty$, the hard scattering mechanism will be the dominant one, since the suppression by powers of α_s goes with powers of $1/\ln(Q)$, whereas the suppression induced by the wave functions in the Feynman mechanism comes with powers of $1/Q$. Formally, the Feynman mechanism represents a power correction to the hard scattering mechanism. But, at any finite momentum transfer it is not possible to decide *a priori* which mechanism dominates. Only explicit calculations of the diagrams for a given exclusive observable, thereby using assumptions on the non-perturbative input, allow a quantitative comparison. In fact, in many exclusive quantities –though not all– there is now convincing phenomenologically evidence that the Feynman mechanism, or its equivalent in other exclusive quantities than form factors, contributes significantly or even dominant in the kinematical regions where data are available today. This is not surprising regarding the fact that Λ_{QCD}/Q is not much smaller than $1/\ln(Q/\Lambda_{QCD})$ in the few GeV region.

According to Drell and Yan [122] an elastic (helicity non-flip) form factor can be represented as the overlap of LCWFs as (in the notation of [120])

$$F(t) = \sum_N F^{(N)}(t) \quad (4.29)$$

hard scattering mechanism	soft-overlap (Feynman) mechanism
additional hard gluons → higher order in $\alpha_s(Q^2)$	asymmetric configuration → suppression by wave function
suppression by powers of $1/\ln(Q)$	suppression by powers of $1/Q$
asymptotically dominant	important at intermediate $ t $

Figure 4.6: Comparison of sources for suppression in the hard scattering mechanism and the soft-overlap (Feynman) mechanism.

with individual Fock state contributions

$$F^{(N)}(t) = \sum_a e_a \sum_j \sum_\beta \int [d\tilde{x}]_N [d^2\tilde{\mathbf{p}}_\perp]_N \Psi_{N\beta}^*(\hat{x}'_i, \hat{\mathbf{p}}'_\perp i) \Psi_{N\beta}(\tilde{x}_i, \tilde{\mathbf{p}}_\perp i) , \quad (4.30)$$

where β labels different spin-flavour combinations of the partons [123] and j runs over all partons of type “ a ”¹. The “Breit-symmetric” frame, detailed in appendix C.1.2, with a purely transverse momentum transfer $\mathbf{q}_\perp^2 = (\mathbf{p}'_\perp - \mathbf{p}_\perp)^2 = -t$ is used to evaluate the overlap. Incoming and outgoing parton momenta in the overlap contributions are related by $p'_i = p_i$ ($i \neq j$) for the spectator partons and $p'_j = p_j + q$ for the active parton which takes the momentum transfer in the scattering. Using the transformations between the symmetric frame and the in/out-hadron frames one can directly express the LCWF arguments for the outgoing hadron (denoted by a hat) in terms of the ones for the incoming hadron (denoted by a tilde) as established in appendix C.1.5

$$\begin{aligned} \hat{x}'_i &= \tilde{x}_i , & \hat{\mathbf{p}}'_\perp i &= \tilde{\mathbf{p}}_\perp i - \tilde{x}_i \mathbf{q}_\perp & \text{for } i \neq j , \\ \hat{x}'_j &= \tilde{x}_j , & \hat{\mathbf{p}}'_\perp j &= \tilde{\mathbf{p}}_\perp j + (1 - \tilde{x}_j) \mathbf{q}_\perp , \end{aligned} \quad (4.31)$$

where the hat/tilde notation could have been dropped for the momentum fractions which are not changed by the boost (2.9). The shifts $-\tilde{x}_i \mathbf{q}_\perp$ result from the transverse boost relating the “in-hadron” and “out-hadron” frames, the active parton additionally takes the overall momentum transfer \mathbf{q}_\perp which is purely transverse in the present frame.

To obtain the contribution of the Feynman mechanism to an elastic form factor the Drell-Yan formula Eq. (4.30) has to be evaluated with the soft parts of the LCWFs $\Psi_{0,N\beta}(x_i, \mathbf{p}_\perp i)$ only, i.e. with their perturbative tails of \mathbf{p}_\perp -dependence removed. The effect of the overlap of the perturbative tails is properly described within the (modified) HSA and must not be double-counted.

From the form of the arguments (4.31) to be used in Eq.(4.30) it is evident that the \mathbf{p}_\perp -dependence of the soft parts of the LCWFs $\Psi_{0,N\beta}(x_i, \mathbf{p}_\perp i)$ completely determines the size of the soft overlap contributions. What renders the overlap integral non-trivial are the shifted arguments in transverse momentum space.

¹Whenever it is necessary to distinguish the momenta of active and spectator partons the active one will be labelled with an index j and the spectators with an index i ($i \neq j$); outgoing momenta will always be indicated by a prime.

In the above considerations the relation between the contribution of the Feynman mechanism to elastic FFs and the \mathbf{p}_\perp -dependence of the soft LCWFs becomes directly evident because of the choice of convenient frames. The question arises whether this close connection is peculiar to chosen frames. Since the result for the overlap contribution is Lorentz invariant, one could use a different frame for the calculation, for instance one where the momentum transfer is not purely transverse. In that case Eq. (4.30) would acquire additional contributions which represent overlap integrals of Fock states with different particle numbers, $N - 1$ and $N + 1$ (see discussion in [123, 124]).

4.2.2 form factors at large $|t|$

Purely theoretical considerations on different reaction mechanisms in hard exclusive reactions at large momentum transfer remain incomplete, since *a priori* unknown non-perturbative matrix elements determine the prefactors and therefore the relative importance of the various contributions. In the following, several exclusive quantities are briefly discussed phenomenologically as examples of how the transverse momentum effects manifest themselves. A consistent phenomenological picture arises.

4.2.2.1 form factor of the pion $F_\pi(Q^2)$

The elastic form factor of the pion F_π is defined from the matrix element of the electromagnetic current operator

$$\langle \pi(P') | j_{e.m.}^\mu | \pi(P) \rangle = e_\pi (P' + P)^\mu F_\pi(Q^2), \quad (4.32)$$

where e_π is the charge of the pion and the momentum transfer is given as $Q^2 = (P' - P)^2$. In obtaining (4.32) the on-shell condition $P^2 = P'^2 = m_\pi^2$ and conservation of the electromagnetic current $\partial_\mu j_{e.m.}^\mu = 0$ was used.

In Fig. 4.7 different contributions to the quantity $Q^2 F_\pi(Q^2)$ are compared to the available experimental data. For the theoretical calculations the asymptotic form of the DA of the lowest Fock state $\phi(x_1, x_2) = 6 x_1 x_2$ was chosen. The \mathbf{p}_\perp -dependence of the soft LCWFs was modelled with a Gaussian ansatz in the form of Eq. (4.28). The contribution obtained in the mHSA is clearly below the data, which are admittedly very uncertain; only statistical errors are shown, for a discussion of systematical problems to extract $F_\pi(Q^2)$ from the data for electroproduction on the proton see [127, 128].

The Feynman (or soft-overlap) contribution is significantly larger, but also seems to be insufficient to explain the data alone. For comparison the soft-overlap contribution obtained with a Gaussian ansatz for the \mathbf{p}_\perp -dependence and containing an additional mass term as suggested by the Brodsky-Huang-Lepage model [129] is also shown. As expected, for larger values of Q^2 the two curves differ substantially, whereas at intermediate momentum transfers they are rather similar; in particular the height of the maximum is almost the same. This behaviour is easy to understand. At small to intermediate relative shifts in the

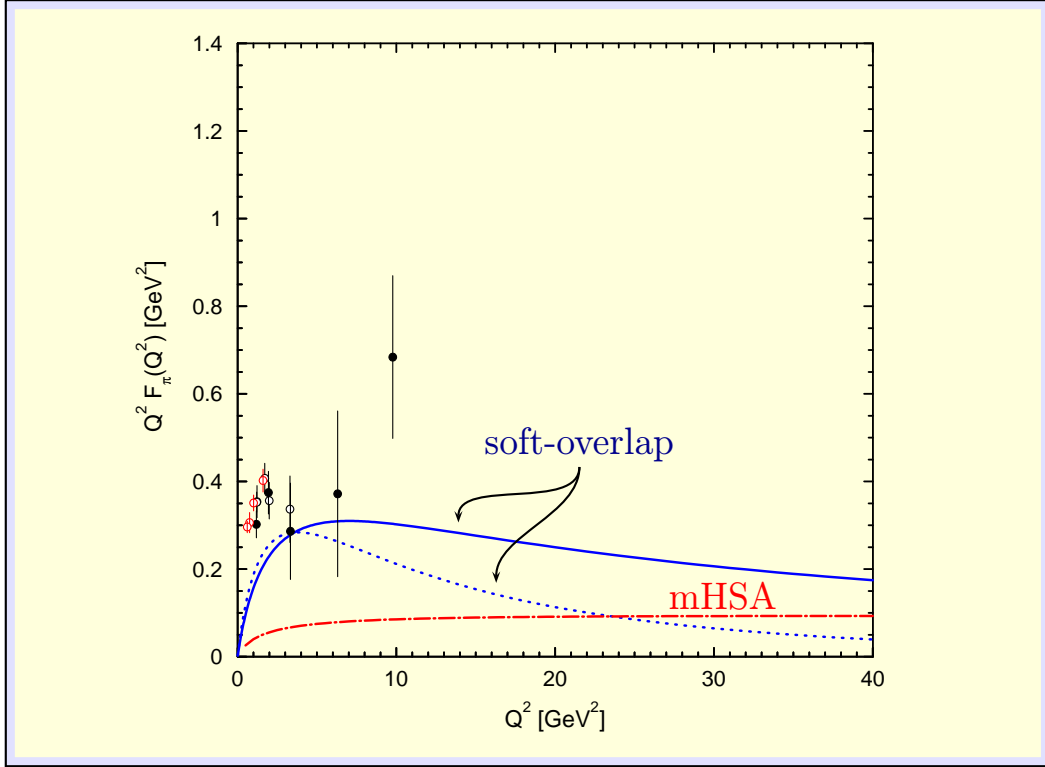


Figure 4.7: The elastic form factor of the pion plotted against Q^2 . The dash-dotted (red) curve represents the result obtained in the mHSA with the asymptotic DA and Gaussian \mathbf{p}_\perp -dependence of Eq. (4.28). The full (blue) line shows the soft-overlap contribution obtained with the same LCWF. For comparison the soft-overlap contribution obtained with a DA with additional mass term is also shown as dotted (blue) curve. Data are taken from [125, 126] (open/full black circles) and [127] (open red circles).

transverse momentum arguments in Eq. (4.30) the results are mainly governed by the width of the LCWFs in \mathbf{p}_\perp space, which is related to the radius of the lowest pion Fock state and thus practically the same in all models. And at larger shifts of arguments the details of the model strongly matter; the tails of the assumed \mathbf{p}_\perp -dependence determine the size of the overlap integral (4.30). Fig. 4.7 corresponds to Fig. 4 of [116] where more details of the calculation are to be found. Some more recent data of the JLAB-F(pi) collaboration [127] are included in Fig. 4.7.

From Fig. 4.7 it is tempting to claim that the data are well explained, if one sums up the mHSA and soft-overlap contributions. It should be mentioned however that more issues related to the pion form factor have been considered. Model calculations within QCD sum rule approaches confirm the principal observation of large soft contributions [130, 131]. Perturbative loop corrections in the HSA are found to be sizable, but strongly depend on the choice of the hard scale in the strong coupling [132, 133, 134, 135, 136, 137, 138]. Loop corrections in the mHSA have not been calculated. LC sum rules indicate that higher twist corrections to the pion form factor might be substantially [131], and the relation between resummed gluon corrections and non-perturbative power corrections has been investigated [139]. The influence of choices for factorisation and renormalisation scales together with an infrared analytic coupling has been considered in

the context of the mHSA [140, 141]. In view of the above listed issues related to the pion form factor it becomes clear that though many subtle problems have been addressed and understanding made considerable progress, it would be premature to claim that the elastic pion form factor is fully understood. Eagerly awaited more precise data certainly will reopen the theoretical discussions. The purpose of the present subsection is merely a comparison of the relative importance of the two reaction mechanisms under consideration, which can be done rather safely without having all smaller details of the full picture.

In conclusion, for the elastic FF of the pion, both reaction mechanisms discussed in the previous subsection are of significant size. Soft-overlap contributions, formally power corrections to the hard scattering, seem to be dominant at small to intermediate momentum transfer. The value of Q^2 for the transition to a kinematical regime where the hard scattering becomes dominant depends on model assumptions of the calculations. Transverse momentum effects are clearly non-negligible up to very high values of momentum transfer $Q^2 \gg 40 \text{ GeV}^2$.

4.2.2.2 elastic form factor of the nucleon

The electromagnetic Dirac-FF, $F_1(Q^2)$, and Pauli-FF, $F_2(Q^2)$, of the nucleon are defined from the matrix element of the electromagnetic current operator

$F_1(Q^2)$

$$\langle N(P', S') | j_{e.m.}^\mu | N(P, S) \rangle \quad (4.33)$$

$$= \bar{u}(P', S') \left\{ \gamma^\mu F_1(Q^2) + \frac{i\sigma^{\mu\nu}\Delta_\nu}{2M} F_2(Q^2) \right\} u(P, S), \quad (4.34)$$

where the momentum transfer is given as $Q^2 = (P' - P)^2$. In obtaining (4.33) the on-shell condition $P^2 = P'^2 = m_N^2$ and conservation of the electromagnetic current $\partial_\mu j_{e.m.}^\mu = 0$ was used. The definition (4.33) implies the normalisations

$$\begin{aligned} F_1^p(0) &= 1 \quad , & F_2^p(0) &= \kappa^p \simeq 1.79, & \text{for the proton} \\ F_1^n(0) &= 0 \quad , & F_2^n(0) &= \kappa^n \simeq -1.81, & \text{for the neutron} \end{aligned} \quad (4.35)$$

where $\kappa^{p/n}$ are the anomalous magnetic moments of proton and neutron.

Alternatively, by use of the Gordon identity the electric and magnetic Sachs FFs [142, 143] can be defined, which are related to the Dirac and Pauli FFs by

$$\begin{aligned} G_E &= F_1 - \tau F_2, \\ G_M &= F_1 + F_2 \end{aligned} \quad (4.36)$$

with the shorthand notation

$$\tau = \frac{Q^2}{4m_N^2}. \quad (4.37)$$

In Fig. 4.8 (left panel) the results for the the magnetic FF of the proton are shown obtained in the mHSA with a whole set of end-point concentrated DAs [144, 145, 102] as suggested by QCD sum-rules [106]. Those DAs have been chosen together with a maximum normalisation to the LCWF, imposed by assuming unity for the probability of the valence Fock state, in order to probe the

maximum contribution to $Q^4 G_M^p(Q^2)$ within the mHSA. The \mathbf{p}_\perp -dependence was modelled with a Gaussian ansatz in the form of Eq. (4.28). Since the difference between G_M^p and F_1^p , corresponding to proton helicity flip, is predicted to be zero in HSA and mHSA, both data sets are shown in comparison.

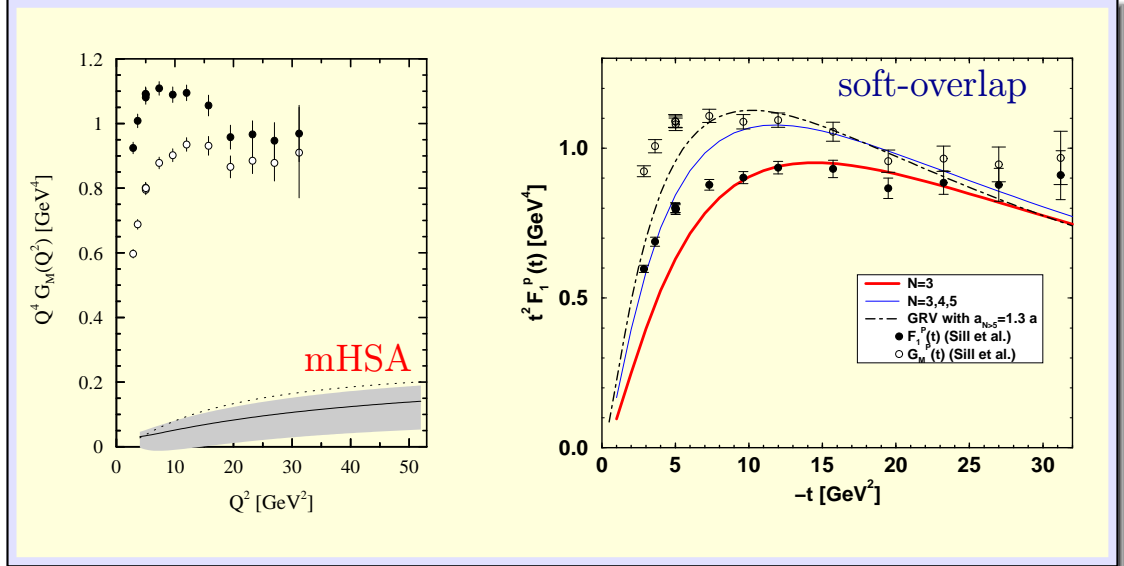


Figure 4.8: The proton magnetic form factor vs. Q^2 . Data are taken from [146]. The G_M^p data are represented by black circles, whereas those for F_1^p are indicated by open circles. *Left:* Contributions obtained in the modified hard scattering approach. The shadowed band indicates the range of predictions derived from the set of DAs determined in [144, 145] in the context of QCD sum rules. The solid (dotted) line corresponds to the COZ [106] (optimised GS) DA. *Right:* Soft-overlap contributions obtained with the Bolz-Kroll DA [118, 147] (see text). Possible improvements by modelling $N = 4, 5$ Fock states or utilising the inclusive PDF data as input are indicated.

Fig. 4.8 (left panel) is similar to Fig. 6 in [114], but shows instead the band of results of the improved and more accurate calculation of [118], which was mentioned in [114], but not shown explicitly. The higher accuracy was obtained by retaining \mathbf{p}_\perp -dependence not only in gluon propagators, but also in the class of fermion propagators which come with a longitudinal scale bilinear in momentum fractions, i.e. of the generic form $x_i y_j Q^2$, and neglecting it only in fermion propagators which come with scales $x_i Q^2$ or $y_i Q^2$ (compare the discussion of scales in subsection 4.2.1). The resulting 9-dimensional integrations are technically very demanding and were fully completed only after the publication of [114]. With the improved accuracy of the calculation the estimates for a maximum of the (modified) hard scattering contributions were altered even more constraining than from the results of the 7-dimensional integrations displayed in [114].

The fact that contributions to the magnetic FF of the proton in the mHSA are down by at least an order of magnitude in comparison with – in this case rather precise – experimental data is understandable. The internal redistribution of the momentum transfer in the proton proceeds via at least two hard gluons. Thus, the suppression of hard scattering contributions, as observed in the pion FF with one hard gluon exchange, is even more pronounced in the proton case. Assuming

a DA of the asymptotic form $\phi(x_i) = 120 x_1 x_2 x_3$ leads to mHSA contributions which are close to zero (with the scales of Fig. 4.8 they would be practically indistinguishable from the zero-line).

When the suppression of the mHSA contribution to the magnetic FF of the proton is more pronounced than for F_π , what is the situation for the soft-overlap contributions to the elastic FF of the proton? Is the tendency of enhanced effects carried on, i.e. are soft-overlap contributions much larger than the ones proceeding via hard gluon scattering? In fact, in [118] it was observed that the soft overlap contributions calculated with end-point concentrated DAs of the COZ type (modelling the \mathbf{p}_\perp -dependence by the Gaussian ansatz (4.28)) overshoot the data by factors 5 - 10, i.e. larger than the (m)HSA contributions by up to two orders of magnitude. There is yet another very strong argument disfavouring endpoint-concentrated proton DAs from the observation that they lead to valence quark distributions much larger at large x than those extracted from DIS data [148]. A model wave function was determined, close to the asymptotic form but not fully symmetric, which provides a soft-overlap contribution in agreement with the data; the mHSA contribution calculated with the same DA is negligible.

The Bolz -Kroll (BK) model wave function for the valence qqq Fock state reads

$$\Psi_{123}(x_i, \mathbf{p}_{\perp i}) \equiv \Psi(x_1, x_2, x_3; \mathbf{p}_{\perp 1}, \mathbf{p}_{\perp 2}, \mathbf{p}_{\perp 3}) = \frac{f_3}{8\sqrt{6}} \phi_{123}(x_i) \Omega_3(x_i, \mathbf{p}_{\perp i}), \quad (4.38)$$

where again the \mathbf{p}_\perp -dependence is give by the ansatz (4.28), and at the input scale $\mu_0 = 1 \text{ GeV}$ the DA has the simple form

$$\phi_{123}(x_i, \mu_0 = 1 \text{ GeV}) = 60 x_1 x_2 x_3 (1 + 3x_1). \quad (4.39)$$

The values of the normalisation f_3 and the transverse size parameter a_3 have been determined in [118] at the scale of reference $\mu_0 = 1 \text{ GeV}$ as

$$f_3 = 6.64 \cdot 10^{-3} \text{ GeV}^2, \quad a_3 = 0.75 \text{ GeV}^{-1}. \quad (4.40)$$

Fig. 4.9 shows the BK model DA in comparison with the COZ DA, the latter as a typical example for the class of end-point concentrated DAs derived from sum rule constraints (see [145, 102] for a detailed discussion on classifications of nucleon DAs from sum-rules). The Bolz-Kroll DA has a much less pronounced asymmetry, where the peak is shifted only moderately away from the symmetric point of $x_1 = 1/3$ to larger values of x_1 . The variable x_1 by construction denotes the momentum fraction which corresponds to an u quark in the proton with spin aligned to the proton spin [118].

Fig. 4.8 (right panel) demonstrates a reasonable agreement of the soft-overlap (Feynman) contribution to the Dirac FF of the proton, obtained with the BK soft LCWF from the Drell-Yan formula (4.30), with the data for $G_M^p(Q^2)$ and $F_1^p(Q^2)$. Possible improvements by generically adding effects of the $N = 4$ ($qqq g$) and $N = 5$ ($qqq \bar{q}q$) Fock states are indicated. More details of this improvement are to be found in [120].

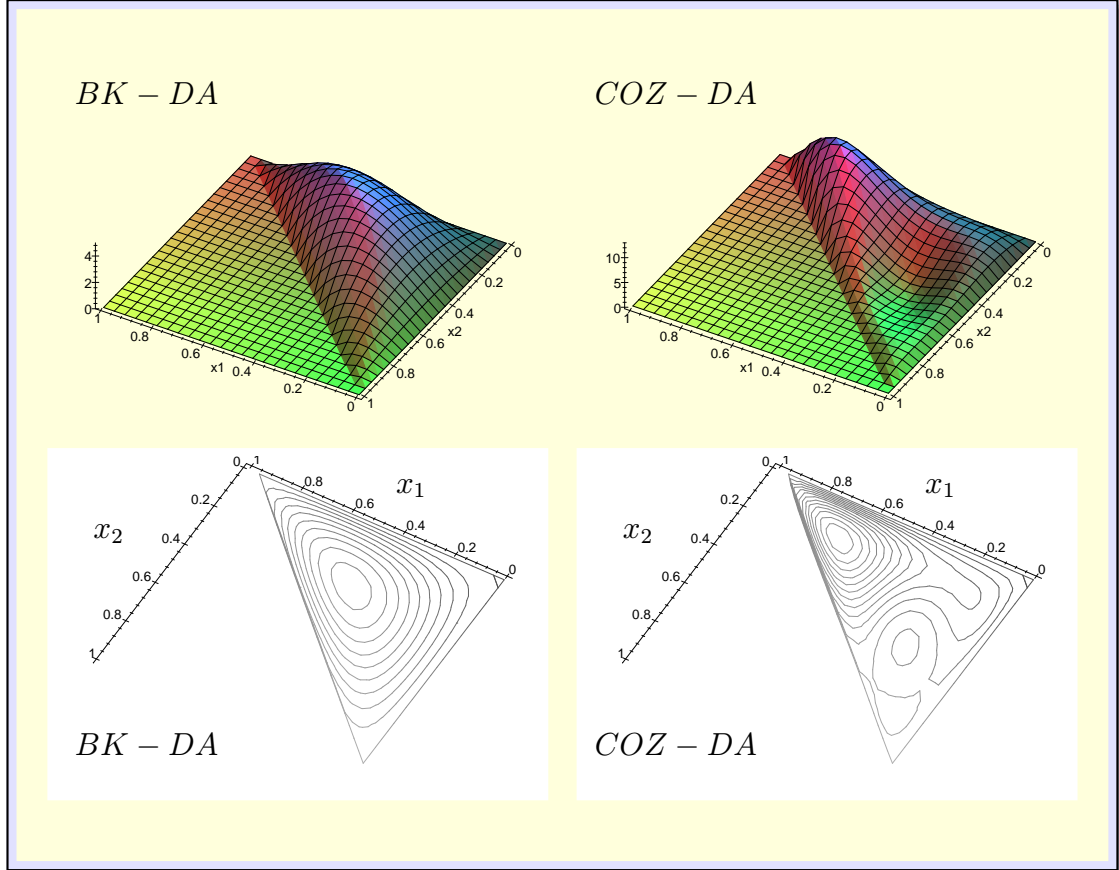


Figure 4.9: Comparison of different DAs for the proton displayed in 3-dimensional and contour plots. *Left:* DA used in the Bolz-Kroll model wave function [118]. *Right:* DA proposed by Chernyak-Ogloblin-Zhitnitsky [106] from sum-rule considerations.

In conclusion, there is phenomenological evidence that the elastic FF of the proton is strongly dominated by the soft-overlap contribution at presently accessible momentum transfers, i.e. up to $Q^2 = 30 \text{ GeV}^2$, and far beyond. The hard scattering mechanism seems to contribute negligibly, though it is generally agreed that it has to take the lead at asymptotically large values of Q^2 . The tendency of a suppressed hard scattering and a large overlap contribution is much more pronounced than observed for the elastic pion FF as was expected from the fact that more hard gluons are necessary for the internal redistribution of the momentum transfer. This confirms the general observations made in [103, 104].

4.2.2.3 pion- γ transition form factor

A further very illustrating example is the pion- γ transition form factor $F_{\pi\gamma}(Q^2)$ which is defined from the $\gamma^*\pi^0 \rightarrow \gamma$ vertex for $e\pi \rightarrow e\gamma$

$$\Gamma_\mu = -ie^2 F_{\pi\gamma}(Q^2) \varepsilon_{\mu\nu\rho\sigma} P_\pi^\nu \epsilon^\rho q^\sigma, \quad (4.41)$$

where P_π and q are the momenta of the initial pion and virtual photon, respectively, and ϵ is the polarisation vector of the final (on-shell) photon. Q^2 is the virtuality of the off-shell photon.

At lowest order pQCD $F_{\pi\gamma}$ is described by a pure QED diagram (see Fig. 4.10 (left panel)), and there is no soft-overlap contribution, since only one hadron is involved in the process ².

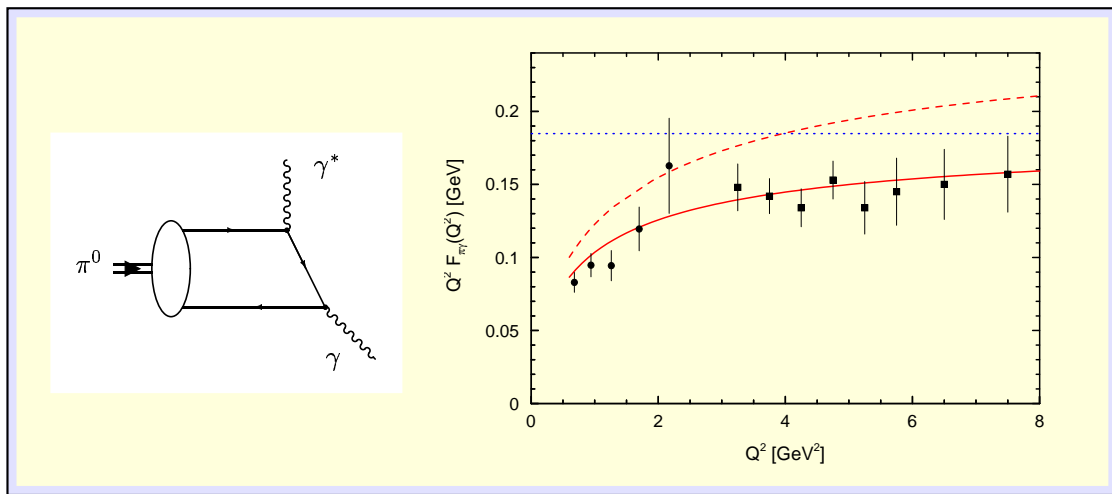


Figure 4.10: Pion- γ transition form factor vs. Q^2 . *Right:* The lowest order diagram for $\gamma^*\pi^0 \rightarrow \gamma$. *Left:* Results from calculation in the mHSA with asymptotic DA (CZ DA) are shown as solid red line (dashed red line) in comparison with the data from CELLO [150] (circles), and CLEO [151] (squares). The level of the pQCD prediction for the asymptotic limit $Q^2 \rightarrow \infty$ is indicated as (blue) dotted line.

In fact, the mHSA contribution obtained with the asymptotic pion DA and ansatz (4.28) for the \mathbf{p}_\perp -dependence describes the data astonishing well as shown in Fig. 4.10 (right panel), which is taken from [116] with the more recent CLEO data [151] added (see also the discussion in [152]). The level of the pQCD prediction for the asymptotic limit $Q^2 \rightarrow \infty$ is indicated as (blue) dotted line in Fig. 4.10 (right panel). For comparison the mHSA contribution obtained with the CZ pion DA is also shown which is significantly off the data. In particular, since the measurement of the more recent CLEO data [151] the pion- γ transition FF provides strong evidence that the pion DA already at intermediate values of Q^2 is rather close to its asymptotic form. No uncertainties from competing reaction mechanisms obscure this observation. Similar conclusions on the form of the pion DA have been also drawn from a local quark hadron duality model [153]. One loop corrections to $F_{\pi\gamma}$ are known to be moderate [154, 134, 136, 155] and do not spoil the general observation in favour of a DA close to the asymptotic form.

In conclusion, the pion- γ transition FF is an example of an exclusive hard quantity, where the transverse momentum effects show up only moderately. The asymptotic limit – one of the very few parameter-free predictions of pQCD – seems to be approached by the data already at intermediate large values of Q^2 . Thus, $F_{\pi\gamma}(Q^2)$ plays a unique rôle in the determination of the pion DA.

²The overlap of the pion LCWF with a wave function describing the hadronic content of the on-shell photon is not only suppressed by factors α_S , but also disfavoured by a helicity mismatch [149].

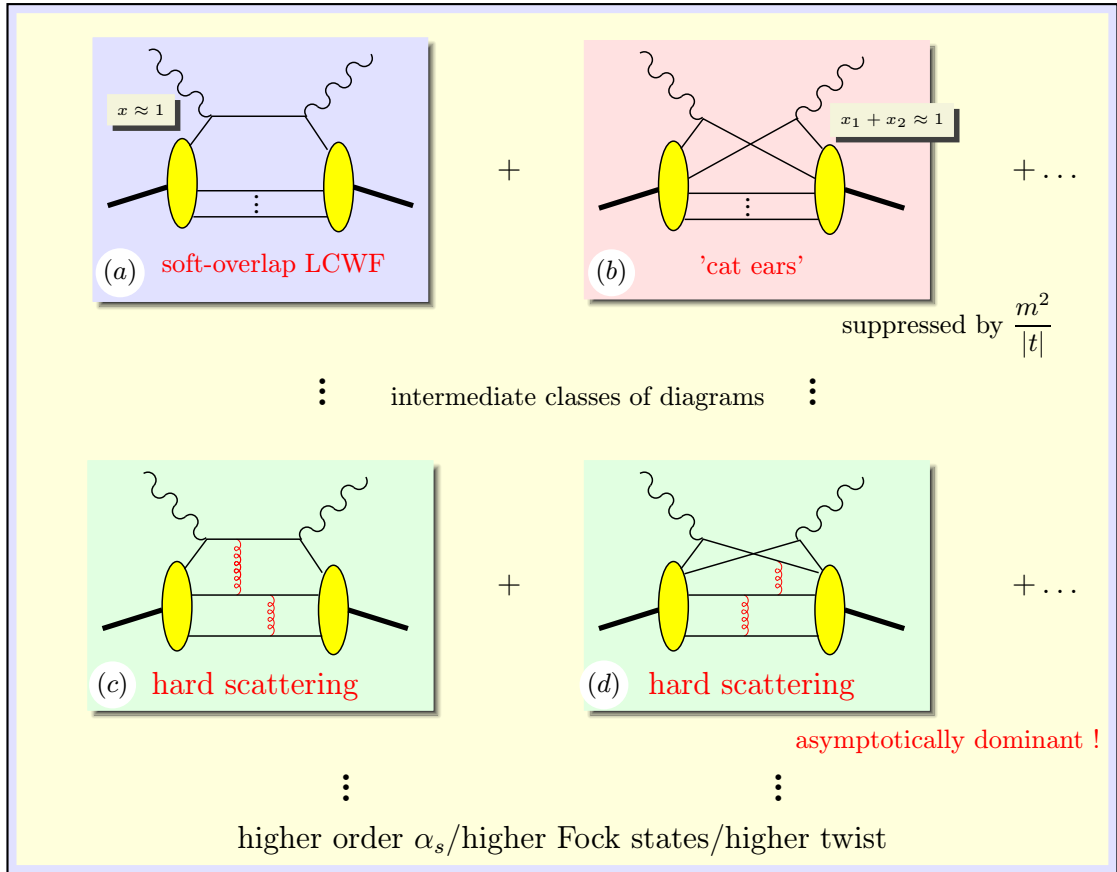


Figure 4.11: Some of the diagrams contributing to WACS ordered with increasing number of hard gluons. The dots between the upper and lower diagrams indicate an intermediate class of diagrams with one exchanged hard gluon, whereas the dots at the bottom stand for diagrams with a higher number of gluons (α_s corrections), and diagrams from higher Fock states (power corrections).

4.2.3 wide angle Compton scattering (WACS)

A process with close relationship to the elastic FF of the proton is real Compton scattering off the proton in the kinematical regime of large $|t|$, or at wide angles³. In the following different contributions to real WACS are compared; results on the kinematical regime of virtual, but not deeply virtual, Compton scattering at wide angles are published in [156]. Examples of diagrams for real WACS are displayed in Fig. 4.11: The soft-overlap mechanism is described by the handbag diagram (a), the contribution from the ‘cat ears’ diagram (b) is suppressed relative to (a). Typical examples for diagrams of hard scattering contributions are displayed in (c) and (d).

4.2.3.1 WACS off protons in the hard scattering approach

Calculations for the Compton scattering process at wide angles in the modified

³Wide angles in the present context refers to angles around 90° corresponding to large momentum transfer, and not backward scattering.

HSA exist only for scattering off pions [157], where no data are available for comparison and a phenomenological discussion, but not for the proton. Thus, in the following results are quoted from a recent leading order calculation of real WACS off protons in the standard HSA [158], i.e. in the approximation of collinear partons, superseding (and partly correcting) earlier calculations [159, 160].

The unpolarised cross section, scaled by s^6 , obtained with different DAs is shown in Fig. 4.12 in comparison to the data. To minimise the influence of choices for the $\alpha_s(\mu)$ argument, the same quantity normalised to the factor $(Q^4 F_1^p(Q^2))^2$, where F_1^p is the Dirac form factor of the proton, is also shown. Uncertainties are expected to cancel from this ratio to a large extent.

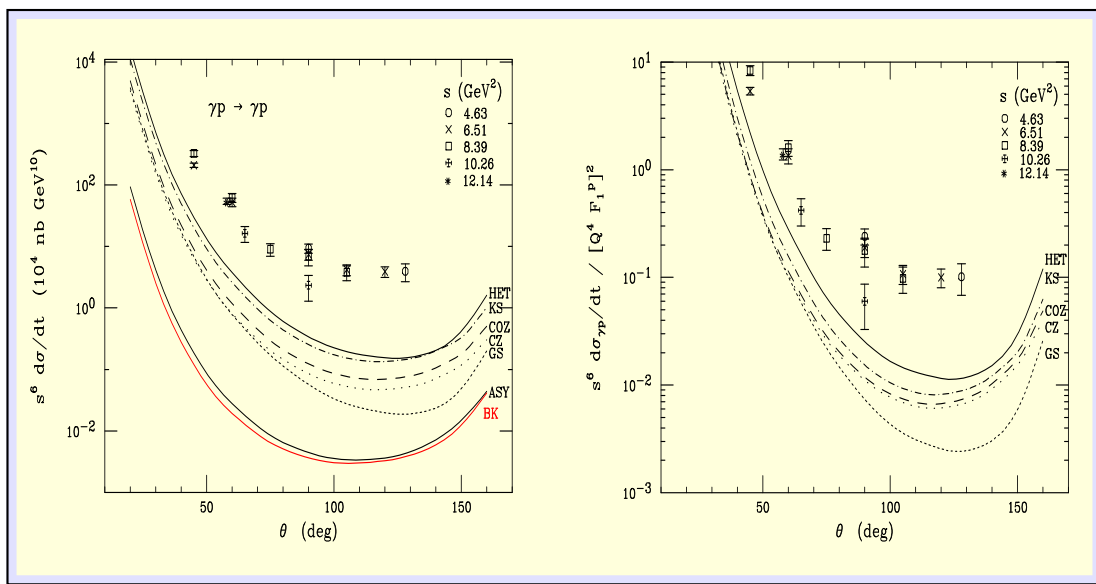


Figure 4.12: *Left:* The hard scattering contribution to the unpolarised differential cross section for WACS obtained with different DAs compared to the data [161]. *Right:* The same quantity scaled by the pQCD result for $(Q^4 F_1^p(Q^2))^2$. Figures reproduced from [158] with one additional curve (BK) provided by the same authors.

Clearly, the results of the hard scattering contributions to the unpolarised cross sections fall short to describe the available data, which are admittedly at rather low momentum transfers. The results obtained with end-point concentrated DAs are 1 - 2 orders of magnitude smaller than the data, the ones obtained with the asymptotic DA and the BK model wave function are about a factor 1000 smaller than the data. From the ratio shown on the RHS the authors of [158] conclude that ‘...it seems unlikely that the elastic proton form factor and the Compton scattering amplitudes are both described by pQCD at presently accessible energies’.^{4,5}

⁴Conclusions from the ratio of $s^6 (d\sigma_{\gamma p}/dt) (Q^4 F_1^p(Q^2))^{-2}$ though should be taken with some care, since the authors of [158] claim a discrepancy of a factor 1/2 in the formulas compared to previous calculations of $F_1^p(Q^2)$, a point which up to now has not been finally clarified.

⁵Note that in [158] ‘pQCD’ is used synonymously for the HSA in the collinear approximation, i.e. for the term which is leading in pQCD at asymptotic large $|t|$. However, it should be stressed that also the handbag contribution is based on a factorisation picture with the hard part described by pQCD and the soft part by a hadronic matrix element.

These results suggest, that hard scattering is not the dominant reaction mechanism at the intermediate large momentum transfer, a situation very similar to the one observed for the elastic nucleon form factors, and less pronounced for the pion form factor.

4.2.3.2 WACS of protons in the soft-overlap approach

soft-overlap
contribution to
WACS

The contribution from the overlap integral of soft LCWFs (Feynman mechanism) to WACS is also denoted as *handbag contribution*, since the amplitude of the process is described by a handbag diagram [162]. This diagram factorises in a hard photon-parton amplitude and a non-perturbative part [120], the latter described by a *generalised parton distribution* at vanishing *skewedness*, which can be calculated from the overlap of LCWFs, as indicated by diagram (a) in Fig. 4.11. The representation of generalised parton distributions as overlap integrals of LCWFs will be discussed in detail in the following section. The contribution from the cat-ears diagram (b) was shown to be suppressed by inverse powers of $|t|$ relative to the handbag diagram [120].

The (unpolarised) differential cross section can be written

$$\begin{aligned} \frac{d\sigma}{dt} &= \frac{2\pi\alpha_{em}^2}{s^2} \left[-\frac{u}{s} - \frac{s}{u} \right] \\ &\times \left\{ \frac{1}{2} \left(R_V^2(t) + R_A^2(t) \right) - \frac{us}{s^2 + u^2} \left(R_V^2(t) - R_A^2(t) \right) \right\} \end{aligned} \quad (4.42)$$

with new form factors [162] specific to Compton scattering depending on $-t$ only

$$\begin{aligned} \sum_a e_a^2 \int_0^1 \frac{dx}{x} P^+ \int \frac{dz^-}{2\pi} e^{ixP^+z^-} \langle P' | \bar{\psi}_a(0) \gamma^+ \psi_a(z^-) - \bar{\psi}_a(z^-) \gamma^+ \psi_a(0) | P \rangle \\ = R_V(t) \bar{u}(P') \gamma^+ u(P) + R_T(t) \frac{i}{2m} \bar{u}(P') \sigma^{\nu} \Delta_\nu u(P) . \end{aligned} \quad (4.43)$$

R_T being related to nucleon helicity flips is neglected in Eq. (4.42). An analogous definition holds for R_A involving the axialvector nucleon matrix element

$$\begin{aligned} \sum_a e_a^2 \int_0^1 \frac{dx}{x} P^+ \int \frac{dz^-}{2\pi} e^{ixP^+z^-} \langle P' | \bar{\psi}_a(0) \gamma^+ \gamma_5 \psi_a(z^-) + \bar{\psi}_a(z^-) \gamma^+ \gamma_5 \psi_a(0) | P \rangle \\ = R_A(t) \bar{u}(P') \gamma^+ \gamma_5 u(P) + R_P(t) \frac{\Delta^+}{2m} \bar{u}(P') \gamma_5 u(P) . \end{aligned} \quad (4.44)$$

In a frame where $\Delta^+ = 0$ – like the CMS-symmetric of appendix C.2.1 – the pseudoscalar form factor R_P decouples from Eq. (4.42).

The new Compton form factors $R_V(t)$, $R_T(t)$, $R_A(t)$, $R_P(t)$ are x^{-1} -moments of generalised parton distributions, which have a representation as overlap integrals of LCWFs. This parallels the situation of elastic form factors, which are x^0 -moments of the same GPDs, and therefore are given by the Drell-Yan overlap formula. Thus, from the knowledge of LCWFs the Compton form factors could be directly calculated. Since the exact LCWFs of nucleons are unknown, it is a good strategy to use additional assumptions on the \mathbf{p}_T -dependence of LCWFs

to establish a connection to related non-perturbative quantities which are rather well-known from experiments.

Assuming the Gaussian model (4.28) for transverse parton momenta the form factors $R_V(t)$ and $R_A(t)$ factorise in ordinary parton distribution functions (PDFs) and a (t, x) -dependent exponential for each N parton Fock state separately

$$R_V^{(N)}(t) = \int_0^1 \frac{dx}{x} \exp \left[\frac{a_N^2 t}{2} \frac{1-x}{x} \right] \times \left\{ e_u^2 [u_v^{(N)}(x) + 2\bar{u}^{(N)}(x)] + e_d^2 [d_v^{(N)}(x) + 2\bar{d}^{(N)}(x)] + e_s^2 2\bar{s}^{(N)}(x) \right\}, \quad (4.45)$$

and analogously for $R_V \rightarrow R_A$, $q(x) \rightarrow \Delta q(x)$. The valence PDF for an N parton Fock state can be calculated from model LCWFs as

$$q_a^{(N)}(x) = \sum_j \sum_\beta \int [dx]_N [d^2\mathbf{k}_\perp]_N \delta(x - x_j) |\Psi_{N\beta}(x_i, \mathbf{k}_{\perp i})|^2 \quad (4.46)$$

where the sum j runs over all partons of type a . The results for the form factors R_V and R_A obtained with the ansatz (4.28) and the BK model DA for the $N = 3$ Fock state are shown in Fig. 4.13 together with estimates for additional contributions from the next higher Fock states ($N = 4, 5$) in a generic model [120].

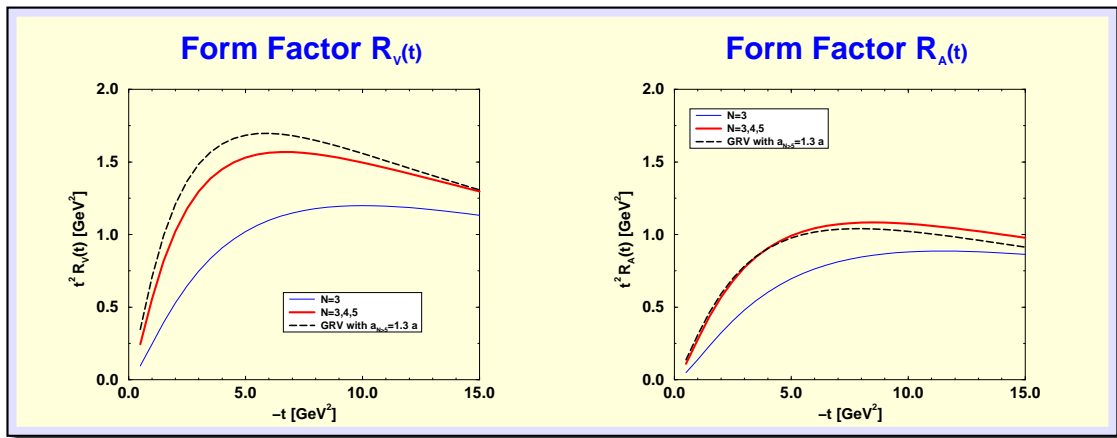


Figure 4.13: CS form factors calculated from the valence Fock state only (thin solid line), $N=3,4,5$ Fock states (thick solid line), and with an additional estimate for higher Fock states (dashed line). *Left:* $R_V(t)$. *Right:* $R_A(t)$.

Under the additional assumption that all Fock states come with the same transverse size parameter $a_N = a$ the sums $\sum_N R_V^{(N)}(t)$ and $\sum_N R_A^{(N)}(t)$ can be directly related to the full proton valence PDFs, i.e. summed over all Fock states, which can be taken from phenomenological parametrisations. An estimate for the effect of all higher Fock states arises. Results for the estimate based on parametrisations for PDFs [163, 164] are also shown in Fig. 4.13. For details see Ref. [120].

Neglecting the effect of the helicity-flip form factor $R_T(t)$ compared to $R_V(t)$, as might be justified by the known suppression of the analogous ratio $F_2^p(t)/F_1^p(t)$,

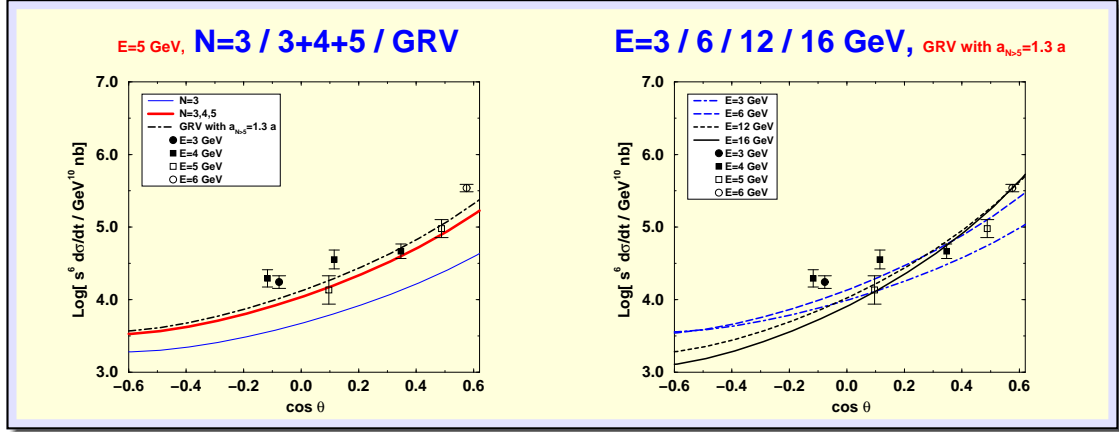


Figure 4.14: Cross sections for WACS obtained from the handbag diagram. Data are from [161]. *Left:* for $E = 5$ GeV the contributions from the valence Fock state, the $N=3,4,5$ Fock states, and for all Fock states are compared. *Right:* the cross sections for different photon energies obtained by the ‘all Fock state estimate’. Data are from [161].

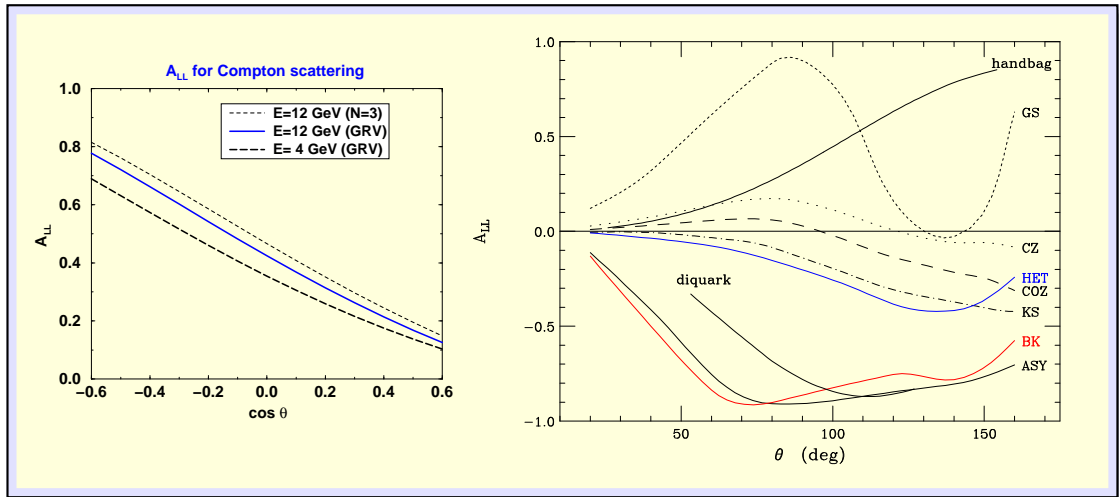


Figure 4.15: Initial state helicity correlation. *Left:* Predictions of the handbag contribution for different energies. *Right:* Comparison of different predictions at $E = 4$ GeV (taken from [158]; additional curve (BK) provided by the same authors).

the cross section of WACS are obtained by inserting the form factors $R_V(t)$ and $R_A(t)$ into Eq. (4.42). Results are displayed in Fig. 4.14 taken from [120]. A comparison shows that the predictions for cross sections from the handbag diagram are much higher than the corresponding ones obtained in the hard scattering picture and can fairly well describe the present data. Note that for a direct comparison a curve was added in Fig. 4.12 (left) obtained within the hard scattering approach in exactly the same way (same value for the parameter f_N) as the other curves in Fig. 4.12, but with the BK distribution amplitude as input.

A_{LL}

Of particular interest is the initial state helicity correlation

$$A_{LL} \frac{d\sigma}{dt} = \frac{1}{2} \left(\frac{d\sigma(\mu = +1, \nu = +1/2)}{dt} - \frac{d\sigma(\mu = +1, \nu = -1/2)}{dt} \right) \quad (4.47)$$

where μ, ν are the helicities of the incoming photon and proton, respectively. The prediction for this quantity from the handbag diagram is distinctively different from predictions obtained in the hard scattering approach, or the diquark model [165].

The JLAB E99-114 collaboration [166] has reported a first yet preliminary measurement of A_{LL} at a c.m.s. scattering angle of 120° which seems to be in agreement with the prediction from the handbag contribution while the HSA calculations fail badly. Further measurements of A_{LL} at higher energies are planned at JLAB.

Perturbative loop corrections to next-to-leading order in α_s to the handbag approach to WACS have been calculated including contributions corresponding to proton helicity flip hadronic matrix elements [167]. The argument for a neglect of helicity flip matrix element is based on the analogy of the ratios $R_T/R_V \simeq F_2/F_1$, which is indicated to behave like $F_2/F_1 \simeq -M^2/t$ by the SLAC data [168]. However, the new JLAB data [169] on F_2 seems to be compatible with a $F_2/F_1 \simeq M/\sqrt{-t}$ behaviour, which in conclusion by analogy would imply a non-negligible correction effect of the R_T form factor to the WACS cross sections, if the JLAB result is confirmed. Huang, Kroll and Morii [167] studied the bearings of the helicity flip form factor R_P on WACS cross sections, and estimated correction effects of about 10%. Moreover, these corrections from a non-negligible R_T lead to a wealth of polarisation phenomena which may be of importance for severe experimental tests of the handbag approach to be expected in the near future.

In conclusion it can be noted that similar to the case of elastic nucleon form factors at intermediate values of $|t|$ there is evidence that also the real WACS off protons is completely dominated by the soft overlap (or handbag) contribution. The size of the contribution calculated from an overlap integral is entirely determined by the functional dependence the partonic transverse momenta in the LCWFs.

It is particularly interesting that the soft physics approach can account for the experimentally observed approximate dimensional counting rule behaviour, at least for Compton scattering and for form factors. This tells us that it is premature to infer the dominance of perturbative physics from the observed scaling behaviour. One may object that the perturbative explanation (leaving aside the logarithms from the running of α_s and from the evolution) works for many exclusive reactions, while in the soft physics approach the approximate counting rule behaviour is accidental, depending on specific properties of a given reaction. In [156] however it was argued that the approximate counting rule behaviour is an unavoidable feature of the soft physics approach related to a scale set by the transverse hadron size.

intrinsic transverse
momenta
determine
soft-overlap
contributions

dimensional
counting rules

4.2.3.3 wide angle meson production

It was shown that also the amplitudes for photoproduction and electroproduction of flavour neutral pseudoscalar and longitudinally polarised vector mesons at large s , $-t$ and $-u$ factorise into parton-level subprocess amplitudes and form factors representing $1/x$ -moments of generalised parton distributions, which can be calculated from overlap integrals of LCWFs [170]. These form factors are of the same type as appear in WACS. It seems however that the contributions from the hadronic component of the photon dominate the photoproduction for values of energy and momentum transfer accessible in current experiments. The measurement of large momentum transfer electroproduction of mesons – though certainly difficult – seems to be feasible at an upgraded JLAB, or at proposed future facilities as ELFE, EVELINE or EIC [170].

4.3 deeply virtual exclusive reactions

In the last 7 years exclusive reactions initiated by a highly virtual photon received a lot of interest. It was realised that these processes are dominated by contributions where only one parton participates in the hard subprocess. Thus, for instance in Compton scattering in the deeply virtual kinematical regime it is the handbag diagram which describes the dominant part of the amplitude (cf. Fig. 4.16).

factorisation of
DVCS

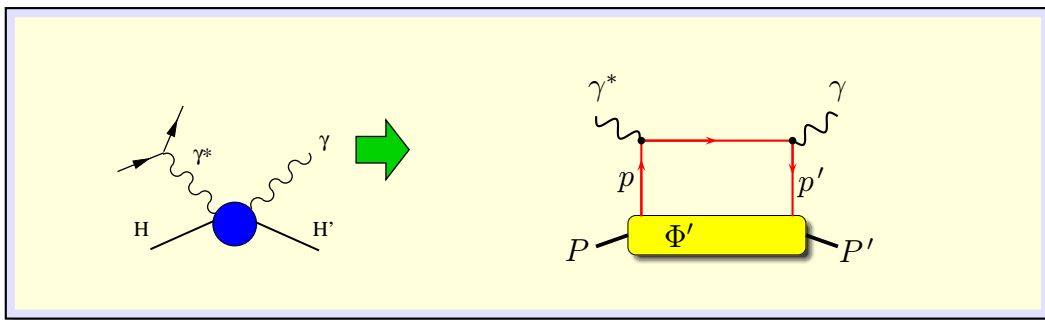


Figure 4.16: The handbag diagram leading to the dominant contribution to the amplitude of Compton scattering in the kinematical regime of a deeply virtual photon.

In close analogy to the Bjorken limit of DIS, there is a kinematical limit of asymptotically rising photon virtuality $Q^2 \rightarrow \infty$ with fixed ratio $x_B = Q^2/(2P \cdot q)$ (while the squared momentum transfer $\Delta^2 = (P' - P)^2$ stays small to avoid a second hard scale) in which the amplitude of the Compton scattering process factorises. The hard partonic subprocess is the (deeply virtual) Compton scattering off a single quark, and the soft part is a hadronic matrix element of a quark field operator describing a quark taken out from the initial proton and reinserted with a different momentum to form the final proton. The quark-quark correlation

function

$$\Phi'(p, P, \Delta) = \int \frac{d^4 z}{(2\pi)^4} e^{i\bar{p}\cdot z} \langle P', S' | \bar{\psi}(\frac{-z}{2}) \psi(\frac{z}{2}) | P, S \rangle, \quad (4.48)$$

where $\bar{p} = (p' + p)/2$, is a direct generalisation of the quark-quark correlation Eq.(3.7) from which the ordinary PDFs are defined as demonstrated in some detail in subsection 3.2. The bilocality of the quark field operator in (4.48) was chosen in a symmetric way which can always be achieved by a translation of the operators. An important difference between the quark-quark correlation of Eq.(3.7) and its generalisation (4.48) is that the initial and final proton states are not identical, but characterised in general by different momentum and spin vectors. Also it should be emphasised that the factorisation in deeply virtual CS takes place on the level of the amplitude of the process, and for DIS it is the cross section which factorises leading to a probabilistic interpretation.

From the quark-quark correlation (4.48) generalised parton distributions are defined as Dirac projections integrated over three quark momentum components, $d\bar{p}^-$ and $d\bar{\mathbf{p}}_\perp$, which constrains the bilocality of the quark field operators to a light-like distance in *minus* directions. The different initial and final states lead to an increased number of independent functions compared to the corresponding ordinary PDFs occurring in forward amplitudes. For instance the leading twist projection with γ^+ defines two functions $H(x, \xi, t)$ and $E(x, \xi, t)$ corresponding to proton helicity non-flip and helicity-flip exactly in the same way as the form factors $F_1(t)$ and $F_2(t)$. With $\bar{P} \equiv (P + P')/2$ the projection with γ^+ defines

$$\bar{P}^+ \int d\bar{p}^- d^2\bar{\mathbf{p}}_\perp \text{Tr} \left(\Phi' \gamma^+ \right) \Big|_{\bar{p}^+ = x\bar{P}^+} = \bar{u}(P', S') \left\{ \gamma^+ H^q(x, \xi, t) + \frac{i\sigma^{+\nu}\Delta_\nu}{2M} E^q(x, \xi, t) \right\} u(P, S), \quad (4.49)$$

where the GPDs $H(x, \xi, t)$ and $E(x, \xi, t)$ depend on the (average) momentum fraction x , the *skewedness* ξ characterising the change of momentum fraction between initial and final quark, and the squared momentum transfer t . A more detailed discussion on GPDs, their properties and interpretation will follow in the next sections.

Also the hard production of mesons in the deeply virtual kinematical regime close to the forward direction receives its dominant contribution from diagrams where only one parton participates in the hard subprocess. At the same order in α_s diagrams occur involving generalised quark distributions and generalised gluon distributions (cf. Fig. 4.17).

Soon after factorisation was made plausible for DVCS [171, 172, 173] and deeply virtual meson production [174] all order factorisation theorems have been developed to leading twist accuracy [175, 176, 177, 178]. Establishing those formal theorems have put the perturbative treatment of DVCS and deeply virtual meson production on the same sound and rigorous mathematical basis as many of the inclusive hard processes.

Hard exclusive reactions in the deeply virtual kinematical regime are difficult to measure. Counting rates and cross sections are small and it is extremely hard

factorisation of
deeply virtual
meson production

factorisation
theorems

first glimpses on
GPDs

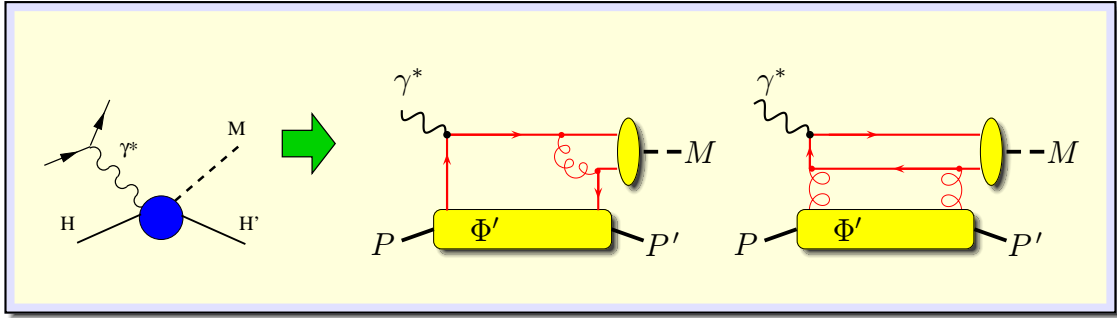


Figure 4.17: Diagrams leading to the dominant contributions to the amplitude of deeply virtual meson production.

to ensure exclusiveness, i.e. to single out experimentally one specific channel from other channels which have a similar signature. For instance, DVCS contributions to cross sections have to be separated from a channel with an additional soft pion in the final state which may go unobserved because of limited detector acceptance in particular in the beam direction. In addition the DVCS contribution has a background by the Bethe-Heitler process consisting of real photon emission by the incoming or outgoing electron. Nevertheless, first observations of DVCS have been reported. In Fig. 4.18 DVCS cross sections (after subtraction from Bethe-Heitler contributions) from the ZEUS experiment at DESY [179] are displayed in comparison with two model predictions.

Measurements of differential cross sections have also been reported by the H1 experiment at DESY [182] shown in Fig. 4.19 as functions of the virtuality of the photon Q^2 and the invariant mass of the final state W . Also here a clear excess over the expected cross section from the Bethe-Heitler process alone is observed.

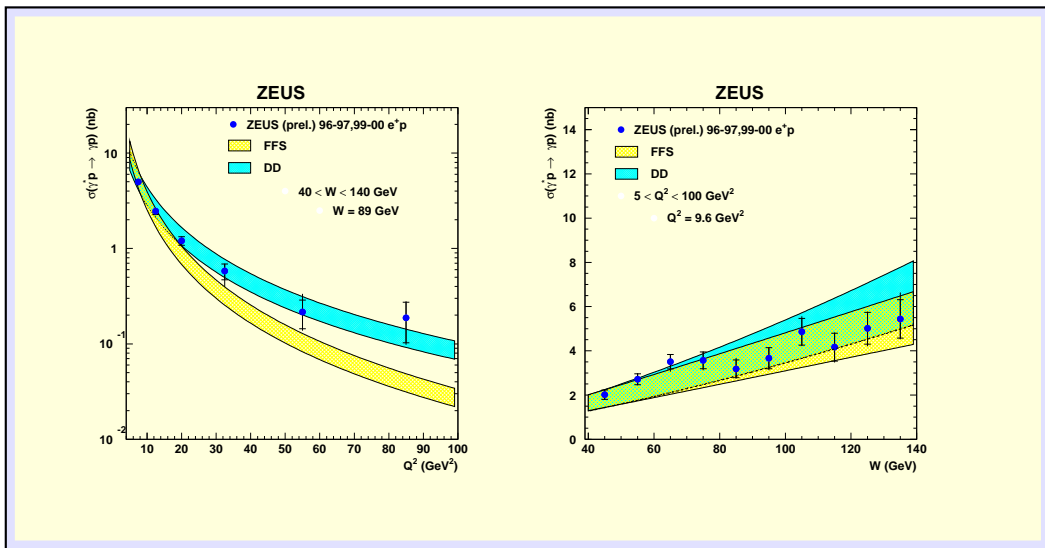


Figure 4.18: Observation of the DVCS reaction $e^+p \rightarrow e^+\gamma p$ at HERA in data taken with the ZEUS detector [179]. Cross section as a function of Q^2 (left panel) and W (right panel) in the kinematic range $5 \leq Q^2 \leq 100 \text{ GeV}^2$ and $40 \leq W < 140 \text{ GeV}$. The data are compared to two theoretical model predictions from [180] and [181].

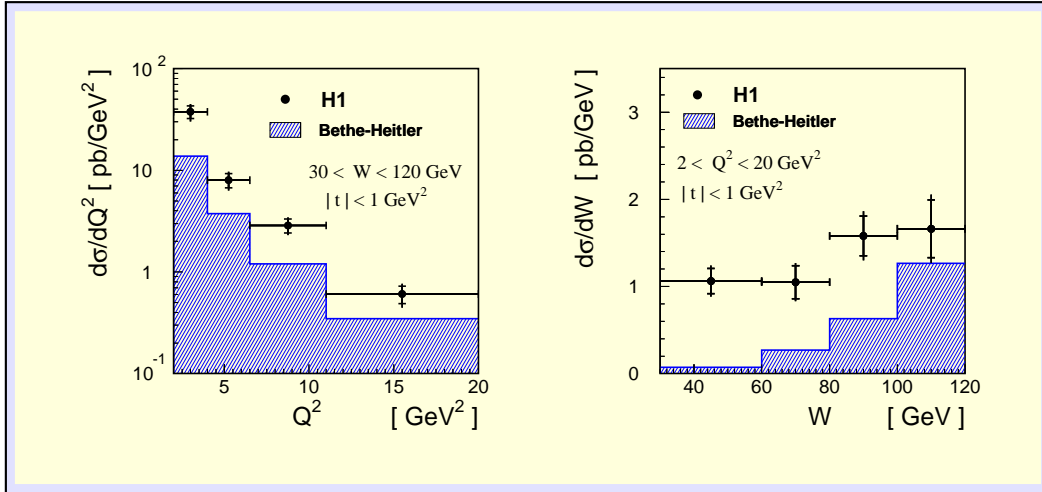


Figure 4.19: Differential cross section measurements for the DVCS reaction $e^+p \rightarrow e^+\gamma p$ from H1 as a function of Q^2 (left) and W (right) [182].

It was pointed out [183] that the Bethe-Heitler process not only plays the rôle of an obstacle as unwanted background, but on the contrary can be made use of as a welcome mechanism enhancing small effects otherwise difficult to access. The QED process of the radiation of a real photon by an electron can be calculated to arbitrary precision and combined with the rather precise data on the nucleon form factors. Having thus a good knowledge on the Bethe-Heitler amplitudes, the DVCS amplitudes can be extracted from interference terms in cross sections. In particular azimuthal asymmetries are suitable for separating out single terms with different angular dependencies. The relevant azimuthal asymmetries have been identified up to and including twist three accuracy [183, 184]. Also beam charge asymmetries, e.g. by comparing electron and positron scattering data, contain valuable information.

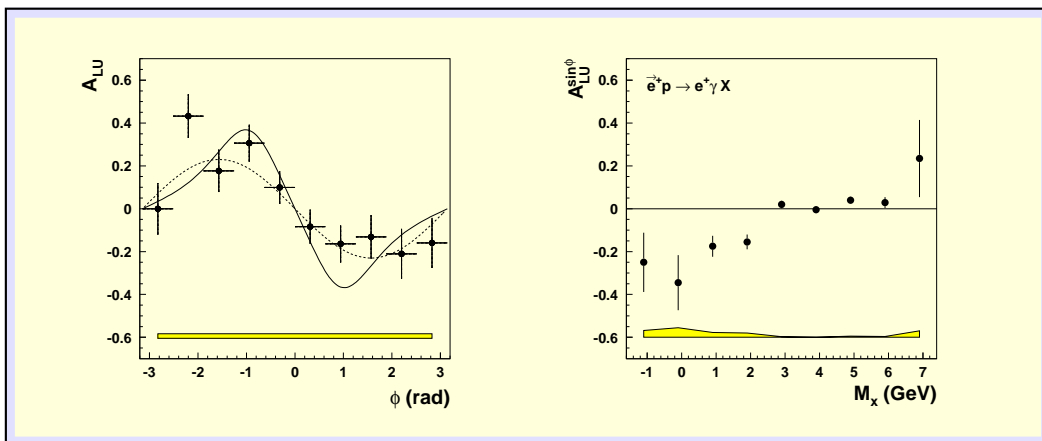


Figure 4.20: The DVCS Single Spin Asymmetry from HERMES [185]. *Left:* Beam-spin asymmetry A_{LU} for hard electroproduction of photons as a function of the azimuthal angle ϕ . The data correspond to the missing mass region between 0.4 and 1.4 GeV. *Right:* The beam-spin analysing power $A_{LU}^{\sin\phi}$ for hard electroproduction of photons on hydrogen as a function of the missing mass.

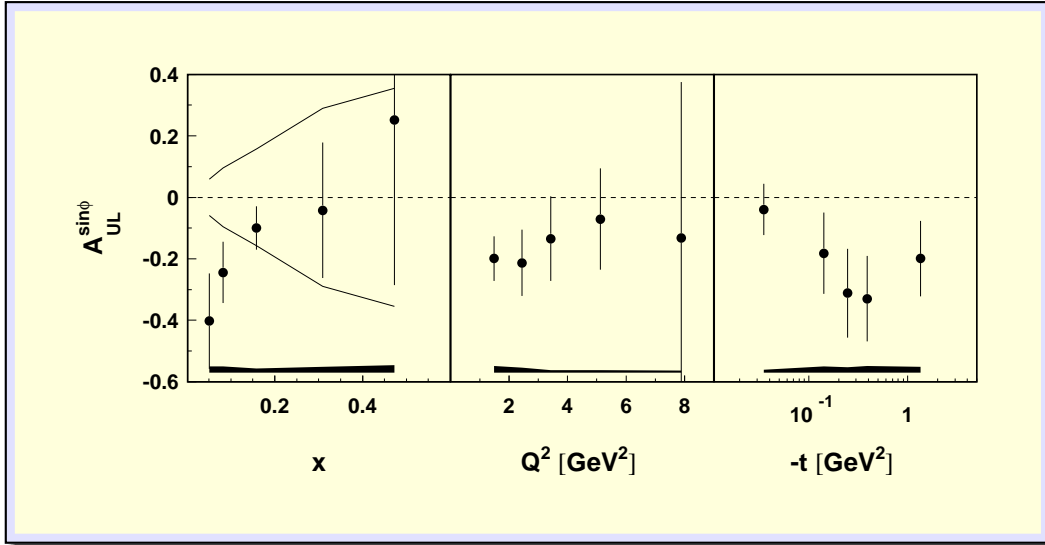


Figure 4.21: Single spin asymmetry for exclusive π^+ production at HERMES [187]. Kinematic dependence of $A_{UL}^{\sin\phi}$ on the variables x , Q^2 , and t for the reaction $e^+ + \bar{p} \rightarrow e'^+ + n + \pi^+$. The error bars and bands represent the statistical and systematic uncertainties, respectively. The solid lines show the upper limits for any asymmetry arising from the transverse target polarization component.

The first measurement of a DVCS azimuthal asymmetry was reported from the HERMES experiment at DESY [185]. The results are shown in Fig. 4.20 together with a fit of a $\sin\phi$ curve to the data (dashed line) and in comparison with a prediction based on a GPD model [186] (solid line). From the experimental setup it is impossible to ensure strict exclusiveness; instead, the data are plotted against the missing mass indicating a clear effect in the exclusive domain.

A similar single spin azimuthal asymmetry in exclusive electroproduction of π^+ mesons on a longitudinally polarised target was observed by HERMES [187] and is shown in Fig. 4.21. A next to leading twist analysis would be necessary for a complete description of the data, but the measurement combined with a similar one on transversely polarised target opens the way to experimentally disentangle the asymmetry arising from the two polarisation components and thus may provide another first glimpse on certain GPDs [187].

4.4 generalised parton distributions

Generalised parton distributions have been first discussed as objects showing evolution behaviour interpolating between the DGLAP evolution of PDFs and the ERBL evolution of DAs [188] and were mentioned in a conference proceeding in the context of helicity flip form factors[189]. The full importance of these generalisations of PDFs went almost unnoticed by the community of hadron physics. Only in 1996 a renewed interest was triggered by a proposal of Ji to access the orbital angular momentum of partons via the GPDs in the DVCS process[171, 172], and very shortly after by two publications of Radyushkin on DVCS [173] and GPDs in hard diffractive electroproduction[174]. In the recent years plenty of publications on GPDs and on the processes involving GPDs appeared. In the present report only some basic features of GPDs are mentioned briefly, before the rôle of transverse momentum dependence is investigated more thoroughly. For more details on GPDs it is referred to the available reviews on the topic, among them [176, 190, 191, 192].

GPDs

Generalised quark distributions of the nucleon at leading twist are defined by projections on different Dirac structures leading to quark helicity non-flip projections (cf. the interpretation of operators in terms of “good” LC components of quark fields worked out in appendix A)

definitions of leading twist GPDs

$$2\bar{P}^+ \sqrt{1 - \xi^2} \mathcal{H}_{\lambda'\lambda}^q \equiv \quad (4.50)$$

$$\begin{aligned} & \bar{P}^+ \int \frac{dz^-}{2\pi} e^{i\bar{x}\bar{P}^+z^-} \langle P', \lambda' | \bar{\psi}\left(\frac{-\bar{z}}{2}\right) \gamma^+ \psi\left(\frac{\bar{z}}{2}\right) | P, \lambda \rangle \\ &= \bar{u}(P', \lambda') \left\{ \gamma^+ H(\bar{x}, \xi, t) + \frac{i\sigma^{\nu\Delta}}{2M} E(\bar{x}, \xi, t) \right\} u(P, \lambda), \end{aligned} \quad (4.51)$$

$$\begin{aligned} & \bar{P}^+ \int \frac{dz^-}{2\pi} e^{i\bar{x}\bar{P}^+z^-} \langle P', \lambda' | \bar{\psi}\left(\frac{-\bar{z}}{2}\right) \gamma^+ \gamma_5 \psi\left(\frac{\bar{z}}{2}\right) | P, \lambda \rangle \\ &= \bar{u}(P', \lambda') \left\{ \gamma^+ \gamma_5 \tilde{H}(x, \xi, t) + \frac{\gamma_5 \Delta^+}{2M} \tilde{E}(x, \xi, t) \right\} u(P, \lambda), \end{aligned} \quad (4.52)$$

where the quantity $\mathcal{H}_{\lambda'\lambda}^q$ was defined for later convenience, and quark helicity flip projections [193]

$$\begin{aligned} & \bar{P}^+ \int \frac{dz^-}{2\pi} e^{i\bar{x}\bar{P}^+z^-} \langle P', \lambda' | \bar{\psi}\left(\frac{-\bar{z}}{2}\right) \sigma^{+j} \gamma_5 \psi\left(\frac{\bar{z}}{2}\right) | P, \lambda \rangle \\ &= \bar{u}(P', \lambda') \left\{ \sigma^{+j} \gamma_5 H_T(x, \xi, t) + \frac{\epsilon^{+j\alpha\beta} \Delta_\alpha \bar{P}_\beta}{M^2} \tilde{H}_T(x, \xi, t) \right. \\ & \quad \left. + \frac{\epsilon^{+j\alpha\beta} \Delta_\alpha \gamma_\beta}{2M} E_T(x, \xi, t) + \frac{\epsilon^{+j\alpha\beta} \bar{P}_\alpha \gamma_\beta}{M} \tilde{E}_T(x, \xi, t) \right\} u(P, \lambda), \end{aligned} \quad (4.53)$$

where λ, λ' denote the proton helicities, and \bar{z} is a shorthand notation for $[0, z^-, \mathbf{0}_\perp]$. Flavour and colour labels are suppressed. The link operator normally needed to render the definition (4.50), (4.52) and (4.53) gauge-invariant does not appear because the gauge $A^+ = 0$ is chosen, which together with an integration path along the *minus* direction reduces the link operator to unity ⁶.

some kinematics

A short digression on the involved kinematics will clarify the meaning of the momenta and momentum fractions occurring in the definitions (cf. appendix C.3). The initial and final hadron states are characterised by the momenta P and P' . In order to parameterise them one defines the average momentum

$$\bar{P} = \frac{1}{2}(P + P'), \quad (4.54)$$

chooses the three-momentum $\bar{\mathbf{P}}$ to be along the \mathbf{e}_3 -axis (see Fig. 4.22, the frame defined this way is named the “average” frame in appendix C.3). One writes in light-cone components

$$\begin{aligned} P &= \left[(1 + \xi)\bar{P}^+, \frac{M^2 + \Delta_\perp^2/4}{2(1 + \xi)\bar{P}^+}, -\frac{\Delta_\perp}{2} \right], \\ P' &= \left[(1 - \xi)\bar{P}^+, \frac{M^2 + \Delta_\perp^2/4}{2(1 - \xi)\bar{P}^+}, +\frac{\Delta_\perp}{2} \right] \end{aligned} \quad (4.55)$$

with the transverse vector Δ_\perp , the plus momentum \bar{P}^+ , and the skewedness parameter

$$\xi = \frac{(P - P')^+}{(P + P')^+}, \quad (4.56)$$

which describes the change in *plus* momentum. The momentum transfer takes the form

$$\Delta = P' - P = \left[-2\xi\bar{P}^+, \frac{\xi(M^2 + \Delta_\perp^2/4)}{(1 - \xi^2)\bar{P}^+}, \Delta_\perp \right], \quad (4.57)$$

and with the parameterisation (4.55) its square reads

$$t = \Delta^2 = -\frac{4\xi^2 M^2 + \Delta_\perp^2}{1 - \xi^2}. \quad (4.58)$$

Notice that the positivity of Δ_\perp^2 implies a minimal value

$$-t_0 = \frac{4\xi^2 M^2}{1 - \xi^2} \quad (4.59)$$

for $-t$ at given ξ , which translates into a maximum allowed ξ at given t . As shown in Fig. 4.22(a) the parton emitted by the hadron has the momentum p , and the one absorbed has momentum p' . The average parton momentum \bar{p} is defined as $(p + p')/2$, in analogy to (4.54), and correspondingly a momentum fraction $\bar{x} = \bar{p}^+/\bar{P}^+$ is introduced. This is Ji's variable x [171].

⁶In the light of the recent discussions about possible time-reversal odd PDFs (cf. the discussion in subsection 3.2.3) this argument needs to be reconsidered critically also for GPDs in future investigations.

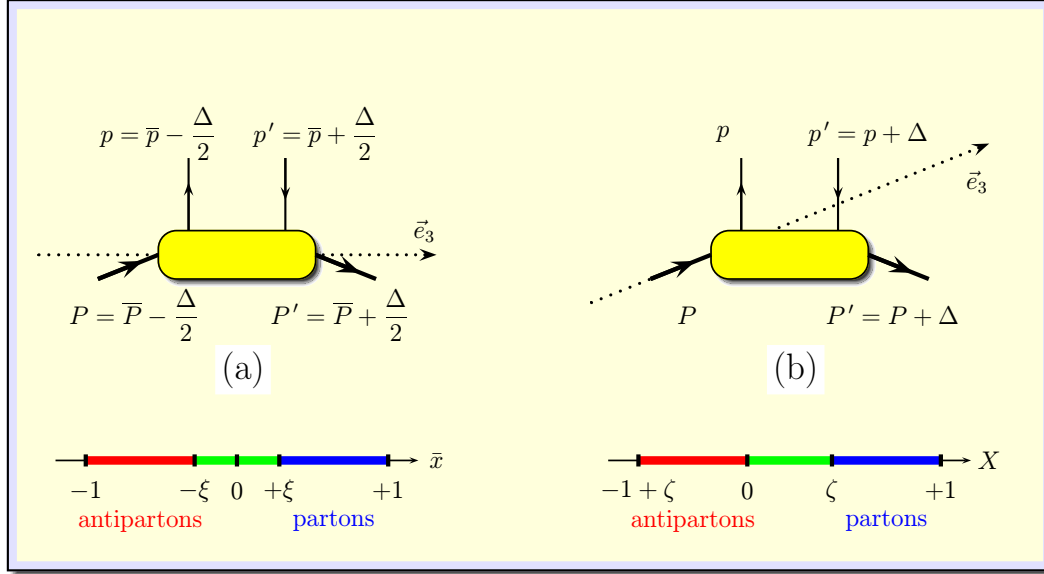


Figure 4.22: Illustration of two common choices to fix the longitudinal direction in the definition of the off-forward hadronic matrix element which defines generalised parton distributions. The flow of momenta is indicated on the lines. *Bottom:* The ranges of momentum fractions for partons, antipartons and the central region specific to GPDs is shown for the two choices ($X \equiv p^+/P^+$, $\zeta \equiv -\Delta^+/P^+$).

In an alternative parametrisation of the hadron momenta frequently found in the literature (see for instance [176]), the three-momentum of the incoming proton is chosen to lie along the \mathbf{e}_3 -axis. In Fig. 4.22 the two different choices are illustrated.

The off-forwardness of the defining hadronic matrix elements, $P' \neq P$, allows for hadron helicity non-flip and helicity flip contributions which enlarges the number of independent functions. For the projections with γ^+ and $\gamma^+\gamma_5$ there are twice as many GPDs than corresponding PDFs, for the projection with $\sigma^{+j}\gamma_5$ four independent functions occur of which one corresponds to the transversity distribution $h_1(x)$ ⁷.

Similarly generalised gluon distributions $H^g(\bar{x}, \xi; t)$ and $E^g(\bar{x}, \xi; t)$ are defined from the Fourier transform of a hadronic matrix element involving two gluon field strength tensors at a light-like distance:

definition of gluon GPDs

$$\begin{aligned}
 & -2 g_{\perp\alpha'\alpha} \int \frac{dz^-}{2\pi} e^{i\bar{x}\bar{p}^+z^-} \langle P', \lambda' | G_c^{+\alpha'}(-\bar{z}/2) G_c^{+\alpha}(\bar{z}/2) | P, \lambda \rangle \\
 & = \bar{u}(P', \lambda') \left\{ \gamma^+ H^g(\bar{x}, \xi; t) + \frac{i\sigma^{+\alpha}\Delta_\alpha}{2M} E^g(\bar{x}, \xi; t) \right\} u(P, \lambda) \quad (4.60)
 \end{aligned}$$

with the transverse metric tensor $g_{\perp}^{\alpha'\alpha}$, which has $g_{\perp}^{11} = g_{\perp}^{22} = -1$ as only non-zero elements.

⁷This result is quoted from Diehl [193] which extends the definitions and corrects the counting of independent functions in the previous literature [194].

The polarised gluon GPDs $\widetilde{H}^g(\bar{x}, \xi; t)$ and $\widetilde{E}^g(\bar{x}, \xi; t)$ are defined from

$$\begin{aligned} & -2i \varepsilon_{\perp \alpha' \alpha} \int \frac{dz^-}{2\pi} e^{i\bar{x}\bar{p}^+ z^-} \langle P', \lambda' | G_c^{+\alpha'}(-\bar{z}/2) G_c^{+\alpha}(\bar{z}/2) | P, \lambda \rangle \\ & = \bar{u}(P', \lambda') \left\{ \gamma^+ \gamma_5 \widetilde{H}^g(\bar{x}, \xi; t) + \frac{\Delta^+ \gamma_5}{2M} \widetilde{E}^g(x, \xi; t) \right\} u(P, \lambda). \end{aligned} \quad (4.61)$$

A direct comparison of the quark GPDs with ordinary PDFs and the nucleon form factor is very illustrative. In Fig. 4.23 the definition of PDFs, form factors and GPDs are listed for the $\bar{\psi}\gamma^+\psi$ quark field operators together with the corresponding diagrams. The differences (as highlighted in the figure by different colours) are:

PDFs: the quark-field operator is *bilocal* with arguments $-\bar{z}/2$ and $+\bar{z}/2$, the initial and final proton state is identical, i.e. it is a *forward* matrix element

FFs: the quark-field operator is *local*, the initial and final proton states are different, i.e. it is a *non-forward* matrix element

GPDs: the quark-field operator is *bilocal* with arguments $-\bar{z}/2$ and $+\bar{z}/2$, the initial and final proton states are different, i.e. it is a *non-forward* matrix element

This comparison reveals that GPDs are hybrid objects combining properties of the ordinary PDFs and elastic FFs. In fact, from the definitions it can be directly read off that GPDs reduce to ordinary PDFs⁸ in the forward limit ($\xi \rightarrow 0, t \rightarrow 0$)

$$H^q(\bar{x}, 0, 0) = f_1^q(\bar{x}) \quad \widetilde{H}^q(\bar{x}, 0, 0) = g_1^q(\bar{x}) \quad H_T^q(\bar{x}, 0, 0) = h_1^q(\bar{x}) \quad (4.62)$$

$$H^g(\bar{x}, 0, 0) = \bar{x} g(\bar{x}) \quad \widetilde{H}^g(\bar{x}, 0, 0) = \bar{x} \Delta g(\bar{x}). \quad (4.63)$$

Furthermore, an integration of the GPDs over $\bar{x} \in [-1, 1]$ together with the exponential factor in the definitions leads to a $\delta(z^-)$, rendering the hadronic matrix element local. Thus, the lowest moments of GPDs are related to parton contributions to elastic form factors. For instance the lowest moment of the unpolarised quark GPD leads to

$$\int_{-1}^1 d\bar{x} H^q(\bar{x}, \xi, t) = F_1^q(t) \quad \text{Dirac FF}, \quad (4.64)$$

which is related the full Dirac form factor by summing over all quarks

$$F_1(t) = \sum_q e_q F_1^q(t) \quad (4.65)$$

⁸Note that the normalisations of gluon GPDs used here correspond to the one of [123, 193] and thus differ from those of Hoodbhoy and Ji [194] by a factor $1/(2\bar{x})$.

comparison
PDF - FF - GPD

forward limit

x^0 -moments

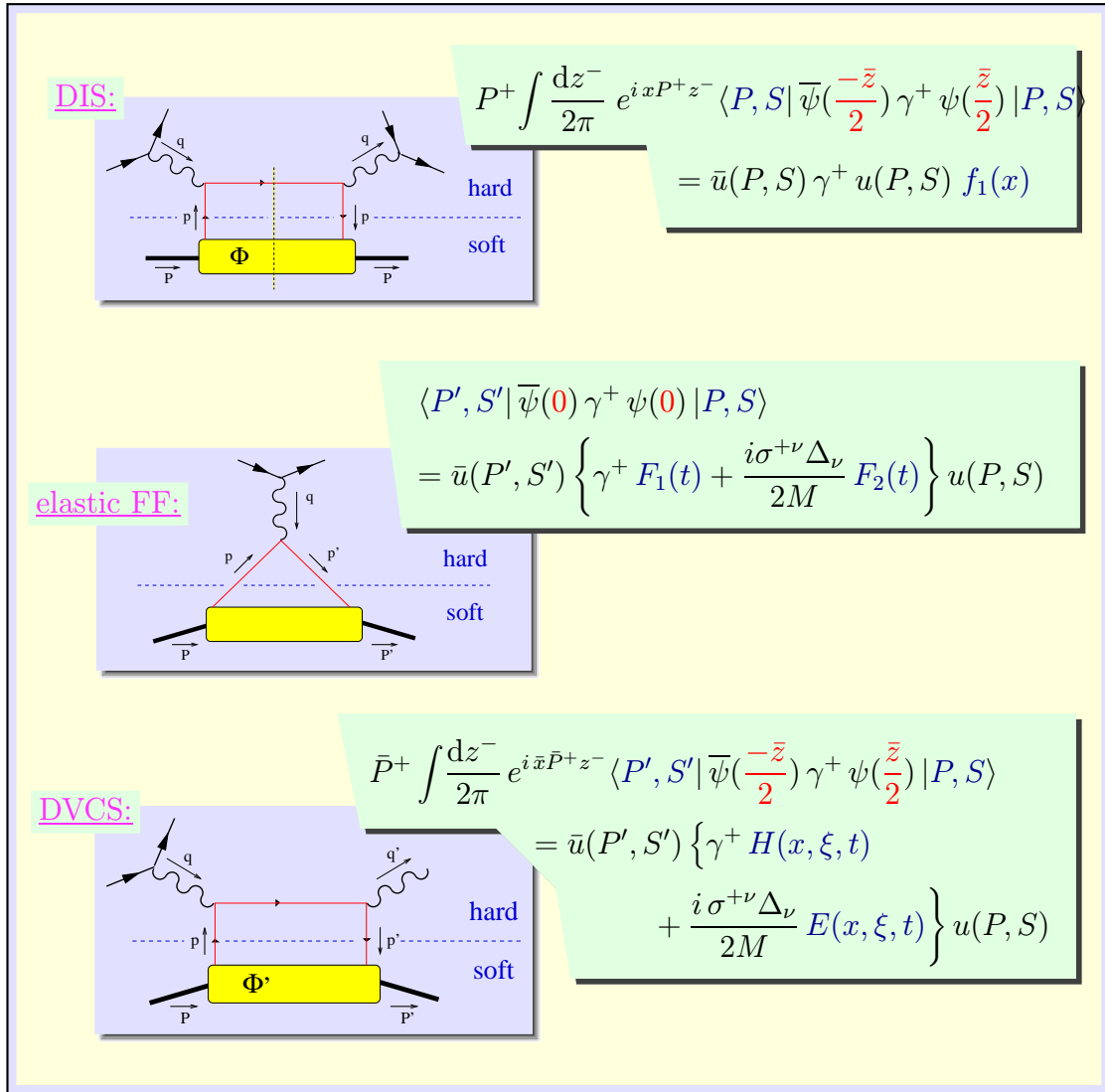


Figure 4.23: Comparison of diagrams for processes involving PDFs, FFs and GPDs together with the respective definitions of these quantities.

Similarly relations of lowest moments of $E^q(\bar{x}, \xi, t)$, $\tilde{H}^q(x, \xi, t)$ and $\tilde{E}^q(x, \xi, t)$ to the quark contributions of Pauli, axial and pseudoscalar FFs exist in the form

$$\int_{-1}^1 d\bar{x} E^q(\bar{x}, \xi, t) \rightarrow F_2^q(t) \quad \text{Pauli FF} \quad (4.66)$$

$$\int_{-1}^1 d\bar{x} \tilde{H}^q(x, \xi, t) \rightarrow G_A^q(t) \quad \text{axial FF} \quad (4.67)$$

$$\int_{-1}^1 d\bar{x} \tilde{E}^q(x, \xi, t) \rightarrow G_P^q(t) \quad \text{pseudoscalar FF} \quad (4.68)$$

Correspondingly the (logarithmic) scale dependence of GPDs is a combination of the DGLAP evolution of ordinary (nucleon) PDFs and the ERBL evolution of (meson) DAs [188, 171, 172, 173, 176]. The generalised evolution kernels are

known two-loop accuracy [195, 196, 197]. Here conformal symmetry has proven to be a particularly useful tool. It implies that leading order kernels can be diagonalised in a basis spanned by Gegenbauer polynomials; beyond leading order conformal symmetry is violated by quantum corrections [198].

From the foregoing brief discussion it becomes obvious that GPDs link many different inclusive and exclusive quantities. In fact, besides the quantities mentioned here GPDs naturally occur in many more processes, like the timelike CS [199], wide angle meson production [170], or in a $\{t, s\} \rightarrow \{s, t\}$ crossed version in proton/antiproton (or $\pi^+\pi^-$) annihilation and two photon processes [200, 201, 202] (cf. Fig. 4.24).

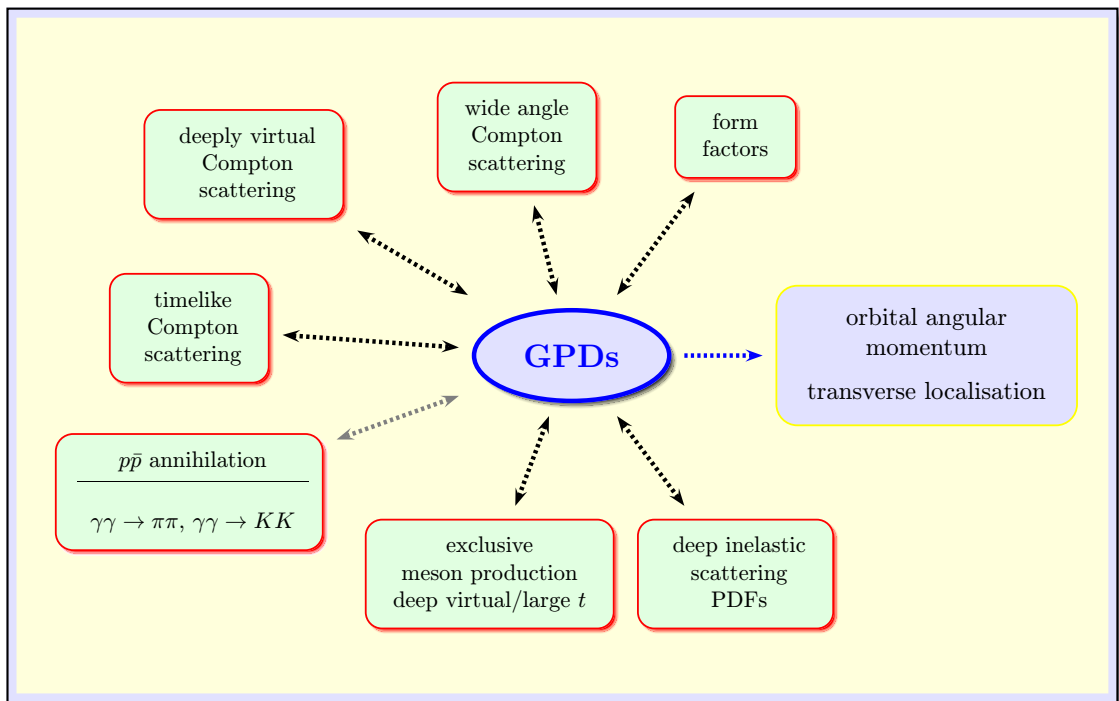


Figure 4.24: Generalised parton distributions provide a unifying formalism linking many inclusive and exclusive quantities and processes.

4.4.1 LCWF overlap representation of GPDs

GPD \leftrightarrow LCWFs

The interpretation of GPDs is largely facilitated by considering a representation as overlap integrals of LCWFs. To this end one can use the LC quantisation techniques and the notions of “good” LC components of the parton fields as introduced in chapter 2.

The bilocal quark field operator in the definition of the unpolarised quark GPD (4.50) can be related to creation and annihilation operators of the “good” LC components of quark fields by writing Eq. (2.35) in the form

$$\frac{1}{\sqrt{2}} \int \frac{dz^-}{2\pi} e^{i\bar{x}\bar{P}^+z^-} \bar{\psi}_q(-\bar{z}/2) \gamma^+ \psi_q(\bar{z}/2)$$

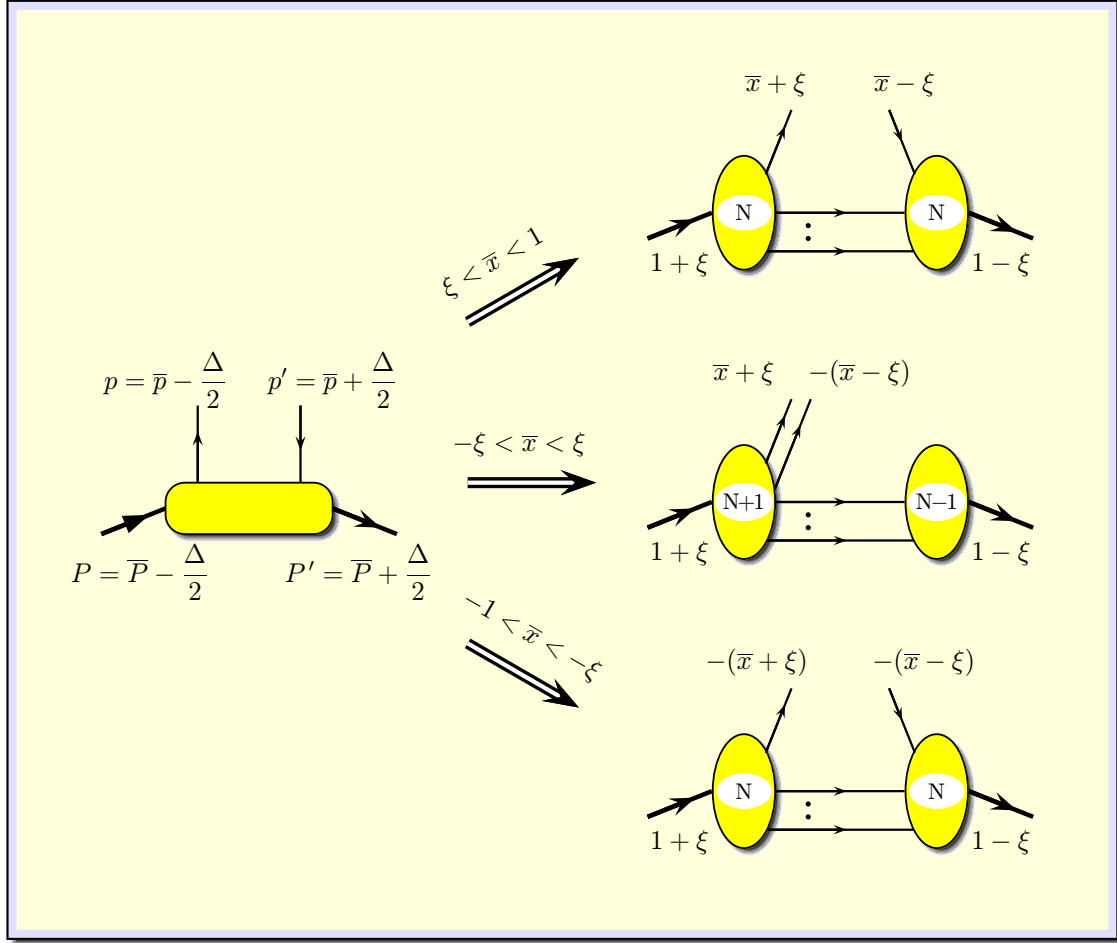


Figure 4.25: Overlap representations for GPDs in different kinematic regions for the case $\xi > 0$. The flow of momenta is indicated on the lines. *Top (bottom) right*: the region $\xi < \bar{x} < 1$ ($-1 < \bar{x} < -\xi$), where the GPDs are given by $N \rightarrow N$ overlaps. *Middle right*: the central region $-\xi < \bar{x} < \xi$, where $N + 1 \rightarrow N - 1$ overlaps are relevant.

$$\begin{aligned}
 &= 2 \int \frac{dp'^+ d^2\mathbf{p}'_{\perp}}{p'^+ 16\pi^3} \Theta(p'^+) \int \frac{dp^+ d^2\mathbf{p}_{\perp}}{p^+ 16\pi^3} \Theta(p^+) \sum_{\mu, \mu'} \\
 &\quad \left\{ \delta(2\bar{x}\bar{P}^+ - p'^+ - p^+) b_q^\dagger(w') b_q(w) u_+^\dagger(w') u_+(w) \right. \\
 &\quad + \delta(2\bar{x}\bar{P}^+ + p'^+ + p^+) d_q(w') d_q^\dagger(w) v_+^\dagger(w') v_+(w) \\
 &\quad + \delta(2\bar{x}\bar{P}^+ + p'^+ - p^+) d_q(w') b_q(w) v_+^\dagger(w') u_+(w) \\
 &\quad \left. + \delta(2\bar{x}\bar{P}^+ - p'^+ + p^+) b_q^\dagger(w') d_q^\dagger(w) u_+^\dagger(w') v_+(w) \right\}, \quad (4.69)
 \end{aligned}$$

which readily allows one to interpret the GPDs in the parton picture [190].

Which of the four terms in (4.69) contributes to the matrix element in (4.50) is determined by the positivity conditions $p^+ \geq 0$ and $p'^+ \geq 0$ for the parton momenta, together with momentum conservation, which imposes $p^+ - p'^+ = P^+ - P'^+ = 2\xi\bar{P}^+$. For definiteness we consider the case $\xi > 0$ in the following, which is relevant for the applications of the GPDs in hard processes that have so far been considered in the literature. In the region $\xi < \bar{x} < 1$ the GPDs describe

the emission of a quark from the nucleon with momentum fraction $\bar{x} + \xi$ and its reabsorption with $\bar{x} - \xi$. In the region $-1 < \bar{x} < -\xi$ one has the emission of an antiquark from the nucleon with momentum fraction $-(\bar{x} + \xi)$ and its reabsorption with $-(\bar{x} - \xi)$. In the third region $-\xi < \bar{x} < \xi$, however, the nucleon emits a quark-antiquark pair. The three cases will be discussed separately firstly focusing on the region $\xi < \bar{x} < 1$ (see Fig. 4.25). The last term in (2.35), going with $b^\dagger(w') d^\dagger(w)$ and describing the absorption of a quark-antiquark pair, does not contribute for $\xi > 0$.

4.4.1.1 the region $\xi < \bar{x} < 1$

The Fock state decomposition (2.24) of the hadronic states is the starting point for the overlap representation of GPDs [120, 123, 124]⁹. The matrix element $\mathcal{H}_{\lambda'\lambda}^q$ defined in Eq. (4.50) is represented as a sum over contributions from separate Fock states

$$\mathcal{H}_{\lambda'\lambda}^q = \sum_N \mathcal{H}_{\lambda'\lambda}^{q(N \rightarrow N)}. \quad (4.70)$$

Using the properties of creation and annihilation operators of the “good” quark LC field components – including their anti-commutation relations – one arrives after a few steps at the overlap representation of the quark GPD in the region $\xi < \bar{x} < 1$:

$$\begin{aligned} \mathcal{H}_{\lambda'\lambda}^{q(N \rightarrow N)} &= \sqrt{1-\xi}^{1-N} \sqrt{1+\xi}^{1-N} \sum_{\beta=\beta'} \sum_j \delta_{s_j q} \\ &\times \int [d\bar{x}]_N [d^2\bar{\mathbf{p}}_\perp]_N \delta(\bar{x} - \bar{x}_j) \Psi_{N,\beta'}^{*\lambda'}(\hat{r}') \Psi_{N,\beta}^\lambda(\tilde{r}), \end{aligned} \quad (4.71)$$

with $r_i = (x_i, \mathbf{p}_{\perp i})$ in the collective notation of Eq. (2.25), and s_j (s'_j) denoting the flavour of the initial (final) active quark. The arguments \tilde{r} (\hat{r}') of the LCWF for the incoming (outgoing) proton are most easily found by considering the momenta of the active and spectator partons in the “average” frame and applying transverse boosts to appropriate hadron frames (cf. appendix C.3). This way relations between \tilde{r} (\hat{r}') and the integration variables \bar{x}_i and $\bar{\mathbf{p}}_{\perp i}$ are found in the form

$$\begin{aligned} \tilde{x}_i &= \frac{\bar{x}_i}{1+\xi}, & \tilde{\mathbf{p}}_{\perp i} &= \bar{\mathbf{p}}_{\perp i} + \frac{\bar{x}_i}{1+\xi} \frac{\Delta_\perp}{2}, & \text{for } i \neq j, \\ \tilde{x}_j &= \frac{\bar{x}_j + \xi}{1+\xi}, & \tilde{\mathbf{p}}_{\perp j} &= \bar{\mathbf{p}}_{\perp j} - \frac{1-\bar{x}_j}{1+\xi} \frac{\Delta_\perp}{2}. \end{aligned} \quad (4.72)$$

and

$$\begin{aligned} \hat{x}'_i &= \frac{\bar{x}_i}{1-\xi}, & \hat{\mathbf{p}}'_{\perp i} &= \bar{\mathbf{p}}_{\perp i} - \frac{\bar{x}_i}{1-\xi} \frac{\Delta_\perp}{2}, & \text{for } i \neq j, \\ \hat{x}'_j &= \frac{\bar{x}_j - \xi}{1-\xi}, & \hat{\mathbf{k}}'_{\perp j} &= \bar{\mathbf{k}}_{\perp j} + \frac{1-\bar{x}_j}{1-\xi} \frac{\Delta_\perp}{2}, \end{aligned} \quad (4.73)$$

respectively. Summation of Eq. (4.71) over N leads to the full expression of $\mathcal{H}_{\lambda'\lambda}^q$ in the region $\xi < \bar{x} < 1$.

⁹The presentation here is an excerpt of the derivation in the context of LC quantisation worked out in [123] where many more details can be found.

4.4.1.2 the region $-1 < \bar{x} < -\xi$

For active *antiquarks* the derivation of the overlap representation of the GPDs goes in full analogy to the one just indicated.

$-1 < \bar{x} < -\xi$

The final result for the region $-1 < \bar{x} < -\xi$ is

$$\begin{aligned} \mathcal{H}_{\lambda'\lambda}^{q(N \rightarrow N)} &= -\sqrt{1-\xi}^{1-N} \sqrt{1+\xi}^{1-N} \sum_{\beta=\beta'} \sum_j \delta_{\bar{s}_j q} \\ &\times \int [d\bar{x}]_N [d^2\bar{\mathbf{p}}_\perp]_N \delta(\bar{x} + \bar{x}_j) \Psi_{N,\beta'}^{*\lambda'}(\hat{r}') \Psi_{N,\beta}^\lambda(\tilde{r}), \end{aligned} \quad (4.74)$$

with the LCWF arguments \tilde{r} and \hat{r}' given by (4.72) and (4.73), respectively.

4.4.1.3 the region $-\xi < \bar{x} < \xi$

As mentioned above, only the case $\xi > 0$ is considered here. Therefore, the quark GPDs in this region describe the emission of a quark-antiquark pair from the initial proton. In the Fock state decompositions of the initial and final protons we thus have to consider only terms where the initial state has the same parton content as the final state plus one additional quark-antiquark pair. We thus have

$-\xi < \bar{x} < \xi$

$$\mathcal{H}_{\lambda'\lambda}^q = \sum_N \mathcal{H}_{\lambda'\lambda}^{q(N+1 \rightarrow N-1)} \quad (4.75)$$

as opposed to (4.70). This particular type of overlap was recently identified in [203] in the context of transition form factors between heavy and light mesons. One arrives at the overlap representation of $\mathcal{H}_{\lambda'\lambda}^q$ in the region $-\xi < \bar{x} < \xi$ for the $N+1 \rightarrow N-1$ transition:

$$\begin{aligned} \mathcal{H}_{\lambda'\lambda}^{q(N+1 \rightarrow N-1)} &= \sqrt{1-\xi}^{2-N} \sqrt{1+\xi}^{-N} \sum_{\beta,\beta'} \sum_{j,j'=1}^{N+1} \frac{1}{\sqrt{n_j n_{j'}}} \delta_{\bar{s}_{j'} s_j} \delta_{s_j q} \delta_{\mu_{j'} - \mu_j} \\ &\times \prod_{\substack{i=1 \\ i \neq j, j'}}^{N+1} \delta_{\mu'_i \mu_i} \delta_{s'_i s_i} \int d\bar{x}_j \prod_{\substack{i=1 \\ i \neq j, j'}}^{N+1} d\bar{x}_i \delta\left(1 - \xi - \sum_{\substack{i=1 \\ i \neq j, j'}}^{N+1} \bar{x}_i\right) \\ &\times \int d^2\bar{\mathbf{p}}_\perp j \prod_{\substack{i=1 \\ i \neq j, j'}}^{N+1} d^2\bar{\mathbf{p}}_\perp i (16\pi^3)^{1-N} \delta^{(2)}\left(\frac{\Delta_\perp}{2} - \sum_{\substack{i=1 \\ i \neq j, j'}}^{N+1} \bar{\mathbf{p}}_\perp i\right) \\ &\times \delta(\bar{x} - \bar{x}_j) \Psi_{N-1,\beta'}^{*\lambda'}(\hat{r}') \Psi_{N+1,\beta}^\lambda(\tilde{r}), \end{aligned} \quad (4.76)$$

The arguments \tilde{r} and \hat{r}' of the wave functions are given in terms of \bar{x}_i and $\bar{\mathbf{p}}_\perp i$ by

$$\begin{aligned} \tilde{x}_i &= \frac{\bar{x}_i}{1+\xi}, & \tilde{\mathbf{p}}_\perp i &= \bar{\mathbf{p}}_\perp i + \frac{\bar{x}_i}{1+\xi} \frac{\Delta_\perp}{2}, & \text{for } i \neq j, j', \\ \tilde{x}_j &= \frac{\bar{x}_j + \xi}{1+\xi}, & \tilde{\mathbf{p}}_\perp j &= \bar{\mathbf{p}}_\perp j - \frac{1 - \bar{x}_j}{1+\xi} \frac{\Delta_\perp}{2}, \\ \tilde{x}_{j'} &= -\frac{\bar{x}_j - \xi}{1+\xi}, & \tilde{\mathbf{p}}_\perp j' &= -\bar{\mathbf{p}}_\perp j - \frac{1 + \bar{x}_j}{1+\xi} \frac{\Delta_\perp}{2}, \end{aligned} \quad (4.77)$$

and

$$\hat{x}'_i = \frac{\bar{x}_i}{1-\xi}, \quad \hat{\mathbf{p}}_{\perp i} = \bar{\mathbf{p}}_{\perp i} - \frac{\bar{x}_i}{1-\xi} \frac{\Delta_{\perp}}{2}, \quad \text{for } i \neq j, j'. \quad (4.78)$$

n_j ($n_{j'}$) in (4.76) is the number of (anti)quarks in the initial proton wave function $\Psi_{N+1,\beta}^{\lambda}(r)$ with the same discrete quantum numbers as the active (anti)quark (cf. [123] for a discussion of the non-trivial statistical factors). As was to be expected, the operator $\bar{\psi}_q \gamma^+ \psi_q$ in (4.50) projects out colour singlet $q\bar{q}$ pairs with total helicity zero in the initial proton LCWF.

4.4.1.4 interpretation of overlap formulas

interpretation of
GPDs

Overlap representation formulas for polarised quark and antiquark GPDs, and for the gluon GPDs – unpolarised and polarised – are to be found in [123]. Having thus established the connection between GPDs and LCWFs in a Fock space decomposition the interpretation of GPDs become evident. Unlike the ordinary PDFs, the GPDs relate different parton configurations. Instead of being parton densities the GPDs are *amplitudes* for a transition between different kinematical situations, where a parton is kicked out from the initial hadron and reinserted with a different momentum to form the final hadron with momentum different from the one of the initial hadron.

In the central region $-\xi < \bar{x} < \xi$ the GPD moreover relates initial and final states not only different in their kinematics, but also with a different parton content. A pair of partons – a quark-antiquark pair, or a pair of gluons – is taken out from an $N + 1$ parton Fock state to form the final $N - 1$ parton Fock state. The full GPDs are obtained by a summation over all Fock states. In this way properties of moments of the full GPDs, i.e. for integrals over $-1 < \bar{x} < 1$, induce constraints and relations between LCWFs with different parton content in the Fock space representation.

Furthermore, the reduction formulas (4.62), (4.63) and (4.64) to (4.68) become obvious in the overlap representation. In the forward limit $\xi \rightarrow 0$, $t \rightarrow 0$ (implying $\Delta_{\perp} \rightarrow 0$) the central region $-\xi < \bar{x} < \xi$ shrinks to zero and the shifts in the initial and final parton momenta in Eqs. (4.72) and (4.73) vanish leading the modulus squared of the LCWFs of Eq. (4.46). Thus, the N parton Fock state contribution to the ordinary PDFs results, to be interpreted as probability density to find a parton with certain momentum fraction \bar{x} inside an N parton Fock state of the hadron under consideration.

generalisation of
the Drell-Yan
formula

Eq. (4.71) is a direct generalisation of the Drell-Yan formula of Eq. (4.30) for elastic form factors which is readily obtained by taking the $\xi = 0$ limit and integrating over \bar{x} .

4.4.2 orbital angular momentum

The 1988 observation by the EMC collaboration [204] that only a small fraction (ca. 20-30 %) of the nucleon spin is explained by the quark and antiquark spins

was confirmed in the meanwhile by several measurements at CERN, SLAC and DESY [205, 206, 207]

$$\Delta\Sigma(5\text{GeV}^2) \sim 0.20 \pm 0.08. \quad (4.79)$$

The rest of the nucleon spin is provided by the polarisation of the gluons and by the orbital angular momentum of quarks and gluons

$$\frac{1}{2} = \frac{\Delta\Sigma(\mu^2)}{2} + \hat{L}_q(\mu^2) + \Delta\hat{G}(\mu^2) + \hat{L}_g(\mu^2). \quad (4.80)$$

First indications on the sign and size of the gluon polarisation have been seen (HERMES@DESY), and precision measurements are on the way (COMPASS@CERN, RHIC-spin@BNL, E-161@SLAC). X. Ji's proposal [171] to access the orbital angular momentum in DVCS initiated lively discussions and renewed the interest in the concept of GPDs which had almost escaped notice before. The proposal is based on a gauge-invariant decomposition of the angular momentum operator

orbital angular momentum of partons

$$\begin{aligned} \mathbf{J}_q &= \int d^3x \psi^\dagger [\boldsymbol{\gamma}\gamma_5 - (\mathbf{x} \times \mathbf{D})] \psi, \\ \mathbf{J}_g &= \int d^3x (\mathbf{x} \times (\mathbf{E} \times \mathbf{B})). \end{aligned} \quad (4.81)$$

Denoting the matrix element of the angular momentum operators as

$$J_{q,g} 2\mathbf{S} = \langle P, S | \mathbf{J}_{q,g} | P, S \rangle \quad (4.82)$$

it was argued that the total angular momentum is related to form factors of the energy-momentum tensor $A(t=0)$ and $B(t=0)$ in the form

$$J_{q,g} = \frac{1}{2} (A_{q,g}(t=0) + B_{q,g}(t=0)) \quad (4.83)$$

with

$$\begin{aligned} \langle P' | T_{q,g}^{\mu\nu} | P \rangle &= \bar{U}(P') \left[A_{q,g}(t) \gamma^{(\mu} \bar{P}^{\nu)} + B_{q,g}(t) \bar{P}^{(\mu} i\sigma^{\nu)\alpha} \Delta_\alpha / (2M) \right. \\ &\quad \left. + C_{q,g}(t) \Delta^{(\mu} \Delta^{\nu)} / M \right] U(P) \end{aligned} \quad (4.84)$$

where brackets denote symmetrisation of indices. The form factors $A(t)$ and $B(t)$ in principle can be measured in non-forward reactions at small but finite values of $-t$ and are related to the first moment of GPDs by

$$\int_{-1}^1 dx x (H_{q,g}(x, \xi, t) + E_{q,g}(x, \xi, t)) = A_{q,g}(t) + B_{q,g}(t). \quad (4.85)$$

A measurement of the t dependence might allow a subsequent extrapolation to $t=0$ and the desired information (cf. [208]).

Ji's proposal has been criticised among others by Jaffe (see [209] and references therein). Jaffe distinguishes between a properly defined 'sum rule', which identifies the expectation value of a local operator in a certain nucleon state with an integral over a distribution measured in an inelastic production involving the same state, and an operator relation. According to this classification Ji's 'spin

partonic interpretation questionable

sum rule' in fact is merely an *operator relation*: there are no parton representations for $\Delta\hat{G}(x)$, \hat{L}_q , \hat{L}_g ; and $\Delta\hat{G}(x)$ is not the the integral of the helicity weighted gluon distribution. There is however a sum rule for the contributions to the nucleon's angular momentum involving proper parton distributions (in LC gauge)[210, 211, 212], but it appears that the respective distributions $L_q(x)$ and $L_g(x)$ are not experimentally accessible¹⁰.

While the proper access o the question of orbital angular momentum of partons is still under debate it was realised however, that GPDs carry most valuable information on hadron substructure of a different kind – though closely related to the angular momentum. The t dependence of GPDs permits the investigation of the absolute localisation of partons in the plane transverse to the direction of hadron motion. The next subsection is devoted to this observation.

4.4.3 transverse localisation of partons

There are several observations indicating the kind of additional information on hadron substructure carried by GPDs compared to the ordinary PDFs.

- It is directly obvious that GPDs carry information on transverse degrees of freedom, since they depend on three variables, $H(x, \xi, t)$, etc.: the momentum transfer $t = \Delta^2$ in general has *longitudinal*¹¹ and *transverse* components.
- The GPDs $E^q(x, \xi, t)$ and $\tilde{E}^q(x, \xi, t)$ describe hadron helicity flip matrix elements where the quark helicity is conserved. These can be non-vanishing only if quarks carry orbital angular momenta.
- Forward hadronic matrix elements are sensitive to distances on the light-cone, i.e. the difference of the arguments ($z - z'$) of the parton field operators, which is the conjugate variable to the sum of incoming and outgoing parton momenta ($k' + k$) (with $k = k'$ in the forward case). Non-forward matrix elements however, are also sensitive to the sum ($z + z'$) which is the conjugate variable to $(k' - k) = P' - P = \Delta$. This gives principally access to the *overall location* of partons[213]. Ralston, Buniy and Jain summarise their observation as “*Measurement of the Δ_T dependence of amplitudes, by Fourier transform, can be inverted to find the spatial \mathbf{b}_\perp location of the partons. The transverse structure is directly observable when amplitudes are measured by interference.*”

A more formal basis can be given to these generic observations. Burkardt found out that for the special case $\xi = 0$ GPDs are Fourier transforms of PDFs in transverse ‘impact parameter’ space

$$H(x, \xi = 0, t = -\Delta_\perp^2) = \int d^2b_\perp e^{-i\Delta_\perp \cdot \mathbf{b}_\perp} f_1(x, b_\perp) \quad (4.86)$$

¹⁰This quandary was summarised by Jaffe as “*What can be interpreted cannot be measured, what can be measured cannot be interpreted*” (quoted from [209]).

¹¹In an infinite momentum frame; otherwise the notion of *longitudinal components* is to be replaced by *plus LC components*

Where are the
quarks
in the nucleon ?

corresponding to

$$f_1(x, \mathbf{b}_\perp) = \int \frac{d^2 \Delta_\perp}{(2\pi)^2} H(x, \xi = 0, -\Delta_\perp^2) e^{i \mathbf{b}_\perp \cdot \Delta_\perp}. \quad (4.87)$$

The impact parameter representation of GPDs was worked out by Diehl [214] for the general case of $\xi \neq 0$ based on the overlap of LCWFs. Here the main results of [214] are quoted for the unpolarised quark GPD.

Diehl noticed that due to Lorentz invariance the invariant momentum transfer depends on the transverse components of proton momenta P and P' only through the combination

$$\mathbf{D}_\perp = \frac{\mathbf{p}'_\perp}{1 - \xi} - \frac{\mathbf{p}_\perp}{1 + \xi}, \quad (4.88)$$

in the form

$$-t = -(p' - p)^2 = \frac{4\xi^2 m^2}{1 - \xi^2} + (1 - \xi^2) \mathbf{D}_\perp^2. \quad (4.89)$$

In the ‘‘average-frame’’ the relation $\overline{\mathbf{D}}_\perp^2 = \Delta_\perp^2 / (1 - \xi^2)^2$ holds. Thus, the Δ_\perp -dependence of the above considerations is replaced by a \mathbf{D}_\perp dependence in the following to avoid reference to a specific choice of transverse momenta \mathbf{P}_\perp and \mathbf{P}'_\perp .

With the phase convention for proton spinors given in [193] one has for the matrix elements $\mathcal{H}_{\lambda'\lambda}$ of Eq. (4.50)

$$\begin{aligned} \mathcal{H}_{++} &= \mathcal{H}_{--} = H - \frac{\xi^2}{1 - \xi^2} E, \\ \mathcal{H}_{-+} &= -(\mathcal{H}_{+-})^* = \frac{D^1 + iD^2}{2m} E, \end{aligned} \quad (4.90)$$

and

$$\begin{aligned} \widetilde{\mathcal{H}}_{++} &= -\widetilde{\mathcal{H}}_{--} = \widetilde{H} - \frac{\xi^2}{1 - \xi^2} \widetilde{E}, \\ \widetilde{\mathcal{H}}_{-+} &= (\widetilde{\mathcal{H}}_{+-})^* = \frac{D^1 + iD^2}{2m} \xi \widetilde{E}. \end{aligned} \quad (4.91)$$

With these preliminaries the matrix elements can now be transformed to transverse impact parameter space,¹²

$$\begin{aligned} \mathcal{I}_{++}(\bar{x}, \xi, \bar{\mathbf{b}}_\perp) &= \int \frac{d^2 \mathbf{D}_\perp}{(2\pi)^2} e^{-i \mathbf{D}_\perp \cdot \bar{\mathbf{b}}_\perp} \mathcal{H}_{++}(\bar{x}, \xi, \mathbf{D}_\perp) \\ &= \frac{1}{4\pi} \int_0^\infty d(\mathbf{D}_\perp^2) J_0(|\mathbf{D}_\perp| |\bar{\mathbf{b}}_\perp|) \left(H - \frac{\xi^2}{1 - \xi^2} E \right), \\ \mathcal{I}_{-+}(\bar{x}, \xi, \bar{\mathbf{b}}_\perp) &= \int \frac{d^2 \mathbf{D}_\perp}{(2\pi)^2} e^{-i \mathbf{D}_\perp \cdot \bar{\mathbf{b}}_\perp} \mathcal{H}_{-+}(x, \xi, \mathbf{D}_\perp) \\ &= \frac{1}{4\pi} \frac{\bar{b}^2 - i\bar{b}^1}{|\bar{\mathbf{b}}_\perp|} \int_0^\infty d(\mathbf{D}_\perp^2) J_1(|\mathbf{D}_\perp| |\bar{\mathbf{b}}_\perp|) \frac{|\mathbf{D}_\perp|}{2m} E, \end{aligned} \quad (4.92)$$

with analogous relations for the other helicity combinations.

¹²Note that the transformation is done for the two transverse dimensions only.

$\bar{x} \in [\xi, 1]$

The derivation of the overlap representation of GPDs in terms of LCWFs as sketched in subsection 4.4.1 can be repeated this time in transverse impact parameter space. The result in the DGLAP region $\bar{x} \in [\xi, 1]$ is found in [193] as

$$\begin{aligned} \mathcal{I}_{\lambda'\lambda}(\bar{x}, \xi, \bar{\mathbf{b}}_{\perp}) &= \sum_{N,\beta} \sqrt{1-\xi^2}^{1-N} \sum_{j=q} \int [d\bar{x}]_N [d^2\bar{\mathbf{b}}_{\perp}]_N \\ &\times \delta(\bar{x} - \bar{x}_j) \delta^{(2)}(\bar{\mathbf{b}}_{\perp} - \bar{\mathbf{b}}_{\perp j}) \tilde{\psi}_{N\beta}^{*\lambda'}(\hat{x}_i, \bar{\mathbf{b}}_{\perp i} - \hat{\mathbf{b}}_{\perp 0}) \tilde{\psi}_{N\beta}^{\lambda}(\tilde{x}_i, \bar{\mathbf{b}}_{\perp i} - \tilde{\mathbf{b}}_{\perp 0}) \end{aligned} \quad (4.93)$$

with wave function arguments

$$\begin{aligned} \tilde{x}_i &= \frac{\bar{x}_i}{1+\xi}, & \hat{x}_i &= \frac{\bar{x}_i}{1-\xi} & \text{for } i \neq j, \\ \tilde{x}_j &= \frac{\bar{x}_j + \xi}{1+\xi}, & \hat{x}_j &= \frac{\bar{x}_j - \xi}{1-\xi}, \end{aligned} \quad (4.94)$$

and transverse locations of the proton states

$$\tilde{\mathbf{b}}_{\perp 0} = \frac{\xi}{1+\xi} \bar{\mathbf{b}}_{\perp j}, \quad \hat{\mathbf{b}}_{\perp 0} = -\frac{\xi}{1-\xi} \bar{\mathbf{b}}_{\perp j}. \quad (4.95)$$

The label j denotes the struck parton and is summed over all quarks with appropriate flavour in a given Fock state, and the labels (N, β) are summed over the corresponding Fock states. The representation in the DGLAP region $x \in [-1, -\xi]$ is obtained from (4.93) by reversing the overall sign, by changing $\delta(x - x_j)$ into $\delta(x + x_j)$, and by summing j over antiquarks.

The wave functions for definite transverse momentum or impact parameter are related by

$$\begin{aligned} \tilde{\psi}_{N\beta}^{\lambda}(x_i, \mathbf{b}_{\perp i} - \mathbf{b}_{\perp}) &= \int [d^2\mathbf{p}_{\perp}]_N \exp\left[i \sum_{i=1}^N \mathbf{p}_{\perp i} \cdot \mathbf{b}_{\perp i}\right] \psi_{N\beta}^{\lambda}(x_i, \mathbf{p}_{\perp i}), \\ \psi_{N\beta}^{\lambda}(x_i, \mathbf{p}_{\perp i} - x_i \mathbf{P}_{\perp}) &= \int [d^2\mathbf{b}_{\perp}]_N \exp\left[-i \sum_{i=1}^N \mathbf{p}_{\perp i} \cdot \mathbf{b}_{\perp i}\right] \tilde{\psi}_{N\beta}^{\lambda}(x_i, \mathbf{b}_{\perp i}) \end{aligned} \quad (4.96)$$

with $\mathbf{b}_{\perp} = \sum_{i=1}^N x_i \mathbf{b}_{\perp i}$ and $\mathbf{P}_{\perp} = \sum_{i=1}^N \mathbf{p}_{\perp i}$, and are normalised to

$$\begin{aligned} P_{N\beta}^{\lambda} &= \int [dx]_N [d^2\mathbf{p}_{\perp}]_N \left| \psi_{N\beta}^{\lambda}(x_i, \mathbf{p}_{\perp i}) \right|^2 \\ &= \int [dx]_N [d^2\mathbf{b}_{\perp}]_N \left| \tilde{\psi}_{N\beta}^{\lambda}(x_i, \mathbf{b}_{\perp i}) \right|^2, \end{aligned} \quad (4.97)$$

where $P_{N\beta}^{\lambda}$ is the probability to find the corresponding Fock state in the proton, so that in total $\sum_{N,\beta} P_{N\beta}^{\lambda} = 1$. The shorthand notation

$$[d^2\mathbf{b}_{\perp}]_N = (4\pi)^{N-1} \prod_{i=1}^N d^2\mathbf{b}_{\perp i} \delta^{(2)}\left(\sum_{i=1}^N x_i \mathbf{b}_{\perp i}\right), \quad (4.98)$$

is used for the N -parton impact parameter integration element.

$\bar{x} \in [-\xi, \xi]$

In the ERBL region $\bar{x} \in [-\xi, \xi]$ Diehl finds

$$\begin{aligned}
 \mathcal{I}_{\lambda\lambda}(\bar{x}, \xi, \bar{\mathbf{b}}_{\perp}) &= \sum_{N, \beta, \beta'} \sqrt{1 - \xi}^{2-N} \sqrt{1 + \xi}^{-N} \sum_{j, j'} \frac{1}{\sqrt{n_j n_{j'}}} & (4.99) \\
 &\times \int d\bar{x}_j \prod_{i \neq j, j'} d\bar{x}_i \delta\left(1 - \xi - \sum_{i \neq j, j'} \bar{x}_i\right) \\
 &\times (4\pi)^{N-1} \int d^2 \bar{\mathbf{b}}_{\perp j} \prod_{i \neq j, j'} d^2 \bar{\mathbf{b}}_{\perp i} \delta^{(2)}\left(\xi \bar{\mathbf{b}}_{\perp j} + \sum_{i \neq j, j'} x_i \bar{\mathbf{b}}_{\perp i}\right) \\
 &\times \delta(\bar{x} - \bar{x}_j) \delta^{(2)}(\bar{\mathbf{b}}_{\perp} - \bar{\mathbf{b}}_{\perp j}) \tilde{\psi}_{N-1, \beta'}^{\lambda'}(\hat{x}_i, \bar{\mathbf{b}}_{\perp i} - \hat{\mathbf{b}}_{\perp 0}) \tilde{\psi}_{N+1, \beta}^{\lambda}(\tilde{x}_i, \bar{\mathbf{b}}_{\perp i} - \tilde{\mathbf{b}}_{\perp 0})
 \end{aligned}$$

with $\tilde{\mathbf{b}}_{\perp 0}$ and $\hat{\mathbf{b}}_{\perp 0}$ as in (4.95) and

$$\begin{aligned}
 \tilde{x}_i &= \frac{\bar{x}_i}{1 + \xi}, & \hat{x}_i &= \frac{\bar{x}_i}{1 - \xi} & \text{for } i \neq j, j', \\
 \tilde{x}_j &= \frac{\xi + \bar{x}_j}{1 + \xi}, & \tilde{x}_{j'} &= \frac{\xi - \bar{x}_{j'}}{1 + \xi}.
 \end{aligned} \tag{4.100}$$

The partons j, j' are the ones emitted from the initial proton, and in (4.99) one has to sum over all quarks j and antiquarks j' with opposite helicities, opposite colour, and appropriate flavour in the initial state proton, over all Fock states $(N+1, \beta)$ containing such a $q\bar{q}$ pair, and over all Fock states $(N-1, \beta')$ of the final state proton with matching quantum numbers for the spectator partons $i \neq j, j'$. The statistical factors n_j ($n_{j'}$) give the number of (anti)quarks in the Fock state $(N+1, \beta)$ that have the same discrete quantum numbers as the (anti)quark pulled out of the target (see [123, 214] for a discussion of the statistical factors).

A few words are in order here for a geometrical interpretation of the results. Inside a proton in a N parton Fock state described by (4.96) the parton i is transversely localised at $\mathbf{b}_{\perp i}$. The wave function $\tilde{\psi}_{N\beta}$ depends only on its position relative to the centre \mathbf{b}_{\perp} of the proton, where the constraint

$$\mathbf{b}_{\perp} = \sum_{i=1}^N x_i \mathbf{b}_{\perp i} \tag{4.101}$$

identifies \mathbf{b}_{\perp} as the *transverse centre of momentum* [216] of the partons in each separate Fock state $(N\beta)$. Note that each parton i contributes to the *transverse centre of momentum* not just by its impact parameter, but additionally weighted with the momentum fraction x_i .¹³

The geometrical situation for the matrix element $\mathcal{I}(\bar{x}, \xi = 0, \bar{\mathbf{b}}_{\perp})$ in the DGLAP region is indicated in Fig. 4.26, where the initial and final proton is depicted as a Lorentz contracted ‘pancake’, and the active parton as wave packets with transverse extension $\sim 1/Q$. The \mathbf{e}_3 axis is chosen to coincide with the transverse centres of proton momenta.

In the case of a non-vanishing change of momentum fraction $\xi \neq 0$ the transverse centres of momenta are shifted resulting from the different weights the active

¹³In [193] the analogy to the centre of mass $\sum m_i \mathbf{r}_i / \sum m_i$ is drawn.

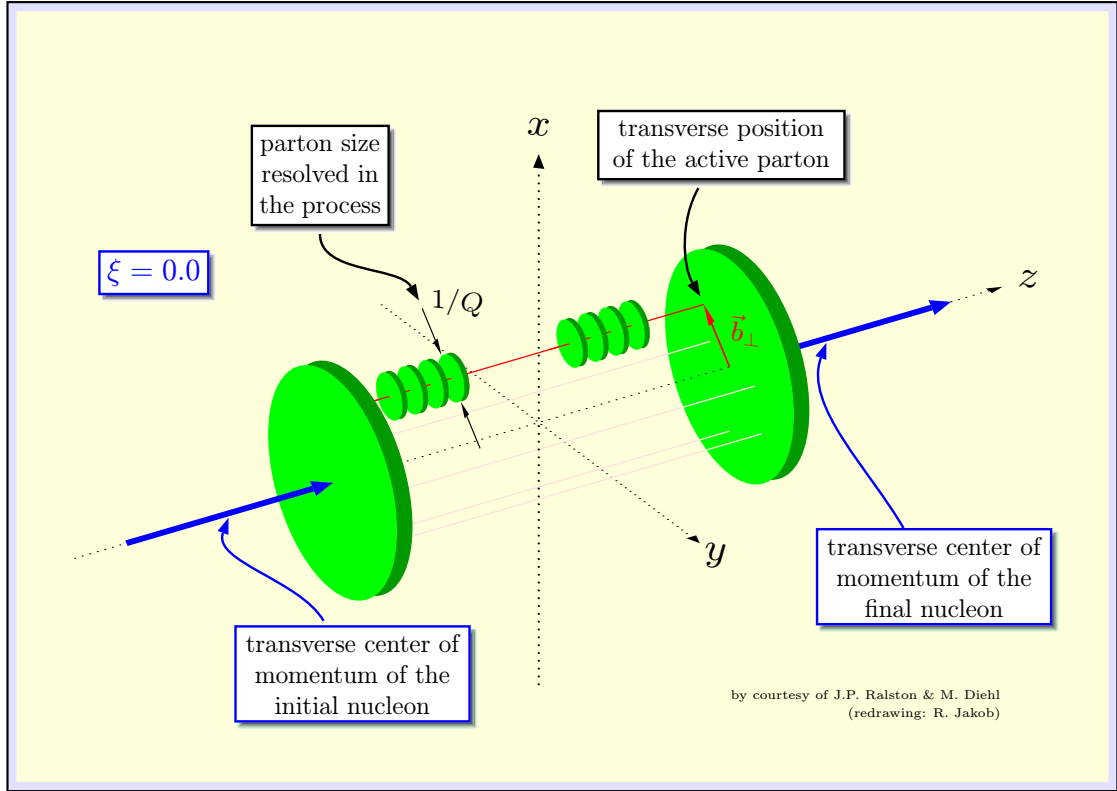


Figure 4.26: Redrawing of Fig. 1 in [215] with $\bar{x} = 0.4$ and $\xi = 0$.

parton brings into the sum $\sum x_i \mathbf{b}_{\perp i}$ before and after the scattering. The shifts in transverse direction out of the \mathbf{e}_3 axis are given by Eqs. (4.95). The geometrical situation is indicated in Fig. 4.27 for the example of $x = 0.4$ and $\xi = 0.3$.

The analogy of *transverse parton localisations* via GPD to optical imaging procedures was noticed by Ralston and Pire [217], who speak about the “...*femtophotography of the interior structure of the proton*”. In [217] and also recently in [218] the analogy with holograms was stressed, where in the case of imaging the nucleon the real Bethe-Heitler amplitude serves as ‘reference beam’ to the complex DVCS amplitude which carries the detailed information on the nucleon substructure.

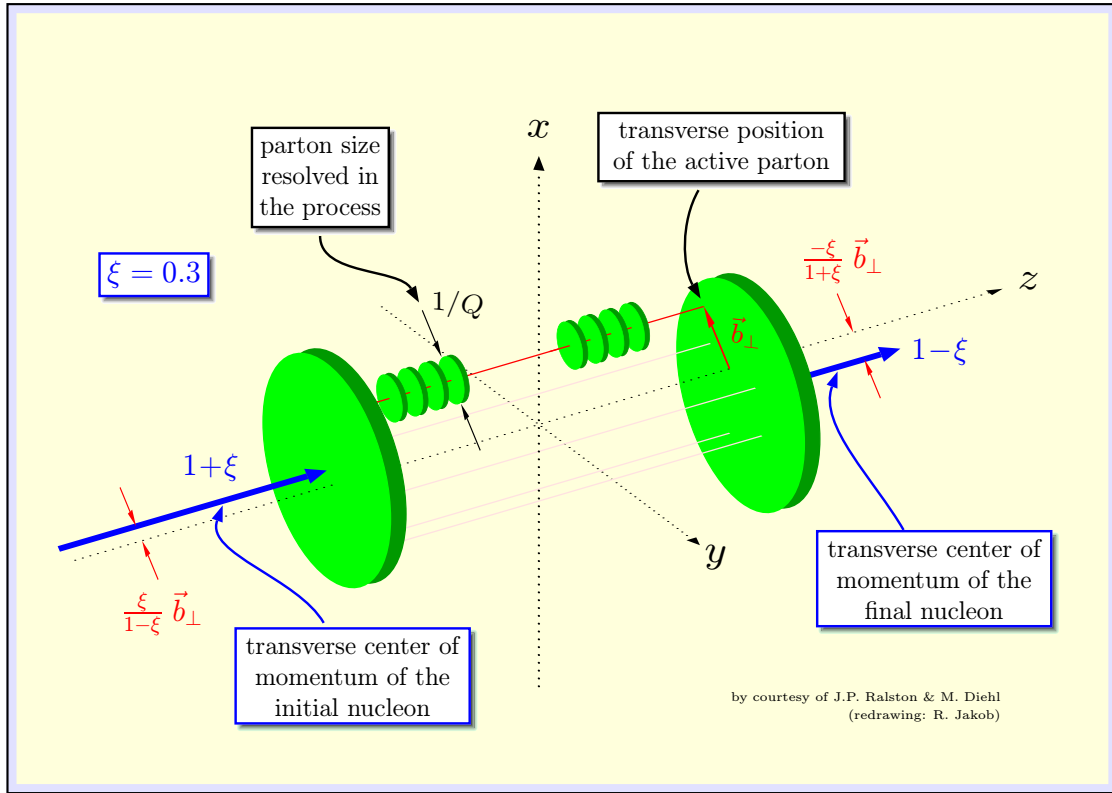


Figure 4.27: Redrawing of Fig. 1 in [213] combined with the generalisation to $\xi \neq 0$ derived by Diehl [214] (cf. Fig. 1 in [214]) for the example of $x = 0.4$ and $\xi = 0.3$. The modulus of longitudinal proton momenta is indicated by the length of arrows.

4.5 summary

In this chapter it was argued by a number of examples discussed on a phenomenological level that the soft overlap contributions (also denoted as Feynman or handbag mechanism) play a significant, in many cases dominant rôle in the description of exclusive processes at intermediate momentum transfers of a few GeV, where data are available (or will become available soon). Since the contributions are calculated from overlap integrals of (soft) LCWFs shifted in their transverse momentum arguments, it is the *a priori* unknown transverse momentum dependence of the (soft) wave functions which is tested in these processes¹⁴. In particular, the case of WACS is instructive, where the recent measurement of the A_{LL} helicity correlation seems to confirm the dominance of the handbag contribution and reveals a behaviour typical for the Compton scattering on a single quark line.

Hard exclusive processes in the kinematical regime of deeply virtual photons are described by a factorisation of the dominant diagrams into hard perturbative partonic subprocesses and soft parts represented by generalised parton distributions. GPDs are very powerful tools for the exploration of hadronic substructure, since they link plenty of hard inclusive and exclusive processes and quantities:

¹⁴The Drell-Yan formula provides an exact relation between the full LCWFs and the elastic FFs.

(elastic) FFs, handbag contributions to wide angle CS and meson production, (semi-)inclusive DIS involving ordinary PDFs (i.e. GPDs in the forward limit), deeply virtual CS and meson production, to name but a few.

One of the main motivations to consider GPDs was the possible access to the orbital angular momentum of partons contributing to the nucleon spin. While this point is still under debate with respect to the correct interpretation of measurable quantities (or at least quantities which might be extractable by extrapolation to kinematical limits) in the context of the parton model, it was realised the GPDs carry more profound and general information. The representation of GPDs as overlap integrals of LCWFs reveals this information most clearly when transformed to impact parameter space [219, 215, 213, 214]. The dependence of GPDs on the transverse components of the external momentum transfer provides access to the absolute position of partons in transverse impact parameter space. This is peculiar to non-forward processes, since forward processes from general principles are sensitive only to relative distances, never to absolute localisations. A generalisation from the special case of vanishing change of longitudinal momentum fractions $\xi = 0$ during the process to the general $\xi \neq 0$ situation reveals an intricate relation between longitudinal momentum fractions and transverse impact parameter space localisations., or transverse momentum distributions, which are conjugate variables.

5

Conclusions and outlook

The present report addresses the rôle of intrinsic transverse momentum in the phenomenology of hard (semi-)inclusive and exclusive reactions. As was argued these effects beyond the parton model are of great importance in the investigation of hadronic substructure. For the understanding of reaction mechanisms and the dominant contributions to many observable quantities the effect of *intrinsic transverse momenta* is a key ingredient.

(semi-)inclusive processes Observables sensitive to *intrinsic transverse momenta* play a key rôle in unravelling the partonic spin contributions to the nucleon spin. In particular the azimuthal angular dependencies of single spin asymmetries allow access to the hitherto unknown transversity distribution function, which completes the leading order picture of quark spin. These findings are summarised in section 3.5.

exclusive processes *Intrinsic transverse momentum* effects manifest themselves in different ways in the kinematical regions of large momentum transfer and of processes initiated by a deeply virtual photon:

- Many wide angle exclusive processes at intermediate momentum transfer probe the *intrinsic transverse momentum dependence* of LCWFs, since significant – and in many cases dominant – contributions can be assigned to overlap integrals of the wave functions, which are shifted in the transverse momentum arguments. The relative importance of partonic transverse momentum effects is strongly enhanced in large $|t|$ exclusive processes, since transverse momenta have to be compared to the relevant longitudinal scales which become small in kinematical end-point regions.
- Consideration of deeply virtual CS and meson production has lead to the introduction of GPDs, which provide a uniform concept and thus

link many inclusive and exclusive quantities. Furthermore, GPDs provide access to the overall localisation of partons in transverse impact parameter space. The key to this most valuable information on hadron substructure is the dependence on *transverse components of momentum transfer*.

These findings are summarised in section 4.5.

In the present report the rôle and importance of intrinsic transverse momentum effects has been discussed mainly from phenomenological perspective. Many more formal aspects have still been not clarified or not even addressed in a satisfactory way. As an example at the end of chapter 3 the interplay of partonic transverse momenta and evolution effects of ordinary PDFs has been briefly sketched. It is this interweaving of perturbative radiative effects and non-perturbative intrinsic partonic properties which makes a proper treatment of the evolution of unintegrated PDFs so difficult, an issue still in its infancy.

Even more problematic, from a principal perspective, the notion of *intrinsic transverse momenta* carries subtle ambiguities in itself. By the definition of the covariant derivative $D^\mu = \partial^\mu + i g_s (\lambda_a/2) A_a^\mu$ (λ_a being the Gell-Mann matrices) the transverse components of the partial derivative, or transverse moments as their conjugate variables, are related to transverse degrees of the gauge field. Since transverse components of the gluon fields are the “good” LC components representing independent dynamical degrees of freedom, transverse momentum effects can be rephrased in terms of additional gluon quanta by means of the equations of motion. For the case of totally inclusive DIS Ellis, Furmanski and Petronzio (EFP) [222] have shown strict equivalence of a field theoretic approach to the operator product expansion. In the course of the proof they introduced the so-called *transverse operator basis* – as opposed to the *collinear operator basis* advocated by Politzer and implemented by Jaffe and Soldate, where off-shellness and transverse momenta are generated dynamically by interaction of partons. In the *transverse operator basis* however off-shellness is eliminated using the equations of motions, but the transverse momentum is retained.

The interpretation of transverse momenta in the present report is done in the spirit of the EFP *transverse operator basis*. One has to be aware that only with this special choice the formal definitions of field theoretical quantities parallel so closely our figurative imagination of transverse momenta of partons inside a compound. This freedom of choice is nothing to be worried about, since it is about the partonic interpretation of effects only. Physical observables in the end are independent of any arbitrary choices, as it should be. We are all used to the fact that the intuitive partonic interpretation of integrated PDFs strictly hold only in a physical, LC gauge and an infinite momentum frame.¹ What worries more, is the question whether the ideas on the transverse momenta developed for inclusive DIS can be taken over unchanged to semi-inclusive reactions, and in particular to observables which depend explicitly on external transverse momentum components.

¹ Alternatively, one can relax the restriction to the infinite momentum frame, when working in LC quantisation and considering only “good” LC components of the fields.

Also for the case of hard exclusive reactions there has been an attempt to find a clear field theoretical definition of transverse momentum effects starting from the consideration of the pion gamma transition form factor [155]. The subject still is not settled on a satisfactory level and certainly needs further investigations.

The eminent importance of *intrinsic transverse momentum effects* in the phenomenology of hard inclusive and exclusive reactions underlines the needs for further theoretical progress on the subject – as was demonstrated in the present report. The communities working in the field of *hadron physics* in the US and in Europe currently undergo a crucial phase of self-organisation. Proposals for future accelerators and dedicated experiments – as ELFE@TESLA, EVELINE or TESLA-N in Europe, or an JLAB upgrade to an energy of 24 GeV, EIC at Brookhaven in the US – are discussed and worked out in detail. Current *hot topics* in hadron physics have been identified as the determination of the *transversity distribution* and the *localisation of partons* via generalised parton distributions (see for instance [223, 224] or [225]). To both topics the understanding of *transverse momentum effects* is an absolutely crucial ingredient. Great opportunities to improve and refine our knowledge of hadron substructure have opened up.

A

Dirac matrices in chiral (Weyl) representation

Dirac matrices: (Weyl or chiral representation) One writes the representation of Dirac matrices compactly in the “bispinor” notation [15]. If $(\sigma^1, \sigma^2, \sigma^3)$ and (ρ^1, ρ^2, ρ^3) are two copies of the standard 2×2 Pauli matrices, any 4×4 Dirac matrix can be represented as $\rho^i \otimes \sigma^j$.

The chiral (Weyl) representation is defined by

$$\gamma^0 = \rho^1 \otimes \mathbf{1} = \begin{pmatrix} 0 & \mathbf{1} \\ \mathbf{1} & 0 \end{pmatrix}; \quad \vec{\gamma} = -i\rho^2 \otimes \vec{\sigma} = \begin{pmatrix} 0 & -\vec{\sigma} \\ \vec{\sigma} & 0 \end{pmatrix}; \quad (\text{A.1})$$

and

$$\gamma_5 = \rho^3 \otimes \mathbf{1} = i\gamma^0\gamma^1\gamma^2\gamma^3 = \begin{pmatrix} \mathbf{1} & 0 \\ 0 & -\mathbf{1} \end{pmatrix}. \quad (\text{A.2})$$

A commonly used basis for the space of all 4×4 matrices are the 16 independent matrices

$$\mathbf{1}, \quad \gamma_5, \quad \gamma^\mu, \quad \gamma^\mu\gamma_5, \quad \sigma^{\mu\nu} \quad (\text{A.3})$$

in terms of which any matrix M can be decomposed as¹

$$M = \frac{\text{Tr}[M \mathbf{1}]}{4} \mathbf{1} + \frac{\text{Tr}[M \gamma_5]}{4} \gamma_5 + \frac{\text{Tr}[M \gamma^\mu]}{4} \gamma_\mu - \frac{\text{Tr}[M \gamma_5 \gamma^\mu]}{4} \gamma_5 \gamma_\mu + \frac{\text{Tr}[M \sigma^{\mu\nu}]}{2 \cdot 4} \sigma_{\mu\nu} \quad (\text{A.4})$$

¹note the minus sign of the 4th term and the extra factor 1/2 in the last term to avoid double counting in the summation over μ and ν .

Instead one can use the alternative basis

$$\begin{aligned} & \gamma^+, \quad \gamma^+ \gamma_5, \quad i \sigma^{i+} \gamma_5, \\ \mathbb{1}, \quad \gamma^i, \quad i \gamma_5, \quad \gamma^i \gamma_5, \quad i \sigma^{ij} \gamma_5, \quad i \sigma^{+-} \gamma_5, \\ & \gamma^-, \quad \gamma^- \gamma_5, \quad i \sigma^{i-} \gamma_5 \end{aligned} \quad (\text{A.5})$$

(where now i, j are purely transverse indices, i.e., $i, j \in \{1, 2\}$) leading to the decomposition²

$$\begin{aligned} M &= \frac{\text{Tr}[M \gamma^+]}{4} \gamma^- - \frac{\text{Tr}[M \gamma^+ \gamma_5]}{4} \gamma^- \gamma_5 + \frac{\text{Tr}[M i \sigma^{i+} \gamma_5]}{4} i \sigma^{i-} \gamma_5 \\ &+ \frac{\text{Tr}[M \mathbb{1}]}{4} \mathbb{1} - \frac{\text{Tr}[M \gamma^i]}{4} \gamma^i - \frac{\text{Tr}[M i \gamma_5]}{4} i \gamma_5 + \frac{\text{Tr}[M \gamma^i \gamma_5]}{4} \gamma^i \gamma_5 \\ &- \frac{\text{Tr}[M i \sigma^{ij} \gamma_5]}{2 \cdot 4} i \sigma^{ij} \gamma_5 - \frac{\text{Tr}[M i \sigma^{+-} \gamma_5]}{4} i \sigma^{+-} \gamma_5 \\ &+ \frac{\text{Tr}[M \gamma^-]}{4} \gamma^+ - \frac{\text{Tr}[M \gamma^- \gamma_5]}{4} \gamma^+ \gamma_5 + \frac{\text{Tr}[M i \sigma^{i-} \gamma_5]}{4} i \sigma^{i+} \gamma_5 \end{aligned} \quad (\text{A.6})$$

Below I list all matrices of the basis (A.5) multiplied from the left by γ^0 , since this is the form relevant for a classification of bilocal quark field operators $\bar{\psi}(z_1) A \psi(z_2)$ according to powers of $1/Q$ and their chiral properties by a simple comparison with the generic pattern given in (2.45). The “effective twist” and chirality of $\bar{\psi}(z_1) A \psi(z_2)$ with $A \in$ basis (A.5) is indicated, as well.

effective twist 2:

$$\begin{aligned} (\gamma^0 \gamma^+) &= \sqrt{2} \begin{pmatrix} 1 & 0 & 0 & 0 \\ 0 & 0 & 0 & 0 \\ 0 & 0 & 0 & 0 \\ 0 & 0 & 0 & 1 \end{pmatrix} & \phi_R^\dagger \phi_R + \phi_L^\dagger \phi_L \\ & \text{chiral even, eff. twist 2} \end{aligned} \quad (\text{A.7})$$

$$\begin{aligned} (\gamma^0 \gamma^+ \gamma_5) &= \sqrt{2} \begin{pmatrix} 1 & 0 & 0 & 0 \\ 0 & 0 & 0 & 0 \\ 0 & 0 & 0 & 0 \\ 0 & 0 & 0 & -1 \end{pmatrix} & \phi_R^\dagger \phi_R - \phi_L^\dagger \phi_L \\ & \text{chiral even, eff. twist 2} \end{aligned} \quad (\text{A.8})$$

$$\begin{aligned} (\gamma^0 i \sigma^{1+} \gamma_5) &= \sqrt{2} \begin{pmatrix} 0 & 0 & 0 & 1 \\ 0 & 0 & 0 & 0 \\ 0 & 0 & 0 & 0 \\ 1 & 0 & 0 & 0 \end{pmatrix} & \phi_L^\dagger \phi_R + \phi_R^\dagger \phi_L \\ & \text{chiral odd, eff. twist 2} \end{aligned} \quad (\text{A.9})$$

$$\begin{aligned} (\gamma^0 i \sigma^{2+} \gamma_5) &= i \sqrt{2} \begin{pmatrix} 0 & 0 & 0 & -1 \\ 0 & 0 & 0 & 0 \\ 0 & 0 & 0 & 0 \\ 1 & 0 & 0 & 0 \end{pmatrix} & -\phi_L^\dagger \phi_R + \phi_R^\dagger \phi_L \\ & \text{chiral odd, eff. twist 2} \end{aligned} \quad (\text{A.10})$$

²again note signs and factors.

effective twist 3:

$$(\gamma^0 \mathbf{1}) = \begin{pmatrix} 0 & 0 & 1 & 0 \\ 0 & 0 & 0 & 1 \\ 1 & 0 & 0 & 0 \\ 0 & 1 & 0 & 0 \end{pmatrix} \quad \begin{array}{l} \chi_L^\dagger \phi_R + \phi_L^\dagger \chi_R + \phi_R^\dagger \chi_L + \chi_R^\dagger \phi_L \\ \text{chiral odd, eff. twist 3} \end{array} \quad (\text{A.11})$$

$$(\gamma^0 \gamma^1) = \begin{pmatrix} 0 & 1 & 0 & 0 \\ 1 & 0 & 0 & 0 \\ 0 & 0 & 0 & -1 \\ 0 & 0 & -1 & 0 \end{pmatrix} \quad \begin{array}{l} \chi_R^\dagger \phi_R + \phi_R^\dagger \chi_R - \phi_L^\dagger \chi_L - \chi_L^\dagger \phi_L \\ \text{chiral even, eff. twist 3} \end{array} \quad (\text{A.12})$$

$$(\gamma^0 \gamma^2) = i \begin{pmatrix} 0 & -1 & 0 & 0 \\ 1 & 0 & 0 & 0 \\ 0 & 0 & 0 & 1 \\ 0 & 0 & -1 & 0 \end{pmatrix} \quad \begin{array}{l} -\chi_R^\dagger \phi_R + \phi_R^\dagger \chi_R + \phi_L^\dagger \chi_L - \chi_L^\dagger \phi_L \\ \text{chiral even, eff. twist 3} \end{array} \quad (\text{A.13})$$

$$(\gamma^0 i \gamma_5) = i \begin{pmatrix} 0 & 0 & -1 & 0 \\ 0 & 0 & 0 & -1 \\ 1 & 0 & 0 & 0 \\ 0 & 1 & 0 & 0 \end{pmatrix} \quad \begin{array}{l} -\chi_L^\dagger \phi_R - \phi_L^\dagger \chi_R + \phi_R^\dagger \chi_L + \chi_R^\dagger \phi_L \\ \text{chiral odd, eff. twist 3} \end{array} \quad (\text{A.14})$$

$$(\gamma^0 \gamma^1 \gamma_5) = \begin{pmatrix} 0 & 1 & 0 & 0 \\ 1 & 0 & 0 & 0 \\ 0 & 0 & 0 & 1 \\ 0 & 0 & 1 & 0 \end{pmatrix} \quad \begin{array}{l} \chi_R^\dagger \phi_R + \phi_R^\dagger \chi_R + \phi_L^\dagger \chi_L + \chi_L^\dagger \phi_L \\ \text{chiral even, eff. twist 3} \end{array} \quad (\text{A.15})$$

$$(\gamma^0 \gamma^2 \gamma_5) = i \begin{pmatrix} 0 & -1 & 0 & 0 \\ 1 & 0 & 0 & 0 \\ 0 & 0 & 0 & -1 \\ 0 & 0 & 1 & 0 \end{pmatrix} \quad \begin{array}{l} -\chi_R^\dagger \phi_R + \phi_R^\dagger \chi_R + \phi_L^\dagger \chi_L + \chi_L^\dagger \phi_L \\ \text{chiral even, eff. twist 3} \end{array} \quad (\text{A.16})$$

$$(\gamma^0 i \sigma^{12} \gamma_5) = i \begin{pmatrix} 0 & 0 & -1 & 0 \\ 0 & 0 & 0 & 1 \\ 1 & 0 & 0 & 0 \\ 0 & -1 & 0 & 0 \end{pmatrix} \quad \begin{array}{l} -\chi_L^\dagger \phi_R + \phi_L^\dagger \chi_R + \phi_R^\dagger \chi_L - \chi_R^\dagger \phi_L \\ \text{chiral odd, eff. twist 3} \end{array} \quad (\text{A.17})$$

$$(\gamma^0 i \sigma^{+-} \gamma_5) = \begin{pmatrix} 0 & 0 & 1 & 0 \\ 0 & 0 & 0 & -1 \\ 1 & 0 & 0 & 0 \\ 0 & -1 & 0 & 0 \end{pmatrix} \quad \begin{array}{l} \chi_L^\dagger \phi_R - \phi_L^\dagger \chi_R + \phi_R^\dagger \chi_L - \chi_R^\dagger \phi_L \\ \text{chiral odd, eff. twist 3} \end{array} \quad (\text{A.18})$$

effective twist 4:

$$(\gamma^0 \gamma^-) = \sqrt{2} \begin{pmatrix} 0 & 0 & 0 & 0 \\ 0 & 1 & 0 & 0 \\ 0 & 0 & 1 & 0 \\ 0 & 0 & 0 & 0 \end{pmatrix} \quad \begin{array}{l} \chi_R^\dagger \chi_R + \chi_L^\dagger \chi_L \\ \text{chiral even, eff. twist 4} \end{array} \quad (\text{A.19})$$

$$(\gamma^0 \gamma^- \gamma_5) = \sqrt{2} \begin{pmatrix} 0 & 0 & 0 & 0 \\ 0 & 1 & 0 & 0 \\ 0 & 0 & -1 & 0 \\ 0 & 0 & 0 & 0 \end{pmatrix} \quad \begin{array}{l} \chi_R^\dagger \chi_R - \chi_L^\dagger \chi_L \\ \text{chiral even, eff. twist 4} \end{array} \quad (\text{A.20})$$

$$(\gamma^0 i \sigma^{1-} \gamma_5) = \sqrt{2} \begin{pmatrix} 0 & 0 & 0 & 0 \\ 0 & 0 & 1 & 0 \\ 0 & 1 & 0 & 0 \\ 0 & 0 & 0 & 0 \end{pmatrix} \quad \begin{array}{l} \chi_L^\dagger \chi_R + \chi_R^\dagger \chi_L \\ \text{chiral odd, eff. twist 4} \end{array} \quad (\text{A.21})$$

$$(\gamma^0 i \sigma^{2-} \gamma_5) = i \sqrt{2} \begin{pmatrix} 0 & 0 & 0 & 0 \\ 0 & 0 & 1 & 0 \\ 0 & -1 & 0 & 0 \\ 0 & 0 & 0 & 0 \end{pmatrix} \quad \begin{array}{l} \chi_L^\dagger \chi_R - \chi_R^\dagger \chi_L \\ \text{chiral odd, eff. twist 4} \end{array} \quad (\text{A.22})$$

B

Sudakov factor

The Sudakov function in impact parameter space $s(\xi, b, Q)$ was derived by Collins and Soper in a paper on $e^+e^- \rightarrow jets$ [66], and ported to exclusive reactions by Botts, Sterman and Li [110, 111, 112]. Expressed in the variables

$$\hat{q} \equiv \ln(\xi Q / \sqrt{2} \Lambda_{QCD}), \quad \hat{b} \equiv \ln(1/b \Lambda_{QCD}) \quad (\text{B.1})$$

it is given in [111, 112] by

$$\begin{aligned} s(\xi, b, Q) = & \frac{2 A^{(1)}}{\beta_0} \hat{q} \ln\left(\frac{\hat{q}}{\hat{b}}\right) - \frac{2 A^{(1)}}{\beta_0} (\hat{q} - \hat{b}) + \frac{4 A^{(2)}}{\beta_0^2} \left(\frac{\hat{q}}{\hat{b}} - 1\right) \\ & - c_1 \frac{A^{(1)} \beta_1}{4 \beta_0^3} \hat{q} \left[\frac{\ln(2\hat{b}) + 1}{\hat{b}} - \frac{\ln(2\hat{q}) + 1}{\hat{q}} \right] \\ & - \left(\frac{4 A^{(2)}}{\beta_0^2} - c_2 \frac{A^{(1)}}{\beta_0} \ln\left(\frac{e^{2\gamma-1}}{2}\right) \right) \ln\left(\frac{\hat{q}}{-\hat{b}}\right) \\ & - c_3 \frac{A^{(1)} \beta_1}{8 \beta_0^3} [\ln^2(2\hat{q}) - \ln^2(-2\hat{b})] \end{aligned} \quad (\text{B.2})$$

with

$$\beta_0 \equiv 11 - \frac{2}{3} n_f, \quad \beta_1 \equiv 102 - \frac{38}{3} n_f, \quad (\text{B.3})$$

and

$$A^{(1)} \equiv \frac{4}{3}, \quad A^{(2)} \equiv \frac{67}{9} - \frac{\pi^2}{3} - \frac{10}{27} n_f + \frac{2\beta_0}{3} \ln\left(\frac{e^\gamma}{2}\right), \quad (\text{B.4})$$

where γ is the Euler constant. Note that in [111, 112] a different convention for the β -function was used with

$$\beta_1^{LS} = \frac{\beta_0}{4}, \quad \beta_2^{LS} = \frac{\beta_1}{16}. \quad (\text{B.5})$$

In Eq. (B.2) factors $c_1 = c_2 = c_3 = 1$ have been inserted to indicate corrections found later. In fact, Bolz [147] derived (see also [117])

$$c_1 = -4, \quad c_3 = 4, \quad (\text{B.6})$$

which was confirmed by Li [226]¹ Stefaniš, Schroers and Kim rederived the Sudakov function and found a further correction amounting to

$$c_2 = \frac{1}{2}. \quad (\text{B.7})$$

As in the original derivation by Collins and Soper [66] also Stefaniš, Schroers and Kim [141] kept explicitly scheme constants C_1 and C_2 related to the ambiguity introduced by the (arbitrary) choice of a factorisation scheme. With the choices

$$C_1^{CS} = C_1^{SSK} = 1, \quad C_2^{CS} = \sqrt{2} C_2^{SSK} = 1 \quad (\text{B.8})$$

Eq. (B.2) is obtained.

¹In the appendix of [226] a complete expression for the function $s(\xi, b, Q)$ including leading and next-to-leading logarithms can be found. The additional terms are negligible for numerical studies.

C

Reference frames for elastic FFs and CS

Various frames of reference for elastic form factors, wide angle Compton scattering and deeply virtual Compton scattering are compiled in this Appendix.

In particular, for the exclusive processes at large momentum transfer, frames in which the momentum transfer has a vanishing LC *plus* component play a special rôle. The evaluation of overlap contributions of LCWFs requires some care. An example is the Drell-Yan overlap formula [122] of the elastic form factor, for which Isgur and Llewellyn Smith [103] observed that different results are obtained in different reference frames. Sawicki [227] has shown the origin of this discrepancy: in certain reference frames there are overlap contributions which are not contained in the Drell-Yan formula; when they are taken into account Lorentz invariance is restored. Recently, the formalism of generalised parton distributions has allowed a more detailed understanding how this can be achieved [120, 123]. However, for an explicit treatment knowledge of higher Fock states of the hadrons is necessary. Thus, for practical model calculations it is preferable to use frames of reference where the momentum transfer has zero LC *plus* component.

Secondly, the arguments in the LCWFs are given by the LC fraction (ratio of LC *plus*-components of parton/hadron momentum), and by the parton transverse momenta (relative to the momentum of the parent hadron). The arguments of the LCWFs are most easily identified in a frame, where the parent hadron has no transverse momentum.

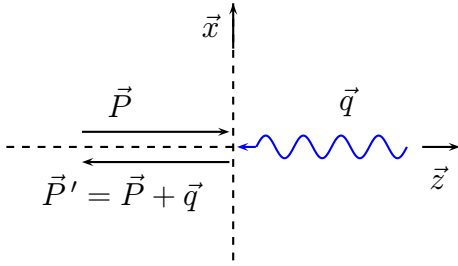
C.1 elastic FF, different reference frames

The elastic nucleon form factor will be considered, i.e. the (sub)process $\gamma^*(\vec{q}) + N(\vec{P}) \rightarrow N(\vec{P}')$.

C.1.1 “Breit-brick wall”

The condition of zero energy transfer defines a class of reference frames known as “Breit frames”. One more condition is to be chosen to completely fix the frame; here a purely longitudinal momentum transfer is chosen.

scattering plane:



define lightlike vectors:

$$\begin{aligned} v^\mu &= [1, 0, \mathbf{0}_\perp] \\ v'^\mu &= [0, 1, \mathbf{0}_\perp] \end{aligned} \quad (\text{C.1})$$

$$\begin{aligned} P &= P^+ v + P^- v' + \mathbf{P}_\perp \\ P' &= P'^+ v + P'^- v' + \mathbf{P}'_\perp \end{aligned} \quad (\text{C.2})$$

In this frame q^μ is purely longitudinal, i.e.

$$\mathbf{P}_\perp = \mathbf{P}'_\perp = \mathbf{q}_\perp = 0 \quad (\text{C.3})$$

and

$$\left. \begin{aligned} P'^0 &= P^0 & (\text{Breit frame}) \\ P'^3 &= -P^3 & (\text{choice of frame}) \end{aligned} \right\} \implies q^+ = P'^+ - P^+ = -\sqrt{2} P^3 \neq 0 \quad (\text{C.4})$$

- The LC components of the involved external vectors are

$$\begin{aligned} P^\mu &= \left[\frac{Q}{\sqrt{2}}, 0, \mathbf{0}_\perp \right], & P'^\mu &= \left[0, \frac{Q}{\sqrt{2}}, \mathbf{0}_\perp \right], \\ q^\mu &= P'^\mu - P^\mu = \left[-\frac{Q}{\sqrt{2}}, \frac{Q}{\sqrt{2}}, \mathbf{0}_\perp \right]. \end{aligned} \quad (\text{C.5})$$

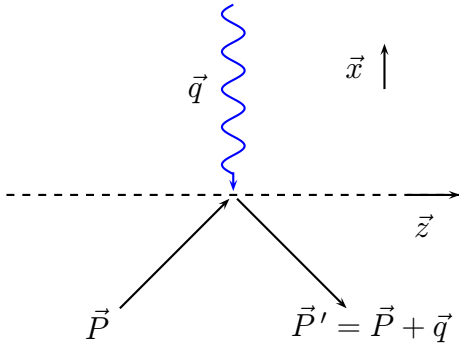
- Parton momenta in the “Breit-brick wall” frame read

$$p_i^\mu = \left[x_i P^+, \frac{p_i^2 + \mathbf{p}_{\perp i}^2}{2 x_i P^+}, \mathbf{p}_{\perp i} \right], \quad p_i'^\mu = \left[x_i' P^+, \frac{p_i'^2 + \mathbf{p}'_{\perp i}{}^2}{2 x_i' P^+}, \mathbf{p}'_{\perp i} \right]. \quad (\text{C.6})$$

C.1.2 “Breit-symmetric”

For the evaluation of overlap contributions a Breit frame combined with a symmetric choice of the z -direction leading to a purely transverse momentum transfer is more suitable.

scattering plane:



define lightlike vectors:

$$\begin{aligned} v^\mu &= [1, 0, \mathbf{0}_\perp] \\ v'^\mu &= [0, 1, \mathbf{0}_\perp] \end{aligned} \quad (\text{C.7})$$

$$\begin{aligned} P &= P^+ v + P^- v' + \mathbf{P}_\perp \\ P' &= P'^+ v + P'^- v' + \mathbf{P}'_\perp \end{aligned} \quad (\text{C.8})$$

In this frame the *plus*-component of the momentum of the incoming proton is not changed in the process, i.e. q^μ is purely transverse

$$\left. \begin{aligned} P'^0 &= P^0 \quad (\text{Breit frame}) \\ P'^3 &= P^3 \quad (\text{choice of frame}) \end{aligned} \right\} \implies q^+ = P'^+ - P^+ = 0 \quad (\text{C.9})$$

and for the transverse components we have

$$\mathbf{P}_\perp = -\mathbf{P}'_\perp = -\frac{\mathbf{q}_\perp}{2}. \quad (\text{C.10})$$

- The LC components of the involved external vectors are

$$\begin{aligned} P^\mu &= \left[P^+, \frac{M^2 + \mathbf{q}_\perp^2/4}{2P^+}, -\frac{\mathbf{q}_\perp}{2} \right], & P'^\mu &= \left[P^+, \frac{M^2 + \mathbf{q}_\perp^2/4}{2P^+}, \frac{\mathbf{q}_\perp}{2} \right], \\ q^\mu &= P'^\mu - P^\mu = [0, 0, \mathbf{q}_\perp]. \end{aligned} \quad (\text{C.11})$$

- Parton momenta in the “Breit-symmetric” frame read

$$p_i^\mu = \left[x_i P^+, \frac{p_i^2 + \mathbf{p}_{\perp i}^2}{2x_i P^+}, \mathbf{p}_{\perp i} \right], \quad p_i'^\mu = \left[x_i' P^+, \frac{p_i'^2 + \mathbf{p}'_{\perp i}{}^2}{2x_i' P^+}, \mathbf{p}'_{\perp i} \right]. \quad (\text{C.12})$$

- The spectator condition for the Feynman (soft overlap) contribution in the “Breit-symmetric” frame takes the form

$$p'_i = p_i \quad \text{for } i \neq j \quad \implies \quad x'_i = x_i; \quad \mathbf{p}'_{\perp i} = \mathbf{p}_{\perp i} \quad (\text{C.13})$$

and for the active quark one finds

$$p'_j = p_j + q \quad \implies \quad x'_j = x_j; \quad \mathbf{p}'_{\perp j} = \mathbf{p}_{\perp j} + \mathbf{q}_\perp. \quad (\text{C.14})$$

Those relations hold exactly without any approximations.

C.1.3 “hadron-in” frame

Utilising the transformation (2.9) one can obtain a frame in which the incoming nucleon has no transverse momentum and we can most easily identify the arguments of its LC wave function, but in which q^μ still has a vanishing *plus*-component and the LC fractions x and x' are the same (quantities in this frame are denoted with a “tilde”).

With the choice $\mathbf{b}_\perp = -\mathbf{q}_\perp/2$ and $b^+ = P^+$ the transformation (2.9) leads to

$$\begin{aligned} P^\mu &\longrightarrow \tilde{P}^\mu = \left[P^+, \frac{M^2}{2P^+}, \mathbf{0}_\perp \right] \\ p_i^\mu &\longrightarrow \tilde{p}_i^\mu = \left[x_i P^+, \frac{p_i^2 + (\mathbf{p}_{\perp i} + x_i \mathbf{q}_\perp/2)^2}{2x_i P^+}, \underbrace{\mathbf{p}_{\perp i} + x_i \mathbf{q}_\perp/2}_{= \tilde{\mathbf{p}}_{\perp i}} \right] \end{aligned} \quad (\text{C.15})$$

The arguments of the incoming proton LC wave function are $\Psi^{in}(x_i, \tilde{\mathbf{p}}_{\perp i})$.

C.1.4 “hadron-out” frame

Similarly, a frame where the outgoing nucleon has no transverse momentum serves to identify the kinematical arguments of its LCWF (quantities are denote with a “hat”).

With the choice $\mathbf{b}_\perp = \mathbf{q}_\perp/2$ and $b^+ = P^+$ the transformation (2.9) leads to

$$\begin{aligned} P'^\mu &\longrightarrow \hat{P}'^\mu = \left[P^+, \frac{M^2}{2P^+}, \mathbf{0}_\perp \right] \\ p_i'^\mu &\longrightarrow \hat{p}_i'^\mu = \left[x_i' P^+, \frac{p_i'^2 + (\mathbf{p}'_{\perp i} - x_i' \mathbf{q}_\perp/2)^2}{2x_i' P^+}, \underbrace{\mathbf{p}'_{\perp i} - x_i' \mathbf{q}_\perp/2}_{= \hat{\mathbf{p}}'_{\perp i}} \right] \end{aligned} \quad (\text{C.16})$$

The arguments of the outgoing proton LC wave function are $\Psi^{out}(x_i', \hat{\mathbf{p}}'_{\perp i})$.

C.1.5 arguments of Ψ^{out} in terms of “hadron-in” quantities

- momentum fractions:

Expressing the arguments of the LC wave function of the outgoing nucleon in terms of “hadron-in” frame quantities thereby using the relations for the spectator partons (C.13) and for the active parton (C.14) leads to

$$\boxed{x_i = \tilde{x}_i = \hat{x}_i = x_i' = \tilde{x}_i' = \hat{x}_i'} \quad (\text{C.17})$$

the fractions are neither changed by the process nor by the transformation (2.9); that’s just how the frames were chosen!

• transverse parton momenta:

For the transverse parton momenta in the outgoing nucleon expressed in terms of “hadron-in” frame quantities one finds (the “primes” on the fractions are now left out)

$$\begin{aligned}
 \hat{\mathbf{p}}'_{\perp i} &\stackrel{\text{(C.16)}}{=} \mathbf{p}'_{\perp i} - x_i \frac{\mathbf{q}_{\perp}}{2} & \text{(C.18)} \\
 \left\{ \begin{array}{ll} \text{(C.13)} & \mathbf{p}_{\perp i} - x_i \frac{\mathbf{q}_{\perp}}{2} & \text{(C.15)} & \tilde{\mathbf{p}}_{\perp i} - x_i \mathbf{q}_{\perp} & i \neq j \\ \text{(C.14)} & \mathbf{p}_{\perp j} + \mathbf{q}_{\perp} - x_j \frac{\mathbf{q}_{\perp}}{2} & \text{(C.15)} & \tilde{\mathbf{p}}_{\perp j} + (1 - x_j) \mathbf{q}_{\perp} & \text{active} \end{array} \right.
 \end{aligned}$$

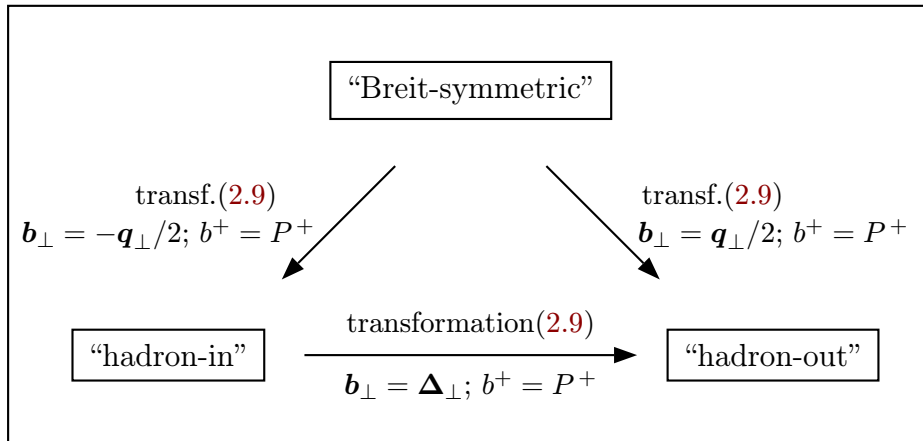
To obtain the above relation one has to

- identify the transverse momenta of the partons in the outgoing nucleon in the “hadron-out” frame to be $\hat{\mathbf{p}}'_{\perp i}$
- express them in terms of “Breit-symmetric” quantities $\mathbf{p}'_{\perp i}$ by (C.16)
- use relations for spectator(C.13)/active parton(s)(C.14) to relate them with $\mathbf{p}_{\perp i}$ and $\mathbf{p}_{\perp j}$, respectively
- and finally, express the results in terms of the transverse parton momenta of the incoming nucleon in the “hadron-in” frame $\tilde{\mathbf{p}}_{\perp i}$ and $\tilde{\mathbf{p}}_{\perp j}$ (C.15).

The above relations are exact; no approximations where made, i.e. the ratios $M^2/(-t)$ and $\mathbf{p}_{\perp}^2/(-t)$, or $p_i^2/(-t)$ are not neglected !

C.1.6 scheme of different reference frames

The “in/hadron-out” frames are related to the “Breit-symmetric” frame by *transverse boosts* (2.9) which leave the LC *plus*-components unchanged. The following scheme may help to visualise the relations between the different coordinate systems:



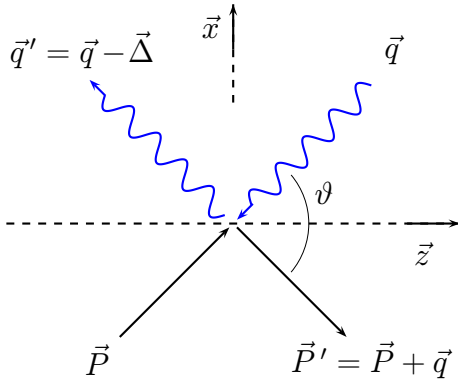
C.2 RCS, different reference frames

Real Compton scattering (RCS) on a nucleon will be considered, i.e., the process $\gamma(\vec{q}) + N(\vec{P}) \rightarrow \gamma(\vec{q}') + N(\vec{P}')$.

C.2.1 “CMS-symmetric”

A centre of mass system (CMS) with the choice of the z -direction as the symmetry axis of the process is a convenient frame for the description of RCS.

scattering plane:



define lightlike vectors:

$$\begin{aligned} v^\mu &= [1, 0, \mathbf{0}_\perp] \\ v'^\mu &= [0, 1, \mathbf{0}_\perp] \end{aligned} \quad (\text{C.19})$$

$$\begin{aligned} P &= P^+ v + P^- v' + \mathbf{P}_\perp \\ P' &= P'^+ v + P'^- v' + \mathbf{P}'_\perp \end{aligned} \quad (\text{C.20})$$

In this frame the LC *plus*-component of the momentum of the incoming nucleon is not changed in the process

$$\left. \begin{aligned} P'^0 &= P^0 \quad (\text{elastic scattering}) \\ P'^3 &= P^3 \quad (\text{choice of frame}) \end{aligned} \right\} \implies \Delta^+ = P'^+ - P^+ = 0 \quad (\text{C.21})$$

and for the transverse components we have

$$\mathbf{P}_\perp = -\mathbf{P}'_\perp = -\frac{\Delta_\perp}{2} \quad (\text{C.22})$$

- The LC components of the involved external vectors are

$$\begin{aligned} P^\mu &= \left[P^+, \frac{M^2 + \Delta_\perp^2/4}{2P^+}, -\frac{\Delta_\perp}{2} \right] & P'^\mu &= \left[P^+, \frac{M^2 + \Delta_\perp^2/4}{2P^+}, \frac{\Delta_\perp}{2} \right] \\ q^\mu &= \left[q^+, \frac{\Delta_\perp^2/4}{2q^+}, \frac{\Delta_\perp}{2} \right] & q'^\mu &= \left[q^+, \frac{\Delta_\perp^2/4}{2q^+}, -\frac{\Delta_\perp}{2} \right] \\ \Delta^\mu &= P'^\mu - P^\mu = q^\mu - q'^\mu = [0, 0, \Delta_\perp]. \end{aligned} \quad (\text{C.23})$$

with $q^+ = (W/\sqrt{2}) - P^+$ and $W^2 = (P + q)^2$; the explicit form of q^+ is ugly, fortunately, it is not needed !

- Parton momenta in the “CMS-symmetric” are

$$p_i^\mu = \left[x_i P^+, \frac{p_i^2 + \mathbf{p}_{\perp i}^2}{2x_i P^+}, \mathbf{p}_{\perp i} \right] \quad p_i'^\mu = \left[x_i' P^+, \frac{p_i'^2 + \mathbf{p}_{\perp i}'^2}{2x_i' P^+}, \mathbf{p}_{\perp i}' \right]. \quad (\text{C.24})$$

Note: $(\mathbf{p}_{\perp i})_y$ are small; but $(\mathbf{p}_{\perp i})_x$ are close to $x_i|\Delta_{\perp}|$.

- The spectator condition for the Feynman (overlap) contribution in the “CMS-symmetric” frame reads

$$p'_i = p_i \quad \text{for } i \neq j \quad \implies \quad x'_i = x_i; \quad \mathbf{p}'_{\perp i} = \mathbf{p}_{\perp i} \quad (\text{C.25})$$

and for the active parton we find

$$p'_j = p_j + \Delta \quad \implies \quad x'_j = x_j; \quad \mathbf{p}'_{\perp j} = \mathbf{p}_{\perp j} + \Delta_{\perp} \quad (\text{C.26})$$

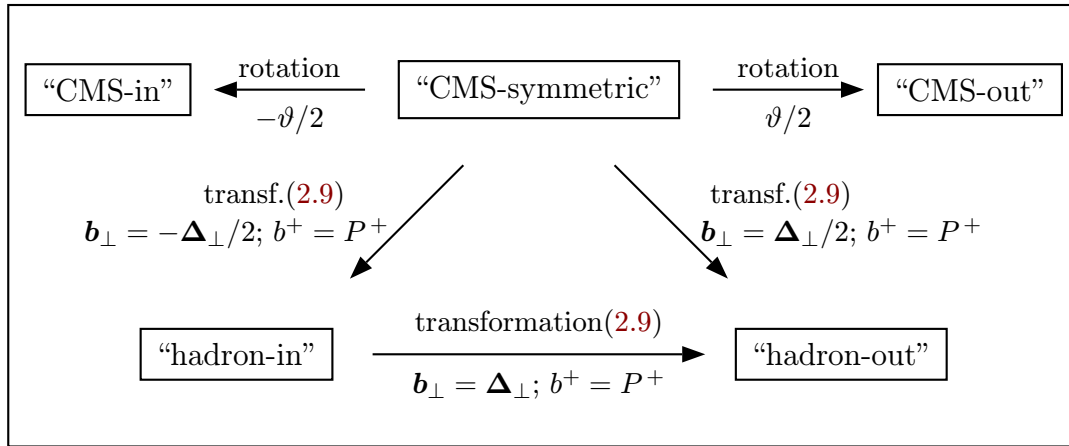
Those relations hold exactly; no approximations are made yet.

C.2.2 scheme of different reference frames

By a rotation about $-\vartheta/2$ ($\vartheta/2$) in the scattering plane the “CMS-symmetric” frame can be transformed in a CMS-frame where \vec{P} (\vec{P}') has no transverse components. Those rotations change the fractions x , x' and, obviously, the transverse momenta of the partons.

Applying *transverse boosts* (2.9) instead also results in frames where \vec{P} (\vec{P}') has no transverse components, but the LC *plus*-components are left unchanged. In lack of better names, we call the resulting frames “hadron-in/out” systems.

The following scheme may help to visualise the relations between the different coordinate systems:



C.2.3 “hadron-in frame”

Utilising the transformation (2.9) one can obtain a frame where the incoming proton has no transverse momentum (quantities in this frame are denoted with a “tilde”). This is a convenient frame to read off the arguments of the light-cone wave function of the incoming proton, i.e., $\Psi^{in}(\tilde{x}_i, \vec{\tilde{k}}_{i\perp})$.

- Starting from the “CMS-symmetric” we get to a (non CMS) hadron-in frame with the help of the transformation (2.9). Δ^μ still has a vanishing LC *plus*-component and the LC fractions x and x' have the same values as in the CMS-symmetric.

With the choice $\mathbf{b}_\perp = -\mathbf{\Delta}_\perp/2$ and $b^+ = P^+$ the transformation (2.9) leads to

$$P^\mu = \left[P^+, \frac{M^2 + \mathbf{\Delta}_\perp^2/4}{2P^+}, -\frac{\mathbf{\Delta}_\perp}{2} \right] \longrightarrow \tilde{P}^\mu = \left[P^+, \frac{M^2}{2P^+}, \vec{0}_\perp \right] \quad (\text{C.27})$$

$$P'^\mu = \left[P^+, \frac{M^2 + \mathbf{\Delta}_\perp^2/4}{2P^+}, \frac{\mathbf{\Delta}_\perp}{2} \right] \longrightarrow \tilde{P}'^\mu = \left[P^+, \frac{M^2 + \mathbf{\Delta}_\perp^2}{2P^+}, \mathbf{\Delta}_\perp \right] \quad (\text{C.28})$$

and

$$\Delta^\mu = [0, 0, \mathbf{\Delta}_\perp] \longrightarrow \tilde{\Delta}^\mu = \left[0, -\frac{\mathbf{\Delta}_\perp^2}{2P^+}, \mathbf{\Delta}_\perp \right]. \quad (\text{C.29})$$

- For the partons inside the incoming nucleon one finds

$$p_i^\mu = \left[x_i P^+, \frac{p_i^2 + \mathbf{p}_{\perp i}^2}{2x_i P^+}, \mathbf{p}_{\perp i} \right] \longrightarrow$$

$$\tilde{p}_i^\mu = \left[x_i P^+, \frac{p_i^2 + (\mathbf{p}_{\perp i} + x_i \mathbf{\Delta}_\perp/2)^2}{2x_i P^+}, \underbrace{\mathbf{p}_{\perp i} + x_i \mathbf{\Delta}_\perp/2}_{= \tilde{\mathbf{p}}_{\perp i}} \right] \quad (\text{C.30})$$

In the “hadron-in” frame $\tilde{\mathbf{p}}_{\perp i} = \mathbf{p}_{\perp i} + x_i \mathbf{\Delta}_\perp/2$ is small compared to $x_i P^+$.

- The parton momenta in the outgoing nucleon are

$$p_i'^\mu = \left[x_i' P^+, \frac{p_i'^2 + \mathbf{p}_{\perp i}'^2}{2x_i' P^+}, \mathbf{p}_{\perp i}' \right] \longrightarrow$$

$$\tilde{p}_i'^\mu = \left[x_i' P^+, \frac{p_i'^2 + (\mathbf{p}_{\perp i}' + x_i' \mathbf{\Delta}_\perp/2)^2}{2x_i' P^+}, \mathbf{p}_{\perp i}' + x_i' \mathbf{\Delta}_\perp/2 \right]. \quad (\text{C.31})$$

The transverse part of the momenta of the partons in the outgoing nucleon, $\tilde{\mathbf{p}}_{\perp i}'$ are not small, but close to $x_i \mathbf{\Delta}_\perp$!

C.2.4 “hadron-out” frame

A frame where the outgoing nucleon has no transverse momentum (quantities in this frame are denoted with a “hat”) is convenient to read off the arguments of

the LC wave function of the outgoing nucleon, i.e., $\Psi^{out}(\hat{x}'_i, \hat{\mathbf{p}}'_{\perp i})$.

- With the choice $\mathbf{b}_{\perp} = \mathbf{\Delta}_{\perp}/2$ and $b^+ = P^+$ one obtains

$$P'^{\mu} = \left[P^+, \frac{M^2 + \mathbf{\Delta}_{\perp}^2/4}{2P^+}, \frac{\mathbf{\Delta}_{\perp}}{2} \right] \longrightarrow \hat{P}'^{\mu} = \left[P^+, \frac{M^2}{2P^+}, \vec{0}_{\perp} \right] \quad (\text{C.32})$$

and

$$\Delta^{\mu} = [0, 0, \mathbf{\Delta}_{\perp}] \longrightarrow \hat{\Delta}^{\mu} = \left[0, \frac{\mathbf{\Delta}_{\perp}^2}{2P^+}, \mathbf{\Delta}_{\perp} \right]. \quad (\text{C.33})$$

- For the partons in the outgoing nucleon one finds

$$\begin{aligned} p_i'^{\mu} &= \left[x'_i P^+, \frac{p_i'^2 + \mathbf{p}_{\perp i}'^2}{2x'_i P^+}, \mathbf{p}'_{\perp i} \right] \longrightarrow \\ \hat{p}_i'^{\mu} &= \left[x'_i P^+, \frac{p_i'^2 + (\mathbf{p}'_{\perp i} - x'_i \mathbf{\Delta}_{\perp}/2)^2}{2x'_i P^+}, \underbrace{\mathbf{p}'_{\perp i} - x'_i \mathbf{\Delta}_{\perp}/2}_{= \hat{\mathbf{k}}'_{\perp i}} \right] \end{aligned} \quad (\text{C.34})$$

We can read off the arguments of the LC wave function of the outgoing nucleon as $\Psi^{out}(\hat{x}'_i, \hat{\mathbf{k}}'_{\perp i})$.

C.2.5 arguments of Ψ^{out} in terms of “hadron-in” quantities

- momentum fractions:

Expressing the arguments of the LC wave function of the outgoing nucleon in terms of “hadron-in” frame quantities thereby using the relations for the spectator partons (C.25) and for the active parton (C.26) leads to

$$\boxed{x_i = \tilde{x}_i = \hat{x}_i = x'_i = \tilde{x}'_i = \hat{x}'_i} \quad (\text{C.35})$$

the fractions are neither changed by the process nor by the transformation (2.9); that’s just how the frames were chosen!

- transverse parton momenta:

For the transverse parton momenta in the outgoing nucleon expressed in terms of “hadron-in” frame quantities we find (the “primes” on the fractions are now left out)

$$\boxed{\begin{aligned} \hat{\mathbf{p}}'_{\perp i} &\stackrel{(\text{C.34})}{=} \mathbf{p}'_{\perp i} - x_i \frac{\mathbf{\Delta}_{\perp}}{2} & (\text{C.36}) \\ \left\{ \begin{array}{ll} \stackrel{(\text{C.25})}{=} \mathbf{p}_{\perp i} - x_i \frac{\mathbf{\Delta}_{\perp}}{2} & \stackrel{(\text{C.30})}{=} \tilde{\mathbf{p}}_{\perp i} - x_i \mathbf{\Delta}_{\perp} & i \neq j \\ \stackrel{(\text{C.26})}{=} \mathbf{p}_{\perp j} + \mathbf{q}_{\perp} - x_j \frac{\mathbf{\Delta}_{\perp}}{2} & \stackrel{(\text{C.30})}{=} \tilde{\mathbf{p}}_{\perp j} + (1 - x_j) \mathbf{\Delta}_{\perp} & \text{active} \end{array} \right. \end{aligned}}$$

To obtain the above relation one has to

- identify the transverse momenta of the partons in the outgoing nucleon in the “hadron-out” frame to be $\hat{\mathbf{p}}_{\perp i}'$;
- express them in terms of “CMS-symmetric” quantities $\mathbf{p}'_{\perp i}$;
- use relations for spectator(C.25)/active parton(s)(C.26) to relate them with $\mathbf{p}_{\perp i}$ and $\vec{p}_{j\perp}$, respectively;
- and finally, express the results in terms of the transverse parton momenta of the incoming nucleon in the “hadron-in” frame $\tilde{\mathbf{p}}_{\perp i}$ and $\tilde{\mathbf{p}}_{\perp j}$.

The above relations are exact; no approximations were made, i.e. the ratios $M^2/(-t)$ and $\mathbf{p}_{\perp}^2/(-t)$, or $p_i^2/(-t)$ are not neglected !

C.2.6 “CMS-in”

Starting from the “CMS-symmetric” frame we get by a simple rotation of $\vartheta/2$ to a CMS system, where the incoming nucleon has no transverse momentum. For convenience we switch to the notation $a^\mu = (a^0, a^1, a^2, a^3)$.

$$\begin{aligned} P^\mu &= (P^0, |\vec{p}| \sin(\vartheta/2), 0, |\vec{p}| \cos(\vartheta/2)) \\ P'^\mu &= (P^0, -|\vec{p}| \sin(\vartheta/2), 0, |\vec{p}| \cos(\vartheta/2)) \end{aligned} \quad (\text{C.37})$$

The rotation in the scattering plane ($x - z$ plane) is done with the help of the matrix

$$\begin{pmatrix} \cos(\vartheta/2) & \sin(\vartheta/2) \\ -\sin(\vartheta/2) & \cos(\vartheta/2) \end{pmatrix} \quad (\text{C.38})$$

leading to the transformations

$$P^\mu \longrightarrow P^{rot,\mu} = (P^0, 0, 0, |\vec{p}|) \quad (\text{C.39})$$

$$\begin{aligned} P'^\mu &\longrightarrow \\ P'^{rot,\mu} &= (P^0, -|\vec{p}| 2 \sin(\vartheta/2) \cos(\vartheta/2), 0, |\vec{p}| (\cos^2(\vartheta/2) - \sin^2(\vartheta/2))) \\ &= (P^0, -|\vec{p}| \sin \vartheta, 0, |\vec{p}| \cos \vartheta) \end{aligned} \quad (\text{C.40})$$

and

$$\begin{aligned} \Delta^\mu &= (0, -|\mathbf{\Delta}_\perp|, 0, 0) = (0, -|\vec{p}| 2 \sin(\vartheta/2), 0, 0) \\ \longrightarrow \Delta^{rot,\mu} &= (0, -|\mathbf{\Delta}_\perp| \cos(\vartheta/2), 0, -|\mathbf{\Delta}_\perp| \sin(\vartheta/2)) \\ &= (0, -|\vec{p}| \sin \vartheta, 0, -|\vec{p}| (1 - \cos \vartheta)) \end{aligned} \quad (\text{C.41})$$

C.2.7 “CMS-out”

Starting from the “CMS-symmetric” frame with the a rotation by $-\vartheta/2$ one gets to a CMS system, where the outgoing nucleon has no transverse momentum.

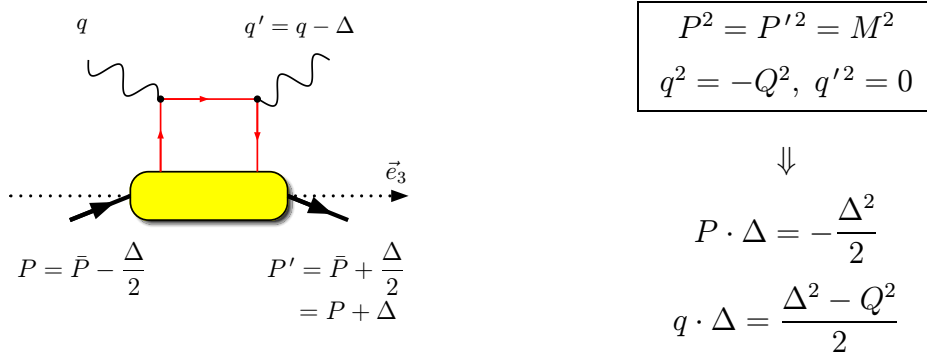
C.3 DVCS, different reference frames

Now we consider deeply virtual Compton scattering on a nucleon, i.e., the process $\gamma^*(\vec{q}) + p(\vec{p}) \rightarrow \gamma(\vec{q}') + p(\vec{P}')$, where $-q^2 = Q^2$ is large.

Unfortunately, there is no useful reference frame where the momentum transfer does not have a *plus* component, i.e. where $\Delta^+ = 0$ (in such a frame the nucleons would be slow).

C.3.1 “average” frame

Close to Ji’s conventions [172, 190] we chose a frame where the longitudinal direction is defined by the nucleon average momentum:



The nucleon average momentum is defined by

$$\bar{P} = (P + P')/2 \quad \text{such that} \quad \begin{cases} P = \bar{P} - \Delta/2 \\ \text{and} \\ P' = \bar{P} + \Delta/2 \end{cases} \quad (\text{C.42})$$

- the Sudakov decomposition of the external vectors reads (with \bar{P} and q chosen to be collinear)

$$\bar{P}^\mu = \left[\bar{P}^+, \frac{\bar{M}^2}{2\bar{P}^+}, \vec{0}_\perp \right] \quad (\text{C.43})$$

$$q^\mu = \left[-x_N \bar{P}^+, \frac{Q^2}{2x_N \bar{P}^+}, \vec{0}_\perp \right] \quad \boxed{x_N = -\frac{q^+}{\bar{P}^+}} \quad (\text{C.44})$$

$$\Delta^\mu = \left[-2\xi \bar{P}^+, \frac{\xi \bar{M}^2}{\bar{P}^+}, \Delta_\perp \right] \quad \boxed{\xi = -\frac{\Delta^+}{2\bar{P}^+}} \quad (\text{C.45})$$

with

$$\bar{M}^2 = \bar{P}^2 = (P + \Delta/2)^2 = M^2 + P \cdot \Delta + \Delta^2/4 = M^2 - \Delta^2/4 \quad (\text{C.46})$$

and

$$\bar{P} \cdot q = \frac{Q^2}{2x_N} - \frac{x_N \bar{M}^2}{2} \implies x_N = \left(-\bar{P} \cdot q + \sqrt{(\bar{P} \cdot q)^2 + Q^2 \bar{M}^2} \right) / \bar{M}^2 \quad (\text{C.47})$$

where the limiting behaviour of x_N is

$$\lim_{\bar{M}^2 \rightarrow 0} x_N = \frac{Q^2}{2\bar{P} \cdot q} \quad (\text{de l'Hospital}).$$

The component Δ^- is determined by

$$\begin{aligned} \bar{P} \cdot \Delta &= (P' + P)/2 \cdot (P' - P) = (P'^2 - P^2)/2 = 0 \\ &= (P + \Delta/2) \cdot \Delta = P \cdot \Delta + \Delta^2/2 \\ &= \bar{P}^+ \Delta^- + \frac{\bar{M}^2}{2\bar{P}^+} \Delta^+ \\ &\implies \Delta^- = -\frac{\bar{M}^2}{2(\bar{P}^+)^2} \Delta^+ = \frac{\xi \bar{M}^2}{\bar{P}^+}. \end{aligned} \quad (\text{C.48})$$

The Mandelstam variable t reads

$$t = \Delta^2 = -4\xi^2 \bar{M}^2 - \Delta_{\perp}^2, \quad (\text{C.49})$$

from which one obtains (by insertion of Eq. (C.49) in Eq. (C.46))

$$\bar{M}^2 (1 - \xi^2) = M^2 + \Delta_{\perp}^2/4 \quad (\text{C.50})$$

or (insert Eq. (C.46) in Eq. (C.49))

$$\Delta^2 = \frac{-4\xi^2 M^2 - \Delta_{\perp}^2}{1 - \xi^2}. \quad (\text{C.51})$$

The momentum of the real photon is

$$q'^{\mu} = (q - \Delta)^{\mu} = \left[(2\xi - x_N) \bar{P}^+, \frac{Q^2 - 2x_N \xi \bar{M}^2}{2x_N \bar{P}^+}, -\Delta_{\perp} \right] \quad (\text{C.52})$$

- for later use we also show the explicit form of the incoming and outgoing nucleon momenta

$$\begin{aligned} P^{\mu} &= (\bar{p} - \Delta/2)^{\mu} = \left[(1 + \xi) \bar{P}^+, \frac{M^2 + \Delta_{\perp}^2/4}{2(1 + \xi) \bar{P}^+}, -\Delta_{\perp}/2 \right] \\ P'^{\mu} &= (\bar{p} + \Delta/2)^{\mu} = \left[(1 - \xi) \bar{P}^+, \frac{M^2 + \Delta_{\perp}^2/4}{2(1 - \xi) \bar{P}^+}, \Delta_{\perp}/2 \right] \end{aligned} \quad (\text{C.53})$$

Note that the minus components can also be written as

$$P^- = \frac{\bar{M}^2 (1 - \xi)}{2\bar{P}^+} \quad P'^- = \frac{\bar{M}^2 (1 + \xi)}{2\bar{P}^+} \quad (\text{C.54})$$

• parton momenta

It is useful to distinguish three different kinematical regions depending on the value of an external momentum fraction variable \bar{x} , which finally will be identified as the momentum fraction of the active parton. The partonic interpretation in the three regions is

in the DGLAP region $\xi < \bar{x} < 1$:

a *quark* is emitted, takes the momentum transfer Δ , and is finally reabsorbed by the hadron.

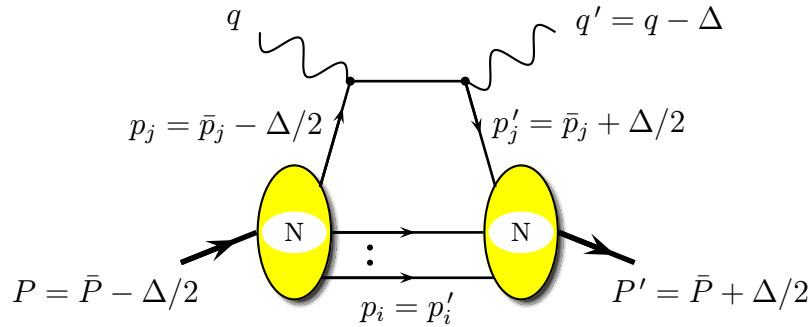
in the ERBL region $-\xi < \bar{x} < \xi$:

a *quark-antiquark pair* is emitted, which takes the momentum transfer Δ ; the rest of the nucleon (spectator system) forms the final hadron .

in the DGLAP region $-1 < \bar{x} < -\xi$

an *antiquark* is emitted, takes the momentum transfer Δ , and is finally reabsorbed by the hadron.

DGLAP regions: ($\xi < \bar{x} < 1$) and ($-1 < \bar{x} < -\xi$)



In order to achieve a formulation symmetric in incoming and outgoing quantities it is useful to define as auxiliary variables the averages of incoming and outgoing parton momenta in the average frame

$$\bar{p}_i = \frac{1}{2}(p_i + p'_i), \quad \bar{x}_i = \frac{\bar{p}_i^+}{\bar{P}^+}, \quad (\text{C.55})$$

which satisfy

$$\bar{P}^+ = \sum_{i=1}^N \bar{p}_i^+ = \sum_{i=1}^N \bar{x}_i \bar{P}^+; \quad \bar{\mathbf{P}}_{\perp} = \sum_{i=1}^N \bar{\mathbf{p}}_{\perp i} \stackrel{\text{average}}{=} \mathbf{0}_{\perp} \quad (\text{C.56})$$

Note: the auxiliary fractions \bar{x}_i correspond to Ji's definition x_{i,J_i} !

The auxiliary \bar{p}_i are identical to the momenta of the spectator partons

$$p_i = p'_i = \bar{p}_i \quad \text{for } i \neq j \quad \implies \quad x_i = x'_i = \bar{x}_i; \quad \mathbf{p}_{\perp i} = \mathbf{p}'_{\perp i} = \bar{\mathbf{p}}_{\perp i} \quad (\text{C.57})$$

and are related to the momentum of the active parton by simple relations

$$\begin{aligned} & p_j = \bar{p}_j - \Delta/2 \quad \text{and} \quad p'_j = \bar{p}_j + \Delta/2 \\ \implies & x_j = \bar{x}_j + \xi \quad \text{and} \quad x'_j = \bar{x}_j - \xi \\ & \mathbf{p}_{\perp j} = \bar{\mathbf{p}}_{\perp j} - \mathbf{\Delta}_{\perp}/2 \quad \text{and} \quad \mathbf{p}'_{\perp j} = \bar{\mathbf{k}}_{\perp j} + \mathbf{\Delta}_{\perp}/2 \end{aligned} \quad (\text{C.58})$$

Note: the fractions x_i are fractional momenta with respect to the *plus* component of the average nucleon momentum \bar{P} !

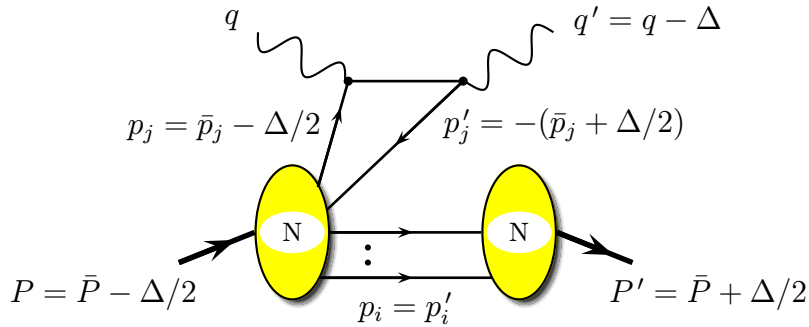
For the calculation of an overlap integral the momentum fractions of the partons with respect to their parent hadron momenta are needed, which are given for the incoming partons as

$$\frac{p_i^+}{P^+} = \frac{\bar{x}_i}{1 + \xi} \quad \text{for } i \neq j; \quad \frac{p_j^+}{P^+} = \frac{\bar{x}_j + \xi}{1 + \xi} \quad \text{active} \quad (\text{C.59})$$

and for the outgoing partons as

$$\frac{p_i'^+}{P'^+} = \frac{\bar{x}_i}{1 - \xi} \quad \text{for } i \neq j; \quad \frac{p_j'^+}{P'^+} = \frac{\bar{x}_j - \xi}{1 - \xi} \quad \text{active} \quad (\text{C.60})$$

ERBL region: $(-\xi < \bar{x} < \xi)$



We label the quark-antiquark pair with indices j for the quark and j' for the antiquark. For $i \neq j, j'$ we again use the auxiliary variables

$$\bar{p}_i = \frac{1}{2} (p_i + p'_i), \quad \bar{x}_i = \frac{\bar{p}_i^+}{P^+}, \quad (\text{C.61})$$

and for j, j' we introduce

$$\bar{p}_j = \frac{1}{2} (p_j - p_{j'}), \quad \bar{x}_j = \frac{\bar{p}_j^+}{P^+}, \quad (\text{C.62})$$

which is half the relative momentum (and momentum fraction) between the active quark and antiquark. It can as well be viewed as the average of p_j and the reverse of the momentum $p_{j'}$ (i.e., $-p_{j'}$), in complete analogy with the definitions (C.55). The auxiliary \bar{p}_i are identical to the momenta of the spectator partons

$$p_i = p'_i = \bar{p}_i \quad \text{for } i \neq j, j' \quad \implies \quad x_i = x'_i = \bar{x}_i; \quad \mathbf{p}_{\perp i} = \mathbf{p}'_{\perp i} = \bar{\mathbf{p}}_{\perp i} \quad (\text{C.63})$$

and are related to the momentum of the active parton by simple relations

$$\begin{aligned} \implies \quad & p_j = \bar{p}_j - \Delta/2 & \text{and} & \quad p_{j'} = -(\bar{p}_j + \Delta/2) \\ & x_j = \bar{x}_j + \xi & \text{and} & \quad x_{j'} = -(\bar{x}_j - \xi) \\ & \mathbf{p}_{\perp j} = \bar{\mathbf{p}}_{\perp j} - \mathbf{\Delta}_{\perp}/2 & \text{and} & \quad \mathbf{p}_{\perp j'} = -(\bar{\mathbf{p}}_{\perp j} + \mathbf{\Delta}_{\perp}/2). \end{aligned} \quad (\text{C.64})$$

Note: the fractions x_i are fractional momenta with respect to the *plus* component of the average nucleon momentum \bar{P} !

For the calculation of an overlap integral the momentum fractions of the partons with respect to their parent hadron momenta are needed, which are given for the incoming partons as

$$\begin{aligned} \frac{p_i^+}{P^+} &= \frac{\bar{x}_i}{1 + \xi} & \text{for } i \neq j, j'; \\ \frac{p_j^+}{P^+} &= \frac{\bar{x}_j + \xi}{1 + \xi}, & \frac{p_{j'}^+}{P^+} &= \frac{-(\bar{x}_j - \xi)}{1 + \xi} \quad \text{active} \end{aligned} \quad (\text{C.65})$$

and for the outgoing partons as

$$\frac{p_i'^+}{p'^+} = \frac{\bar{x}_i}{1 - \xi} \quad \text{for } i \neq j, j'. \quad (\text{C.66})$$

C.3.2 “hadron-in” frame

To identify the arguments of the LC wave function for the incoming nucleon we may use a transverse boost (2.9) with $\mathbf{b}_{\perp} = -\mathbf{\Delta}_{\perp}/2$ and $b^+ = (1 + \xi) \bar{P}^+$ to a frame where p has no transverse component (quantities in this frame are denoted with a “tilde”).

$$\begin{aligned} P^\mu &= \left[(1 + \xi) \bar{P}^+, \frac{M^2 + \mathbf{\Delta}_{\perp}^2/4}{2(1 + \xi)\bar{P}^+}, -\frac{\mathbf{\Delta}_{\perp}}{2} \right] \\ \longrightarrow \quad \tilde{P}^\mu &= \left[(1 + \xi) \bar{P}^+, \frac{M^2}{2(1 + \xi)\bar{P}^+}, \mathbf{0}_{\perp} \right] \end{aligned} \quad (\text{C.67})$$

and

$$\begin{aligned} \Delta^\mu &= \left[-2\xi \bar{P}^+, \frac{\xi \bar{M}^2}{\bar{P}^+}, \mathbf{\Delta}_{\perp} \right] \\ \longrightarrow \quad \tilde{\Delta}^\mu &= \left[-2\xi \bar{P}^+, -\frac{\Delta^2 + \mathbf{\Delta}_{\perp}^2/(1 + \xi)^2}{2\xi \bar{P}^+}, \frac{\mathbf{\Delta}_{\perp}}{1 + \xi} \right] \end{aligned} \quad (\text{C.68})$$

spectator partons

$$\begin{aligned} p_i^\mu &= \left[\bar{x}_i \bar{P}^+, \frac{p_i^2 + \mathbf{p}_{\perp i}^2}{2\bar{x}_i \bar{P}^+}, \mathbf{p}_{\perp i} \right] \\ \longrightarrow \quad \tilde{p}_i^\mu &= \left[\bar{x}_i \bar{P}^+, \frac{p_i^2 + \left(\mathbf{p}_{\perp i} + \frac{\bar{x}_i}{1 + \xi} \mathbf{\Delta}_{\perp}/2 \right)^2}{2\bar{x}_i \bar{P}^+}, \underbrace{\mathbf{p}_{\perp i} + \frac{\bar{x}_i}{1 + \xi} \mathbf{\Delta}_{\perp}/2}_{= \tilde{\mathbf{p}}_{\perp i}} \right] \end{aligned} \quad (\text{C.69})$$

active parton

$$p_j^\mu = \left[(\bar{x}_j + \xi) \bar{P}^+, \frac{p_j^2 + \mathbf{p}_{\perp j}^2}{2(\bar{x}_j + \xi) \bar{P}^+}, \mathbf{p}_{\perp j} \right] \quad (\text{C.70})$$

$$\longrightarrow \tilde{p}_j^\mu = \left[(\bar{x}_j + \xi) \bar{P}^+, \frac{p_j^2 + \left(\mathbf{p}_{\perp j} + \frac{\bar{x}_j + \xi}{1 + \xi} \Delta_{\perp} / 2 \right)^2}{2(\bar{x}_j + \xi) \bar{P}^+}, \underbrace{\mathbf{p}_{\perp j} + \frac{\bar{x}_j + \xi}{1 + \xi} \Delta_{\perp} / 2}_{= \tilde{\mathbf{p}}_{\perp j}} \right]$$

$$p_{j'}^\mu = \left[-(\bar{x}_j - \xi) \bar{P}^+, \frac{p_{j'}^2 + \mathbf{p}_{\perp j'}^2}{-2(\bar{x}_j - \xi) \bar{P}^+}, \mathbf{p}_{\perp j'} \right] \quad (\text{C.71})$$

$$\longrightarrow \tilde{p}_{j'}^\mu = \left[-(\bar{x}_j - \xi) \bar{P}^+, \frac{p_{j'}^2 + \left(\mathbf{p}_{\perp j'} - \frac{\bar{x}_j - \xi}{1 + \xi} \Delta_{\perp} / 2 \right)^2}{-2(\bar{x}_j - \xi) \bar{P}^+}, \underbrace{\mathbf{p}_{\perp j'} - \frac{\bar{x}_j - \xi}{1 + \xi} \Delta_{\perp} / 2}_{= \tilde{\mathbf{p}}_{\perp j'}} \right]$$

The arguments of the LCWF for the incoming nucleon become (DGLAP and ERBL, respectively)

$$\Psi^{in} \left(\tilde{x}_i = \frac{\bar{x}_i}{1 + \xi}, \tilde{\mathbf{k}}_{\perp i}; \tilde{x}_j = \frac{\bar{x}_j + \xi}{1 + \xi}, \tilde{\mathbf{p}}_{\perp j} \right)$$

$$\Psi^{in} \left(\tilde{x}_i = \frac{\bar{x}_i}{1 + \xi}, \tilde{\mathbf{p}}_{\perp i}; \tilde{x}_j = \frac{\bar{x}_j + \xi}{1 + \xi}, \tilde{\mathbf{p}}_{\perp j}; \tilde{x}_{j'} = \frac{-(\bar{x}_j - \xi)}{1 + \xi}, \tilde{\mathbf{p}}_{\perp j'} \right) \quad (\text{C.72})$$

C.3.3 “hadron-out” frame

To identify the arguments of the LC wave function for the outgoing nucleon we may use a boost with $\mathbf{b}_{\perp} = \Delta_{\perp} / 2$ and $b^+ = (1 - \xi) \bar{P}^+$ to a frame where P' has no transverse component (quantities in this frame are denoted with a “hat”).

$$P'^{\mu} = \left[(1 - \xi) \bar{P}^+, \frac{M^2 + \Delta_{\perp}^2 / 4}{2(1 - \xi) \bar{P}^+}, \frac{\Delta_{\perp}}{2} \right]$$

$$\longrightarrow \hat{P}'^{\mu} = \left[(1 - \xi) \bar{P}^+, \frac{M^2}{2(1 - \xi) \bar{P}^+}, \mathbf{0}_{\perp} \right] \quad (\text{C.73})$$

spectator partons

$$p_i'^{\mu} = \left[\bar{x}_i \bar{P}^+, \frac{p_i'^2 + \mathbf{p}_{\perp i}'^2}{2\bar{x}_i \bar{P}^+}, \mathbf{p}_{\perp i}' \right] \quad (\text{C.74})$$

$$\longrightarrow \hat{p}_i'^{\mu} = \left[\bar{x}_i \bar{P}^+, \frac{p_i'^2 + \left(\mathbf{p}_{\perp i}' - \frac{\bar{x}_i}{1 - \xi} \Delta_{\perp} / 2 \right)^2}{2\bar{x}_i \bar{P}^+}, \underbrace{\mathbf{p}_{\perp i}' - \frac{\bar{x}_i}{1 - \xi} \Delta_{\perp} / 2}_{= \hat{\mathbf{p}}_{\perp i}'} \right]$$

active parton

$$p_j'^{\mu} = \left[(\bar{x}_j - \xi) \bar{P}^+, \frac{p_j'^2 + \mathbf{p}'_{\perp j}{}^2}{2(\bar{x}_j + \xi) \bar{P}^+}, \mathbf{p}'_{\perp j} \right] \quad (\text{C.75})$$

$$\longrightarrow \hat{p}_j'^{\mu} = \left[(\bar{x}_j - \xi) \bar{P}^+, \frac{p_j'^2 + \left(\mathbf{p}'_{\perp j} + \frac{\bar{x}_j - \xi}{1 - \xi} \frac{\Delta_{\perp}}{2} \right)^2}{2(\bar{x}_j - \xi) \bar{P}^+}, \underbrace{\mathbf{p}'_{\perp j} - \frac{\bar{x}_j - \xi}{1 - \xi} \frac{\Delta_{\perp}}{2}}_{= \tilde{\mathbf{k}}_{j\perp}'} \right]$$

The arguments of the LC wave function for the outgoing nucleon are (DGLAP and ERBL, respectively)

$$\Psi^{out} \left(\hat{x}'_i = \frac{\bar{x}_i}{1 - \xi}, \hat{\mathbf{p}}'_{\perp i}; \hat{x}'_j = \frac{\bar{x}_j - \xi}{1 - \xi}, \hat{\mathbf{p}}'_{\perp j} \right)$$

$$\Psi^{out} \left(\hat{x}'_i = \frac{\bar{x}_i}{1 - \xi}, \hat{\mathbf{p}}'_{\perp i} \right) \quad (\text{C.76})$$

C.3.4 arguments of LCWFs in terms of auxiliary variables

DGLAP regions: ($\xi < \bar{x} < 1$) and ($-1 < \bar{x} < -\xi$)

LCWF arguments for the incoming hadron (i.e., the momenta of the partons belonging to the incoming hadron in the hadron-in frame) are related to the momenta in the average-frame by

$$\tilde{x}_i = \frac{\bar{x}_i}{1 + \xi}, \quad \tilde{\mathbf{p}}_{\perp i} = \bar{\mathbf{p}}_{\perp i} + \frac{\bar{x}_i}{1 + \xi} \frac{\Delta_{\perp}}{2} \quad \text{for } i \neq j,$$

$$\tilde{x}_j = \frac{\bar{x}_j + \xi}{1 + \xi}, \quad \tilde{\mathbf{p}}_{\perp j} = \bar{\mathbf{p}}_{\perp j} - \frac{1 - \bar{x}_j}{1 + \xi} \frac{\Delta_{\perp}}{2}. \quad (\text{C.77})$$

Likewise, the LCWF arguments for the outgoing hadron (i.e., the momenta of the partons belonging to the outgoing hadron in the hadron-out frame) are related to the momenta in the average-frame by

$$\hat{x}'_i = \frac{\bar{x}_i}{1 - \xi}, \quad \hat{\mathbf{p}}'_{\perp i} = \bar{\mathbf{p}}_{\perp i} - \frac{\bar{x}_i}{1 - \xi} \frac{\Delta_{\perp}}{2} \quad \text{for } i \neq j,$$

$$\hat{x}'_j = \frac{\bar{x}_j - \xi}{1 - \xi}, \quad \hat{\mathbf{p}}'_{\perp j} = \bar{\mathbf{p}}_{\perp j} + \frac{1 - \bar{x}_j}{1 - \xi} \frac{\Delta_{\perp}}{2}. \quad (\text{C.78})$$

ERBL region: ($-\xi < \bar{x} < \xi$)

LCWF arguments for the incoming hadron are related to the parton momenta in the average-frame by

$$\tilde{x}_i = \frac{\bar{x}_i}{1 + \xi}, \quad \tilde{\mathbf{p}}_{\perp i} = \bar{\mathbf{p}}_{\perp i} + \frac{\bar{x}_i}{1 + \xi} \frac{\Delta_{\perp}}{2} \quad \text{for } i \neq j, j',$$

$$\tilde{x}_j = \frac{\bar{x}_j + \xi}{1 + \xi}, \quad \tilde{\mathbf{p}}_{\perp j} = \bar{\mathbf{p}}_{\perp j} - \frac{1 - \bar{x}_j}{1 + \xi} \frac{\Delta_{\perp}}{2},$$

$$\tilde{x}_{j'} = -\frac{\bar{x}_j - \xi}{1 + \xi}, \quad \tilde{\mathbf{p}}_{\perp j'} = -\bar{\mathbf{p}}_{\perp j} - \frac{1 + \bar{x}_j}{1 + \xi} \frac{\Delta_{\perp}}{2}, \quad (\text{C.79})$$

and that the LCWF arguments for the outgoing hadron are given by

$$\hat{x}'_i = \frac{\bar{x}_i}{1-\xi}, \quad \hat{\mathbf{p}}'_{\perp i} = \bar{\mathbf{p}}_{\perp i} - \frac{\bar{x}_i}{1-\xi} \frac{\Delta_{\perp}}{2} \quad \text{for } i \neq j, j'. \quad (\text{C.80})$$

C.3.5 arguments of Ψ^{out} in terms of “hadron-in” quantities

spectator partons

use

$$X_i = \frac{\bar{x}_i}{1+\xi} \quad \Longrightarrow \quad \bar{x}_i = X_i(1+\xi) \quad (\text{C.81})$$

to obtain

$$X'_i = \frac{\bar{x}_i}{1-\xi} = \boxed{\frac{X_i(1+\xi)}{1-\xi}} \quad (\text{C.82})$$

for the transverse momentum

$$\begin{aligned} \hat{\mathbf{p}}'_{\perp i} &= \mathbf{p}'_{\perp i} - \frac{\bar{x}_i}{1-\xi} \frac{\Delta_{\perp}}{2} = \mathbf{p}_{\perp i} - \frac{\bar{x}_i}{1-\xi} \frac{\Delta_{\perp}}{2} = \tilde{\mathbf{p}}_{\perp i} - \frac{\bar{x}_i}{1+\xi} \frac{\Delta_{\perp}}{2} - \frac{\bar{x}_i}{1-\xi} \frac{\Delta_{\perp}}{2} \\ &= \tilde{\mathbf{p}}_{\perp i} - \frac{\Delta_{\perp}}{2} \left(X_i + X_i \frac{1+\xi}{1-\xi} \right) = \boxed{\tilde{\mathbf{p}}_{\perp i} - \frac{X_i}{1-\xi} \Delta_{\perp}} \end{aligned} \quad (\text{C.83})$$

active parton

use

$$X_j = \frac{\bar{x}_j + \xi}{1+\xi} \quad \Longrightarrow \quad \bar{x}_j = X_j(1+\xi) - \xi \quad (\text{C.84})$$

to obtain

$$X'_j = \frac{\bar{x}_j - \xi}{1-\xi} = \boxed{\frac{X_j(1+\xi) - 2\xi}{1-\xi}} \quad (\text{C.85})$$

for the transverse momentum

$$\begin{aligned} \hat{\mathbf{p}}'_{\perp j} &= \mathbf{p}'_{\perp j} - \frac{\bar{x}_j - \xi}{1-\xi} \frac{\Delta_{\perp}}{2} = \mathbf{p}_{\perp j} + \Delta_{\perp} - \frac{\bar{x}_j - \xi}{1-\xi} \frac{\Delta_{\perp}}{2} \\ &= \tilde{\mathbf{p}}_{\perp j} - \frac{\bar{x}_j + \xi}{1+\xi} \frac{\Delta_{\perp}}{2} + \Delta_{\perp} - \frac{\bar{x}_j - \xi}{1-\xi} \frac{\Delta_{\perp}}{2} \\ &= \tilde{\mathbf{p}}_{\perp j} + \frac{\Delta_{\perp}}{2} \left(2 - X_j - \frac{X_j(1+\xi) - 2\xi}{1-\xi} \right) = \boxed{\tilde{\mathbf{p}}_{\perp j} + \frac{1-X_j}{1-\xi} \Delta_{\perp}} \end{aligned} \quad (\text{C.86})$$

note: the transverse part of the momentum transfer in the “hadron-in” frame is given as (see Eq. (C.68))

$$\vec{\Delta}_{\perp} = \frac{\Delta_{\perp}}{1+\xi} \quad (\text{C.87})$$

C.3.6 “ γ^* -nucleon c.m.”-frame

Alternatively, one can chose the momentum of the incoming nucleon p and of the virtual photon q to be collinear.

This is not the “hadron-in” frame from above, since there the photon momentum \tilde{q}^μ has a non-vanishing transverse component.

$$\begin{aligned}
 P^\mu &= \left[P^+, \frac{M^2}{2P^+}, \vec{0}_\perp \right] \\
 \Delta^\mu &= \left[-\zeta P^+, \frac{\zeta M^2 + \Delta_\perp^2}{2P^+(1-\zeta)}, \Delta_\perp \right] \\
 q^\mu &= \left[-x_N P^+, \frac{Q^2}{2x_N P^+}, \vec{0}_\perp \right] \\
 P'^\mu &= P^\mu + \Delta^\mu = \left[(1-\zeta)P^+, \frac{M^2 + \Delta_\perp^2}{2P^+(1-\zeta)}, \Delta_\perp \right] \quad (C.88)
 \end{aligned}$$

Partons in the incoming nucleon have momenta

$$p_i^\mu = \left[X_i P^+, \frac{p_i^2 + \mathbf{p}_{\perp i}^2}{2X_i P^+}, \mathbf{p}_{\perp i} \right], \quad (C.89)$$

and partons in the outgoing nucleon

$$\begin{aligned}
 p_i'^\mu &= p_i^\mu \quad \text{for } i \neq j \\
 p_j'^\mu &= p_j^\mu + \Delta^\mu \\
 &= \left[(X_j - \zeta)P^+, \frac{p_j'^2 + (\mathbf{p}_{\perp j} + \Delta_\perp)^2}{2(X_j - \zeta)P^+}, \mathbf{p}_{\perp j} + \Delta_\perp \right] \quad \text{active (C.90)}
 \end{aligned}$$

a boost with $\vec{b} = \Delta_\perp$ and $b^+ = (1-\zeta)P^+$ leads to a frame, where the outgoing nucleon has no transverse momentum components

$$P'^\mu \longrightarrow \check{P}'^\mu = \left[(1-\zeta)P^+, \frac{M^2}{2(1-\zeta)P^+}, \vec{0}_\perp \right] \quad (C.91)$$

and

$$\begin{aligned}
 p_i' &\longrightarrow \check{p}_i' = \left[X_i P^+, \frac{p_i'^2 + (\mathbf{p}_{\perp i} - \frac{X_i}{1-\zeta} \Delta_\perp)^2}{2X_i P^+}, \mathbf{p}_{\perp i} - \frac{X_i}{1-\zeta} \Delta_\perp \right] \quad \text{for } i \neq j \\
 p_j' &\longrightarrow \check{p}_j' = \left[(X_j - \zeta)P^+, \frac{p_j'^2 + (\mathbf{p}_{\perp j} + \frac{1-X_j}{1-\zeta} \Delta_\perp)^2}{2(X_j - \zeta)P^+}, \mathbf{p}_{\perp j} + \frac{1-X_j}{1-\zeta} \Delta_\perp \right] \quad (C.92)
 \end{aligned}$$

such that the arguments for the outgoing nucleon wave function read (DGLAP region)

$$\Psi^{out} \left(\frac{X_i}{1-\zeta}, \mathbf{p}_{\perp i} - \frac{X_i}{1-\zeta} \Delta_\perp; \frac{X_j - \zeta}{1-\zeta}, \mathbf{p}_{\perp j} + \frac{1-X_j}{1-\zeta} \Delta_\perp \right) \quad (C.93)$$

C.3.7 relation to X and ζ variables

Using the variable (compare Radyushkin [176] Eq. (9.5) and Ji [190] Eq. (23)).

$$\zeta = \frac{2\xi}{1+\xi} \quad (\text{C.94})$$

we get

$$\begin{aligned} X'_i &= \frac{X_i}{1-\zeta} & \hat{\mathbf{p}}_{\perp i} &= \tilde{\mathbf{p}}_{\perp i} - \frac{X_i}{1-\zeta} \vec{\Delta}_{\perp} \\ X'_j &= \frac{X_j - \zeta}{1-\zeta} & \hat{\mathbf{p}}_{\perp j} &= \mathbf{p}_{\perp j} + \frac{1-X_j}{1-\zeta} \vec{\Delta}_{\perp} \end{aligned} \quad (\text{C.95})$$

D

List of Acronyms

A list of acronyms used throughout the text:

CMS	centre of mass system
DA	distribution amplitude
DIS	deep inelastic scattering
DVCS	deeply virtual Compton scattering
FF	form factor
GPD	generalised parton distribution
HSA	hard scattering approach
mHSA	modified hard scattering approach
LCWF	light cone wave function
PDF	parton distribution function
PPF	parton fragmentation function
pQCD	perturbative Quantum Chromo Dynamics
QCD	Quantum Chromo Dynamics
RCS	real Compton scattering
WACS	wide angle Compton scattering

publications by
the author
marked with '=>'

Bibliography

- [1] J. C. Collins, D. E. Soper and G. Sterman, "Factorization Of Hard Processes In QCD," in: *Perturbative Quantum Chromodynamics*, edited by A. H. Mueller (World Scientific, Singapore 1989).
- [2] D. E. Soper, "The Parton Model And The Bethe-Salpeter Wave Function," *Phys. Rev. D* **15** (1977) 1141, (SPIRES); D. E. Soper, "Partons And Their Transverse Momenta In QCD," *Phys. Rev. Lett.* **43** (1979) 1847, (SPIRES).
- [3] A. H. Mueller, "Cut Vertices And Their Renormalization: A Generalization Of The Wilson Expansion," *Phys. Rev. D* **18** (1978) 3705, (SPIRES).
- [4] G. Curci, W. Furmanski and R. Petronzio, "Evolution Of Parton Densities Beyond Leading Order: The Nonsinglet Case," *Nucl. Phys. B* **175** (1980) 27, (SPIRES).
- [5] J. C. Collins and D. E. Soper, "Parton Distribution And Decay Functions," *Nucl. Phys. B* **194** (1982) 445, (SPIRES).
- [6] R. L. Jaffe, "Parton Distribution Functions For Twist Four," *Nucl. Phys. B* **229** (1983) 205, (SPIRES).
- [7] E. Rutherford, "The Scattering of the α and β Rays and the Structure of the Atom," *Proceedings of the Manchester Literary and Philosophical Society*, IV, 55, pp. 18-20 (presented on March 7, 1911).
- [8] J. H. Christenson, G. S. Hicks, L. M. Lederman, P. J. Limon, B. G. Pope and E. Zavattini, "Observation Of Massive Muon Pairs In Hadron Collisions," *Phys. Rev. Lett.* **25** (1970) 1523, (SPIRES).
- [9] S. D. Drell and T. Yan, "Massive Lepton Pair Production In Hadron - Hadron Collisions At High-Energies," *Phys. Rev. Lett.* **25** (1970) 316, (SPIRES); S. D. Drell and T. Yan, "Partons and their applications at high energies," *Annals Phys.* **66** (1971) 578, (SPIRES).
- [10] A.H. Compton, "A quantum theory of the scattering of X-rays by light elements," *Phys. Rev.* **21** (1923) 483; A.H. Compton, "The spectrum of scattered X-rays," *Phys. Rev.* **22** (1923) 409.
- [11] P. A. Dirac, "Forms Of Relativistic Dynamics," *Rev. Mod. Phys.* **21** (1949) 392, (SPIRES); H. Leutwyler and J. Stern, "Relativistic Dynamics On A Null Plane," *Annals Phys.* **112** (1978) 94, (SPIRES).

-
- [12] J. B. Kogut and D. E. Soper, “Quantum Electrodynamics In The Infinite Momentum Frame,” *Phys. Rev.* **D1**, 2901 (1970), (SPIRES).
- [13] Z. Dziembowski, “On Uniqueness Of Relativistic Nucleon State,” *Phys. Rev.* **D37**, 768 (1988), (SPIRES).
- [14] S. J. Brodsky and G. P. Lepage, “Exclusive Processes In Quantum Chromodynamics,” in: *Perturbative Quantum Chromodynamics*, edited by A. H. Mueller (World Scientific, Singapore 1989).
- [15] R. L. Jaffe, “Spin, twist and hadron structure in deep inelastic processes,” in: *Lectures on QCD, Erice 1995*, edited by F. Lenz, [hep-ph/9602236](#), (SPIRES).
- [16] J. C. Collins, “Light-cone variables, rapidity and all that,” [hep-ph/9705393](#), (SPIRES).
- [17] J. P. Ralston and D. E. Soper, “Production Of Dimuons From High-Energy Polarized Proton-Proton Collisions,” *Nucl. Phys. B* **152** (1979) 109, (SPIRES).
- [18] P. J. Mulders and R. D. Tangerman, “The complete tree-level result up to order $1/Q$ for polarized deep-inelastic leptonproduction,” *Nucl. Phys. B* **461** (1996) 197 [Erratum-ibid. B **484** (1996) 538] (SPIRES).
- [19] D. W. Sivers, “Single Spin Production Asymmetries From The Hard Scattering Of Pointlike Constituents,” *Phys. Rev. D* **41** (1990) 83 [*Annals Phys.* **198** (1990) 371], (SPIRES); D. W. Sivers, “Hard Scattering Scaling Laws For Single Spin Production Asymmetries,” *Phys. Rev. D* **43** (1991) 261, (SPIRES).
- ⇒ [20] R. Jakob, P. J. Mulders and J. Rodrigues, “Modelling quark distribution and fragmentation functions,” *Nucl. Phys.* **A626** (1997) 937, (SPIRES).
- [21] J. Rodrigues, “Modelling Quark and Gluon Correlation Functions,” Ph.D. thesis, VU Amsterdam, 2001, unpublished.
- [22] H. Burkhardt and W. N. Cottingham, “Sum Rules For Forward Virtual Compton Scattering,” *Annals Phys.* **56** (1970) 453, (SPIRES).
- [23] M. Burkardt, “Delta Functions In Higher Twist Parton Distribution. Physical Interpretation And Consequences For G(2) And H(2) Sum Rules,” *Talk given at the 10th International Symposium on High Energy Spin Physics (SPIN 92), Nagoya, Japan, 9-14 Nov 1992*, (SPIRES).
- [24] M. Burkardt, “On the possible violation of sum rules for higher twist parton distributions,” *Phys. Rev. D* **52** (1995) 3841, (SPIRES).
- [25] A. De Rujula, J. M. Kaplan and E. De Rafael, “Elastic Scattering Of Electrons From Polarized Protons And Inelastic Electron Scattering Experiments,” *Nucl. Phys. B* **35** (1971) 365, (SPIRES); K. Hagiwara, K. i. Hikasa

-
- and N. Kai, “Time Reversal Odd Asymmetry In Semiinclusive Leptoproduction In Quantum Chromodynamics,” *Phys. Rev. D* **27** (1983) 84, (SPIRES); D. Atwood, G. Eilam and A. Soni, “Transverse tau polarization in decays of the top and bottom quarks in the Weinberg model of CP nonconservation,” *Phys. Rev. Lett.* **71** (1993) 492, (SPIRES).
- [26] J. C. Collins, “Fragmentation of transversely polarized quarks probed in transverse momentum distributions,” *Nucl. Phys. B* **396** (1993) 161, (SPIRES).
- [27] J. w. Qiu and G. Sterman, “Single Transverse Spin Asymmetries,” *Phys. Rev. Lett.* **67** (1991) 2264, (SPIRES).
- [28] J. w. Qiu and G. Sterman, “Single Transverse Spin Asymmetries In Direct Photon Production,” *Nucl. Phys. B* **378** (1992) 52, (SPIRES).
- [29] D. Boer, P. J. Mulders and O. V. Teryaev, “Single spin asymmetries from a gluonic background in the Drell-Yan process,” *Phys. Rev. D* **57** (1998) 3057, (SPIRES).
- [30] M. Anselmino, M. Boglione and F. Murgia, “Single spin asymmetry for p (polarized) $p \rightarrow \pi X$ in perturbative QCD,” *Phys. Lett. B* **362** (1995) 164, (SPIRES).
- [31] M. Anselmino and F. Murgia, “Single spin asymmetries in p(pol.) p and anti-p(pol.) p inclusive processes,” *Phys. Lett. B* **442** (1998) 470, (SPIRES).
- [32] D. Boer, “Investigating the origins of transverse spin asymmetries at RHIC,” *Phys. Rev. D* **60** (1999) 014012, (SPIRES).
- [33] D. Boer and P. J. Mulders, “Time-reversal odd distribution functions in leptoproduction,” *Phys. Rev. D* **57** (1998) 5780, (SPIRES).
- [34] S. J. Brodsky, D. S. Hwang and I. Schmidt, “Final-state interactions and single-spin asymmetries in semi-inclusive deep inelastic scattering,” *Phys. Lett. B* **530** (2002) 99, (SPIRES).
- [35] J. C. Collins, “Leading-twist single-transverse-spin asymmetries: Drell-Yan and deep-inelastic scattering,” *Phys. Lett. B* **536** (2002) 43, (SPIRES).
- [36] X. d. Ji and F. Yuan, “Parton distributions in light-cone gauge: Where are the final-state interactions?,” *Phys. Lett. B* **543** (2002) 66, (SPIRES).
- [37] A. V. Belitsky, X. Ji and F. Yuan, “Final state interactions and gauge invariant parton distributions,” *Nucl. Phys. B* **656** (2003) 165, (SPIRES).
- [38] S. J. Brodsky, P. Hoyer, N. Marchal, S. Peigne and F. Sannino, “Structure functions are not parton probabilities,” *Phys. Rev. D* **65** (2002) 114025, (SPIRES).
- [39] J. Levelt and P. J. Mulders, “Quark correlation functions in deep inelastic semiinclusive processes,” *Phys. Rev. D* **49** (1994) 96, (SPIRES).

-
- [40] P. J. Mulders and J. Rodrigues, “Transverse momentum dependence in gluon distribution and fragmentation functions,” *Phys. Rev. D* **63** (2001) 094021, (SPIRES).
- [41] A. Bacchetta and P. J. Mulders, “Deep inelastic lepton production of spin-one hadrons,” *Phys. Rev. D* **62** (2000) 114004, (SPIRES).
- ⇒ [42] A. Bianconi, S. Boffi, R. Jakob and M. Radici, “Two-hadron interference fragmentation functions. I: General framework,” *Phys. Rev. D* **62** (2000) 034008, (SPIRES).
- [43] R. L. Jaffe, “Can transversity be measured?,” [hep-ph/9710465](#), (SPIRES).
- [44] R. L. Jaffe, X. m. Jin and J. Tang, “Interference fragmentation functions and the nucleon’s transversity,” *Phys. Rev. Lett.* **80** (1998) 1166, (SPIRES).
- [45] A. A. Henneman, D. Boer and P. J. Mulders, “Evolution of transverse momentum dependent distribution and fragmentation functions,” *Nucl. Phys. B* **620** (2002) 331, (SPIRES).
- [46] D. Boer, “Sudakov suppression in azimuthal spin asymmetries,” *Nucl. Phys. B* **603** (2001) 195, (SPIRES).
- [47] O. Martin, A. Schäfer, M. Stratmann and W. Vogelsang, “Soffer’s inequality and the transversely polarized Drell-Yan process at next-to-leading order,” *Phys. Rev. D* **57** (1998) 3084, (SPIRES); O. Martin, A. Schäfer, M. Stratmann and W. Vogelsang, “Transverse Double-Spin Asymmetries For Muon Pair Production In P P Collisions,” *Phys. Rev. D* **60** (1999) 117502, (SPIRES).
- [48] J. Soffer, M. Stratmann and W. Vogelsang, “Accessing transversity in double-spin asymmetries at the BNL-RHIC,” *Phys. Rev. D* **65** (2002) 114024, (SPIRES); D. de Florian, J. Soffer, M. Stratmann and W. Vogelsang, “Bounds on transverse spin asymmetries for Lambda baryon production in p p collisions at BNL RHIC,” *Phys. Lett. B* **439** (1998) 176, (SPIRES).
- [49] V. Barone, A. Drago and P. G. Ratcliffe, “Transverse polarisation of quarks in hadrons,” *Phys. Rept.* **359** (2002) 1, (SPIRES).
- [50] E. Leader, “Spin In Particle Physics,” *Cambridge Monogr. Part. Phys. Nucl. Phys. Cosmol.* **15** (2001) 1, (SPIRES).
- ⇒ [51] D. Boer, R. Jakob and P. J. Mulders, “Angular dependences in electroweak semi-inclusive lepton production,” *Nucl. Phys. B* **564** (2000) 471, (SPIRES).
- [52] J. C. Collins, S. F. Heppelmann and G. A. Ladinsky, “Measuring transversity densities in singly polarized hadron-hadron and lepton - hadron collisions,” *Nucl. Phys. B* **420** (1994) 565, (SPIRES).
- [53] A. Airapetian *et al.* [HERMES Collaboration], “Observation of a single-spin azimuthal asymmetry in semi-inclusive pion electro-production,” *Phys. Rev.*

-
- Lett. **84** (2000) 4047, (SPIRES); A. Airapetian *et al.* [HERMES Collaboration], “Single-spin azimuthal asymmetries in electroproduction of neutral pions in semi-inclusive deep-inelastic scattering,” Phys. Rev. D **64** (2001) 097101, (SPIRES).
- [54] A. Bravar [Spin Muon Collaboration], “Hadron azimuthal distributions and transverse spin asymmetries in DIS of leptons off transversely polarized targets from SMC,” Nucl. Phys. Proc. Suppl. **79** (1999) 520, (SPIRES).
- [55] M. Boglione and P. J. Mulders, “Azimuthal spin asymmetries in semi-inclusive production from positron proton scattering,” Phys. Lett. B **478** (2000) 114, (SPIRES).
- [56] A. V. Efremov, K. Goeke and P. Schweitzer, “Azimuthal asymmetry in electroproduction of neutral pions in semi-inclusive DIS,” Phys. Lett. B **522** (2001) 37, (SPIRES); A. V. Efremov, K. Goeke and P. Schweitzer, “Erratum to ‘Azimuthal asymmetry in electro production of neutral pions in semiinclusive DIS’ published in Phys. Lett. B522 (2001) 37,” [hep-ph/0204056](#).
- [57] E. De Sanctis, W. D. Nowak and K. A. Oganessian, “Single-spin azimuthal asymmetries in the ‘reduced twist-3 approximation’,” Phys. Lett. B **483** (2000) 69, (SPIRES); K. A. Oganessian, N. Bianchi, E. De Sanctis and W. D. Nowak, “Investigation of single spin asymmetries in pi+ electroproduction,” Nucl. Phys. A **689** (2001) 784, (SPIRES).
- [58] S. Wandzura and F. Wilczek, “Sum Rules For Spin Dependent Electroproduction: Test Of Relativistic Constituent Quarks,” Phys. Lett. B **72** (1977) 195, (SPIRES).
- [59] D. L. Adams *et al.* [FNAL-E704 Collaboration], “Analyzing power in inclusive pi+ and pi- production at high x(F) with a 200-GeV polarized proton beam,” Phys. Lett. B **264** (1991) 462, (SPIRES).
- [60] M. Boglione and E. Leader, “Reassessment of the Collins mechanism for single-spin asymmetries and the behavior of Delta(d)(x) at large x,” Phys. Rev. D **61** (2000) 114001, (SPIRES).
- ⇒ [61] D. Boer, R. Jakob and P. J. Mulders, “Asymmetries in polarized hadron production in e+ e- annihilation up to order 1/Q,” Nucl. Phys. **B504** (1997) 345, (SPIRES).
- ⇒ [62] D. Boer, R. Jakob and P. J. Mulders, “Leading asymmetries in two-hadron production in e+ e- annihilation at the Z pole,” Phys. Lett. **B424** (1998) 143, (SPIRES).
- [63] A. V. Efremov, O. G. Smirnova and L. G. Tkachev, “Study of T-odd quark fragmentation function in Z0 → 2-jet decay,” in *C98/07/02* Nucl. Phys. Proc. Suppl. **74** (1999) 49, (SPIRES).
- [64] J. C. Collins and G. A. Ladinsky, “On pi - pi correlations in polarized quark fragmentation using the linear sigma model,” [hep-ph/9411444](#).

- [65] X. Artru and J. C. Collins, “Measuring transverse spin correlations by 4 particle correlations in $e^+ e^- \rightarrow 2$ jets,” *Z. Phys. C* **69** (1996) 277, (SPIRES).
- [66] J. C. Collins and D. E. Soper, “Back To Back Jets In QCD,” *Nucl. Phys. B* **193** (1981) 381 [Erratum-ibid. *B* **213** (1983) 545], (SPIRES).
- [67] S. Boffi, C. Giusti, F. D. Pacati, and M. Radici, *Electromagnetic Response of Atomic Nuclei*, Vol. 20 of *Oxford Studies in Nuclear Physics* (Oxford University Press, Oxford, 1996).
- [68] A. Bacchetta, “Probing the transverse spin of quarks in deep inelastic scattering,” Ph.D. thesis, VU Amsterdam, 2002, unpublished.
- [69] A. M. Kotzinian and P. J. Mulders, “Probing transverse quark polarization via azimuthal asymmetries in leptonproduction,” *Phys. Lett. B* **406** (1997) 373, (SPIRES).
- [70] R. L. Jaffe, “Deep Inelastic Structure Functions In An Approximation To The Bag Theory,” *Phys. Rev. D* **11** (1975) 1953, (SPIRES).
- [71] C. J. Benesh and G. A. Miller, “Valence Quark Distributions In The Soliton Bag Model,” *Phys. Lett. B* **215** (1988) 381, (SPIRES); C. J. Benesh and G. A. Miller, “Deep Inelastic Scattering In A Modified Bag Model,” *Phys. Rev. D* **38** (1988) 48, (SPIRES).
- [72] A. W. Schreiber, A. I. Signal and A. W. Thomas, “Structure Functions In The Bag Model,” *Phys. Rev. D* **44** (1991) 2653, (SPIRES).
- [73] X. Song and J. S. McCarthy, “Model Calculation Of Nucleon Structure Functions,” *Phys. Rev. D* **49** (1994) 3169 [Erratum-ibid. *D* **50** (1994) 4718], (SPIRES).
- [74] M. Ropele, M. Traini and V. Vento, “Parton Polarization And Constituent Quarks,” *Nucl. Phys. A* **584** (1995) 634, (SPIRES); S. Scopetta, V. Vento and M. Traini, “Towards a unified picture of constituent and current quarks,” *Phys. Lett. B* **421** (1998) 64, (SPIRES); S. Scopetta, V. Vento and M. Traini, “Polarized structure functions in a constituent quark scenario,” *Phys. Lett. B* **442** (1998) 28, (SPIRES); M. Traini, A. Mair, A. Zambarda and V. Vento, “Constituent Quarks And Parton Distributions,” *Nucl. Phys. A* **614** (1997) 472, (SPIRES).
- [75] R. G. Roberts and G. G. Ross, “Quark Model Description of Polarised Deep Inelastic Scattering and the prediction of g_2 ,” *Phys. Lett. B* **373** (1996) 235, (SPIRES).
- [76] V. Barone, T. Calarco and A. Drago, “A confinement model calculation of $h_1(x)$,” *Phys. Lett. B* **390** (1997) 287, (SPIRES); V. Barone, T. Calarco and A. Drago, “Gluon spin in a quark model,” *Phys. Lett. B* **431** (1998) 405, (SPIRES).

-
- [77] H. Weigel, L. P. Gamberg and H. Reinhardt, “Nucleon Structure Functions from a Chiral Soliton,” *Phys. Lett. B* **399** (1997) 287, (SPIRES); H. Weigel, L. P. Gamberg and H. Reinhardt, “Polarized nucleon structure functions within a chiral soliton model,” *Phys. Rev. D* **55** (1997) 6910, (SPIRES); H. Weigel, L. P. Gamberg and H. Reinhardt, “Unpolarized Nucleon Structure Functions In The Nambu-Jona-Lasinio Chiral Soliton Model,” *Mod. Phys. Lett. A* **11** (1996) 3021, (SPIRES); L. P. Gamberg, H. Reinhardt and H. Weigel, “Odd structure functions from a chiral soliton,” *Phys. Rev. D* **58** (1998) 054014, (SPIRES); H. Weigel, E. Ruiz Arriola and L. P. Gamberg, “Hadron structure functions in a chiral quark model: Regularization, scaling and sum rules,” *Nucl. Phys. B* **560** (1999) 383, (SPIRES).
- [78] D. Diakonov, V. Y. Petrov, P. V. Pobylitsa, M. V. Polyakov and C. Weiss, “Unpolarized and polarized quark distributions in the large- $N(c)$ limit,” *Phys. Rev. D* **56** (1997) 4069, (SPIRES); P. V. Pobylitsa, M. V. Polyakov, K. Goeke, T. Watabe and C. Weiss, “Isovector unpolarized quark distribution in the nucleon in the large- $N(c)$ limit,” *Phys. Rev. D* **59** (1999) 034024, (SPIRES); K. Goeke, P. V. Pobylitsa, M. V. Polyakov, P. Schweitzer and D. Urbano, “Quark distribution functions in the chiral quark-soliton model: Cancellation of quantum anomalies,” *Acta Phys. Polon. B* **32** (2001) 1201, (SPIRES); A. V. Efremov, K. Goeke and P. V. Pobylitsa, “Gluon and quark distributions in large $N(c)$ QCD: Theory vs. phenomenology,” *Phys. Lett. B* **488** (2000) 182, (SPIRES); P. Schweitzer, D. Urbano, M. V. Polyakov, C. Weiss, P. V. Pobylitsa and K. Goeke, “Transversity distributions in the nucleon in the large- $N(c)$ limit,” *Phys. Rev. D* **64** (2001) 034013, (SPIRES).
- [79] H. Meyer and P. J. Mulders, “Polarized And Unpolarized Structure Functions In A Diquark Model For The Nucleon,” *Nucl. Phys. A* **528** (1991) 589, (SPIRES).
- [80] M. Nzar and P. Hoodbhoy, “Quark fragmentation functions in a diquark model for proton and Lambda hyperon production,” *Phys. Rev. D* **51** (1995) 32, (SPIRES).
- [81] B. Q. Ma, I. Schmidt, J. Soffer and J. J. Yang, “Quark distributions of octet baryons from $SU(3)$ symmetry,” *Phys. Rev. D* **65** (2002) 034004, (SPIRES).
- ⇒ [82] A. Bianconi, S. Boffi, R. Jakob and M. Radici, “Two-hadron interference fragmentation functions. II: A model calculation,” *Phys. Rev. D* **62** (2000) 034009, (SPIRES).
- ⇒ [83] M. Radici, R. Jakob and A. Bianconi, “Accessing transversity with interference fragmentation functions,” *Phys. Rev. D* **65** (2002) 074031, (SPIRES).
- [84] W. Melnitchouk, A. W. Schreiber and A. W. Thomas, “Deep inelastic scattering from off-shell nucleons,” *Phys. Rev. D* **49** (1994) 1183, (SPIRES).
- ⇒ [85] A. Bacchetta, S. Boffi and R. Jakob, “Semi-inclusive structure functions in the spectator model,” *Eur. Phys. J.* **A9** (2000) 131, (SPIRES).

- [86] F. E. Close and A. W. Thomas, "The Spin And Flavor Dependence Of Parton Distribution Functions," *Phys. Lett. B* **212** (1988) 227, (SPIRES).
- [87] M. Glück, E. Reya and A. Vogt, "Dynamical parton distributions of the proton and small x physics," *Z. Phys. C* **67** (1995) 433, (SPIRES).
- [88] M. Glück, E. Reya, M. Stratmann and W. Vogelsang, "Next-to-leading order radiative parton model analysis of polarized deep inelastic lepton - nucleon scattering," *Phys. Rev. D* **53** (1996) 4775, (SPIRES).
- [89] J. Soffer, "Positivity constraints for spin dependent parton distributions," *Phys. Rev. Lett.* **74** (1995) 1292, (SPIRES).
- [90] V. N. Gribov and L. N. Lipatov, "Deep Inelastic E P Scattering In Perturbation Theory," *Yad. Fiz.* **15** (1972) 781 [*Sov. J. Nucl. Phys.* **15** (1972) 438], (SPIRES); Y. L. Dokshitzer, "Calculation Of The Structure Functions For Deep Inelastic Scattering And E+ E- Annihilation By Perturbation Theory In Quantum Chromodynamics. (In Russian)," *Sov. Phys. JETP* **46** (1977) 641 [*Zh. Eksp. Teor. Fiz.* **73** (1977) 1216], (SPIRES); G. Altarelli and G. Parisi, "Asymptotic Freedom In Parton Language," *Nucl. Phys. B* **126** (1977) 298, (SPIRES).
- [91] R. G. Roberts, "The Structure Of The Proton: Deep Inelastic Scattering," *Cambridge, UK: Univ. Pr. (1990) 182 p. (Cambridge monographs on mathematical physics)*.
- [92] R. D. Peccei, "High-energy lepton hadron scattering as a probe of QCD," *UCLA-92-TEP-5 Lectures given at SLAC Summer Inst., SLAC, Aug 5-16, 1991*.
- [93] Y. L. Dokshitzer, D. Diakonov and S. I. Troian, "Hard Processes In Quantum Chromodynamics," *Phys. Rept.* **58** (1980) 269, (SPIRES).
- [94] A.-K. Kashani-Poor, " Q^2 -Evolution k_T -abhängiger Parton-Verteilungsfunktionen" Diploma thesis, Goethe Universität Frankfurt, 1997, (in German), unpublished.
- [95] V. L. Chernyak, A. R. Zhitnitsky and V. G. Serbo, "Asymptotic Hadronic Form-Factors In Quantum Chromodynamics," *JETP Lett.* **26** (1977) 594 [*Pisma Zh. Eksp. Teor. Fiz.* **26** (1977) 760], (SPIRES).
- [96] V. L. Chernyak and A. R. Zhitnitsky, "Asymptotic Behavior Of Exclusive Processes In QCD," *Phys. Rept.* **112** (1984) 173, (SPIRES).
- [97] A. V. Efremov and A. V. Radyushkin, "Factorization And Asymptotical Behavior Of Pion Form-Factor In QCD," *Phys. Lett. B* **94** (1980) 245, (SPIRES).
- [98] G. P. Lepage and S. J. Brodsky, "Exclusive Processes In Quantum Chromodynamics: Evolution Equations For Hadronic Wave Functions And The Form-Factors Of Mesons," *Phys. Lett. B* **87** (1979) 359, (SPIRES).

-
- [99] G. P. Lepage and S. J. Brodsky, "Exclusive Processes In Perturbative Quantum Chromodynamics," Phys. Rev. D **22** (1980) 2157, (SPIRES).
- [100] A. Duncan and A. H. Mueller, "Asymptotic Behavior Of Composite Particle Form-Factors And The Renormalization Group," Phys. Rev. D **21** (1980) 1636, (SPIRES); A. Duncan and A. H. Mueller, "Asymptotic Behavior Of Exclusive And Almost Exclusive Processes," Phys. Lett. B **90** (1980) 159, (SPIRES).
- [101] G. P. Lepage and S. J. Brodsky, "Exclusive Processes In Quantum Chromodynamics: The Form-Factors Of Baryons At Large Momentum Transfer," Phys. Rev. Lett. **43** (1979) 545 [Erratum-ibid. **43** (1979) 1625], (SPIRES).
- [102] N. G. Stefanis, "The physics of exclusive reactions in QCD: Theory and phenomenology," Eur. Phys. J. direct C **7** (1999) 1, (SPIRES).
- [103] N. Isgur and C. H. Llewellyn Smith, "The Applicability Of Perturbative QCD To Exclusive Processes," Nucl. Phys. B **317** (1989) 526, (SPIRES).
- [104] A. V. Radyushkin, "Hadronic Form-Factors: Perturbative QCD Versus QCD Sum Rules," in *C90-10-08.1* Nucl. Phys. A **532** (1991) 141, (SPIRES).
- [105] V. L. Chernyak and A. R. Zhitnitsky, "Exclusive Decays Of Heavy Mesons," Nucl. Phys. B **201** (1982) 492 [Erratum-ibid. B **214** (1983) 547], (SPIRES); V. L. Chernyak, A. R. Zhitnitsky and I. R. Zhitnitsky, "Meson Wave Functions And SU(3) Symmetry Breaking," Nucl. Phys. B **204** (1982) 477 [Erratum-ibid. B **214** (1983) 547], (SPIRES).
- [106] V. L. Chernyak, A. A. Ogloblin and I. R. Zhitnitsky, "The Wave Functions Of The Octet Baryons," Z. Phys. C **42** (1989) 569 [Yad. Fiz. **48** (1988) SJNCA,48,896-904.1988) 1410], (SPIRES)
- [107] M. Gari and N. G. Stefanis, "Electromagnetic Form-Factors Of The Nucleon From Perturbative QCD And QCD Sum Rules," Phys. Lett. B **175** (1986) 462, (SPIRES).
- [108] I. D. King and C. T. Sachrajda, "Nucleon Wave Functions And QCD Sum Rules," Nucl. Phys. B **279** (1987) 785, (SPIRES).
- [109] N. G. Stefanis and M. Bergmann, "On the Nucleon distribution amplitude: the Heterotic solution," Phys. Rev. D **47** (1993) 3685, (SPIRES).
- [110] J. Botts and G. Sterman, "Hard Elastic Scattering In QCD: Leading Behavior," Nucl. Phys. B **325** (1989) 62, (SPIRES); J. Botts and G. Sterman, "Sudakov Effects In Hadron-Hadron Elastic Scattering," Phys. Lett. B **224** (1989) 201 [Erratum-ibid. B **227** (1989) 501], (SPIRES); J. F. Botts, "Hard Elastic Scattering In QCD: Leading Behavior," Ph.D.thesis, Stony Brook NY, 1989, UMI-90-10466.
- [111] H. n. Li and G. Sterman, "The Perturbative pion form-factor with Sudakov suppression," Nucl. Phys. B **381** (1992) 129, (SPIRES).

- [112] H. n. Li, "Sudakov suppression and the proton form-factor in QCD," Phys. Rev. D **48** (1993) 4243, (SPIRES).
- ⇒ [113] R. Jakob and P. Kroll, "The Pion form-factor: Sudakov suppressions and intrinsic transverse momentum," Phys. Lett. B **315** (1993) 463 [Erratum-ibid. B **319** (1993) 545], (SPIRES).
- ⇒ [114] J. Bolz, R. Jakob, P. Kroll, M. Bergmann and N. G. Stefanis, "A Critical analysis of the proton form-factor with Sudakov suppression and intrinsic transverse momentum," Z. Phys. C **66** (1995) 267, (SPIRES).
- ⇒ [115] J. Bolz, R. Jakob, P. Kroll, M. Bergmann and N. G. Stefanis, "Neutron form-factor: Sudakov suppression and intrinsic transverse size effect," Phys. Lett. B **342** (1995) 345, (SPIRES).
- ⇒ [116] R. Jakob, P. Kroll and M. Raulfs, "Meson - photon transition form-factors," J. Phys. G **22** (1996) 45, (SPIRES).
- ⇒ [117] M. Dahm, R. Jakob and P. Kroll, "A Perturbative approach to B decays into two pi mesons," Z. Phys. C **68** (1995) 595, (SPIRES).
- [118] J. Bolz and P. Kroll, "Modelling the nucleon wave function from soft and hard processes," Z. Phys. A **356** (1996) 327, (SPIRES).
- [119] G. P. Lepage, S. J. Brodsky, T. Huang and P. B. Mackenzie, "Hadronic Wave Functions In QCD," in *C81-08-16.10 CLNS-82/522 Invited talk given at Banff Summer Inst. on Particle Physics, Banff, Alberta, Canada, Aug 16-28, 1981*.
- ⇒ [120] M. Diehl, T. Feldmann, R. Jakob and P. Kroll, "Linking parton distributions to form factors and Compton scattering," Eur. Phys. J. **C8** (1999) 409, (SPIRES).
- [121] R. P. Feynman, "Photon hadron interactions" (Benjamin, Reading, MA, 1972).
- [122] S. D. Drell and T. M. Yan, "Connection Of Elastic Electromagnetic Nucleon Form-Factors At Large Q^2 And Deep Inelastic Structure Functions Near Threshold," Phys. Rev. Lett. **24** (1970) 181, (SPIRES).
- ⇒ [123] M. Diehl, T. Feldmann, R. Jakob and P. Kroll, "The overlap representation of skewed quark and gluon distributions," Nucl. Phys. B **596** (2001) 33 [Erratum-ibid. B **605** (2001) 647], (SPIRES).
- [124] S. J. Brodsky, M. Diehl and D. S. Hwang, "Light-cone wavefunction representation of deeply virtual Compton scattering," Nucl. Phys. B **596** (2001) 99, (SPIRES).
- [125] C. J. Bebek *et al.*, "Measurement Of The Pion Form-Factor Up To $Q^2 = 4\text{ GeV}^2$," Phys. Rev. D **13** (1976) 25, (SPIRES).

-
- [126] C. J. Bebek *et al.*, “Electroproduction Of Single Pions At Low Epsilon And A Measurement Of The Pion Form-Factor Up To $Q^2 = 10\text{GeV}^2$,” Phys. Rev. D **17** (1978) 1693, (SPIRES).
- [127] J. Volmer *et al.* [The Jefferson Lab F(pi) Collaboration], “New results for the charged pion electromagnetic form-factor,” Phys. Rev. Lett. **86** (2001) 1713, (SPIRES).
- [128] J. Volmer, “The Pion Charge Form Factor via Pion Electroproduction on the Proton,” Ph.D. thesis, VU Amsterdam, 2000, unpublished.
- [129] S. J. Brodsky, T. Huang and G. P. Lepage, “Hadronic Wave Functions And High Momentum Transfer Interactions In Quantum Chromodynamics,” In **Banff 1981, Proceedings, Particles and Fields 2**, 143-199.
- [130] V. A. Nesterenko and A. V. Radyushkin, “Sum Rules And Pion Form-Factor In QCD,” Phys. Lett. B **115** (1982) 410, (SPIRES).
- [131] V. M. Braun, A. Khodjamirian and M. Maul, “Pion form factor in QCD at intermediate momentum transfers,” Phys. Rev. D **61** (2000) 073004, (SPIRES).
- [132] R. D. Field, R. Gupta, S. Otto and L. Chang, “Beyond Leading Order QCD Perturbative Corrections To The Pion Form-Factor,” Nucl. Phys. B **186** (1981) 429, (SPIRES).
- [133] F. M. Dittes and A. V. Radyushkin, “Radiative Corrections To The Pion Form-Factor In Quantum Chromodynamics,” Sov. J. Nucl. Phys. **34** (1981) 293, (SPIRES); R. S. Khalmuradov and A. V. Radyushkin, “One Loop Corrections To Pion Form-Factor In QCD In A Lightlike Gauge,” Sov. J. Nucl. Phys. **42** (1985) 289, (SPIRES);
- [134] E. P. Kadantseva, S. V. Mikhailov and A. V. Radyushkin, “Total α_s corrections to processes $\gamma^*\gamma^* \rightarrow \pi_0$ and $\gamma^*\pi \rightarrow \pi$ in a perturbative QCD,” Sov. J. Nucl. Phys. **44** (1986) 326, (SPIRES).
- [135] E. Braaten and S. M. Tse, “Perturbative QCD Correction To The Hard Scattering Amplitude For The Meson Form-Factor,” Phys. Rev. D **35** (1987) 2255, (SPIRES).
- [136] F. del Aguila and M. K. Chase, “Higher Order QCD Corrections To Exclusive Two Photon Processes,” Nucl. Phys. B **193** (1981) 517, (SPIRES).
- [137] A. Szczepaniak, A. Radyushkin and C. R. Ji, “Consistent analysis of $O(\alpha(s))$ corrections to pion elastic form factor,” Phys. Rev. D **57** (1998) 2813, (SPIRES).
- [138] B. Melic, B. Nizic and K. Passek, “Complete next-to-leading order perturbative QCD prediction for the pion form factor,” Phys. Rev. D **60** (1999) 074004, (SPIRES).

- [139] A. I. Karanikas and N. G. Stefanis, “Analyticity and power corrections in hard-scattering hadronic functions,” *Phys. Lett. B* **504** (2001) 225, (SPIRES).
- [140] N. G. Stefanis, W. Schroers and H. C. Kim, “Pion form factors with improved infrared factorization,” *Phys. Lett. B* **449** (1999) 299, (SPIRES); N. G. Stefanis, W. Schroers and H. C. Kim, “Infrared-finite factorization and renormalization scheme for exclusive processes. Application to pion form factors,” [hep-ph/9812280](#).
- [141] N. G. Stefanis, W. Schroers and H. C. Kim, “Analytic coupling and Sudakov effects in exclusive processes: Pion and $\gamma^*\gamma \rightarrow \pi_0$ form factors,” *Eur. Phys. J. C* **18** (2000) 137, (SPIRES).
- [142] F. J. Ernst, R. G. Sachs and K. C. Wali, “Electromagnetic Form Factors of the Nucleon,” *Phys. Rev.* **119** (1960) 1105.
- [143] R. G. Sachs, *Phys. Rev.* **126** (1962) 2256.
- [144] M. Bergmann and N. G. Stefanis, “Heterotic approach to the nucleon distribution amplitude,” *Phys. Lett. B* **325** (1994) 183, (SPIRES).
- [145] M. Bergmann and N. G. Stefanis, “Bounds On G_N^M/G_P^M From QCD Sum Rules,” *Phys. Rev. D* **48** (1993) 2990, (SPIRES).
- [146] S. Rock *et al.*, “Measurement Of Elastic Electron - Neutron Cross-Sections Up To $Q^2 = 10 (\text{GeV}/c)^2$,” *Phys. Rev. Lett.* **49** (1982) 1139, (SPIRES); R. G. Arnold *et al.*, “Measurement Of Elastic Electron Scattering From The Proton At High Momentum Transfer,” *Phys. Rev. Lett.* **57** (1986) 174, (SPIRES). S. Platchkov *et al.*, “Deuteron $A(Q^2)$ Structure Function And The Neutron Electric Form-Factor,” *Nucl. Phys. A* **510** (1990) 740, (SPIRES); S. Rock *et al.*, “Measurement of elastic electron - neutron scattering and inelastic electron - deuteron scattering cross-sections at high momentum transfer,” *Phys. Rev. D* **46** (1992) 24, (SPIRES); A. Lung *et al.*, “Measurements of the electric and magnetic form-factors of the neutron from $Q^2 = 1.75 (\text{GeV}/c)^2$ to $4 (\text{GeV}/c)^2$,” *Phys. Rev. Lett.* **70** (1993) 718, (SPIRES); A. F. Sill *et al.*, “Measurements of elastic electron - proton scattering at large momentum transfer,” *Phys. Rev. D* **48** (1993) 29, (SPIRES).
- [147] J. Bolz, “Das Nukleon im modifizierten harten Streubild,” Ph.D. thesis, Bergische Universität Wupertal, 1995, (in German), unpublished.
- [148] A. Schafer, L. Mankiewicz and Z. Dziembowski, “A Bound For The Three Quark Component Of The Nucleon Wave Function,” *Phys. Lett. B* **233** (1989) 217, (SPIRES).
- [149] P. Kroll, *private communication*.
- [150] H. J. Behrend *et al.* [CELLO Collaboration], “A Measurement Of The π_0 , η And η' Electromagnetic Form-Factors,” *Z. Phys. C* **49** (1991) 401, (SPIRES).

-
- [151] J. Gronberg *et al.* [CLEO Collaboration], “Measurements of the meson photon transition form factors of light pseudoscalar mesons at large momentum transfer,” *Phys. Rev. D* **57** (1998) 33, (SPIRES).
- [152] P. Kroll and M. Raulfs, “The $\pi\gamma$ transition form factor and the pion wave function,” *Phys. Lett. B* **387** (1996) 848, (SPIRES).
- [153] S. V. Mikhailov and A. V. Radyushkin, “The Pion Wave Function And QCD Sum Rules With Nonlocal Condensates,” *Phys. Rev. D* **45** (1992) 1754, (SPIRES).
- [154] E. Braaten, “QCD Corrections To Meson - Photon Transition Form-Factors,” *Phys. Rev. D* **28** (1983) 524, (SPIRES).
- [155] I. V. Musatov and A. V. Radyushkin, “Transverse momentum and Sudakov effects in exclusive QCD processes: $\gamma^*\gamma\pi_0$ form factor,” *Phys. Rev. D* **56** (1997) 2713, (SPIRES).
- ⇒ [156] M. Diehl, T. Feldmann, R. Jakob and P. Kroll, “Skewed parton distributions in real and virtual Compton scattering,” *Phys. Lett.* **B460** (1999) 204, (SPIRES).
- [157] C. Coriano and H. n. Li, “QCD sum rule and perturbative QCD approaches to pion Compton scattering,” *Phys. Lett. B* **309** (1993) 409, (SPIRES).
- [158] T. C. Brooks and L. J. Dixon, “Recalculation of proton Compton scattering in perturbative QCD,” *Phys. Rev. D* **62** (2000) 114021, (SPIRES).
- [159] A. S. Kronfeld and B. Nizic, “Nucleon Compton scattering in perturbative QCD,” *Phys. Rev.* **D44** (1991) 3445, (SPIRES).
- [160] M. Vanderhaeghen, P. A. Guichon and J. Van de Wiele, *Nucl. Phys.* **A622** (1997) 144c, (SPIRES).
- [161] M. A. Shupe *et al.*, “Neutral Pion Photoproduction And Proton Compton Scattering At Large Angles,” *Phys. Rev.* **D19** (1979) 1921, (SPIRES).
- [162] A. V. Radyushkin, “Nonforward parton densities and soft mechanism for form factors and wide-angle Compton scattering in QCD,” *Phys. Rev.* **D58** (1998) 114008, (SPIRES).
- [163] M. Glück, E. Reya and A. Vogt, “Dynamical parton distributions revisited,” *Eur. Phys. J.* **C5** (1998) 461, (SPIRES).
- [164] M. Glück, E. Reya, M. Stratmann and W. Vogelsang, “Next-to-leading order radiative parton model analysis of polarized deep inelastic lepton - nucleon scattering,” *Phys. Rev.* **D53** (1996) 4775, (SPIRES).
- [165] P. Kroll, M. Schürmann and W. Schweiger, “Exclusive photon - proton reactions at moderately large momentum transfer,” *Int. J. Mod. Phys.* **A6** (1991) 4107, (SPIRES).

- [166] A. Nathan, for the E99-114 JLAB collaboration, talk presented at the workshop on exclusive processes, Newport News (2002).
- [167] H. W. Huang, P. Kroll and T. Morii, “Perturbative and non-perturbative QCD corrections to wide-angle Compton scattering,” *Eur. Phys. J. C* **23** (2002) 301, (SPIRES).
- [168] L. Andivahis *et al.*, “Measurements of the electric and magnetic form-factors of the proton from $Q^2 = 1.75 \text{ GeV}/c^2$ to $8.83 \text{ GeV}/c^2$,” *Phys. Rev. D* **50** (1994) 5491, (SPIRES).
- [169] M. K. Jones *et al.* [Jefferson Lab Hall A Collaboration], “ $G(E(p))/G(M(p))$ ratio by polarization transfer in $e(\text{pol.}) p \rightarrow e p(\text{pol.})$,” *Phys. Rev. Lett.* **84** (2000) 1398, (SPIRES).
- [170] H. W. Huang and P. Kroll, “Large momentum transfer electroproduction of mesons,” *Eur. Phys. J. C* **17** (2000) 423, (SPIRES).
- [171] X. D. Ji, “Gauge invariant decomposition of nucleon spin,” *Phys. Rev. Lett.* **78** (1997) 610, (SPIRES).
- [172] X. D. Ji, “Deeply-virtual Compton scattering,” *Phys. Rev. D* **55** (1997) 7114, (SPIRES).
- [173] A. V. Radyushkin, “Scaling Limit of Deeply Virtual Compton Scattering,” *Phys. Lett. B* **380** (1996) 417, (SPIRES).
- [174] A. V. Radyushkin, “Asymmetric gluon distributions and hard diffractive electroproduction,” *Phys. Lett. B* **385** (1996) 333, (SPIRES).
- [175] J. C. Collins, L. Frankfurt and M. Strikman, “Factorization for hard exclusive electroproduction of mesons in QCD,” *Phys. Rev. D* **56** (1997) 2982, (SPIRES).
- [176] A. V. Radyushkin, “Nonforward parton distributions,” *Phys. Rev. D* **56** (1997) 5524, (SPIRES).
- [177] J. C. Collins and A. Freund, “Proof of factorization for deeply virtual Compton scattering in QCD,” *Phys. Rev. D* **59** (1999) 074009, (SPIRES).
- [178] X. D. Ji and J. Osborne, “One-loop corrections and all order factorization in deeply virtual Compton scattering,” *Phys. Rev. D* **58** (1998) 094018, (SPIRES).
- [179] ZEUS collaboration, “Measurement of deeply virtual Compton scattering cross section at HERA,” Submitted to the XXXIst International Conference on High Energy Physics, 24-31 July, 2002, Amsterdam, The Netherlands
- [180] L. L. Frankfurt, A. Freund and M. Strikman, “Diffractive exclusive photo-production in DIS at HERA,” *Phys. Rev. D* **58** (1998) 114001 [Erratum-*ibid.* *D* **59** (1999) 119901], (SPIRES).

-
- [181] A. Donnachie and H. G. Dosch, “Diffractive exclusive photon production in deep inelastic scattering,” *Phys. Lett. B* **502** (2001) 74, (SPIRES).
- [182] C. Adloff *et al.* [H1 Collaboration], “Measurement of deeply virtual Compton scattering at HERA,” *Phys. Lett. B* **517** (2001) 47, (SPIRES).
- [183] M. Diehl, T. Gousset, B. Pire and J. P. Ralston, “Testing the handbag contribution to exclusive virtual Compton scattering,” *Phys. Lett. B* **411** (1997) 193, (SPIRES).
- [184] A. V. Belitsky, D. Muller, L. Niedermeier and A. Schafer, “Leading twist asymmetries in deeply virtual Compton scattering,” *Nucl. Phys. B* **593** (2001) 289, (SPIRES); A. V. Belitsky, D. Muller, L. Niedermeier and A. Schafer, “Deeply virtual Compton scattering in next-to-leading order,” *Phys. Lett. B* **474** (2000) 163, (SPIRES); A. V. Belitsky and D. Muller, “Twist-three effects in two-photon processes,” *Nucl. Phys. B* **589** (2000) 611, (SPIRES); A. V. Belitsky, A. Kirchner, D. Muller and A. Schafer, “Twist-three observables in deeply virtual Compton scattering on the nucleon,” *Phys. Lett. B* **510** (2001) 117, (SPIRES); A. V. Belitsky, D. Muller and A. Kirchner, “Theory of deeply virtual Compton scattering on the nucleon,” *Nucl. Phys. B* **629** (2002) 323, (SPIRES).
- [185] A. Airapetian *et al.* [HERMES Collaboration], “Measurement of the beam spin azimuthal asymmetry associated with deeply-virtual Compton scattering,” *Phys. Rev. Lett.* **87** (2001) 182001, (SPIRES).
- [186] N. Kivel, M. V. Polyakov and M. Vanderhaeghen, “DVCS on the nucleon: Study of the twist-3 effects,” *Phys. Rev. D* **63** (2001) 114014, (SPIRES).
- [187] A. Airapetian *et al.* [HERMES Collaboration], “Single-spin azimuthal asymmetry in exclusive electroproduction of π^+ mesons,” *Phys. Lett. B* **535** (2002) 85, (SPIRES).
- [188] F. M. Dittes, D. Muller, D. Robaschik, B. Geyer and J. Horejsi, “The Altarelli-Parisi Kernel As Asymptotic Limit Of An Extended Brodsky-Lepage Kernel,” *Phys. Lett. B* **209** (1988) 325, (SPIRES); D. Muller, D. Robaschik, B. Geyer, F. M. Dittes and J. Horejsi, “Wave functions, evolution equations and evolution kernels from light-ray operators of QCD,” *Fortsch. Phys.* **42** (1994) 101, [hep-ph/9812448](#), (SPIRES).
- [189] P. Jain and J. P. Ralston, “Measuring chirally odd wave functions with helicity flip form-factors,” [hep-ph/9305250](#).
- [190] X. D. Ji, “Off-forward parton distributions,” *J. Phys. G* **24** (1998) 1181, (SPIRES).
- [191] A. V. Radyushkin, “Generalized parton distributions,” [hep-ph/0101225](#).
- [192] K. Goeke, M. V. Polyakov and M. Vanderhaeghen, “Hard exclusive reactions and the structure of hadrons,” *Prog. Part. Nucl. Phys.* **47** (2001) 401, (SPIRES).

- [193] M. Diehl, “Generalized parton distributions with helicity flip,” *Eur. Phys. J. C* **19** (2001) 485, (SPIRES).
- [194] P. Hoodbhoy and X. D. Ji, “Helicity-flip off-forward parton distributions of the nucleon,” *Phys. Rev. D* **58** (1998) 054006, (SPIRES).
- [195] A. V. Belitsky, D. Muller, L. Niedermeier and A. Schafer, “Two-loop effects in the evolution of non-forward distributions,” *Phys. Lett. B* **437** (1998) 160, (SPIRES).
- [196] A. V. Belitsky, A. Freund and D. Muller, “Evolution kernels of skewed parton distributions: Method and two-loop results,” *Nucl. Phys. B* **574** (2000) 347, (SPIRES).
- [197] A. Freund and M. F. McDermott, “Next-to-leading order evolution of generalized parton distributions for HERA and HERMES,” *Phys. Rev. D* **65** (2002) 056012 [Erratum-ibid. *D* **66** (2002) 079903], (SPIRES). A. Freund and M. McDermott, “A detailed next-to-leading order QCD analysis of deeply virtual Compton scattering observables,” *Eur. Phys. J. C* **23** (2002) 651, (SPIRES).
- [198] D. Muller, “Conformal constraints and the evolution of the nonsinglet meson distribution amplitude,” *Phys. Rev. D* **49** (1994) 2525, (SPIRES); A. V. Belitsky and D. Muller, “Predictions from conformal algebra for the deeply virtual Compton scattering,” *Phys. Lett. B* **417** (1998) 129, (SPIRES); A. V. Belitsky and D. Muller, “Next-to-leading order evolution of twist-two conformal operators: The abelian case,” *Nucl. Phys. B* **527** (1998) 207, (SPIRES); A. V. Belitsky and D. Muller, “Broken conformal invariance and spectrum of anomalous dimensions in QCD,” *Nucl. Phys. B* **537** (1999) 397, (SPIRES).
- [199] E. R. Berger, M. Diehl and B. Pire, “Timelike Compton scattering: Exclusive photoproduction of lepton pairs,” *Eur. Phys. J. C* **23** (2002) 675, (SPIRES).
- [200] M. Diehl, T. Gousset, B. Pire and O. Teryaev, “Probing partonic structure in $\gamma^*\gamma \rightarrow \pi\pi$ near threshold,” *Phys. Rev. Lett.* **81** (1998) 1782, (SPIRES); M. Diehl, T. Gousset and B. Pire, “Exclusive production of pion pairs in $\gamma^*\gamma$ collisions at large Q^2 ,” *Phys. Rev. D* **62** (2000) 073014, (SPIRES).
- [201] M. Diehl, P. Kroll and C. Vogt, “The annihilation of virtual photons into pseudoscalar mesons,” *Eur. Phys. J. C* **22** (2001) 439, (SPIRES); M. Diehl, P. Kroll and C. Vogt, “The handbag contribution to $\gamma\gamma \rightarrow \pi\pi$ and KK ,” *Phys. Lett. B* **532** (2002) 99, (SPIRES).
- [202] M. Diehl, P. Kroll and C. Vogt, “Two-photon annihilation into baryon antibaryon pairs,” *Eur. Phys. J. C* **26** (2003) 567, (SPIRES).
- [203] S. J. Brodsky and D. S. Hwang, “Exact light-cone wavefunction representation of matrix elements of electroweak currents,” *Nucl. Phys. B* **543** (1999) 239, (SPIRES).

-
- [204] J. Ashman *et al.* [European Muon Collaboration], “A Measurement Of The Spin Asymmetry And Determination Of The Structure Function $G(1)$ In Deep Inelastic Muon Proton Scattering,” *Phys. Lett. B* **206** (1988) 364, (SPIRES).
- [205] B. Adeva *et al.* [Spin Muon Collaboration], “Spin asymmetries $A(1)$ of the proton and the deuteron in the low x and low Q^2 region from polarized high energy muon scattering,” *Phys. Rev. D* **60** (1999) 072004, (SPIRES).
- [206] K. Abe *et al.* [E143 Collaboration], “Measurements of the Q^2 dependence of the proton and deuteron spin structure functions $g_1(p)$ and $g_1(d)$,” *Phys. Lett. B* **364** (1995) 61, (SPIRES).
- [207] K. Ackerstaff *et al.* [HERMES Collaboration], “Flavor decomposition of the polarized quark distributions in the nucleon from inclusive and semi-inclusive deep-inelastic scattering,” *Phys. Lett. B* **464** (1999) 123, (SPIRES).
- [208] B. W. Filippone and X. D. Ji, “The spin structure of the nucleon,” *Adv. Nucl. Phys.* **26** (2001) 1, (SPIRES).
- [209] R. L. Jaffe, “The theory of the nucleon spin,” *Phil. Trans. Roy. Soc. Lond. A* **359** (2001) 391, (SPIRES).
- [210] S. V. Bashinsky and R. L. Jaffe, “Quark and gluon orbital angular momentum and spin in hard processes,” *Nucl. Phys. B* **536** (1998) 303, (SPIRES).
- [211] P. Hagler and A. Schafer, “Evolution equations for higher moments of angular momentum distributions,” *Phys. Lett. B* **430** (1998) 179, (SPIRES).
- [212] A. Harindranath and R. Kundu, “On orbital angular momentum in deep inelastic scattering,” *Phys. Rev. D* **59** (1999) 116013, (SPIRES).
- [213] J. P. Ralston, R. V. Buniy and P. Jain, “Electromagnetic form factors and the localization of quark orbital angular momentum in the proton,” [hep-ph/0206063](#).
- [214] M. Diehl, “Generalized parton distributions in impact parameter space,” *Eur. Phys. J. C* **25** (2002) 223, (SPIRES).
- [215] J. P. Ralston and P. Jain, “Exploring the micro-structure of the proton: From form factors to DVCS,” [hep-ph/0207129](#).
- [216] M. Burkardt, “Off-forward parton distributions and impact parameter dependent parton structure,” [hep-ph/0008051](#).
- [217] J. P. Ralston and B. Pire, “Femto-photography of protons to nuclei with deeply virtual Compton scattering,” *Phys. Rev. D* **66** (2002) 111501, (SPIRES).
- [218] A. V. Belitsky and D. Muller, “Nucleon hologram with exclusive lepton production,” *Nucl. Phys. A* **711** (2002) 118, (SPIRES).

-
- [219] M. Burkardt, "Impact parameter dependent parton distributions and off-forward parton distributions for $\zeta \rightarrow 0$," Phys. Rev. D **62** (2000) 071503, (SPIRES).
- [220] M. Burkardt, "Impact parameter space interpretation for generalized parton distributions," Int. J. Mod. Phys. A **18** (2003) 173, (SPIRES);
- [221] M. Burkardt, "Impact parameter dependent parton distributions and transverse single spin asymmetries," Phys. Rev. D **66** (2002) 114005, (SPIRES).
- [222] R. K. Ellis, W. Furmanski and R. Petronzio, "Unraveling Higher Twists," Nucl. Phys. B **212** (1983) 29, (SPIRES).
- ⇒ [223] N. Bianchi and R. Jakob, "Summary report of the spin physics working group," presented at the 9th International Workshop on Deep Inelastic Scattering (DIS 2001), April 2001, Bologna, hep-ph/0108078.
- ⇒ [224] N. Bianchi and R. Jakob, "Nucleon insights: echoes from QCD-N'02", Report on the European Workshop on the QCD Structure of the Nucleon (QCD-N'02), April 2002, Ferrara, CERN COURIER, Vol.42, No.6
- [225] J. D. Bjorken, "Intersections 2000: What's new in hadron physics," AIP Conf. Proc. **549** (2002) 211, (SPIRES).
- [226] H. n. Li, "Applicability of perturbative QCD to $B \rightarrow D$ decays," Phys. Rev. D **52** (1995) 3958, (SPIRES).
- [227] M. Sawicki, "Soft Charge Form-Factor Of The Pion," Phys. Rev. D **46** (1992) 474, (SPIRES); M. Sawicki, "Light front limit in a rest frame," Phys. Rev. D **44** (1991) 433, (SPIRES).